UNIVERSITY OF SOUTHAMPTON

FACULTY OF MEDICINE

Clinical and Experimental Sciences

Peptides of the renin angiotensin system and their potential roles in idiopathic pulmonary fibrosis

by

Samantha Marie Maitland

Thesis for the degree of Doctor of Philosophy

September 2015

UNIVERSITY OF SOUTHAMPTON

ABSTRACT

FACULTY OF MEDICINE

Clinical and Experimental Sciences

Thesis for the degree of Doctor of Philosophy

PEPTIDES OF THE RENIN ANGIOTENSIN SYSTEM AND THEIR POTENTIAL ROLES IN IDIOPATHIC PULMONARY FIBROSIS

By Samantha Marie Maitland

Idiopathic pulmonary fibrosis (IPF) is a progressive, irreversible disease of the lung, characterised by excessive extracellular matrix (ECM) deposition and loss of pulmonary function.

Fibroblasts are the main cell type responsible for ECM deposition and peptides from the renin-angiotensin system (RAS) have been shown to modulate fibroblast function. Angiotensin (ANG)-II, has been shown to exert profibrotic effects on human cardiac fibroblasts, such as increased collagen deposition. ANGII is known to bind to two receptors (AT_1R and AT_2R), with profibrotic effects attributed to AT_1R.

ANGII is cleaved to form ANG(1-7). This peptide has been shown to exert antifibrotic effects on fibroblasts, such as decreased cell proliferation, via binding to the Mas receptor. However, most investigations have been performed in rat fibroblasts. Another related peptide called ANG(1-9), has also been shown to exert antifibrotic effects on fibroblasts, via binding to AT_2R, again this work has only been performed in rat fibroblasts.

The main aims of this thesis were to investigate the effects of ANGII and related peptides on signalling pathways in both IPF derived and healthy human lung fibroblasts (HLFs) and to explore the effects of ANG peptides on HLF function. A second aim was to characterise Mas receptor expression on HLFs.

The effects of ANGII, ANG(1-7) and six related peptides on intracellular Ca^{2+} release were explored and the ability of ANGII to phosphorylate ERK was also investigated. Fibroblast functions in response to both ANGII and ANG(1-7) were also examined, including proliferation, collagen deposition, matrix metalloproteinase (MMP) and cytokine secretion. Receptor involvement was investigated with telmisartan (AT_1R antagonist), PD-123319 (AT_2R antagonist) and A-779 (Mas receptor antagonist). Mas receptor expression on HLFs was also investigated with immunocytochemistry and radioligand binding studies.

ANGI ANGII and ANGIII caused intracellular Ca^{2+} release via AT_1R. ANGII also induced ERK phosphorylation, although this did not translate to fibroblast function. No effects of ANGII were observed on cell proliferation, collagen deposition, MMP secretion or IL-6 production.

In the Ca^{2+} assay, ANG(1-7) and ANG(1-9) partially inhibited the responses to both ANGII and ANGIII. These effects did not appear to be modulated by AT_2R or the Mas receptor, indicating a novel binding site for these two peptides. The effects of ANG(1-7) did not appear to correlate with functional activity, with no reduction in cell proliferation or collagen deposition observed with this peptide. Immunocytochemistry showed clear nuclear expression of the Mas receptor in HLFs, with very low cell surface expression, providing an explanation for the lack of functional response.

Together these results indicate that although many ANG peptides can affect intracellular signalling pathways, peptides from the RAS do not affect functional responses of HLFs.

Contents

Contents i

List of tables v

List of figures vii

DECLARATION OF AUTHORSHIP xi

Acknowledgements xiii

Definitions and Abbreviations xv

Chapter 1. Introduction 1

1.1 Idiopathic Pulmonary Fibrosis 2

1.1.1 Introduction 2

1.1.2 Diagnosis 2

1.1.3 Prognosis 3

1.1.4 Treatment 4

1.1.5 Aetiology 5

1.1.6 Pathogenesis 5

1.2 Extracellular matrix 7

1.2.1 Collagens 7

1.2.2 Matrix-metalloproteases. 8

1.3 Transforming Growth Factor-β 9

1.4 Fibroblasts 14

1.4.1 Fibroblasts in normal epithelial repair 14

1.4.2 Fibroblasts in idiopathic pulmonary fibrosis 15

1.5 Renin-angiotensin system 18

1.5.1 Basic renin-angiotensin system 18

1.5.2 Peptides and receptors of the renin-angiotensin system 19

1.5.3 Inhibitors of the renin angiotensin system 25

1.6 Angiotensin peptides in the pathogenesis of IPF 28

1.6.1 Angiotensin II 28

1.6.2 Angiotensin(1-7) 30

1.6.3 Related peptides 31

1.6.4 Clinical Evidence for the role of the RAS in IPF 32

1.7 Limitations of pulmonary fibrosis animal models 33
1.8 Aims 34

Chapter 2. Materials and Methods 37
2.1 Materials. 38
2.2 Buffers and Reagents 38
2.2.1 Basic Buffers 38
2.2.2 Cell Culture 38
2.2.3 FLIPR buffers 39
2.2.4 Collagen Assays 39
2.2.5 Zymography 39
2.2.6 Western blotting 39
2.2.7 Radioligand Binding 39
2.3 Cell Culture 40
2.3.1 Isolating fibroblasts from human lung tissue. 40
2.3.2 Cell maintenance 40
2.4 Fluorescence imaging plate reader 40
2.5 Western blots 42
2.6 Fibroblast proliferation assay 43
2.7 Collagen Assays 43
2.8 Gelatin Zymography 44
2.9 Enzyme-linked immunosorbent assay 45
2.10 Immunocytochemistry 45
2.11 Fibroblast membrane preparation for radioligand binding 45
2.11.1 Preparation of fibroblast membranes 46
2.11.2 Protein Assays for membrane protein concentration 46
2.12 Radioligand binding 46
2.12.1 Simple binding experiments 46
2.12.2 Competitive binding assays 48
2.13 Statistical analysis. 48

Chapter 3. Calcium mobilisation in human lung fibroblasts 49
3.1 Background 50
3.2 Protocols 52
3.2.1 Calcium signalling experiments 52
3.2.2 ERK phosphorylation 53
3.3 Results 54

3.3.1 Reproducibility of Fibroblast Ca^{2+} responses 54
3.3.2 Effects of angiotensin peptides on calcium mobilisation 55
3.3.3 Inhibitory effects of angiotensin peptides 57
3.3.4 Further investigations into the activity of ANG(1-7) and ANG(1-9). 61
3.3.5 Investigations into the activity of angiotensin I 65
3.3.6 ERK Phosphorylation 68
3.4 Discussion 70

Chapter 4. Effects of angiotensin peptides on human lung fibroblast function 79
4.1 Background 80
4.2 Protocols 82
4.2.1 Patient characteristics 82
4.2.2 Angiotensin II 82
4.2.3 Angiotensin(1-7) 83
4.2.4 Angiotensin inhibitors 83
4.3 Results 84
4.3.1 Angiotensin peptides and human lung fibroblast function 84
4.3.2 Angiotensin inhibitor effects 100
4.4 Discussion 111

Chapter 5. Angiotensin receptor expression in human lung fibroblasts 127
5.1 Background 128
5.2 Protocols 129
5.2.1 Immunocytochemistry 129
5.2.2 Radioligand binding 129
5.3 Results 130
5.3.1 Mas receptor immunocytochemistry 130
5.3.2 Radioligand binding 134
5.4 Discussion 145

Chapter 6. Final discussion 151
6.1 Discussion 152
6.2 Further work 159
6.2.1 Calcium mobilisation in human lung fibroblasts 159
6.2.2 ERK phosphorylation 160
6.2.3 Receptor Expression 160
6.2.4 Fibroblast functions 161

List of References..... 163

8. Appendix 184

List of tables

Table 1-1. IPF diagnostic criteria. 3

Table 1-2. Matrixmetalloproteinase (MPP) family subtypes 8

Table 1-3. Circulating plasma concentrations of angiotensin peptides. 21

Table 1-4. Affinity of different angiotensin peptides at angiotensin receptors. 22

Table 3-1. Affinity of different angiotensin peptides at angiotensin receptors. 50

Table 3-2. pEC_{50} values of peptides in healthy and IPF cells. 56

Table 3-3. Maximal responses to peptides in healthy and IPF cells. 56

Table 3-4. The percentage of inhibition of ANGII and ANGIII in the presence of ANG(1-7) and ANG(1-9) in healthy fibroblasts. 60

Table 3-5. The percentage of inhibition of ANGII and ANGIII in the presence of ANG(1-7) and ANG(1-9) in IPF fibroblasts. 60

Table 3-6. Effects of ANG(1-7) and ANG(1-9) on ANGII and ANGIII pEC_{50} values in healthy fibroblasts. 61

Table 3-7. Effects of ANG(1-7) and ANG(1-9) on ANGII and ANGIII pEC_{50} values in IPF fibroblasts. 61

Table 3-8. Human plasma concentrations of angiotensin peptides. 73

Table 4-1. Summary of patient characteristics. Characteristics of the donors from which fibroblasts were isolated for functional studies. 82

Table 5-1. Different angiotensin receptor agonists/antagonists and their binding sites. 138

List of figures

Figure 1-1. Fibroblastic foci. 4

Figure 1-2. IPF is a multifactorial disease. 6

Figure 1-3. Basic structure of TGF-β large latent complex. 10

Figure 1-4. Basic TGF-β signalling pathway. 11

Figure 1-5. Wound healing response. 14

Figure 1-6. Intracellular signalling in fibroblasts important in ECM and β1 integrin interaction. 15

Figure 1-7. The basic renin angiotensin system. 19

Figure 1-8. ANGII and related peptides. 20

Figure 1-9. The signalling pathway involved in intracellular calcium release. 22

Figure 2-1. Diagrammatic representation of FLIPR experiment. 41

Figure 2-2. Gelatin zymography method. 44

Figure 2-3. Radioligand binding experimental set up. 47

Figure 2-4. Total and non-specific binding of the radioligand. 47

Figure 3-1. Diagrammatic representation of desensitisation experiments. 52

Figure 3-2. Ca^{2+} responses to ANGII. 54

Figure 3-3. Dose response curves to angiotensin peptides. 55

Figure 3-4. Dose-response curves to angiotensin peptides in the presence of antagonists. 57

Figure 3-5. The ability of angiotensin peptides to inhibit ANGII. 58

Figure 3-6. The ability of angiotensin peptides to inhibit ANGIII. 59

Figure 3-7. Effects of antagonists on ANG(1-7) induced inhibition. 62

Figure 3-8. Effects of antagonists on ANG(1-9) induced inhibition. 62

Figure 3-9. Inhibition curves to ANG(1-9). 63

Figure 3-10. Inhibition curves to ANG(1-7). 64

Figure 3-11. Inhibition curves to ANG(1-9) in the presence and absence of captopril. 65

Figure 3-12. Desensitisation of the Ca^{2+} response to ANGII. 66

Figure 3-13. ANGI induced desensitisation of the Ca^{2+} response to ANGII. 66

Figure 3-14. ANGI induced desensitisation of the Ca^{2+} response to ANGII in the presence and absence of captopril. 67

Figure 3-15. ANGI dose response curves in the presence and absence of captopril. 68

Figure 3-16. Western blot investigating ERK phosphorylation in response to ANGII. 68

Figure 3-17. Western blot quantification. 69

Figure 4-1. Initial proliferation experiments in serum free media. 84

Figure 4-2. The effect of ANGII on human lung fibroblast proliferation in the presence of 10% newborn calf serum. 85

Figure 4-3. The effect of ANGII on human lung fibroblast proliferation in the presence of 0.4% newborn calf serum. 86

Figure 4-4. The effects of 1μM ANG(1-7) and 10μM A-779 on 10% newborn calf serum induced proliferation. 87

Figure 4-5. The effects of 10μM ANG(1-7) and 10μM A-779 on 10% newborn calf serum induced proliferation. 88

Figure 4-6. Effects of TGF-β1 on collagen production. 89

Figure 4-7. Effect of TGF-β1 on ANGII induced collagen production. 90

Figure 4-8. Effects of ANGII on TGF-β1 induced collagen production. 91

Figure 4-9. Effects of ANG(1-7) on serum induced collagen production. 92

Figure 4-10. Effects of ANG(1-7) on TGF-B induced collagen production. 93

Figure 4-11. Effect of A-779 on ANG(1-7) modulated collagen production. 94

Figure 4-12. Effects of ANG(1-7) preincubation on TGF-β1 induced collagen production. 95

Figure 4-13. The effects of ANGII and TGF-β1 on matrix metalloproteinase-1 secretion. 96

Figure 4-14. MMP-2 production in the presence of ANGII and TGF-β1. 97

Figure 4-15. Relative changes in MMP-2 production in the presence of ANGII or TGF-β1. 97

Figure 4-16. Effects of ANGII and TGF-β1 on interleukin-6 secretion. 98

Figure 4-17. Effects of ANGII and TGF-β1 on latency associated peptide secretion. . 99

Figure 4-18. The effect of captopril on baseline collagen levels. 100

Figure 4-19. The effect of telmisartan on baseline collagen levels. 101

Figure 4-20. Effects of captopril on interleukin-6 secretion. 102

Figure 4-21. The effect of angiotensin inhibitors on baseline interleukin-6 secretion. 103

Figure 4-22. The effects of angiotensin inhibitors on 10% newborn calf serum induced interleukin-6. 104

Figure 4-23. The effects of angiotensin inhibitors on TGF-β1 induced interleukin-6 secretion. 104

Figure 4-24. The effect of captopril on TGF-β1 secretion. 105

Figure 4-25. The effects of angiotensin inhibitors on baseline TGF-β1 secretion.. 106

Figure 4-26. The effect of angiotensin inhibitors on 10% newborn calf serum induced TGF-β1. 106

Figure 4-27. The effect of captopril on MMP-1 secretion. 107

Figure 4-28. The effect of angiotensin inhibitors on baseline MMP-1 secretion.... 108

Figure 4-29. The effects of angiotensin inhibitors on 10% newborn calf serum induced MMP-1...... 109

Figure 4-30. The effects of angiotensin inhibitors on TGF-β1 induced MMP-1...... 109

Figure 5-1. Cytoplasmic anti-Mas staining in permeabilised human lung fibroblasts. 130

Figure 5-2. Cytoplasmic anti-Mas in non-permeabilised human lung fibroblasts. 131

Figure 5-3. Secondary antibody staining alone...... 131

Figure 5-4. Staining with extracellular anti-Mas in non-permeabilised human lung fibroblasts. 132

Figure 5-5. Staining with extracellular anti-Mas in non-permeabilised human lung fibroblasts. 132

Figure 5-6. Effects of A-779 on extracellular anti-Mas staining...... 133

Figure 5-7. Effects of A-779 and 0.5% newborn calf serum on cytoplasmic anti-Mas staining. 134

Figure 5-8. Total and non-specific binding of [^{125}I]-A-779...... 135

Figure 5-9. Total and non-specific binding of [^{125}I]-ANG(1-7)...... 136

Figure 5-10. Specific binding in the presence of saponin. 137

Figure 5-11. Binding of [^{125}I]-ANG(1-7) in the presence of increasing membrane protein. 137

Figure 5-12. Binding of 0.2nM [^{125}I]-ANG(1-7) in presence of different cold ligands.139

Figure 5-13. Binding of 0.52nM [^{125}I]-ANG(1-7) in the presence of different cold ligands. 139

Figure 5-14. Total and NSB observed with [^{125}]I-Sarile. 140

Figure 5-15. Specific binding of [^{125}I]-Sarile over time. 141

Figure 5-16. Homologous competition assays with [^{125}I]-Sarile. 142

Figure 5-17. Homologous competition assays with [^{125}I]-Sarile. 142

Figure 5-18. Heterologous competition of [^{125}I]-Sarile. 143

Figure 5-19. Inhibition of [^{125}I]-Sarile with ANGII and telmisartan. 144

DECLARATION OF AUTHORSHIP

I, Samantha Marie Maitland, declare that the thesis entitled: PEPTIDES OF THE RENIN ANGIOTENSIN SYSTEM AND THEIR POTENTIAL ROLES IN IDIOPATHIC PULMONARY FIBROSIS, and the work presented in the thesis are both my own, and have been generated by me as the result of my own original research.

I confirm that:

- this work was done wholly or mainly while in candidature for a research degree at this University;
- where any part of this thesis has previously been submitted for a degree or any other qualification at this University or any other institution, this has been clearly stated;
- where I have consulted the published work of others, this is always clearly attributed;
- where I have quoted from the work of others, the source is always given. With the exception of such quotations, this thesis is entirely my own work;
- I have acknowledged all main sources of help;
- where the thesis is based on work done by myself jointly with others, I have made clear exactly what was done by others and what I have contributed myself;
- none of this work has been published before submission.

Signed: ……..

Date:……..

Acknowledgements

I would like to thank my supervisors Jane Warner, David Hall and Tony Sampson for all their help, guidance and support.

Thanks to my fellow students Mel Jannaway and Andy Hutton for helping to obtain human lung tissue, which is used to culture fibroblasts. And again thanks to Andy for helping to culture and maintain these cells.

Valerie Morrison at GSK for all her support in the lab and for helping to maintain my cell lines, this helped make starting experiments much smoother.

A really big thank you to all staff in histopathology and on theatre reception, nurses on wards D2 and E4, and to all patients who agreed to donate lung tissue to us. Without whom, none of this research would have been possible.

Ben Johnson and Serena Chee from the target lung group, who took on the role of consenting patients and coordinating lung tissue for us during the last year. This was really helpful and relieved some of the stress involved in the final year of our PhDs.

Also thanks to my parents and my non-PhD friends for lending an ear and supporting me through the harder times, with general PhD stress and failed experiments, even though they didn't always fully understand what I was talking about. Thanks for listening anyway it was really appreciated!

Definitions and Abbreviations

ACE – Angiotensin converting enzyme.

AEC – Alveolar epithelial cell

AGT- Angiotensinogen

Akt – Protein kinase B

ALI – Acute lung injury

AMPS – Ammonium persulphate solution

ANG – Angiotensin

AP - Aminopeptidase

BALF – Bronchoalveolar lavage fluid

BFGF – Basic fibroblast growth factor

BFS – Bovine foetal serum

Bpa – Benzoyl-l-phenylalanine

BSA – Bovine serum albumin

CPW – Cells per well

CXCR4 – Human chemokine receptor type 4

DTT – DL-Dithiothreitol

DPM – disintegrations per minute

DMEM – Dulbecco's modified eagles medium.

ECM – Extracellular matrix

EC_{50} – Concentration causing 50% excitatory response

ELISA – Enzyme linked immunosorbent assay

EMT – Epithelial mesenchymal transition

ER – Endoplasmic reticulum

FAK – Focal adhesion kinase

FCS – Foetal calf serum

FEV1 – Forced expiratory volume in one second

FLIPR – Fluorescence imaging plate reader.

FVC – Forced vital capacity

GPCR – G-protein coupled receptor

HBSS – Hanks balanced salt solution

HEK – Human embryonic kidney

HLF – Human lung fibroblast

IC_{50} – Concentration causing 50% inhibition

ILD – Interstitial lung disease

IPF – Idiopathic pulmonary fibrosis

IP_3 – Inositol 1,4,5-trisphosphate

LTBP – Latent TGF-β binding protein

MMP – Matrix-metalloproteinase

MPA – Methionine proximity assay

NCS – Newborn calf serum

NEP – Neprilysin

NO – Nitric oxide

NRK – Normal rat kidney

NSB – Non-specific binding

PAI – Plasminogen activator inhibitor

PBS – Phosphate Buffered Saline

PFA – Paraformaldehyde

PDGF – Platelet derived growth factor

PEI - Polyethylenimine

PIP_2 – Phosphatidylinositol 4,5-bisphosphate

PIP_3 – Phosphatidylinositol 3,4,5-trisphosphate

PLC – Phospholipase C

RAS – Renin-angiotensin system

SDS – Sodium Dodecyl Sulphate

SGH – Southampton General Hospital

SMA – Smooth muscle actin

TEMED – Tetramethylethenediamine

TGF – Transforming growth factor

TIMP – Tissue inhibitor of metalloproteinase

TMB - 3,3',5,5'-tetramethylbenzidine

Chapter 1. Introduction

1.1 Idiopathic Pulmonary Fibrosis

1.1.1 Introduction

Idiopathic pulmonary fibrosis (IPF) is characterized by the progressive deposition of scar tissue in the lungs and loss of pulmonary function. The prognosis for a patient with IPF is poor, with an average life expectancy of 3 to 5 years after diagnosis (Raghu *et al.*, 2006). The only therapy available for patients with advanced IPF is lung transplantation; however, this only offers a 5 year post-transplantation survival rate of 44% (King *et al.*, 2011), indicating the need for research into new treatments for this disease.

1.1.2 Diagnosis

IPF is classified by the American Thoracic Society and the European Respiratory Society (ATS/ERS, 2000) as 'a specific form of chronic fibrosing interstitial pneumonia limited to the lung and associated with the histological appearance of usual interstitial pneumonia (UIP) on surgical (thoracoscopic or open) lung biopsy. The aetiology is unknown'.

IPF is one of many fibrotic diseases that can affect the lung, that are collectively known as interstitial lung disease (ILD). Accurate diagnosis of IPF is often difficult, with four major and three minor criteria needing to be met before a diagnosis of IPF can be considered, these are set out in **Table 1-1** below. All diagnostic criteria discussed in this section are taken from the ATS/ERS international consensus statement for IPF.

IPF is a peripheral, bibasilar disease, usually beginning in the subpleural regions of the lower lobes of the lung. The classic histopathological pattern for IPF is usual interstitial pneumonia (UIP), this is characterised by a heterogeneous pattern of areas of normality, fibrosis and honeycombing (degradation of the alveolar walls and enlargement of air spaces). This pattern is unique to IPF and allows distinction from many other ILDs, such as asbestosis and scleroderma.

Major	Minor
Exclusion of other known causes of ILD, such as certain drug toxicities, environmental exposures and connective tissue diseases	Age >50
Abnormal pulmonary function studies that include evidence of restriction (reduced vital capacity often with an increased FEV1/FVC ratio) and impaired gas exchange (increased AaPo2 with rest or exercise or decreased DL_{CO}	Insidious onset of otherwise unexplained dyspnoea on exertion
Bibasilar reticular abnormalities with minimal ground glass opacities on high resolution CT scans	Duration of illness ≥3 months
Transbronchial lung biopsy or bronchoalveolar lavage showing no features to support an alternative diagnosis	Bibasilar, inspiratory crackles (dry or 'Velcro' type in quality)

Table 1-1. IPF diagnostic criteria. All four major and at least three of the minor criteria must be met before a diagnosis of IPF can be considered. FEV1 is the forced expiratory volume in one second. FVC (forced vital capacity), is the total volume that can be expelled from the lungs after maximum inhalation. Table taken from the ATS/ERS international consensus statement for IPF.

The age of the patient is also important in determining the likelihood of an IPF diagnosis, with most patients typically above 40 years of age. Incidence increases further with ageing, with two thirds of patients above 60 years with an average diagnosis age of 66.

1.1.3 Prognosis

Determining the prognosis of individual patients is difficult, due to the lack of definitive and widely accepted clinical markers for the indication of disease progression. Also IPF is a highly variable disease with patients either being classified as 'slow' or 'rapid' progressors. Another reason for the unpredictability of patient prognosis is that a high number of patients may undergo periods of acute exacerbations with no obvious cause; these periods lead to a worsening of symptoms and are linked with high mortality rates (Moeller *et al.*, 2009). Although the course of IPF is extremely variable between patients, the underlying histopathological features are consistent. As mentioned above, most patients have increased collagen deposition, large areas of lung fibrosis and honeycombing with areas of dense populations of fibroblasts and myofibroblasts (**Figure 1-1**) known as fibroblastic foci (Yamashita *et al.*, 2009). The numbers of these fibrotic foci are an important marker and correlate well with the speed of disease progression and prognosis.

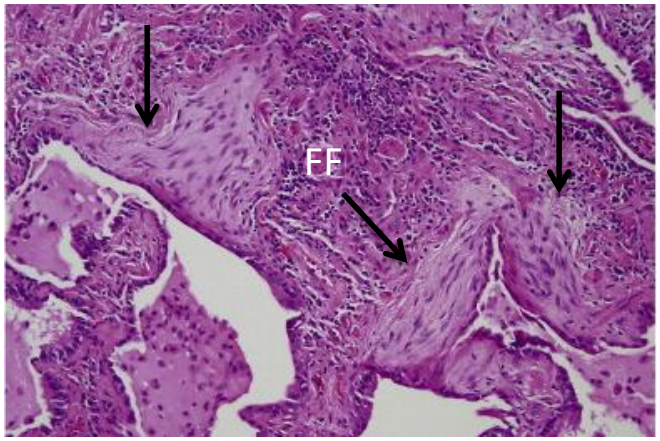

Figure 1-1. Fibroblastic foci. Fibroblastic foci (indicated by arrows) are characteristic of a patient with IPF (Katzenstein *et al.*, 2008). The number of fibroblastic foci present in the lung generally correlates to the rate of disease progression.

1.1.4 Treatment

There are currently two licensed drugs for patients with IPF. Pirfenidone, (licensed for use in Europe in 2011) is an antifibrotic drug that has proved effective for the treatment of IPF. The exact mechanism of action of this drug is unclear, but it has been shown to decrease fibroblast proliferation, transforming growth factor (TGF)-β levels, as well as TGF-β induced collagen production (Di Sario *et al.*, 2002; Lin *et al.*, 2009). There are, however, many limitations with this treatment; although pirfenidone significantly slows disease progression, it does not actually cure or halt the development of disease (Taniguchi *et al.*, 2010). Although this drug is quite well tolerated in patients, there are many serious adverse effects associated with pirfenidone, such as photosensitivity and anorexia (Maher, 2010). Ongoing treatment with pirfenidone is also extremely expensive, at approximately £25000 per annum (Raghu and Thickett, 2013).

Nintedanib, a small molecule tyrosine kinase inhibitor, has also been approved (Feb 2015) for the treatment of IPF. Nintedanib has been shown to interfere with a number of important process involved in IPF disease progression, such as fibroblast proliferation and migration, as well as extracellular matrix (ECM) secretion (Wollin *et al.*, 2015). However, in a similar manner to pirfenidone, nintedanib does not actually cure IPF, but only slows disease progression. A significantly slower decline in force vital capacity (FVC) was observed with nintedanib in two 12 month, random, double-blind placebo controlled trials (Richeldi *et al.*, 2014). This drug also seems to have less serious adverse effects than pirfenidone, with gastrointestinal effects, such as diarrhoea and nausea, being the most commonly reported adverse events in these clinical trials.

Both currently available IPF treatments, pifendione (for patients with mild to moderate disease), and nintedanib (for mild to severe disease) have serious downfalls in that they only slow disease progression, with mortality still the end point for every patient with IPF. This therefore still represents a major unmet medical need, with the need for more research into this disease area.

1.1.5 Aetiology

The aetiology of IPF is currently unknown, with a number of potential causes and risk factors all contributing to the onset of disease. These include inhaled toxins such as cigarette smoke and dust from metal, wood and asbestos. Viral infections, in particular the herpes virus have also been implicated in the pathogenesis of IPF, although no definitive link has been proven (Gross and Hunninghake, 2001). Genetics are also thought to play a role in some patients with IPF, with 0.5-3.7% of cases thought to have a genetic component, although this value may be higher as many cases of familial IPF are often missed (King *et al.*, 2011). IPF also has a slightly higher prevalence in males with an incidence of 7 cases per 100,000 in females and 10 cases per 100,000 in males. The incidence of IPF also increases with age, with most patients being between the ages of 50 and 75 (Selman *et al.*, 2001).

1.1.6 Pathogenesis

IPF is a multifactorial condition, with a number of processes contributing to disease progression (**Figure 1-2**). An increased number of fibroblasts are present in the lungs of patients with IPF (as shown in **Figure 1-1**), leading to an increase in ECM deposition and fibrosis. TGF-β is well known to increase fibroblast ECM production and has been shown to be upregulated in IPF lungs (Bergeron *et al.*, 2003). An upregulation of platelet derived growth factor (PDGF) has also been demonstrated (Antoniades *et al.*, 1990), PDGF is a well known mitogen and chemoattractant for fibroblasts and smooth muscle cells, and is also capable of stimulating fibroblast collagen production.

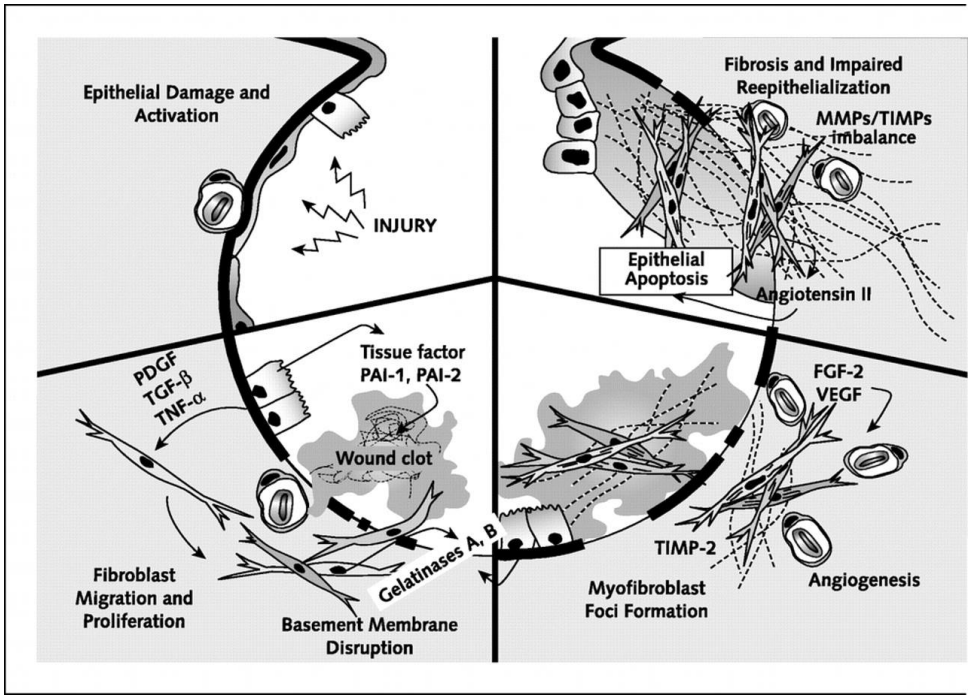

Figure 1-2. IPF is a multifactorial disease. IPF is driven by a number of different factors, dysregulation of transforming growth factor (TGF)-β, platelet derived growth factor (PDGF), plasminogen activator inhibitors (PAI), matrix metalloproteinases (MMPs) and tissue inhibitors of metalloproteinases (TIMPs) lead to epithelial cell apoptosis, increasing numbers of fibroblasts and myofibroblasts as well as upregulated ECM deposition. (Selman *et al.*, 2001).

It is thought that this increased number of fibroblasts could also be a response to increased alveolar epithelial cell (AEC) damage and death, with AECs in IPF shown to have an increase in the apoptotic Fas-signalling pathway (Selman and Pardo, 2006). Also in patients with lung fibrosis, areas of alveolar type II cell damage were associated with increased levels of pro-apoptotic BAX and p53 expression, with a loss of anti-apoptotic Bcl-2 expression (Guinee *et al.*, 1997). There are many environmental factors that may be responsible for the initial AEC damage, such as viruses and cigarette smoke (see section 1.1.5).

Although many of the defective mechanisms that seem to contribute to IPF are well characterised, it is unknown what is actually responsible for altering these processes, and what causes these patients to develop an irreversible fibrotic response to injury.

Many of the factors that are involved in the progression of IPF are discussed in more detail below.

1.2 Extracellular matrix

1.2.1 Collagens

Collagens are the main class of structural proteins present in ECM and over 20 different types of collagen have been identified (Suki *et al.*, 2005). Although there are differences in the structure of each collagen, the basic architecture is similar with the presence of a well characterised collagen triple-helix. (Brodsky and Ramshaw, 1997). The fibrillar collagens I, II and III are the most abundant collagens present in the human lung (van Kuppevelt *et al.*, 1995). Collagen I mainly co-localises with collagen III and together these are responsible for maintaining the structural architecture of the alveolar wall and vasculature (Suki *et al.*, 2005). Collagen II is another significant structural collagen, but is mainly confined to cartilage in the large airways (van Kuppevelt *et al.*, 1995). Collagen IV, another key collagen in the lung, is found in the basement membrane and is responsible for maintaining tensile strength at the blood-air interface (Berg *et al.*, 1998). Other key, but less common collagens include type V and VI, which are responsible for adhesion and fibril formation. Increased collagen production is a pivotal feature of IPF, with many differences in collagen expression in IPF lungs previously described.

Studies have shown that collagen deposition is not only elevated in IPF, but is also dysregulated. Although early studies showed there to be no change in collagen amount between healthy and IPF lungs (Fulmer *et al.*, 1980), and rather suggested that the fibrotic response observed in IPF was entirely due to irregular deposition of collagen, in response to high enzymatic degradation of previously existing ECM. Bronchoalveolar lavage fluid (BALF) from patients with IPF also showed an upregulation in collagenase content indicating a high enzymatic breakdown of collagen (Gadek *et al.*, 1979). It was also demonstrated that IPF lungs had a higher ratio of collagen I to collagen III than control lungs (Seyer *et al.*, 1976), further indicating that the composition of newly deposited collagen is unusual in IPF. In a more recent finding (Leeming *et al.*, 2012), breakdown products of collagen I, III, V and VI were significantly increased in the serum of IPF patients when compared to controls, again indicating high collagen degradation in these patients.

Other investigations have demonstrated that collagen content in IPF lungs is elevated (Selman *et al.*, 1986), although in this study the specific collagen types that were upregulated were not investigated. The authors also demonstrated a reduction in collagen breakdown, which does not agree with previous findings. One explanation for this is the area of the lung under investigation, Gadek *et al* (1979) looked at BALF and this may not be representative of the

alveolar environment, which is the main site of fibrosis in the IPF lung. Leeming et al examined the serum of IPF patients, which again may not be indicative of the fibrotic environment. However, Selman *et al* (1986) analysed parenchymal biopsies from fibrotic lung, which is likely to be more indicative of localised areas of disease.

Although there is a large body of evidence illustrating defective collagen deposition and excess production of ECM in IPF, the cause of these abnormal processes is relatively unknown and need to be further explored.

1.2.2 Matrix-metalloproteases.

As mentioned briefly in section 1.2.1, collagenase in BALF was upregulated in IPF patients (Gadek *et al.*, 1979). Collagenase, otherwise known as MMP-1 is a member of the matrix metalloproteinase (MMP) family. MMPs are zinc dependent endopeptidases that are collectively responsible for the degradation of most ECM components (Birkedal-Hansen *et al.*, 1993). Depending on substrate and amino acid sequence similarities, the MMP family can be sorted into distinct separate subtypes (Verma and Hansch, 2007), as shown in **Table 1-2**.

Subtype	**MMPs**
Collagenases	1,8,13,18
Gelatinases	2,9
Stromelysins	3,10,11,27
Membrane-type MMPs	14,15,16,17,24,25
Matrilysins	7,26
Other	12,19,20,21,22,23,28,29

Table 1-2. Matrixmetalloproteinase (MPP) family subtypes (Verma and Hansch, 2007).

As MMPs are responsible for the degradation of ECM components, normal lung architecture is dependent on a delicate balance between MMP activity and collagen production. Therefore, differences in the expression of MMPs could play important roles in IPF disease progression, with many MMPs implicated in the pathogenesis of IPF. Microarray analysis revealed that MMP-1, MMP-2, MMP-7 and MMP-28 gene expressions are increased in IPF lung (Pardo *et al.*, 2008). At the protein and gene level, MMP-3 has also been shown to be highly upregulated in

the lungs of patients with IPF when compared to control (Yamashita *et al.*, 2011). These authors also demonstrated that rats, which had transient adenoviral vector-mediated recombinant MMP-3 expression, showed increased pulmonary myofibroblast accumulation and fibrosis, further illustrating the role of this MMP in IPF.

The gelatinases MMP-2 and MMP-9 have also been shown in many studies to be upregulated in IPF; MMP-9 mRNA expression was significantly elevated in fibroblasts derived from IPF lung (Ramos *et al.*, 2001), with the same study also revealing a trend towards higher MMP-2 mRNA expression in IPF fibroblasts. Both MMP-2 and MMP-9 levels were also shown to be significantly higher in BALF from IPF patients (Lemjabbar *et al.*, 1999), with the same investigation also demonstrating elevated MMP-9 production by alveolar macrophages derived from these patients. This increased MMP-9 level in IPF patient BALF was further confirmed by more recent research (Willems *et al.*, 2013), with an upregulation in MMP-8 expression also observed in this study.

The most confounding of these observations is the increased level of MMP-1 in IPF (Pardo *et al.*, 2008), with the main substrates for this MMP being the fibrous collagens type I and III, both of which are elevated in IPF. These findings appear to be paradoxical; however, when studied more closely, MMP-1 has been shown to localise with AECs and macrophages, with no expression observed in myofibroblastic foci (Selman *et al.*, 2000). This finding indicates that MMP-1 may play a more pivotal role in the honeycombing features of IPF rather than the fibrotic component. It was also established that tissue inhibitor of metalloproteinase (TIMP) - 2 expression was increased in myofibroblastic foci (Fukuda *et al.*, 1998; Selman *et al.*, 2000), this highlights the profibrotic nature of these foci, with TIMP-2 providing a stable non-degrading environment, allowing cumulative and progressive ECM deposition. These observations demonstrate the complex nature of IPF, with varying microenvironments within the lung all contributing to disease progression.

1.3 Transforming Growth Factor-β

TGF-β1, a well-known profibrotic cytokine, is part of the TGF-β superfamily that consists of over 40 different genes, coding for TGF-β1 to β5. TGF-β1, β2 and β3 are found in humans and other mammals and are known to have very diverse effects on embryonic development and tissue function.

TGF-β is secreted in its latent form as a dimeric complex, consisting of C-terminal mature TGF-β non-covalently linked to N-terminal latency associated peptide (LAP). Two molecules of this pro-TGF-β are linked by disulphide bonds and form the small latent TGF-β complex. This small

latent complex can also associate with latent TGF-β binding protein (LTBP) to form the large latent TGF-β complex (Saharinen *et al.*, 1999), (**Figure 1-3**) most cells secrete TGF-β in the form of this large latent complex. The main function of LTBP is to interact with ECM components via its N-terminus, allowing for direct co-localisation of TGF-β with the ECM. This large latent complex can be cleaved to allow the release of the small latent complex.

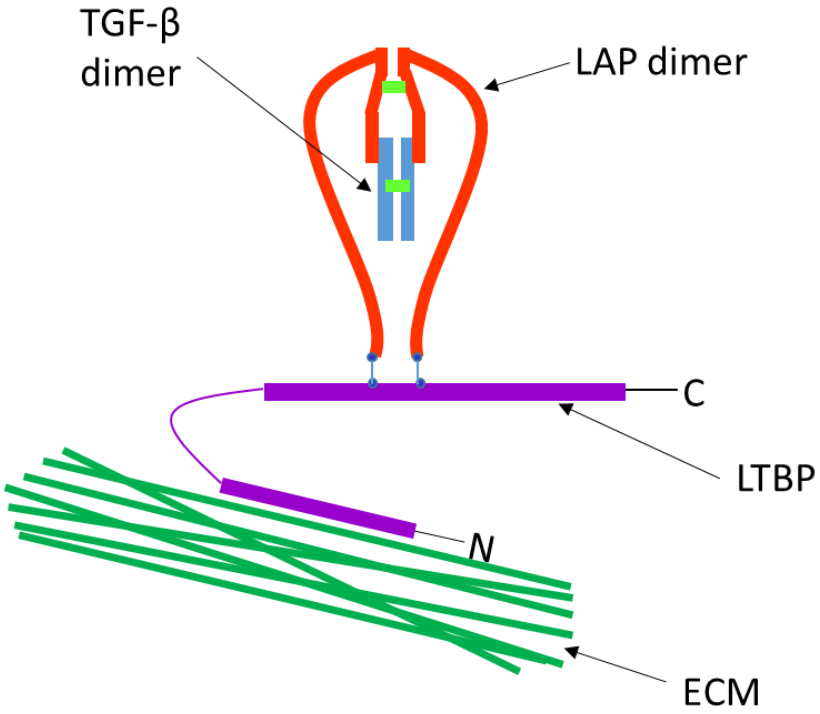

Figure 1-3. **Basic structure of TGF-β large latent complex.** TGF-β as part of the large latent complex exists as a TGF-β homodimer, bound to two molecules of latency associated peptide (LAP). LAP then binds a further protein, known as latent TGF-β binding peptide (LTBP), which interacts with extracellular matrix (ECM) via its N-terminus.

A number of factors cause release of active TGF-β from the small latent complex, such factors include proteases such as cathepsin D and plasmin (Lyons *et al.*, 1988), integrin αvβ6 (Munger *et al.*, 1999) and nitric oxide (Metukuri *et al.*, 2009). Upon activation, TGF-β is then free to bind to TGF-β receptors, there are two main TGF-β receptors, named TGFβR1 and 2, these receptors are serine/threonine kinases that exist as homodimers in the cell membrane (**Figure 1-4**) and are present on most mammalian cell types (Kingsley, 1994).

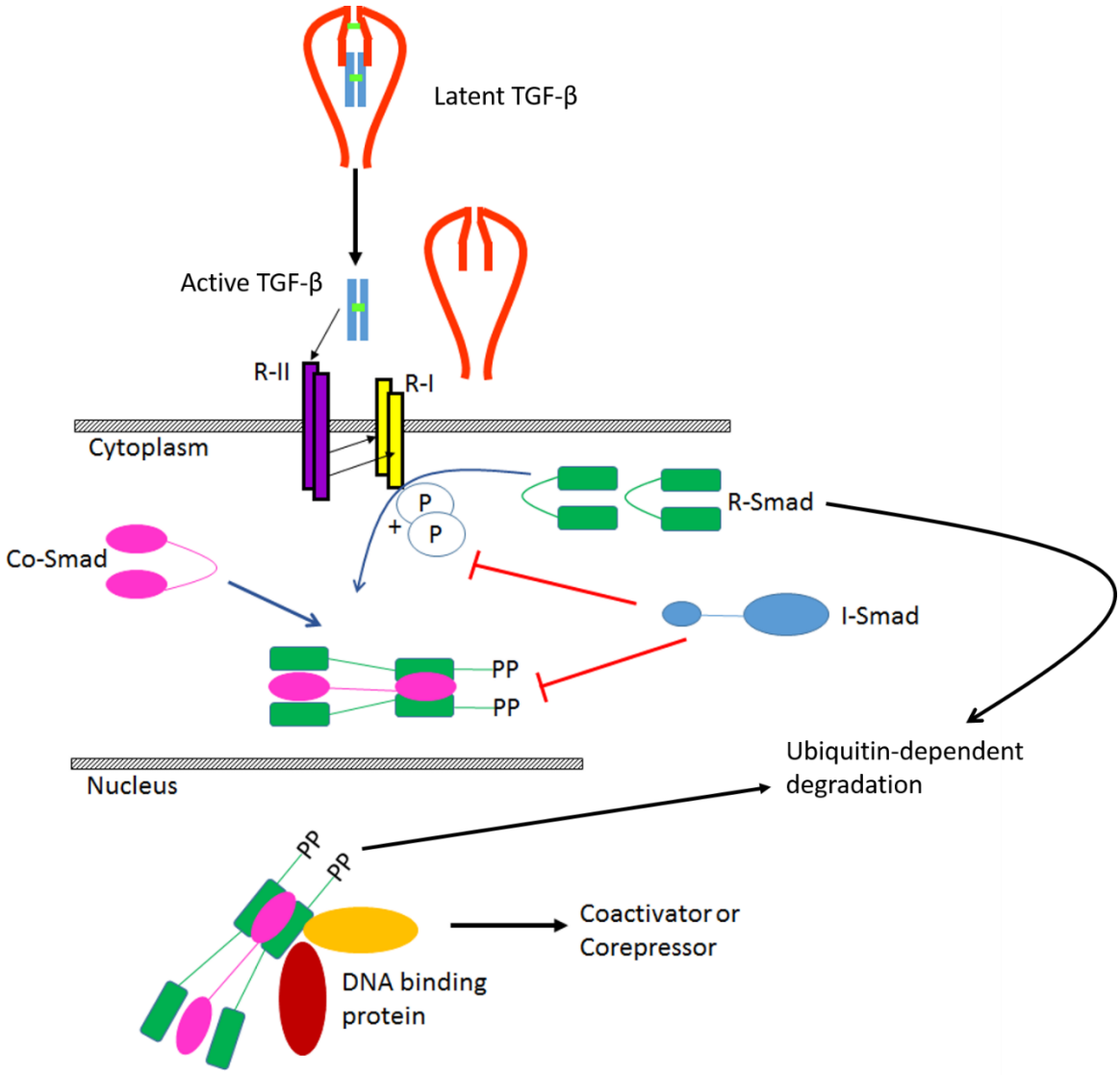

Figure 1-4. Basic TGF-β signalling pathway. TGF-β dissociates from latency associated peptide (LAP) and binds to TGF-β receptor II. This interaction causes heterodimerisation of the two receptor subtypes I and II (R-I and R-II), causing activation of receptor I. Receptor type I then causes phosphorylation of regulatory (R) Smads allowing them to localise with common mediator (Co) Smads. This R/Co-Smad complex then translocates to the nucleus where it can modulate gene transcription. Inhibitory (I) Smads can negatively regulate this pathway by competing for the receptor or for Co-Smads (adapted from (Miyazono, 2000)).

TGF-β peptides have high affinity for TGFβR2, with no binding affinity for TGFβR1. Upon binding of the ligand dimer to TGFβR2, this receptor co-localises with a TGFβR1 dimer to form a large complex, consisting of two receptor homodimers (**Figure 1-4**), this interaction causes activation of TGFβR1.

The main intracellular signalling pathway activated by TGFβR1 is the Smad pathway. Many different types of Smad proteins exist and are classified into three groups known as regulatory

(R), common mediator (Co) and inhibitory (I). The main R-Smads phosphorylated by TGFβR1 are Smad2/3, upon phosphorylation, these R-Smads form complexes with Co-Smads, with Smad 4 being the only Co-Smad known to exist in humans. This Smad complex then translocates to the nucleus, where it affects the transcription of mRNA for many different cellular processes including cell growth and ECM production. I-Smads (Smad6/7) negatively regulate TGF-β signalling by competing for interaction with either Co-Smad or the receptor (Miyazono, 2000).

TGF-β1 has been shown to positively regulate expression of itself in a number of cells types, including a human embryonic lung fibroblast line (MRC5s) (Van Obberghen-Schilling *et al.*, 1988). TGF-β1 mRNA expression was upregulated at 3 hours following treatment with TGF-β1, with this upregulated expression still maintained at 18 hours. The same study also demonstrated the secretion of TGF-β1 protein by normal rat kidney (NRK) cells following treatment with TGF-β1. If uncontrolled, due to low levels of I-Smad for example, this cycle of positive regulation by TGF-β1 could easily lead to high levels of this cytokine in many organ systems, including the lung.

TGF-β1 is a highly profibrotic cytokine and has been shown to play important roles in the pathogenesis of IPF. TGF-β1 has been shown to be upregulated in epithelial cells and the sub-epithelial matrix in later stage IPF, the amount of TGF-β2 and β3, however, appears to be unaffected (Khalil *et al.*, 1996). It is important to note, however, that this study measured both latent and active TGF-β and therefore the proportion of active TGF-β present may vary from the total cytokine measured.

Khalil et al (Khalil *et al.*, 2001) observed detectable levels of active TGF-β1 in the BALF of IPF patients, whereas no active cytokine was observed in healthy control samples. Interestingly in the IPF patients, higher levels of active TGF-β1 were observed in BALF from the lower compared to upper lobes. This fits well with IPF disease progression, with the first clinical features of the disease appearing in the lower lobes of the lung, highlighting the role of TGF-β1 in the pathogenesis of IPF. The same authors observed decreased expression of TGFβR1 in all cells around areas of honeycomb cysts in IPF patients, except for interstitial fibroblasts that expressed both receptor types. As downstream processes mediated by TGFβR1 include decreased cell growth and increased ECM deposition, this reduced expression in epithelial cells around honeycomb cysts allows for proliferation and regeneration of this cell type. The co-expression of receptors on mesenchymal cells promotes ECM deposition; this differential expression in receptor levels in both cell types is likely to maintain the IPF lung in a constant repair state.

TGF-β exerts many of its profibrotic effects directly on fibroblasts; although this cytokine has been shown to inhibit proliferation of most cell types, including human AECs (Fjellbirkeland *et al.*, 2003), it actually induces proliferation in fibroblasts via the induction of fibroblast growth factor (FGF) -2 (Kay *et al.*, 1998; Strutz *et al.*, 2001). TGF-β1 also stimulates the release of PDGF and tumour necrosis factor (TNF)-α by monocytes (McCartney-Francis *et al.*, 1990), both of which are mitogenic for fibroblasts, hence further promoting proliferation. Proliferation of this cell type will inevitably lead to increased ECM deposition. Another mechanism by which TGF-β drives an increase in fibroblast population is via epithelial mesenchymal transition (EMT), TGF-β1 demonstrates the ability to induce EMT in rat (Willis *et al.*, 2005) as well as human (Kasai *et al.*, 2005) AECs, marked by an increase in α-smooth muscle actin (α-SMA) staining.

TGF-β not only promotes an increased population of fibroblasts, but also stimulates fibroblasts to increase ECM production, both TGF-β1 and β3 were shown to increase collagen production in HLFs (Eickelberg *et al.*, 1999), another study also demonstrated that TGF-β1 increased the expression of collagen I and fibronectin in human serosal fibroblasts (Mulsow *et al.*, 2005).

One study demonstrated the ability of both TGF-β1 and β3 to decrease MMP-1 and increase MMP-2 expression in HLFs (Eickelberg *et al.*, 1999). Both of these changes are important in driving a profibrotic state in the pulmonary environment, a decrease in MMP-1 production will lead to a reduction in collagen degradation, contributing to fibrosis. Collagen IV, an integral component of epithelial cell basement membrane is a known substrate for MMP-2 (Zeng *et al.*, 1999). Increases in the expression of this MMP is likely to cause high degradation of the basement membrane, and to trigger the wound healing response (see section 1.4.1). Repeated degradation of the basement membrane may lead to the dysregulated wound healing response observed in IPF, where the lung undergoes repeated cycles of damage and repair. Further research into the effects on MMP-1 expression also demonstrated a decrease in the expression of this MMP in response to TGF-β in human dermal fibroblasts (Yuan and Varga, 2001), this effect was also likely mediated by the Smad pathway.

The effects of TGF-β on MMP-1 expression, however, do appear to be controversial; in contrast to the findings in the two studies described above, Asano et al observed an increase in both MMP-1 and MMP-2 in response to TGF-β1 in HLFs (Asano *et al.*, 2010). An increase in MMP-1 may also be capable of promoting a fibrotic environment, as excess degradation of collagen I and III may lead to increased and dysregulated deposition of these collagens by fibroblasts, a feature which is characteristic of fibrosis. Also, as discussed in section 1.2.2, upregulation in MMP-1 expression in IPF may actually be responsible for honeycombing features of the disease, rather than the fibrosis itself.

The evidence supporting the increase in MMP-2 in response to TGF-β1 appears to be resounding, with further investigations supporting this finding in both human dermal (Lee *et al.*, 2010) and gingival (Overall *et al.*, 1989) fibroblasts. The induction of MMP-2 by TGF-β1 may play an important role in further activation of latent TGF-β1. Yu and Stamenkovic (Yu and Stamenkovic, 2000) observed that both membrane bound MMP-9 and MMP-2 have the ability to cleave and therefore activate latent TGF-β1. This suggests another positive feedback loop upon which TGF-β1 is able to cause further activation of itself and therefore drive a profibrotic environment. This finding also further demonstrates the profibrotic nature of MMP-2.

1.4 Fibroblasts

1.4.1 Fibroblasts in normal epithelial repair

It is thought that fibrogenesis associated with IPF is caused either by long-term exposure to tissue damaging irritants, or by dysregulation of the normal wound healing response (Wynn, 2011). In normal response to injury (shown in **Figure 1-5**) fibroblasts and circulating fibrocytes are recruited to the site of injury where many differentiate into myofibroblasts.

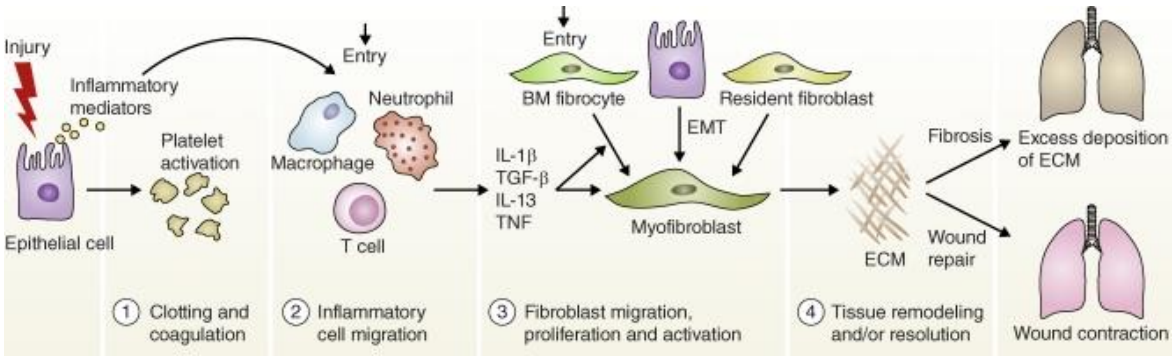

Figure 1-5. Wound healing response. Upon initial injury (1), leukocytes are recruited to the site of damage (2). These cells release a number of cytokines inducing fibroblast recruitment, proliferation and activation (3), activated myofibroblasts deposit extracellular matrix (ECM) (4), and then undergo apoptosis in healthy conditions. Failure to apoptose can lead to excess ECM deposition and fibrosis. (Wynn, 2011).

Myofibroblasts are the main cells responsible for the deposition of ECM components (fibronectin, collagen and proteoglycans etc). Myofibroblasts are contractile fibroblasts and once deposition of the ECM is complete, myofibroblasts contract this matrix, bringing healthy epithelial cells to the edge of the wound. These epithelial cells then migrate over the ECM forming a new monolayer before re-differentiating into a functional epithelium.

Upon ECM contraction in normal pulmonary conditions, β1 integrin on the fibroblast cell surface acts as a mechanoreceptor, inducing dephosphorylation of focal adhesion kinase (FAK), inactivating phosphotidylinositol 3-kinase (PI3K) and Akt and therefore initiating cell apoptosis (Xia *et al.*, 2004; Nho *et al.*, 2005), as depicted in **Figure 1-6**.

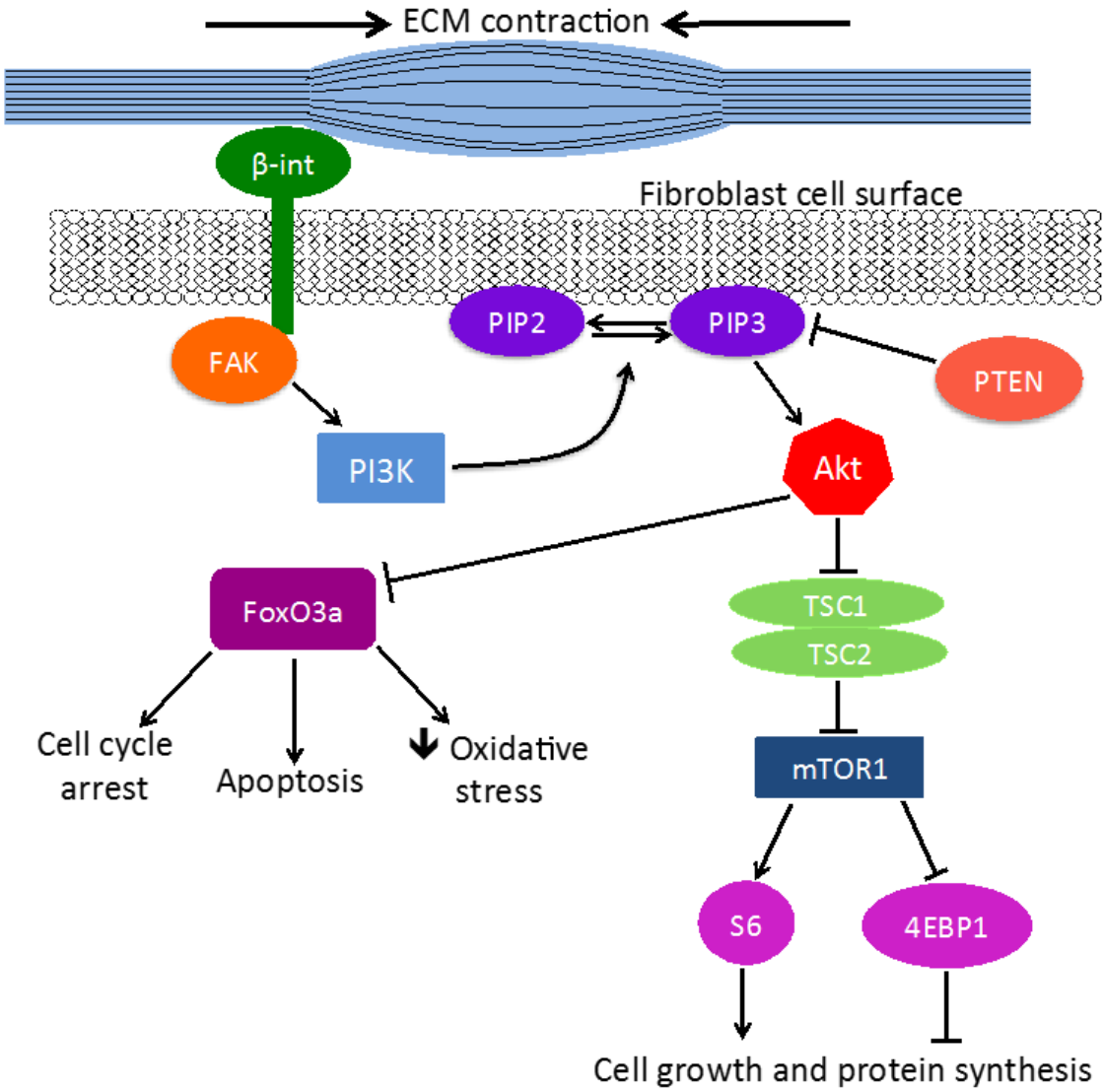

Figure 1-6. Intracellular signalling in fibroblasts important in ECM and β1 integrin interaction. β1 integrin interactions with ECM in either the contracted or non-contracted state induces differences in the phosphorylation of focal adhesion kinase (FAK) and eventually protein kinase B (Akt), initiating either apoptosis and cell cycle arrest via FoxO3a or cell proliferation and protein synthesis via mTOR1 signalling.

1.4.2 Fibroblasts in idiopathic pulmonary fibrosis

As mentioned briefly, patients with IPF have high number of fibroblasts within the lung, which accumulate in areas known as fibroblastic foci (**Figure 1-1**). As fibroblasts and myofibroblasts are responsible for the deposition of ECM, they are important cells in the progression of IPF disease, and are a widely studied cell population.

There are a number of factors that may influence this increased population of fibroblasts in the IPF lung. AECs from IPF patients have been shown to be susceptible to apoptosis (Guinee *et al.*, 1997); high alveolar cell death means higher numbers of fibroblasts are recruited to the site of damage to aid the normal repair response. These fibroblasts can be recruited, either from the circulation or from a resident fibroblast population in the lung. Another source of fibroblasts is from EMT, where differentiated epithelial cells undergo conversion into fibroblasts and myofibroblasts. EMT has been found to be an important process in IPF, and (as mentioned in section 1.3) TGF-β has been found to be a major inducer of EMT in a number of different tissues including the lung (Crosby and Waters, 2010). TGF-β is also thought to play other important roles in tissue repair such as activation of matrix formation, by increasing fibroblast expression of fibronectin and collagen (Sacco *et al.*, 2004). TGF-β also causes activation of FAK and Akt in fibroblasts (**Figure 1-6**), both of which are components of anti-apoptotic pathways (Horowitz and Thannickal, 2006). Myofibroblasts from IPF patients have also been shown to be resistant to FasL induced apoptosis (Moodley *et al.*, 2004).

As mentioned in section 1.4.1, once wound healing is complete, contraction of the ECM induces fibroblast apoptosis in normal pulmonary conditions. However, it has been shown recently that IPF cells are resistant to this mechanically induced apoptosis, due to unusually low levels of PTEN in turn leading to higher Akt activity (Nho *et al.*, 2013) and protection against apoptosis (**Figure 1-6**). Abnormalities in this pathway have also been shown to drive proliferation of IPF fibroblasts cultured on collagen I matrices (Nho *et al.*, 2011). These anti-apoptotic characteristics may lead to an excess population of fibroblasts in this patient group; however observations in this area vary, with fibroblasts from IPF lung shown to have a higher number of spontaneously apoptotic cells in culture (Ramos *et al.*, 2001).

Fibroblasts cultured from IPF lung have also been shown to have higher staining of the myofibroblast marker α-SMA than healthy fibroblasts (Ramos *et al.*, 2001; Moodley *et al.*, 2004; Bocchino *et al.*, 2010), providing further evidence for higher numbers of myofibroblasts in this patient population. As myofibroblasts are highly profibrotic, increased number of these cells is likely to lead to elevated collagen production by IPF fibroblasts compared to control cells, which has been confirmed in culture (Ramos *et al.*, 2001; Bocchino *et al.*, 2010).

Proliferation rates of fibroblasts from fibrotic human lung have also been shown to differ to those of HLFs (Raghu *et al.*, 1988), fibroblasts from patients with early fibrosis with alveolitis demonstrate highly upregulated growth rates compared to control, whereas growth of fibroblasts from densely fibrotic tissue was markedly impeded. Another investigation (Jordana *et al.*, 1988) also illustrated the difference between healthy and fibrotic lung fibroblasts, with

high rates of proliferation observed in the fibrotic phenotype. These fibroblasts were also taken from patients with early stage fibrosis (3-12 months since onset of symptoms). In contradiction to Jordana et al, Ramos et al (Ramos *et al.*, 2001) observed a reduced growth rate in fibroblasts from IPF lung, although the disease state in this patient population was likely to be progressed (22 ± 6 months after onset of symptoms). These observations indicate that the highly proliferative fibroblast phenotype may be responsible for driving the initial fibrotic response and disease progression, but may become less important in later, more fibrotic stages of the disease.

Interleukin (IL)-6, a cytokine involved in inflammation, is released by fibroblasts in response to a number of profibrotic substances, including TGF-β and PDGF. It has been demonstrated that IL-6 inhibits proliferation of HLFs, but is actually mitogenic for fibroblasts derived from IPF lung (Moodley *et al.*, 2003b). This again highlights the differences in the proliferative response between the two phenotypes. As TGF-β is upregulated in IPF lung, this is likely to induce IL-6 release from IPF fibroblasts, and hence further drive proliferation in this cell type. The same group (Moodley *et al.*, 2003a) also demonstrated differential effects of IL-6 on fibroblast apoptosis, with IL-6 enhancing Fas-induced apoptosis in HLFs and inhibiting this apoptosis in IPF derived fibroblasts. The effects of IL-6 on both proliferation and apoptosis are likely to contribute to the increased fibroblast population observed in the IPF lung.

It has also been demonstrated more recently, that the ECM in the pulmonary environment can have a direct effect on fibroblast function. Marinković et al (Marinković *et al.*, 2013) cultured both healthy and IPF fibroblasts on surfaces with varying stiffness that spanned the range of healthy and fibrotic lung matrix. Both fibroblast phenotypes demonstrated increasing basal proliferation rates on stiffer matrices, with HLFs proliferating at a much higher rate than IPF cells on these surfaces. The same study also illustrated increased contractile ability of both cell phenotypes on stiffer matrices (representative of later stage lung fibrosis), with IPF cells demonstrating higher contractile capability that healthy cells. This increased contractile ability is indicative of higher numbers of profibrotic myofibroblasts, although the levels of α-SMA were not investigated. Interestingly, no differences in fibroblast function were observed between the two phenotypes when cultured on the 'softer' matrices, representative of healthy lung parenchyma.

These results fit well with the proliferative differences observed between healthy and IPF fibroblasts discussed earlier. Increasing matrix stiffness (as observed in later stage IPF) appears to cause decreased proliferation and increased contractile function of IPF fibroblasts compared to healthy controls, indicating a higher proportion of the contractile myofibroblasts

phenotype in these cultures. These results indicate that the ECM itself may be responsible for promoting the IPF phenotype, creating a feedback loop, leading to progressive ECM deposition and worsening of disease.

Fibroblasts, more importantly myofibroblasts, are the main cells responsible for the deposition of ECM in response to epithelial injury, and play an important role in repairing and remodelling the pulmonary environment. These basic and very important functions of fibroblasts and their potential dysregulation in IPF, make these cells an interesting therapeutic target for the treatment of this disease.

1.5 Renin-angiotensin system

There are many processes that are abnormally regulated in the fibrotic lung; however, the factors responsible for initiating and driving these profibrotic mechanisms remain unknown. Peptides of the renin-angiotensin (RAS) system (primarily angiotensin (ANG) II) have recently been implicated in the pathogenesis of IPF; the RAS is discussed in more detail below.

1.5.1 Basic renin-angiotensin system

The RAS (depicted in **Figure 1-7**) is one of the most widely studied hormonal systems and plays an important role in the regulation of blood pressure, and fluid and electrolyte balance (Schwacke *et al.*, 2013). The primary precursor component of the RAS is angiotensinogen (AGT), this is an α2-globulin consisting of 452 amino acids (Eggena *et al.*, 1976). The 10 amino acid peptide ANG I, is cleaved from the N-terminus of AGT by renin (Schwacke *et al.*, 2013). Two further amino acids are cleaved from the C-terminal end of ANGI by ANG converting enzyme (ACE) or chymase to produce ANGII. ANGII is the most widely studied peptide of the RAS and is the endogenous ligand for both ANG receptor 1 and 2 (AT_1R and AT_2R respectively) (de Gasparo *et al.*, 2000).

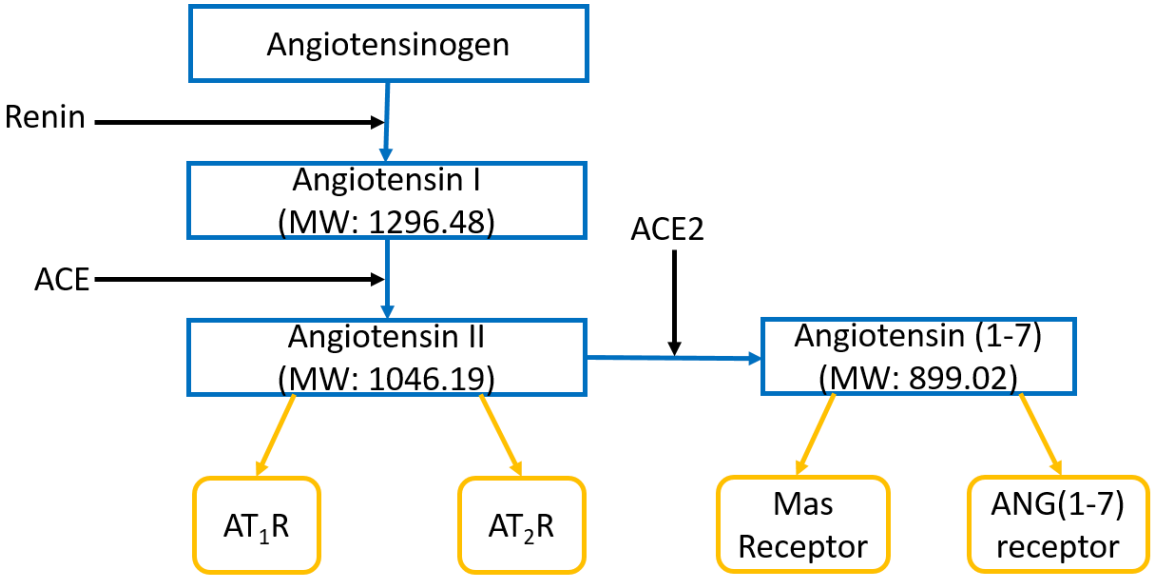

Figure 1-7. The basic renin angiotensin system. The enzymatic formation and molecular weights of the main angiotensin peptides, ANGI, ANGII and ANG(1-7) and their binding sites.

ANGII acts to cause vasoconstriction via binding to AT_1R and vasodilation via binding to AT_2R. ANGII also stimulates the adrenal cortex to release the hormone aldosterone, which causes reabsorption of sodium (and hence water) by the kidney, acting to increasing blood pressure (de Gasparo *et al.*, 2000). The enzyme ACE2 further cleaves ANGII to ANG(1-7) (Tipnis *et al.*, 2000) which is the endogenous ligand for the recently characterised G-protein coupled receptor (GPCR) Mas (Santos *et al.*, 2003b) (**Figure 1-7**). ANG(1-7) is a vasodilatory peptide, acting via Mas to oppose the effects of ANGII (Benter *et al.*, 1993).

1.5.2 Peptides and receptors of the renin-angiotensin system

The RAS peptide family consists of many more peptide fragments than the well known, ANGI, ANGII and ANG(1-7). Schwake et al (2013) detected 20 different peptide fragments that were composed of five or more amino acids, nine of which are shown in **Figure 1-8** (the peptides in colour indicate peptides that were investigated in the current study). The authors also proposed that ACE, ACE2, chymase, neprilysin (NEP), and aminopeptidases (AP) A and N are the main proteolytic enzymes responsible for the breakdown of ANG peptides.

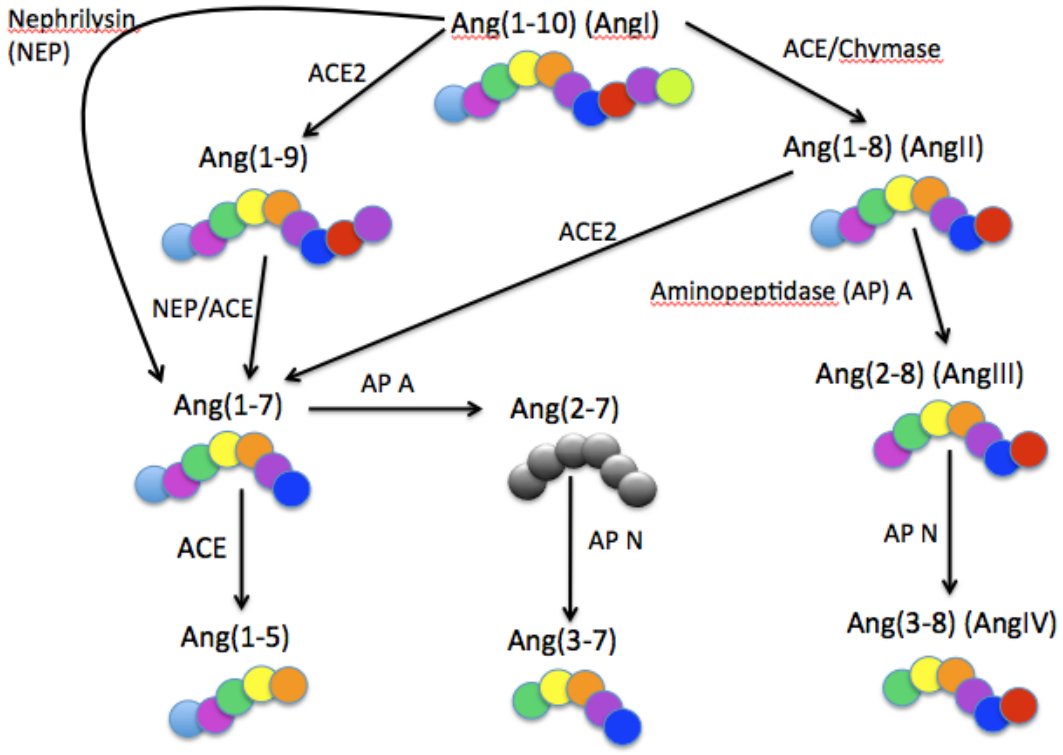

Figure 1-8. ANGII and related peptides. Diagram showing the enzymatic formation of ANGII and related peptides, adapted from (Schwacke *et al.*, 2013). ACE – Angiotensin converting enzyme, NEP – Neprilysin, AP – Aminopeptidase, ○ = Aspartic acid, ● = arginine, ● = valine, ● = tyrosine, ● = isoleucine, ● = histidine, ● = proline, ● = phenylalanine, ● = leucine.

As mentioned previously, ANGII is cleaved to ANG(1-7) by ACE2. Another substrate for ACE2 is ANGI, with one amino acid cleaved to form ANG(1-9), ANG(1-9) itself is then cleaved by ACE to form ANG(1-7) (Donoghue *et al.*, 2000), providing an alternative pathway for the production of this peptide. As mentioned above, ANG(1-7) acts via the Mas receptor to oppose the effects of ANGII. This is not the only mechanism by which ANG(1-7) opposes the actions of ANGII, ANG(1-7) is also a substrate for ACE and therefore competes with ANGI. ANG(1-7) has been shown to completely inhibit ACE in human plasma and atrial tissue (Roks *et al.*, 1999), which would lead to reduced ANGII production and thus prevent increases in blood pressure. ACE also degrades bradykinin, a vasodilatory peptide, therefore ANG(1-7) can also compete with this peptide, prolonging its presence in the blood and enhancing its vasodilatory properties (Tom *et al.*, 2001).

Other peptides derived from ANGI include ANGIII, ANGIV, ANG(3-7) and ANG(1-5); the circulating plasma concentrations for most of these peptides can be found in **Table 1-3**. Of the nine peptides depicted above, most have been shown be biologically active. Although ANG(1-5) is widely regarded to be biologically inactive (Schwacke *et al.*, 2013), this peptide has been

shown to inhibit ACE with similar potencies to that of ANGI (Roks *et al.*, 1999). However, ANG(1-5) did not affect arterial contractions in the same investigation.

Peptide	**Human plasma concentration (pM)**
ANGI (1-10)	19.5±2.4 – 304±43
ANGII (1-8)	13.9±2.0 - 32±6.0
ANGIII (2-8)	2.9±1.0
ANGIV (3-8)	>30
ANG(1-7)	1.0±0.2
ANG(1-9)	<2.1

Table 1-3. Circulating plasma concentrations of angiotensin peptides. Values from normotensive male subjects (Lawrence *et al.*, 1990; Matsui *et al.*, 1999).

ANGII is well known to bind to AT_1R and AT_2R; these receptors are class A (rhodopsin like) GPCRs (Oliveira *et al.*, 2007) with about 30% sequence identity (Kambayashi *et al.*, 1993; Hunyady *et al.*, 2000). However, despite similarities in their basic structures, these two receptors have been shown to act differently upon agonist binding. AT_1R is rapidly internalised, whereas AT_2R remains on the cell surface (Thomas *et al.*, 1996). Upon binding of ANGII to AT_1R the main signalling pathway is activation of phospholipase C (PLC), initiating inositol phosphate responses and hence generating intracellular Ca^{2+} release (**Figure 1-9**). AT_1R also activates further intracellular signalling pathways such as stimulation of tyrosine kinase and the JAK-STAT pathway; whereas AT_2R binding stimulates tyrosine phosphatases and causes apoptosis (Hunyady *et al.*, 2000).

The binding characteristics of ANGII to AT_1R are fairly well characterised, with Tyr^4 and Phe^8 important in both binding and agonistic properties of ANGII, by interacting with Asp^{111} and His^{256} of AT_1R respectively (Miura *et al.*, 1999). The COOH terminal end of ANGII has been shown to be essential for binding of this peptide, with ANG(5-8) shown to be the smallest COOH terminal peptide to demonstrate inhibitory effects against ^{125}[I]-ANGII (Capponi and Catt, 1979). The same study also showed that in order to stimulate release of aldosterone from canine adrenal medulla cells, Tyr^4 was also required, demonstrating the need for this amino acid in the activation of AT_1R. Asp^1 does not appear to be required for the activation of AT_1R as the COOH terminal peptide ANG(2-8) exhibited similar binding affinities for AT_1R, and was also capable of stimulating aldosterone release in a similar manner to ANGII.

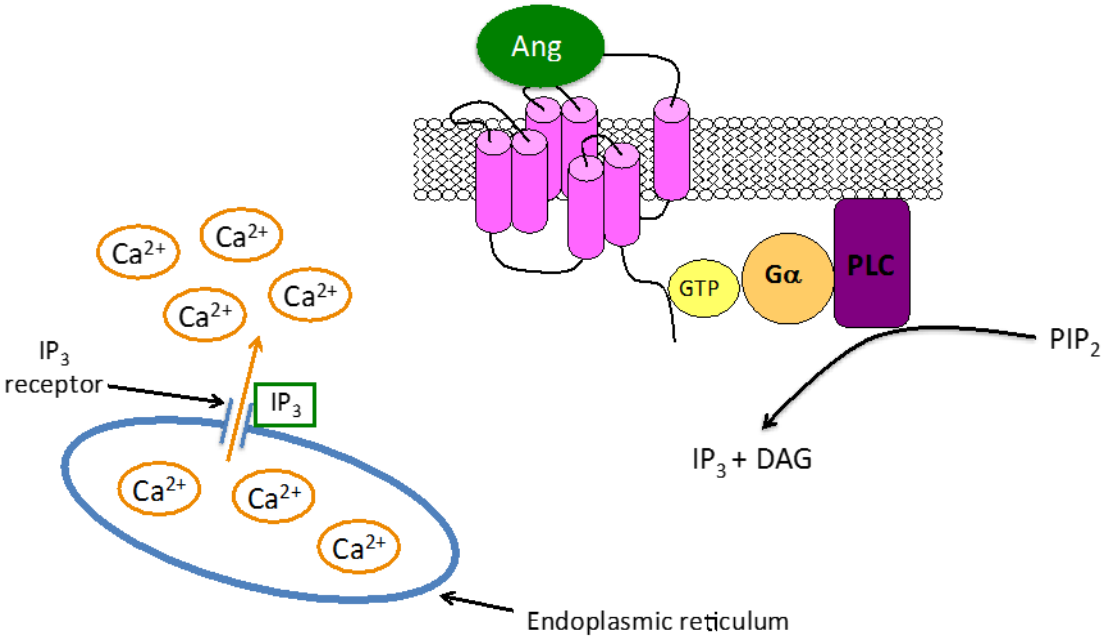

Figure 1-9. The signalling pathway involved in intracellular calcium release. Upon binding of ANGII to AT_1R, phospholipase C (PLC) is activated and cleaves phosphatidylinositol-4,5-bisphosphate (PIP_2) to form inositol 1,4,5-trisphospate (IP_3) and diacyl glycerol (DAG). IP_3 then binds to IP_3 sensitive calcium channels on the smooth endoplasmic reticulum (ER) surface to allow influx of calcium into the cell cytosol.

ANG(2-8) (otherwise known as ANGIII), produced by cleavage of ANGII, is another relatively important peptide of the RAS. This peptide has been shown to have comparable functions to ANGII, with elevated blood pressure and increased aldosterone release observed in humans following ANGIII infusion (Suzuki *et al.*, 1984). ANGIII also has a similar affinity to ANGII for both AT_1R and AT_2R (Bosnyak *et al.*, 2011). **Table 1-4** lists the affinities of ANGII, ANGIII, ANGIV and ANG(1-7) for different ANG receptors.

Peptide	**AT_1R**	**AT_2R**	**AT_4R**	**Mas**
ANGII	7.92×10^{-9}	5.22×10^{-10}	1.10×10^{-5}	5.33×10^{-8}
ANGIII	2.11×10^{-8}	6.48×10^{-10}	N/A	4.52×10^{-7}
ANGIV	$>1 \times 10^{-5}$	4.68×10^{-8}	2.40×10^{-8}	1.24×10^{-6}
ANG(1-7)	$>1 \times 10^{-5}$	2.46×10^{-7}	0.80×10^{-5}	6.90×10^{-9}

Table 1-4. Affinity of different angiotensin peptides at angiotensin receptors. All data shown are IC_{50} values from competitive binding studies (Handa, 2000; Santos *et al.*, 2003a; Bosnyak *et al.*, 2011).

Specific ligand/receptor amino acid interactions responsible for ligand binding can be identified using the methionine proximity assay (MPA), where site-directed mutagenesis replaces specific amino acids in the receptor structure with a methionine (Met) residue. One

amino acid of the peptide of interest (usually Val^3 in the case of ANGII) is also replaced with *p*-benzoyl-l-phenylalanine (Bpa) to produce a photoreactive radiolabelled peptide (^{125}I-Sar^1Bpa^3-ANGII). Bpa has been shown to have high selectivity towards binding Met residues within physical proximity. Proteolytic cleavage of this Met residue with cyanogen bromide causes detectable release of the radiolabelled peptide, and thus confirms binding of the peptide to this residue, establishing this site as a ligand contact point. This method has been adopted by Fillion et al, who have shown there to be at least 38 ligand/receptor contact points between ANGII and AT_1R. The authors used these results together with 15 ligand/receptor contact points already determined by previous MPA studies, to perform homology modelling (Fillion *et al.*, 2013). The amino acid sequence of AT_1R was fit to GPCR crystal structure templates of bovine rhodopsin, human β_2-adrenergic receptor and human chemokine receptor type 4 (CXCR4). Results from this showed extracellular loop 2 in AT_1R to be important in the binding of ANGII. A β-hairpin fold in this extracellular loop, together with two disulphide bridges, is responsible for opening and shaping the ligand binding site (Fillion *et al.*, 2013). The authors also observed that ANGII adopted a vertical binding mode, allowing for multiple contacts along the extracellular surface, as well as within the transmembrane domain of the receptor. Another earlier study investigating the binding of ANGII to AT_1R with MPA demonstrated Ile^{172} in transmembrane domain 7 of AT_1R as a ligand contact point (Boucard *et al.*, 2000). This further confirms the 'extended' structure of ANGII when binding AT_1R, with contact points spanning from extracellular loop 2, to transmembrane domain 7.

Further publications using conventional x-ray crystallography and site-directed mutagenesis, investigated the binding of ANGII and the AT_1R inverse agonist olmesartan to AT_1R (Zhang *et al.*, 2015a). Tyr^{35}, Trp^{84} and Arg^{167} of AT_1R were shown to be essential for the binding of both olmesartan and ANGII. Displacement of [^{125}I]-olemartan from different AT_1R mutants by other AT_1R inhibitors such as candesartan and telmisartan demonstrated that these ligand/receptor contact points were conserved amongst all the inhibitors tested. The same group also studied the binding of the AT_1R antagonist ZD7155 by crystallography in another publication (Zhang *et al.*, 2015b). This antagonist was also shown to adopt a similar binding mode to olmesartan, with the binding pocket for both compounds consisting of residues from all seven transmembrane domains, as well as from extracellular loops one and two, further demonstrating a conserved binding pocket for AT_1R antagonists.

There is also evidence to support the existence of an AT_4 receptor, AT_4R is a transmembrane insulin-regulated aminopeptidase (IRAP). ANGIV is thought to be the main ligand for AT_4R, with this peptide causing vasodilation via this receptor (Patel *et al.*, 1998). ANG(3-7) has also been shown to bind to this receptor with relatively high affinity (Handa, 2000). AT_4R

expression has been shown in many physiological systems such as the heart, kidneys and on vascular smooth muscle (Paul *et al.*, 2006), expression has also been illustrated in porcine pulmonary aortic endothelial cells, indicating a presence of this receptor in the lung (Patel *et al.*, 1998).

The actions of ANG(1-9) have been more recently investigated, and this peptide has been shown to exert functions that potentially oppose those of ANGII. Cha et al (Cha *et al.*, 2013) found that ANG(1-9) induced atrial natiuretic peptide release in isolated rat atria via AT_2R, implicating the importance of ANG(1-9) in vasodilation. ANG(1-9) has also been shown to protect against hypertrophy in cardiomyocytes, again via AT_2R (Flores-Muñoz *et al.*, 2011), further demonstrating the protective effects of this peptide.

As mentioned previously, the Mas receptor has recently been characterised as an endogenous receptor for ANG(1-7). Gironacci et al (Gironacci *et al.*, 2011) investigated the early fate of the Mas receptor upon binding by ANG(1-7). This group demonstrated both a time and dose dependent reduction in receptor sensitivity to ANG(1-7), indicating internalisation of the Mas receptor. In an agonist free environment, Mas was mostly located on the cell membrane and the endoplasmic reticulum of human embryonic kidney (HEK)-293T cells, but began to relocate to intracellular vesicles within five minutes of stimulation with 1μM ANG(1-7). By 10 minutes, half of the Mas receptor had undergone endocytosis with this effect partially inhibited by the Mas antagonist A-779.

There is also emerging evidence to suggest that a second ANG(1-7) receptor subtype exists. In the aorta of Sprague-Dawley rats it was demonstrated that the vasodilatory effects of ANG(1-7) were not inhibited by the addition of A-779; this vasodilatory effect was, however, blocked by the addition of D-Pro^7-ANG(1-7). This indicates that D-Pro^7-ANG(1-7) and A-779 are acting on two separate receptor populations, and that ANG(1-7) was causing vasodilation via a receptor population separate from the Mas receptor (Silva *et al.*, 2007). Another study looking at hepatic perfusion pressure in rats, showed inhibition of ANGII induced increases in perfusion pressure in the presence of ANG(1-7). This vasodilatory effect of ANG(1-7) was once again inhibited by D-Pro^7-ANG(1-7) but not A-779, indicating a novel receptor population for ANG(1-7) (Herath *et al.*, 2013), although this effect is currently rodent specific and has not yet been documented in humans.

This separate ANG(1-7) receptor population could be attributed to Mas-related G protein-coupled receptor member D (mrgD). ANG(1-7) has been shown to activate this receptor in transfected COS (fibroblast like cells) and HEK293 cells (Gembardt *et al.*, 2008). Other more novel members of the RAS peptide family have also been shown to bind to mrgD. Alamandine, a peptide very similar in structure to ANG(1-7), has been shown to have similar effects to

ANG(1-7) upon binding to mrgD (Lautner *et al.*, 2013). The only difference between these two peptides is the replacement of the N-terminal alanine in ANG(1-7) with an aspartate residue. Lautner et al demonstrated a relaxation in mouse aortic rings in response to both ANG(1-7) and alamandine. Interestingly the relaxation in response to ANG(1-7) was inhibited by both A-779 and D-pro^7-ANG(1-7), but the response to alamandine was only inhibited by D-pro^7-ANG(1-7). The role of mrgD in these alamandine induced effects was confirmed by binding studies with fluorescently labelled alamandine. Binding was observed in mrgD transfected CHO cells that was blocked by both D-pro^7-ANG(1-7) and β-alanine, which is a known agonist for mrgD (Milasta *et al.*, 2006). The results from this study indicate that ANG(1-7) is able to bind both Mas and mrgD to induce vasorelaxation and that alamandine is only capable of binding to mrgD to induce the same effects.

Alamandine is known to be formed by two distinct mechanisms, one is the direct decarboxylation of the ANG(1-7) N-terminal alanine. The other is by cleavage of another novel ANG peptide, ANG A, by ACE2. Both of these mechanisms were demonstrated in the Lautner et al study described above. ANG A is a peptide similar in structure to ANGII, with the N terminal alanine replaced with an aspartate molecule, the same difference that is observed between ANG(1-7) and alamandine. ACE2 can cleave the C-terminal phenylalanine of ANG A to form alamandine.

The presence of ANG A in human serum was first reported by Jankowski et al (Jankowski *et al.*, 2007). The formation of this peptide was shown to be via decarboxylation of Ala^1. ANG A was also shown to cause vasocontriction in isolated rat kidney (although at a lower level to that observed with ANGII), via AT_1R dependent mechanisms. This peptide has also been shown to cause increases in blood pressure in Wistar rats, in similar manner to ANGII. The effects of both of these peptides on blood pressure were blocked by the AT_1R antagonist losartan (Coutinho *et al.*, 2014).

1.5.3 Inhibitors of the renin angiotensin system.

1.5.3.1 Angiotensin receptor 1 antagonists

As AT_1R is an extremely important receptor involved in vasoconstriction and blood pressure regulation, many AT_1R receptor antagonists are clinically available for the treatment of hypertension. This class of drugs all share the common suffix 'sartan' and there are many available compounds in this family, such as losartan, olmesartan and candesartan.

Telmisartan is another member of this class, and is the AT_1R antagonist chosen for use in the current investigation. Telmisartan is a potent antagonist, preventing binding of [^{125}I]-ANGII to

intact rat VSMCs with an IC_{50} of 9.2 ± 0.8 x10^{-9} M. An even higher potency for AT_1R was observed in VSMC membrane preparations, with an IC_{50} of 2.9 ± 0.5 x10^{-9} M. [H^3]-telmisartan was also shown to reach equilibrium with AT_1R approximately one hour after addition to intact rat VSMCs (Maillard *et al.*, 2002).

Telmisartan demonstrates a clear competitive profile when added simultaneously with a competing agonist (such as ANGII), with a clear rightward shift in the ANGII dose response curve observed in the presence of telmisartan. However, telmisartan also demonstrates insurmountable antagonism, causing a reduction in the maximal response to ANGII and this occurs when cells are preincubated with the antagonist prior to ANGII addition. This insurmountable antagonism appears to be due, at least in part, to slow dissociation of telmisartan from AT_1R, with a dissociation half-time of approximately 75 mins. The addition of other competing agonists (ANGII) or antagonists (candesartan, losartan) did not affect this dissociation half-time. (Maillard *et al.*, 2002).

Telmisartan was shown to specifically antagonise AT_1R in rat lung tissue preparations against [^{125}I]-ANGII, losartan was also shown to cause complete displacement of the radioligand in these preparations, whereas the AT_2R antagonist PD-123319 (discussed below) had no effect. In contrast, neither telmisartan nor losartan inhibited [^{125}I]-ANGII binding to rat adrenal medulla tissue preparations, but PD-123319 caused complete inhibition of radioligand binding. These results show that telmisartan does not antagonise AT_2R (Wienen *et al.*, 1993). Telmisartan was also shown in the same study to have no effect on either renin or ACE activity.

1.5.3.2 Angiotensin receptor 2 antagonists

AT_2R is less clinically exploited than AT_1R and therefore few characterised antagonists are targeted to this receptor. One available antagonist for this receptor is PD-123319 (also named EXP655), one of the first studies investigating the selectivity of this non-peptide compound was performed by Chiu et al, in the rat adrenal cortex (Chiu *et al.*, 1989). EXP655 (as this compound was currently known at the time) was shown to inhibit 20% of the binding of [^{125}I]-ANGII, while Dup753 (AT_1R antagonist) blocked 80% of [^{125}I]-ANGII binding, indicating these compounds were acting on two distinct receptor sites. Further experiments performed in rat adrenal medulla showed that EXP655 blocked 90% of [^{125}I]-ANGII binding with an IC_{50} of 3 x 10^{-8}M.

EXP655 was also synthesised in 1991 by Blankley et al (Blankley *et al.*, 1991), who renamed this compound PD-123319 (as it is mostly known today). Following the blocking of AT_1R, PD-123319 was shown to antagonise binding of ANGII to the remaining receptor population with

an IC_{50} of 3.4 x 10^{-8}M. This was a similar value to that obtained by Chiu et al above. This compound was also shown to have no antagonistic effects on other receptor systems such as α1 or α2 adrenergic receptors, dopamine or muscarinic receptors. Most importantly, PD-123319 did not demonstrate any inhibitory actions against ACE. PD-123319 also did not inhibit ANGII induced contractions in rabbit aortic preparations, indicating that this compound has no antagonistic effects on AT_1R.

1.5.3.3 Mas receptor antagonists

The Mas receptor was defined as a receptor for ANG(1-7) fairly recently in 2003 (Santos *et al.*, 2003b). Prior to this discovery, work from the same group also characterised a specific antagonist against ANG(1-7) (Santos *et al.*, 1994), this antagonist was d-ala^7-ANG(1-7), or as it is better known, A-779. This antagonist was shown to inhibit many of the *in vivo* effects of ANG(1-7), such as antidiuretic effects and changes in blood pressure. Also, A-779 did not significantly compete with [^{125}I]-ANGII in adrenal cortical membrane preparations, even at a concentration of 1μM. A-779 also did not affect contractile effects of ANGII, bradykinin or substance P in rat ileum. Indicating that this antagonist is extremely selective for ANG(1-7) (Santos *et al.*, 1994).

In Mas transfected CHO cells, A-779 was shown to antagonise binding of [^{125}I]-ANG(1-7) with an IC_{50} of 0.3nM in whole cell preparations. Neither AT_1R or AT_2R antagonists (CV-11974 or PD-123319 respectively) competed with [^{125}I]-ANG(1-7) for the Mas receptor (Santos *et al.*, 2003b). More recent studies have further demonstrated the lack of affinity of A-779 for both AT_1R and AT_2R, with minimal displacement of the non-specific antagonist [^{125}I]-Sar^{1}Ile^8-ANGII from HEK293 cells transfected with either receptor. IC_{50} values of greater than 1 x 10^5 M were reported for A-779 against both receptor types (Bosnyak *et al.*, 2011).

1.5.3.4 Angiotensin converting enzyme inhibitors

Angiotensin converting enzyme (ACE) is important for the endogenous production of ANGII and is therefore another important therapeutic target for the treatment of hypertension. There are many clinically available ACE inhibitors that belong to the drug family with the common suffix 'pril'. Compounds from this class include lisinopril, enalapril and ramipril.

The ACE inhibitor chosen for use in the current investigation is captopril. Captopril has been shown to inhibit ACE activity with an IC_{50} of 16.71μM when the competing substrate is ANGI (Ben Henda *et al.*, 2013). Captopril has also been shown to inhibit binding of another inhibitor (ramiprilat) to ACE in a number of rat tissues, with the IC_{50} of captopril ranging from 2.86 ± 0.22 x10^7 M (rat lung) to 10.85 ± 2.96 x10^7 M (rat kidney cortex) (Grima *et al.*, 1991).

Captopril also exerts many actions that are RAS independent. ACE is also known to degrade bradykinin (Hornig *et al.*, 1997), therefore some of the vasodilatory effects of ACE inhibitors (such as captopril) have been attributed to the prolonged vasodilatory effects of bradykinin via binding to the B_2-receptor. Captopril has also been shown to inhibit prolidase (Ganapathy *et al.*, 1985), an enzyme important in collagen resynthesis. Captopril has been shown to inhibit rat prolidases with a K_i (inhibitory constant) of 25-35μM (Ganapathy *et al.*, 1985). Human skin fibroblasts deficient in prolidase have been shown to have impaired collagen production (Dolenga and Hechtman, 1992).

1.6 Angiotensin peptides in the pathogenesis of IPF

There is a large body of evidence indicating the existence of a local RAS in the pulmonary environment. High expression of the two main RAS enzymes ACE and ACE2 has been demonstrated in the lung. ACE is highly expressed in the alveolar capillary endothelium (Orte *et al.*, 2000), and ACE2 expression has been illustrated in both airway epithelium and parenchyma (Jia *et al.*, 2005). The presence of locally expressed ACE is likely to lead to high concentrations of ANGII, which when coupled with high pulmonary ACE2 expression could lead to increased levels of ANG(1-7) and related peptides within the lung. High levels of RAS peptides could feasibly affect the pathogenesis of many lung diseases including IPF. Differential expression levels of these enzymes may also play important roles in the pathogenesis of IPF, Li et al (Li *et al.*, 2008) demonstrated a 92% and 74% reduction in levels of ACE2 mRNA and enzyme activity respectively in IPF derived lung tissue, which is in turn likely to drive increased levels of ANGII in the lungs of these patients.

1.6.1 Angiotensin II

The profibrotic characteristics of ANGII and its potential role in the pathogenesis of IPF have been widely explored. Much of the evidence available for ANGII in IPF comes from *in vivo* systems; elevated ACE levels in the BALF from IPF patients has been demonstrated (Specks *et al.*, 1990), which could feasibly lead to increased levels of ANGII in these patients (**Figure 1-7**). Molteni et al (Molteni *et al.*, 2007) also determined that two ACE inhibitors (captopril and lisinopril) attenuated radiation induced pulmonary fibrosis in rats. Captopril has also been shown to reduce AEC apoptosis and fibrosis in the bleomycin rat model of pulmonary fibrosis (Wang *et al.*, 2000).

Further to ACE inhibitors, there is a large body of evidence demonstrating that AT_1R antagonists such as candesartan (Otsuka *et al.*, 2004) and losartan (Yao *et al.*, 2006) also

attenuate bleomycin induced pulmonary fibrosis. Waseda et al (Waseda *et al.*, 2008) not only confirmed that AT_1R antagonists protect against bleomycin induced fibrosis, but also indicated a similar role for AT_2R antagonists, with PD-123319 reducing lung fibrosis in a similar manner to the AT_1R antagonist olmesartan. Lung samples obtained from IPF patients also showed an upregulation in both AT_1R and AT_2R mRNA levels when compared to healthy donor tissue, further indicating a role for these receptors in IPF disease progression (Königshoff *et al.*, 2007).

Although the benefit of blocking both ANGII production and its receptor mediated effects is evident, there is little investigation into the individual profibrotic mechanisms exerted by this peptide *in vivo*. However, there are a number of *in vitro* studies investigating the effects of ANGII on individual cell types, most notably, the pulmonary fibroblast.

ANGII has been shown to induce proliferation in HLFs and mouse lung fibroblasts (Marshall *et al.*, 2000; Königshoff *et al.*, 2007). Marshall et al also suggested that this increase in cell proliferation was at least in part due to ANGII induced TGF-β. This idea that ANGII may increase TGF-β expression in HLFs was more recently confirmed (Uhal *et al.*, 2007), and it was also determined, by addition of a TGF-β1 neutralising antibody, that this cytokine was capable of reducing fibroblast AGT expression. These results may indicate an autocrine feedback loop involving TGF-β1 and ANGII. It was also confirmed that the mitogenic effect of ANGII on HLFs was via AT_1R, demonstrated by the addition of losartan (Marshall *et al.*, 2000). Another study also observed a link between ANGII and TGF-β1 release, this time in rat cardiac fibroblasts (Lee *et al.*, 1995). Treatment with ANGII increased TGF-β1 mRNA levels by four hours that was maintained to at least 24 hours, also active TGF-β1 release by fibroblasts in response to ANGII was not only detected but also neutralised by TGF-β1 antibody.

ANGII has also been shown to induce collagen synthesis in HLFs, and this was again shown to be via binding to AT_1R (Marshall *et al.*, 2004), the same study also confirmed this *in vivo*; ANGII levels in rat lung were elevated in response to bleomycin, correlating with an increase in lung collagen production. Ramipril and losartan both significantly reduced these ANGII and lung collagen levels. This ability of ANGII to increase collagen production both *in vitro* and *in vivo* again appears to be at least partially due to TGF-β1 activation (Marshall *et al.*, 2004). The evidence for the effects of ANGII on HLFs is limited; however, many of the profibrotic actions of ANGII have been extensively studied in human cardiac fibroblasts (HCFs). As with the previous study in HLFs, ANGII has been shown to induce collagen synthesis in HCFs in a number of studies (Hafizi *et al.*, 1998; Chen *et al.*, 2004), with this being demonstrated as an AT_1R dependent response (Hafizi *et al.*, 1998; Hafizi *et al.*, 2004). The observed effect of ANGII on HCF proliferation *in vitro* appears to be highly variable, ANGII was shown to induce protein synthesis in HCFs via AT_1R but to have no effect on DNA synthesis or cell number (Hou *et al.*,

2000), indicating that ANGII has no effect on fibroblast proliferation. This observation was supported by further studies; Hafizi et al (Hafizi *et al.*, 2004) showed that whilst ANGII induced a dose-dependent increase in collagen production, fibroblast proliferation was unaltered. However, in a number of other studies, ANGII has been shown to increase fibroblast proliferation (Agocha *et al.*, 1997; Kawano *et al.*, 2000). The variability in the response to ANGII is likely due to the difficulty in reproducing the *in vivo* environment, as cells cultured on plastic are likely to behave in a different manner to those cultured in 3D matrices such as collagen gel.

Another cell type on which the effects of ANGII have been well characterised is the AEC. As mentioned earlier, one of the main driving forces of IPF disease progression is thought to be AEC apoptosis, causing a constant activation of the wound healing response and hence increased ECM production.

Captopril has been shown to inhibit Fas-induced apoptosis in human AECs (Uhal *et al.*, 1998), further investigations demonstrated that ACE inhibitors blocked AGT induced apoptosis but had no effect on apoptosis induced by purified ANGII (Wang *et al.*, 1999). As ACE is a key enzyme involved in the production of ANGII from AGT and is blocked by captopril, these observations clearly indicate that the production of ANGII plays an important role in this apoptotic pathway. Additional research from the same laboratory demonstrated that the ANGII driven apoptosis was purely mediated by AT_1R (Papp *et al.*, 2002), with complete inhibition of the apoptotic response observed in the presence of losartan.

Further evidence to suggest ANGII is involved in IPF disease progression comes from the comparative studies between healthy and IPF lung tissue and fibroblasts. Uhal et al (Uhal *et al.*, 2007) demonstrated that IPF derived fibroblasts expressed AGT and TGF-β1 mRNA, at higher levels than HLFs. IPF fibroblasts also produced higher levels of AGT, ANGII and TGF-β1 protein, suggesting an upregulation of RAS activity in this cell population.

1.6.2 Angiotensin(1-7)

In contrast to ANGII, ANG(1-7) has been shown to exhibit antifibrotic properties, with a number of *in vivo* studies providing evidence of the protective functions of ANG(1-7). Shenoy et al (Shenoy *et al.*, 2010) demonstrated an abrogation of bleomycin induced pulmonary fibrosis, in rats treated intratracheally with either ANG(1-7) or ACE2 lentiviral delivered genes. ANG(1-7) has also been shown to protect against fibrosis caused by lipopolysaccharide induced lung injury (Chen *et al.*, 2013), and that this protective effect was generated via binding to the Mas receptor. These antifibrotic effects of ANG(1-7) were likely to be, at least in part, due to altered TGF-β signalling as decreased levels of this cytokine were observed in ANG(1-7) treated animals. This study, amongst others have shown that ANG(1-7) not only protects

against the fibrotic response caused by lung injury, but also against acute lung injury (ALI) itself.

The observation that ANG(1-7) is capable of modulating TGF-β signalling has been confirmed in the *in vitro* setting. Morales et al (Morales *et al.*, 2014) showed an increase in TGF-β mRNA expression in mouse myoblasts in response to ANGII, they also demonstrated that ANG(1-7) was capable of inhibiting this increased TGF-β expression and that this was via the Mas receptor. A second study also showed the inhibitory effects of ANG(1-7) on both TGF-β mRNA expression and secretion of active cytokine in rat proximal tubular NEK-52E cells, a reversal in this inhibitory activity of ANG(1-7) was observed in the presence of the Mas antagonist A-779 (Chou *et al.*, 2013).

As with ANGII, there are a number of studies investigating the effects of ANG(1-7) on fibroblasts. However, most studies exploring these effects of ANG(1-7) have been performed in rat cardiac fibroblasts, with an extremely limited number of investigations in human fibroblasts. ANG(1-7) has been shown to decrease foetal calf serum (FCS) induced proliferation and collagen production in rat fibroblasts (McCollum *et al.*, 2012). The authors also concluded that ANG(1-7) inhibited proliferation via the Mas receptor (by the addition of A-779); however, the mechanism by which collagen synthesis was inhibited was not investigated. A second study in rat cardiac fibroblasts (Iwata *et al.*, 2005) again illustrated the antifibrotic effects of ANG(1-7), this peptide was shown not only to reduce baseline collagen production (in the absence of serum), but also to inhibit ANGII induced collagen synthesis in this cell type. This group also investigated the binding of [^{125}I]-ANG(1-7) to rat cardiac fibroblasts and found a receptor density of 131 fmol/mg, this population was likely to be the Mas receptor as specific binding was displaced by A-779 and by increasing concentrations of ANG(1-7).

1.6.3 Related peptides

There is limited information on the potential roles of other ANG peptides in the pathogenesis of IPF. As mentioned in section 1.5.2, ANG(1-9) has been shown to have opposing effects to ANGII in a number of systems via binding to AT_2R. Antifibrotic actions of ANG(1-9) have also been demonstrated in rat cardiac fibroblasts (Flores-Munoz *et al.*, 2012), with decreased proliferation and downregulation of collagen I mRNA observed in the presence of this peptide. Both of these ANG(1-9) mediated effects were blocked by the addition of PD-123319, indicating that this peptide was again acting via AT_2R.

ANGIII has been shown to upregulate TGF-β gene expression and to increase production of the ECM component fibronectin in rat kidney fibroblasts (Ruiz-Ortega *et al.*, 1998). This may

suggest a profibrotic role of ANGIII, although this remains relatively unexplored. This peptide has been shown to behave in similar manner to ANGII in a number of systems, causing increased blood pressure and aldosterone release in humans (discussed in section 1.5.2), as well as demonstrating similar affinities for AT_1R and AT_2R. These similarities with ANGII, indicate that ANGIII is likely to have a similar role in IPF pathogenesis.

Proliferative effects of ANGIV have been demonstrated in rabbit cardiac fibroblasts (Wang *et al.*, 1995), with increases in DNA and RNA synthesis observed in the presence of this peptide. The same group has also demonstrated the presence of AT_4R in this cell type. In contrast to these results, Marshall et al (Marshall *et al.*, 2000) found no proliferative effect of ANGIV in a study on a human foetal fibroblast cell line (HFL-1). Although as the latter study was not performed in primary cells, care needs to be taken not to over compare these results.

Currently, investigations into the effects of ANG(1-5) and ANG(3-7) on fibroblasts are limited. Also none of the studies discussed in this section were performed in primary human fibroblasts, or in pulmonary fibroblasts. This indicates a need for more research in this area to determine the potential effects, if any, of these peptide fragments in the pathogenesis of IPF.

1.6.4 Clinical Evidence for the role of the RAS in IPF

The clinical evidence for the effectiveness of RAS manipulation in IPF is limited, one small clinical trial (Couluris *et al.*, 2012) indicated that the AT_1R antagonist losartan stabilised lung function (% predicted forced vital capacity) in 12 of 17 IPF patients over the 12 month course of the study. These results are promising and represent the need of a larger, placebo-controlled clinical trial to investigate the effects of AT_1R inhibition in IPF.

The evidence for the effectiveness of ACE inhibition in IPF does not appear to be as promising. One study (Nadrous *et al.*, 2004), although retrospective, found no beneficial effects of ACE inhibitors in the mean survival time of IPF patients. The results of this study should not be over-interpreted, however, as many factors could reduce the effectiveness of ACE inhibitors in this setting. Although many factors were accounted for, such as smoking status, age and FVC, patient compliance in taking their drug is a major limitation in this study. Also six different ACE inhibitors were the focus of investigation, with many patients also likely to have been prescribed varying drug concentrations.

The small number of clinical trials in this field, indicate the need for more investigations into the clinical relevance of RAS manipulation in patients with IPF.

1.7 Limitations of pulmonary fibrosis animal models

As mentioned in section 1.6.1, candesartan has been shown to reduce bleomycin induced fibrosis *in vivo,* indicating that ANGII may induce fibrosis via this receptor (Otsuka *et al.*, 2004). Losartan has also been shown to attenuate bleomycin induced fibrosis *in vivo* (Yao *et al.*, 2006). However, both of these studies looked at the effects of bleomycin up to 21 days after a single intratracheally administered dose. It has been demonstrated that the fibrosis induced by a single dose of intratracheal bleomycin does not resemble human IPF (Borzone *et al.*, 2001), with the main reason being the reversible nature of the fibrosis induced in this model; therefore care should be taken when extrapolating data from this model to the human disease state.

There are several animal models of fibrosis available with a number of methods and substances used to induce lung injury, these include bleomycin, FITC and irradiation. These models allow for histological and biological changes during fibrosis to be observed; however, none are able to replicate the complicated progressive nature of human IPF (Moeller *et al.*, 2006). In these animal models, the main aim is to attempt to prevent the formation of fibrosis or to completely reverse it, and all these studies were performed in animals with the known ability to regenerate their alveolar structures (Gauldie and Kolb, 2008). Therefore the fibrotic response begins to reverse once the stimulus is removed and this does not appear to occur in humans (Moeller *et al.*, 2006). Also, humans do not usually present for treatment for the disease until chronic stage, whereas animal models are mainly working to prevent fibrosis from developing (Gauldie and Kolb, 2008). Another consideration to take into account with fibrosis animal models is the age factor, with IPF not usually developing in humans until age 50 and above, whereas the animals used in these models are usually used within a few weeks or months after birth, which again may not provide a suitable comparison to the human disease (Gauldie and Kolb, 2008).

The irradiation model is a reliable method of inducing fibrosis, with the fibrotic response dependent on the size and length of the radiation dose administered; this makes the model extremely predictable and also closely mimics the long time frame required for induction of fibrosis in humans. However, this advantage is also the model's main practical disadvantage (Moeller *et al.*, 2006), with fibrosis taking more than 30 weeks to develop in some cases (Moore and Hogaboam, 2008). This model is also extremely variable between strains of mice, with C3H/HeJ and CBA/J being resistant to irradiation induced fibrosis and C57Bl/6 being prone to irradiation induced fibrosis. There also appears to be gender based differences in this model with female C57Bl/6 mice being more sensitive to fibrosis than males (Moore and Hogaboam, 2008).

The bleomycin model is the most widely used fibrosis model today. Although there are a number of advantages associated this model, such as a wide variety of administration routes (intratracheal and intravenous etc) and with it being the most characterised animal model of fibrosis with reproducible induction of fibrotic changes, there are also a number of disadvantages with this model. The main one of which is the variability observed between different mice strains and the reversible nature of the fibrotic response (Moore and Hogaboam, 2008). Balb/c mice show limited fibrosis in this model, while C57Bl/6 mice are more susceptible to fibrosis. While the fibrotic response observed between days 14-21 after intratracheal administration of bleomycin is quite reproducible, the fibrosis observed 28 days post-dose becomes more variable, with many reports documenting a reversal of fibrosis after this point, indicating that the disease may be self-limiting in mice (Moore and Hogaboam, 2008). As IPF is not reversible, this model may not be a particularly representative model of the disease, and this reversal of the fibrotic response does not allow for the long-term study of disease progression. Also whilst the bleomycin model is clinically relevant for patients developing pulmonary fibrosis whilst undergoing chemotherapy, this model is not representative of the idiopathic nature of IPF disease pathology.

As there are no real transferable models of human IPF, other methods to investigate mechanisms of fibrosis are required. It is hoped that human, primary, pulmonary derived fibroblasts in culture will allow for more accurate study of fibrotic mechanisms. The effects of RAS peptides on this cell population will be the main focus of this thesis.

1.8 Aims

As there are very few studies investigating the effects of ANGII, ANG(1-7) and related peptides on HLF activity, there are three main aims to this project:

1. To determine the effects of ANGII, ANG(1-7) and related peptides on fibroblast activity, such as intracellular calcium release, collagen deposition and MMP production.

2. To determine any differences in the effects of ANG peptides on fibroblast activity between healthy and IPF derived HLFs.

3. To investigate the ANG receptors present on HLFs, with the main focus on the Mas receptor.

We hypothesise that ANG receptors are present on HLFs and that there are differences in the effects of ANG peptides on healthy and IPF derived fibroblasts. This may provide evidence for the RAS being a useful beneficial therapeutic target for the future treatment of IPF.

Chapter 2. Materials and Methods

2.1 Materials.

Angiotensin peptides were from Bachem; Radioligands [^{125}I]-[Sar^{1},Ile^{8}]-ANGII, [^{125}I]-ANG(1-7) (Custom made) and [^{125}I]-D-ala^{7}-ANG(1-7) were from PerkinElmer; Cytoplasmic and extracellular Anti-Mas (Rabbit IgG) were from Cambridge Biosciences; Alexa fluor 488™ conjugated Goat anti-Rabbit IgG and Hoechst dye were from Invitrogen; p44/42 MAPK (ERK1/2) and phospho-p44/42 MAPK (ERK1/2) rabbit monoclonal antibodies were from New England Biolabs; Supersignal™ west pico chemiluminescent substrate, PageRuler™ prestained protein ladder and TMB chromagen solution were from Life Technologies; Ionomycin, Saturated picric acid, collagen type I , protease inhibitor cocktail and standard experimental reagents were from Sigma Aldrich; tissue culture reagents were from either GE healthcare, Life Technologies or Sigma Aldrich; Plasticware was from greiner bio-one or BD-Biosciences.

2.2 Buffers and Reagents

All buffers were made up in distilled water unless otherwise stated.

2.2.1 Basic Buffers

PBS contained 137mM NaCl, 2.7mM KCl, 1.8mM KH_2PO_4 and 10mM Na_2HPO_4 ; **PBS tween** contained PBS with 0.05% tween; **Saline** contained 155mM NaCl; **Tyrodes buffer** contained 1.8mM $CaCl_2$, 5.6mM D-glucose, 2.7mM KCl, 1.05mM $MgCl_2$, 137mM NaCl, 0.4mM NaH_2PO_4.

2.2.2 Cell Culture

GSK DMEM contained DMEM with 25mM HEPES, supplemented with 4mM L-glutamine, 100 units/ml penicillin, 100µg/ml streptomycin, 2.5µg/ml amphotericin B and 10% foetal calf serum (FCS);

Soton DMEM contained DMEM supplemented with 2mM L-glutamine, 100 units/ml penicillin, 100µg/ml streptomycin, 1/100 dilution of commercially available non-essential amino acids (GE healthcare), 1mM sodium pyruvate and 10% newborn calf serum (NCS).

Two different media compositions were used, depending on the previously existing cell culture protocols at the stated institutions. This was the only reason for the differences between the two types of media used in this project.

2.2.3 FLIPR buffers

FLIPR buffer contained Tyrodes buffer supplemented with 20mM HEPES, 11.9mM $NaHCO_3$, 500μM brilliant black, 2.5mM probenicid and 0.1% BSA and balanced to a pH of 7.4 with NaOH; **Loading Buffer** contained FLIPR buffer with 2mM FLUO4-AM.

2.2.4 Collagen Assays

Sirius red contained 1mg/ml Sirius red dissolved in saturated aqueous picric acid; **Bouins fluid** contained 15ml saturated picric acid, 5ml formaldehyde and 1ml glacial acid.

2.2.5 Zymography

Running buffer contained 0.325M Tris; 0.1% SDS with a final pH of 8.8; **Stacking buffer** contained 0.125M Tris, 0.1% SDS, final pH of 6.8; **Electrode buffer** contained 25mM Tris, 0.1% SDS, 0.192M glycine with a final pH of 8.3; **Zymography sample buffer** contained 125mM Tris, 0.2% SDS and 50% glycerol final pH of 6.8; **Zymography wash buffer** contained 20mM Tris, 2.5% Triton-X 100, with a final pH of 7.8; **Ca^{2+} Zymography wash buffer** contained 20mM Tris 10mM, $CaCl_2$, 5μM $ZnCl_2$ and 1% Triton-X 100 with a final pH of 7.8; **Coomassie blue stain** contained 0.5% Coomassie blue, 45% Methanol, 10% acetic acid; **Destain** contained 10% methanol and 10% acetic acid.

2.2.6 Western blotting

Resolving buffer contained 1.5M Tris base, final pH of 8.8; **Stacking buffer** contained 0.5M Tris base, final pH of 6.8; **Laemmli buffer (2X)** contained 500mM Tris base, 138.7mM SDS, 522.4μM bromophenol blue and 20% v/v glycerol, final pH of 6.8; **Running Buffer (5X)** contained 125mM Tris Base, 959.2mM glycine and 17.3mM SDS.

2.2.7 Radioligand Binding

HEPES buffer contained 50mM HEPES, balanced to pH 7.4 with KOH; **Binding buffer** contained HEPES buffer with 0.1% BSA.

2.3 Cell Culture

2.3.1 Isolating fibroblasts from human lung tissue.

Human lung samples were either obtained from patients undergoing lung resection surgery for lung carcinoma at Southampton General Hospital (SGH) (Approved by Southampton and South West Hants A ethical committee; NREC number 08/H0502/32), or from deceased organ donors at GlaxoSmithKline [GSK]. Both IPF and non-fibrotic lung donors were available at GSK. The human biological samples were sourced ethically and their research use was in accord with the terms of the informed consents. Lung tissue was chopped into cubic fragments of approximately 8mm^3 and fibroblasts allowed to grow out over 10-14 days in DMEM, at 37°C with 5% CO_2 in 6-well plates. Fibroblasts were monitored closely to ensure that areas of over confluency did not develop, if this began to occur then cells were passaged as normal into 25cm^2 flasks (two wells of a 6 well plate were combined into one 25cm^2 flask).

Cultured cells were shown to be fibroblasts by immunocytochemistry, with positive staining for CD90 (anchoring protein expressed by many cell types including leukocytes, endothelial cells and fibroblasts) and negative staining for CD45 (leukocytes) and epcam (epithelial cells). Only a small proportion of fibroblasts stained positive for α-SMA, until 48 hour treatment with 9ng/ml TGF-β1 which induced positive staining in most cells, indicating a shift to the more active myofibroblastic phenotype.

2.3.2 Cell maintenance

Fibroblasts were maintained in DMEM, at 37°C with 5% CO_2, with media changed three times weekly. Cells were grown to 90% confluency in 25cm^2 flasks before trypsinisation and passage into 75cm^2 flasks. Once confluent, cell number was determined with either a haemocytometer (at Southampton) or cell counter (chemometec nucleocounter NC-300) (at GSK) and plated out at the cell density required for individual experiments. All experiments were performed in fibroblasts at passage 3-8.

2.4 Fluorescence imaging plate reader

Fluorescence imaging plate reader (FLIPR) experiments were performed at GSK Stevenage.

Cells were seeded at 1x10^4 cells per well in clear bottomed, black-walled 96 well plates, grown to confluency, and treated with 2ng/ml TGF-β1 (in serum free GSK DMEM) overnight before starting the experiment. Pretreatment with TGF-β1 increases the Ca^{2+} release observed in the

presence of ANGII (previously established at GSK), which was likely due to increased AT_1R expression (Renzoni *et al.*, 2004).

All reagents for the experiment were diluted in FLIPR buffer.

Serum free DMEM was replaced with loading buffer and cells were incubated at 37°C for 1 hour to allow the FLUO-4AM to enter the cell cytoplasm. Increases in the fluorescence of FLUO-4AM indicates increases in cytoplasmic Ca^{2+} concentration.

Using a FLIPR tetra, 50µl of peptide was added to each well containing loading buffer. Fluorescence was measured every 2 seconds for 3 minutes before simultaneous addition of 5mM $MnCl_2$ and 5µM ionomycin (final concentrations), fluorescence was measured for a further 3 minutes at 6 second intervals.

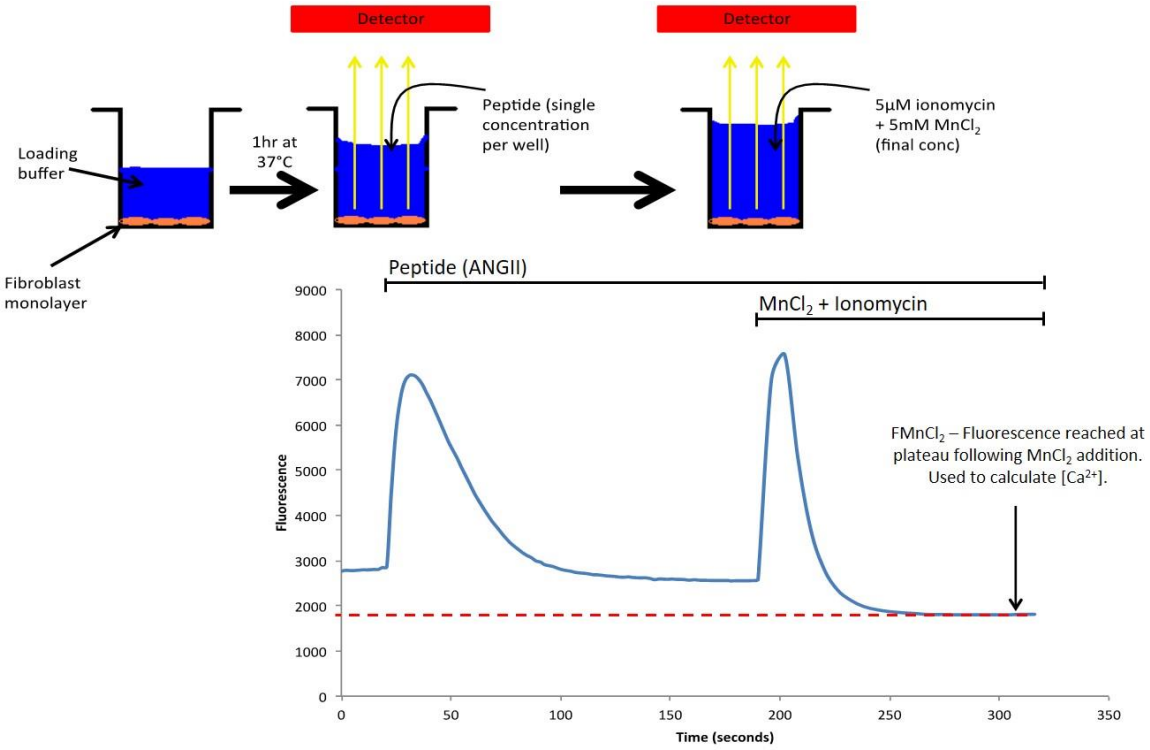

Figure 2-1. Diagrammatic representation of FLIPR experiment. The fluorescence emitted upon both peptide and ionomycin/$MnCl_2$ addition was recorded by a FLIPR tetra. Graph shows a typical trace plotted by the FLIPR tetra, peaks represent high transient levels of intracellular calcium release upon peptide addition. This is an original trace plotted from fluorescence values upon ANGII addition.

Addition of ionomycin raises intracellular Ca^{2+} levels causing saturation of FLUO-4AM (second peak in **Figure 2-1**), which is then quenched by the high concentrations of Mn^{2+} ions. The value of the fluorescent plateau reached after the addition of the $MnCl_2$ mixture (**Figure 2-1**) was used to calculate the changes in cytosolic calcium concentration over the course of the experiment,

using the following equation, as previously described by Grynkiewicz et al (Grynkiewicz *et al.*, 1985).

$$[Ca^{2+}] = K_d \times \frac{[F - Fmin]}{[Fmax - F]}$$

Equation 2-1. Calculation of Ca^{2+} concentration from fluorescent values. *F* is fluorescence; K_d is the dissociation constant of FLUO-4AM binding to calcium and is known to be 345nM. F_{max} and F_{min} are the maximum and minimum fluorescence intensities possible when FLUO-4AM is saturated with calcium (F_{max}) and when FLUO-4AM is in a calcium free environment (F_{min}).

$MnCl_2$ does not completely quench the FLUO-4AM signal, but does reduce fluorescence to a consistent level each time. This value is used to calculate F_{min} and F_{max}, using correction factors that were previously determined at GSK (as shown below).

$$F_{min} = \frac{F_{MnCl_2}}{8.3}$$

$$F_{max} = F_{MnCl_2} \times 9.4$$

Equation 2-2. Equation for calculation of F_{min} and F_{max}. The correction factors shown above can be used to calculate the minimum and maximum fluorescence of FLUO-4AM (F_{min} and F_{max} respectively).

Background fluorescence (the level of free FLUO-4AM that remained in the supernatant) was calculated by adding loading buffer to four wells of cells, incubating for 1 hour and transferring the supernatant to four empty wells containing no cells. The average background fluorescence was then subtracted from the fluorescent values of the experiment.

2.5 Western blots

Fibroblasts were seeded at a density of $4x10^5$ per well in a 6 well plate and incubated at 37°C with 5% CO_2 overnight in Soton DMEM.

Prior to treatment, HLFs were serum starved for 30 minutes in hanks balanced salt solution (HBSS) containing Mg^{2+} and Cl^-. Cells were treated with varying concentrations of ANGII or with H_2O_2 (as a positive control) for 10 minutes and lysed with Laemmli buffer containing 40mM DL-Dithiothreitol (DTT). Lysate was denatured by boiling, and 30µl of each sample was run at 100v for approximately 2 hours, through a 10.6% acrylamide, 0.02% SDS resolving gel with a 4% acrylamide 0.1% SDS stacking gel poured on top. Molecular weight marker (PageRuler™) was run alongside samples.

Protein bands were then transferred to nitrocellulose membrane under a current of 300mA for 1.5 hours, between blotting pads soaked in running buffer containing 20% methanol. Membranes were then blocked with 3% milk protein in 0.5% PBS tween before overnight incubation at room temperature with primary antibody. Membranes were then washed with 0.5% PBS tween, prior to a 1 hour incubation at room temperature with secondary HRP conjugated antibody (goat anti-Rabbit). Membranes were then washed 3 times in 0.5% PBS tween and treated with Supersignal™ west pico chemiluminescent substrate for 2 mins. Membranes were then exposed to x-ray film to allow visualisation of protein bands. Bands were quantified by densitometric analysis using image J.

2.6 Fibroblast proliferation assay

Fibroblasts were seeded at a density of $1x10^4$ per well in flat-bottomed 96 well plates, incubated at 37°C with 5% CO_2 overnight and maintained in Soton DMEM containing 10% NCS. Fibroblasts were then treated with the relevant peptides/inhibitors and NCS concentrations.

Cells were fixed in formyl saline at 24, 48, 72 and 120 hour time points (depending on the individual experiment), rinsed with PBS and air dried overnight. Methylene blue was added to each well for one hour to allow staining of the cell nuclei; cells were then rinsed thoroughly with saline solution to remove all free dye. Plates were air dried overnight, dye liberated with acid:alcohol and absorbance read at 650nm. Fibroblasts were also seeded at known density (0 – 50 cells per well) and stained in the same manner to allow for the production of a standard curve. Experimental cell numbers were then calculated from absorbance values using this standard curve.

2.7 Collagen Assays

HLFs were seeded at $5x10^4$ cells per well in 24 well plates, incubated at 37°C with 5% CO_2 overnight in Soton DMEM before peptide treatments.

Cells were then maintained in DMEM with 0.5% NCS containing 100μM L-ascorbate for 6 days (Chen *et al.*, 2009) without media change. Ascorbate was added as this is an important component required for synthesis of hydroxyproline in collagen. Collagen staining was carried out following peptide treatments as described previously (Tullberg-Reinert and Jundt, 1999); in brief, cell layers were fixed in Bouins fluid, washed extensively with PBS and stained with Sirius red. Any unbound dye was removed by extensive washing with 0.01M HCl. Bound dye

was then dissolved using 0.5M NaOH, the solutions transferred to a 96 well plate and read at 550nm. Collagen amount per well was calculated from absorbance values using a standard curve.

2.8 Gelatin Zymography

Cell supernatants were prepared in zymography sample buffer with added bromophenol blue to ensure samples were visible upon gel loading. Samples (10µl) were run at 30mA for approximately 1 hour on a 0.1% gelatin and 7.5% acrylamide gel, to allow separation of protein bands (**Figure 2-2**); MMP standards and molecular weight marker (Pageruler™) were run alongside samples.

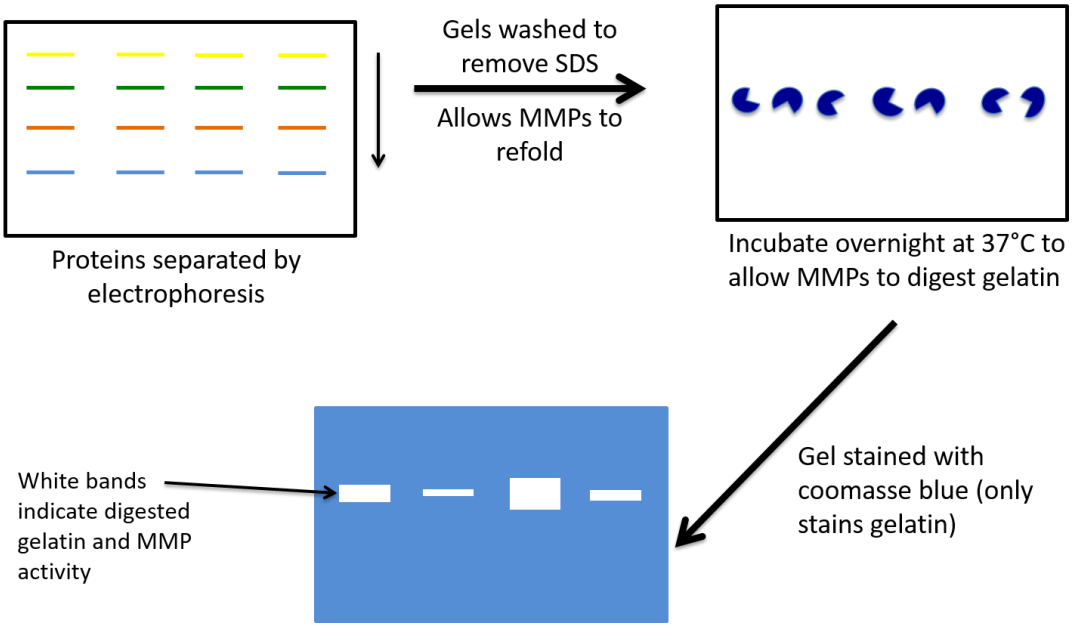

Figure 2-2. Gelatin zymography method. Matrix metalloproteinases (MMP) were separated by gel electrophoresis, washed and incubated at 37°C overnight in zymography buffer containing calcium. Gels were then stained with coomassie blue, white bands indicate MMP activity.

After electrophoresis, gels were given two 20-minute washes in zymography wash buffer to remove SDS and to allow refolding of proteins, before a further 20-minute wash in Ca^{2+} zymography buffer. Gels were then incubated overnight at 37°C in fresh Ca^{2+} zymography buffer to allow the reactivation of gelatinases. Coomassie blue stain was then added to the gels, to fix the gelatinases and to stain any undigested gelatin. Excess stain was then removed by washing with destain, rendering any bands on the gel visible. Gels were then scanned and densitometric analysis used to calculate relative changes in MMP activity.

2.9 Enzyme-linked immunosorbent assay

Cells were seeded at a density of $5x10^4$ cpw in 24 well plates and incubated at 37°C with 5% CO_2 overnight in Soton DMEM. Cells were treated with various ANG peptide concentrations or 2ng/ml TGF-β1. Supernatants were harvested at 24, 48 and 72 hours and run through sandwich enzyme linked immunosorbent assays (ELISA) for MMP-1, IL-6, TGF-β1 or latency associated peptide (LAP) according to manufacturer's instructions.

In brief, high binding 96 well plates were coated with specific capture antibody for the protein of interest overnight at room temperature. Plates were blocked with 1% BSA for one hour, washed with PBS tween and supernatants added to the plate for two hours. Plates were washed again and incubated with specific detection antibody for the protein of interest for a further two hours. Plates were washed again and incubated in the dark for 20 minutes with streptavidin-horse radish peroxidase (HRP). Plates were washed a final time before the addition of 3,3',5,5'-tetramethylbenzidine (TMB) substrate solution for a further 20 minutes. Reaction was stopped with 1M HCl and absorbances were read at 450nm.

2.10 Immunocytochemistry

HLFs, seeded at a density of $3x10^4$ on $12mm^2$ cover slips coated in 1% BSA, were incubated at 37°C with 5% CO_2 overnight in soton DMEM. Cells were then fixed with 4% paraformaldehyde (PFA) for 30 minutes on ice. For long-term storage, PBS was added to each well and the plate sealed and stored at 4°C.

Cells were permeabilised with 0.1% Triton-x before incubation with primary anti-Mas antibody (rabbit IgG) for 2 hours at room temperature in the dark. Cells were then rinsed three times with PBS tween before the addition of Alexo fluor® 488 conjugated anti-rabbit IgG, for 1 hour at room temperature in the dark. This allowed for the detection of cell bound Anti-Mas with Hoechst stain used as a nuclear marker. Cells were rinsed again in PBS tween, coverslips mounted on to slides with ProLong® diamond mounting solution and imaged used a fluorescence microscope.

2.11 Fibroblast membrane preparation for radioligand binding

All binding experiments and preparations were performed at GSK Stevenage.

2.11.1 Preparation of fibroblast membranes

Cells from 30-40 T175 flasks of confluent fibroblasts (maintained with GSK DMEM) were scraped from flasks using a cell scraper and combined to form one cell pellet, which was kept at -80°C until needed. To make the membrane suspension, the pellet was defrosted on ice, in HEPES buffer supplemented with protease inhibitor cocktail (2mM AEBSF, 0.3μM Aprotinin, 130μM Bestatin, 1mM EDTA, 14μM E-64 and 1μM Leupepin). The cell suspension was homogenised and then spun at 500g for 20 minutes at 4°C. The supernatant was withdrawn and re-spun at approximately 48,000g for 30 minutes. The membrane pellet was resuspended in HEPES buffer and aliquots were stored at -80°C.

2.11.2 Protein Assays for membrane protein concentration

A BSA standard curve (in PBS) of 0.1-2mg/ml was produced in duplicate and 6 serial dilutions of stock membrane suspension (produced in method section 2.11.1) were produced in PBS. A solution of BCA (reagent A) and $CuS0_4$ (reagent B) was prepared according to manufacturer's instructions and added to a 96 well plate containing the membrane samples above. The plate was incubated at 37°C for 30 minutes and then read at 565nm. The amount of protein per membrane sample was then calculated from the standard curve.

2.12 Radioligand binding

2.12.1 Simple binding experiments

To determine whether the receptors of interest were present on fibroblast membrane, simple radioligand binding experiments were performed.

Fibroblast membrane suspension (containing varying amounts of membrane protein) was incubated with either 0.1 or 0.3nM of [^{125}I]-labelled ligand. To determine the total and non-specific binding (NSB), this experiment was performed, in parallel, in the presence and absence of unlabelled cold ligand (**Figure 2-3**).

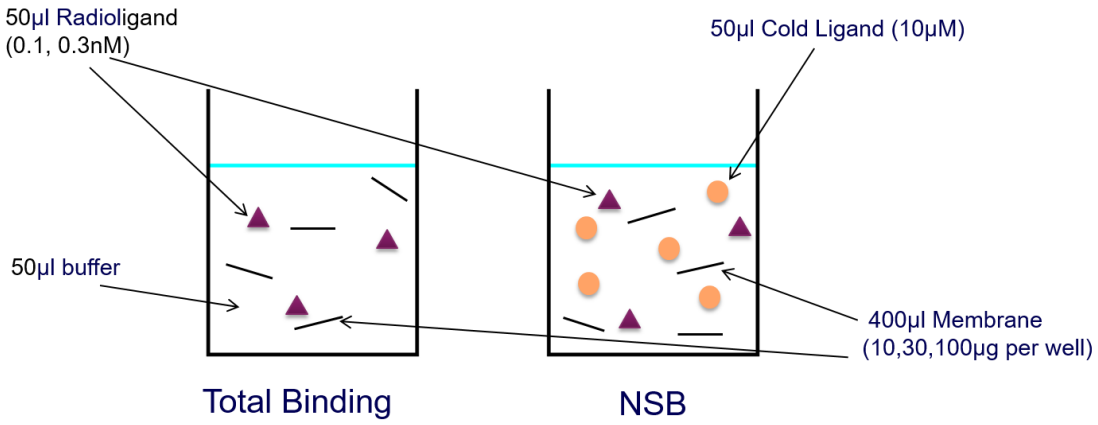

Figure 2-3. Radioligand binding experimental set up. Fibroblast membrane was incubated in the presence and absence of cold ligand to measure non-specific binding (NSB) and total binding of the radioligand respectively.

Cold ligand is a non-radiolabelled ligand that binds to the receptor of interest, as well as NSB sites, but the cold ligand has a separate population of NSB sites from the radiolabelled ligand and hence does not displace the radiolabelled ligand from its own NSB sites (as depicted in **Figure 2-4**). This allows specific binding of the radioligand to be determined.

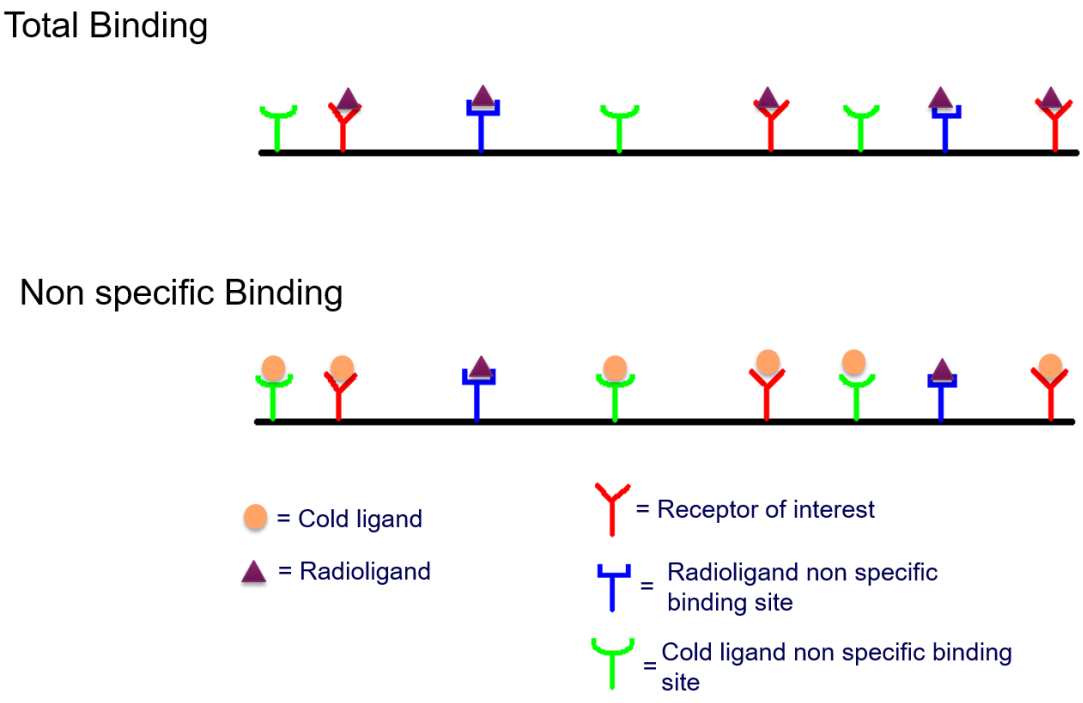

Figure 2-4. Total and non-specific binding of the radioligand. Total binding (top) measures the binding of radioligand to its specific and non-specific binding (NSB) sites in the absence of cold ligand. NSB (bottom) is the binding of the radioligand to NSB binding sites only, and is measured in the presence of 10µM cold ligand.

Total binding of the radioligand (measured in the absence of cold ligand) is the binding of the radioligand to both the receptor of interest and to its NSB sites. NSB of the radioligand is determined in the presence of cold ligand. Together these two values allow for the calculation of the specific binding of the radioligand.

At the end of the incubation step, the suspensions were vacuum filtered through GF/B, filter mats, rinsing three times with HEPES buffer (at 4°C). The filter mat was then dried and placed in polypropylene tubes. Filtration removed unbound radioligand and allowed the membrane bound radioligand alone to be measured using a gamma counter. The disintergrations per minute (DPM) that were measured directly related to radioligand concentration.

To allow for the measurement of the exact radioligand concentration that was used for each individual experiment, 10µl of the radioligand solution was added to three polypropylene tubes, and DPMs of these samples along with the specific activity of the radioligand were used to calculate radioligand concentration.

2.12.2 Competitive binding assays

Homologous competition assays were run in duplicate in the presence of 30µg of fibroblast membrane per well, two single concentrations of [^{125}I]-ligand were run in the presence of increasing concentrations of the unlabelled [I] version of the same ligand. Heterologous competition assays were run in a similar manner, however, the cold ligands in this case were antagonists, used to determine the specific receptor(s) responsible for the binding signal observed. All reagents were diluted in binding buffer for this experiment.

After a two-hour incubation at room temperature, the plate was filtered and dried as described in section 2.12.1.

2.13 Statistical analysis.

All statistical analysis was carried out using GraphPad Prism.

Two way ANOVA with Bonferroni correction for multiple comparisons was used to compare dose response curves where stated, ANOVA was structured with repeated measures for both peptide concentration and cell line to allow comparison between inhibitors.

Statistical comparisons were performed using non-parametric tests, either Wilcoxon matched-pairs signed rank. Mann-Whitney test or Friedman test (where stated).

Chapter 3. Calcium mobilisation in human lung fibroblasts

3.1 Background

The RAS (as shown in **Figure 1-7**) has been implicated in the pathogenesis of IPF. As mentioned earlier, the two mostly widely studied peptides of this system for their potential roles in fibrosis are ANGII and ANG(1-7). There are however many more peptides derived from ANGI whose implications in fibrosis remain relatively unexplored. **Figure 1-8** depicts the more complicated renin angiotensin peptide system and the enzymatic formation of these peptides.

Currently there are four known ANG receptors, AT_1R, AT_2R, AT_4R and Mas (Unger *et al.*, 2011), with the binding of many ANG peptides to these receptors investigated. As mentioned previously, ANGII is a potent agonist for both AT_1R and AT_2R and has also been shown to bind with low affinity to both AT_4R (Handa, 2000) and the Mas receptor (Santos *et al.*, 2003a). ANGIII, ANGIV and ANG(1-7) have also been shown to bind to these receptors with varying affinities, all of which can be found in **Table 3-1**.

Peptide	**AT_1R**	**AT_2R**	**AT_4R**	**Mas**
ANGII	$7.92x10^{-9}$	$5.22x10^{-10}$	$1.10x10^{-5}$	$5.33x10^{-8}$
ANGIII	$2.11x10^{-8}$	$6.48x10^{-10}$	N/A	$4.52x10^{-7}$
ANGIV	$>1x10^{-5}$	$4.68x10^{-8}$	$2.40x10^{-8}$	$1.24x10^{-6}$
ANG(1-7)	$>1x10^{-5}$	$2.46x10^{-7}$	$0.80x10^{-5}$	$6.90x10^{-9}$

Table 3-1. Affinity of different angiotensin peptides at angiotensin receptors. All data shown are IC_{50} values from competition binding studies (Handa, 2000; Santos *et al.*, 2003a; Bosnyak *et al.*, 2011)

ANG(1-9) has also been shown to bind to both AT_1R and AT_2R with pK_i values of 6.61 and 6.28 respectively (Flores-Muñoz *et al.*, 2011). ANG(3-7) has been shown to bind to AT_4R with high affinity (pK_i of 8.97) (Handa, 2000). However, little is known about the activity of ANG(1-5), with this peptide thought to be biologically inactive (Schwacke *et al.*, 2013).

As mentioned in section 1.5.2, the main signalling pathway activated by ANGII upon binding to AT_1R is activation of PLC, which is responsible for the cleavage of phosphatidylinositol-4,5-bisphosphate (PIP_2) to inositol 1,4,5-trisphospate (IP_3) and diacyl glycerol (DAG). IP_3 then acts on IP_3 dependent calcium channels on the endoplasmic reticulum (ER) (**Figure 1-9**) causing an influx of Ca^{2+} from the ER into the cell cytoplasm, as reviewed by Clapham (Clapham, 2007). Elevated intracellular Ca^{2+} levels can then act on plasma membrane Ca^{2+} channels causing further influx of Ca^{2+} from the extracellular environment. This can cause downstream

activation of extracellular signal-related kinase (ERK)-1/2 (May *et al.*, 2014), a member of the mitogen activated protein kinase (MAPK) family. Rises in intracellular Ca^{2+} are detected by calmodulin (CaM), a Ca^{2+} binding protein. The calcium-calmodulin complex is then able to activate calcium-calmodulin dependent kinase (CaMK)-II (Clapham, 2007), which in turn can lead to downstream ERK phosphorylation (Abraham *et al.*, 1997). ERK1/2 phosphorylation can affect many cellular functions, such as proliferation, ECM deposition and cell survival. Increases in intracellular Ca^{2+} can also cause downstream phosphorylation of ERK1/2 via PKC dependent mechanisms (Booz *et al.*, 1994).

The ability of ANGII to induce intracellular Ca^{2+} release has been demonstrated in a number of different organ derived fibroblasts such as skin (Nickenig *et al.*, 1997; Ceolotto *et al.*, 1998) and cardiac fibroblasts (Fareh *et al.*, 1995).

Previous work has suggested that at least ANGI, ANGII, ANGIII and ANGIV are capable of inducing intracellular Ca^{2+} release in other cell types, such as neuroblastoma cells (Ransom *et al.*, 1992). ANG(1-7) has been shown previously to have no effect on basal Ca^{2+} levels in mesangial cells (Chansel *et al.*, 2001; Zimpelmann and Burns, 2009). However the actions of ANG(1-5), ANG(3-7) and ANG(1-9) on intracellular Ca^{2+} release remain relatively unexplored.

None of the work described above was carried out in human lung fibroblasts (HLFs); therefore one aim of this chapter was to determine the ability of eight ANG peptides (as shown in colour in **Figure 1-8**) to manipulate intracellular Ca^{2+} release in HLFs. The second aim of this chapter was to determine whether there were any differences in the activity of these ANG peptides in healthy and IPF derived HLFs, as this has not been investigated previously. IPF derived fibroblasts are known to be phenotypically different to healthy fibroblasts, they have been shown to be more proliferative and to have much higher α-SMA staining (Moodley *et al.*, 2003b) indicating a higher number of myofibroblast cells in culture. These differences suggest that they may respond in a different manner to healthy fibroblasts.

The ability of ANGII to induce intracellular signalling processes downstream of intracellular Ca^{2+} release were also explored. ERK1/2 phosphorylation in response to ANGII was investigated in HLFs.

3.2 Protocols

3.2.1 Calcium signalling experiments

Intracellular Ca^{2+} mobilisation was performed using a FLIPR tetra, according to section 2.4. Dose response curves to ANGI, ANGII, ANGIII, ANGIV, ANG(1-7), ANG(1-9), ANG(1-5) and ANG(3-7) were constructed, with concentrations ranging from 0.5nM to 10μM. Any peptides that successfully increased intracellular Ca^{2+} were retested following a 15 minute preincubation with the AT_1R antagonist telmisartan (10nM), the AT_2R antagonist PD-123319 (1μM) or the Mas antagonist A-779 (10μM) to determine mechanism of action.

Peptides that did not cause intracellular Ca^{2+} release were retested as antagonists, ANGII and ANGIII dose response curves were constructed in both HLFs and IPF derived fibroblasts that were preincubated with 10μM 'inactive' peptide for 15 minutes. Peptides that demonstrated antagonistic properties against ANGII were retested in the presence of PD-123319 (1μM), A-779 (10μM) and D-pro^7-ANG(1-7) (10μM) (a second ANG(1-7) inhibitor discussed in section 1.5.2) to further explore this mechanism.

The ability of increasing concentrations of ANGI and ANGII to desensitise the response to a subsequent high dose of ANGII (10μM) was also investigated as depicted in **Figure 3-1**.

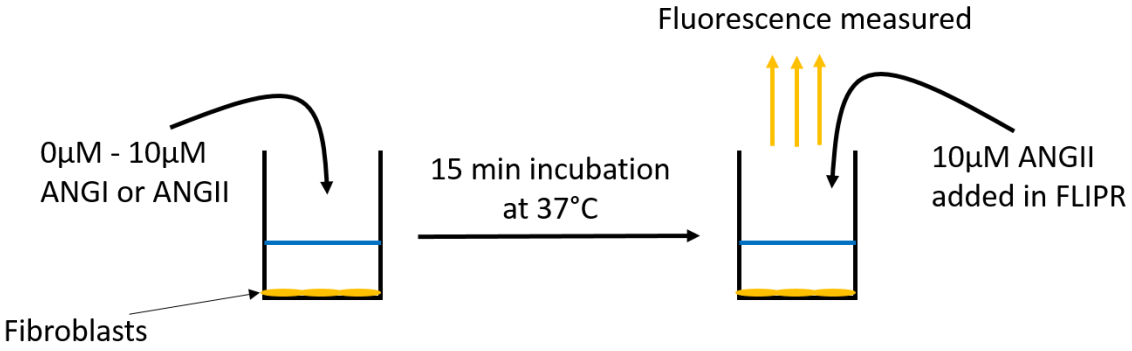

Figure 3-1. Diagrammatic representation of desensitisation experiments. Diagram showing the time course of additions used for investigation into receptor desensitisation.

Fibroblasts were incubated for 15 minutes with increasing concentrations of either ANGI or ANGII before the addition of 10μM ANGII. The change in fluorescence induced by the addition of 10μM ANGII was recorded by the FLIPR tetra and calcium values calculated as described in section 2.4.

3.2.2 ERK phosphorylation

ERK1/2 MAPK phosphorylation was analysed by Western blot (as described in section 2.5). HLFs were incubated with 0.01 - 10μM ANGII or 8mM H_2O_2 (positive control) for 10 minutes before cells were lysed and run as described above.

3.3 Results

3.3.1 Reproducibility of Fibroblast Ca^{2+} responses

ANGII has been reported to induce Ca^{2+} mobilisation in many organ derived fibroblasts such as skin fibroblasts (Ceolotto *et al.*, 1998). As ANGII is a well described Ca^{2+} agonist, this peptide was used a positive control to ensure that the fibroblast lines used were responding in the expected manner. ANGII was able to induce Ca^{2+} mobilisation in both healthy and IPF fibroblasts. Although the peak Ca^{2+} responses for both cell types were variable with average responses of 309 ± 50.5nM for healthy fibroblasts and 137.9 ± 28.1nM for IPF fibroblasts (ranges of 225.9 ± 19.07 to 400.4 ± 28.9nM and 91.5 ± 23.9 to 188.5 ± 35.8nM respectively), the potency of ANGII remained consistent between cell lines (**Figure 3-2**). IPF fibroblasts also appeared to have higher variability between experiments from the same cell line.

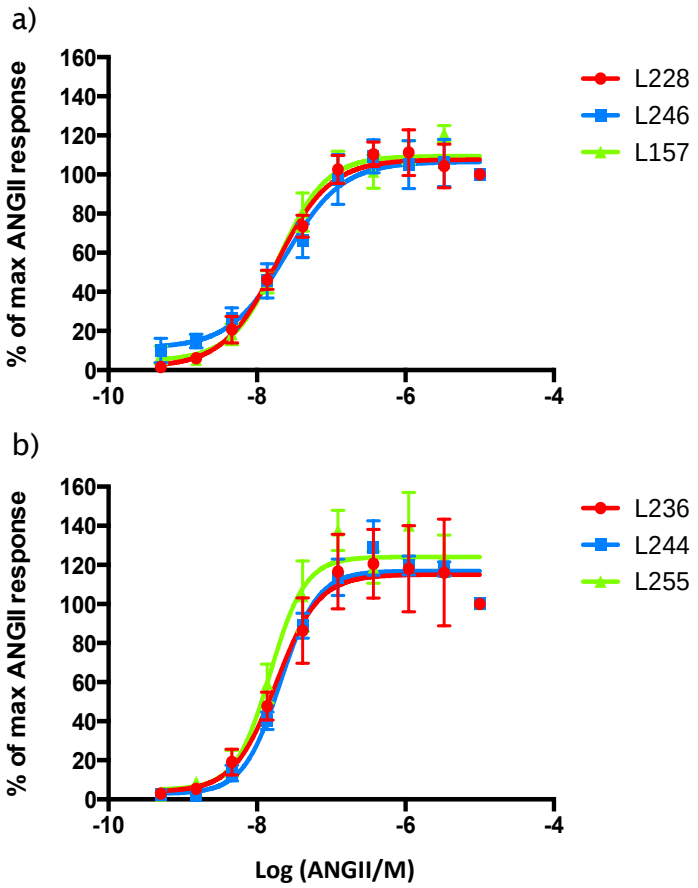

Figure 3-2. Ca^{2+} responses to ANGII. Ca^{2+} responses were expressed as a percentage of the fitted maximum ANGII response in a) healthy fibroblasts and b) IPF derived fibroblasts. ANGII dose response curves were run a minimum of three times per cell line. Data shown are mean ± SEM

3.3.2 Effects of angiotensin peptides on calcium mobilisation

Dose response curves to eight ANG peptides were performed. ANGI, ANGII, ANGIII and ANGIV were able to mobilise Ca^{2+} in both healthy and IPF cell lines (**Figure 3-3**). ANGII and ANGIII had similar maximal effects and no significant difference was observed in the EC_{50} values between healthy and IPF fibroblast lines (**Table 3-2**). ANG(1-5), ANG(1-7), ANG(1-9) and ANG(3-7) did not induce Ca^{2+} mobilisation in this assay.

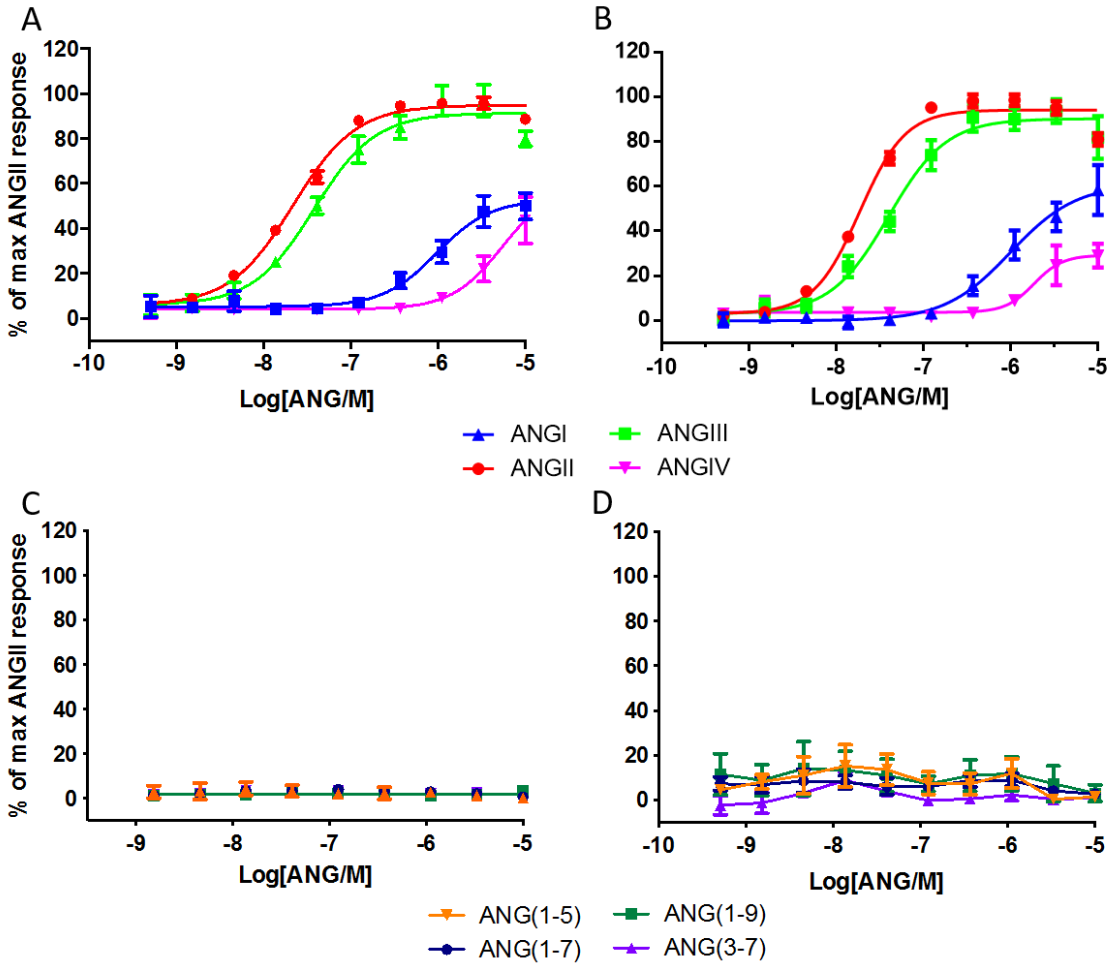

Figure 3-3. Dose response curves to angiotensin peptides. Treatment with increasing concentrations of four angiotensin peptides caused dose dependent increases in intracellular Ca^{2+} release in both healthy (n=3) (A) and IPF fibroblasts (n=3) (B). ANGII and ANGIII acted as full agonists, ANGI acted as a partial and ANGIV as a weak agonist. The remaining peptides tested had no effect on Ca^{2+} mobilisation in either healthy (C) or IPF fibroblasts (D). All data are expressed as percentage of the fitted maximum ANGII response and are the pooled mean ± SEM from all experiments.

A significant difference was observed in the maximal responses (**Table 3-3**) to ANGII between healthy and IPF fibroblasts ($p<0.0001$). A similar effect was observed with ANGIII ($p<0.05$). ANGI acted as a partial agonist with maximal responses of 54.9±6.4% and 53.6±10.9% of the ANGII responses in healthy and IPF cells respectively. As ANGIV acted as very weak agonist,

the maximal responses for this peptide were not well defined and therefore not included in analysis.

Peptide	**Healthy pEC_{50}**	**IPF pEC_{50}**	**Statistically significant?**
ANGI	5.87 ± 0.2	6.12 ± 0.1	No
ANGII	7.67 ± 0.01	7.72 ± 0.04	No
ANGIII	7.43 ± 0.02	7.22 ± 0.2	No
ANGIV	4.92 ± 0.15	4.67 ± 0.11	No

Table 3-2. pEC_{50} values of peptides in healthy and IPF cells. Data shown are mean ± SEM

Peptide	**Healthy maximal response (nM)**	**IPF maximal response (nM)**	**Statistically significant?**
ANGI	170.4 (105.2-269.1)	57.62 (33.94-134.1)	$p<0.05$
ANGII	277.5 (240.3-403.7)	133.5(115.7-158.5)	$p<0.0001$
ANGIII	308.8 (157.2-373.0)	119.5 (77.82-174.3)	$p<0.01$

Table 3-3. Maximal responses to peptides in healthy and IPF cells. Data shown are median with IQR (Statistical comparison with Mann Whitney U-test).

To determine the site of action of the four active ANG peptides, fibroblasts were pre-incubated with either 10nM telmisartan (AT_1R antagonist), 1μM PD-123319 (AT_2R antagonist) or 10μM A-779 (Mas receptor antagonist) for 15 minutes before peptide addition. Ca^{2+} responses were completely inhibited in the presence of telmisartan, with no effect on peak Ca^{2+} responses observed in the presence of the remaining two antagonists (**Figure 3-4**).

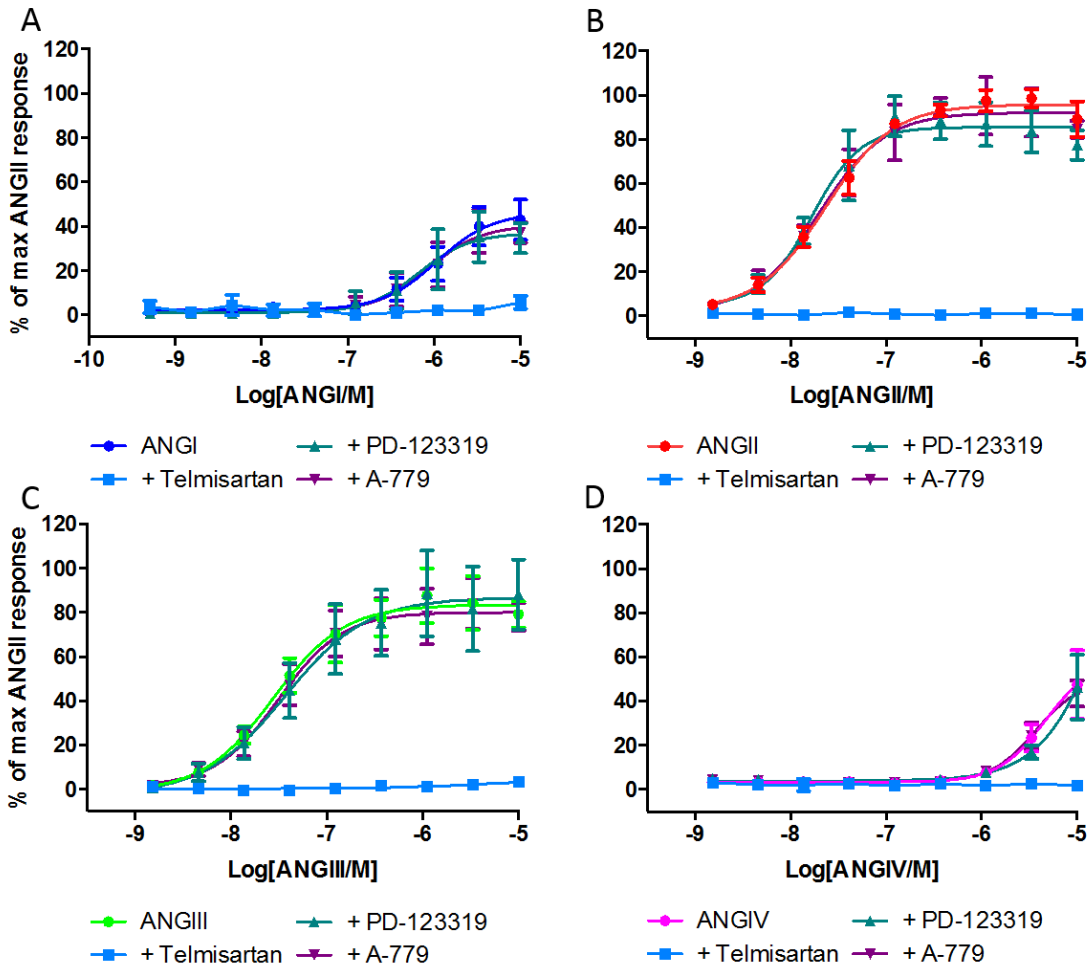

Figure 3-4. Dose-response curves to angiotensin peptides in the presence of antagonists. Healthy human lung fibroblasts were pre-treated for 15 minutes with telmisartan (10nM), PD-123319 (1μM) or A-779 (10μM). Telmisartan caused complete inhibition of the Ca^{2+} response to ANGI (A), ANGII (B), ANGIII (C) and ANGIV (D); PD-123319 and A-779 had no effect on Ca^{2+} mobilisation induced by any of the angiotensin peptides in healthy fibroblasts (n=3). All data are expressed as percentage of the fitted maximum ANGII response and are the pooled mean ± SEM from all experiments.

Telmisartan also completely inhibited Ca^{2+} mobilisation in IPF cells in the same manner as shown in **Figure 3-4** (data not shown).

3.3.3 Inhibitory effects of angiotensin peptides

As ANG(1-5), ANG(1-7), ANG(1-9) and ANG(3-7) failed to mobilise Ca^{2+} in this assay, the ability of these peptides to act as antagonists was investigated. Fibroblasts were pre-incubated with 10μM of each peptide, 15 minutes before the addition of either ANGII or ANGIII.

ANG(1-7) and ANG(1-9) caused significant inhibition of the Ca^{2+} responses to ANGII (**Figure 3-5**) and ANGIII (**Figure 3-6**) in both healthy and IPF fibroblasts.

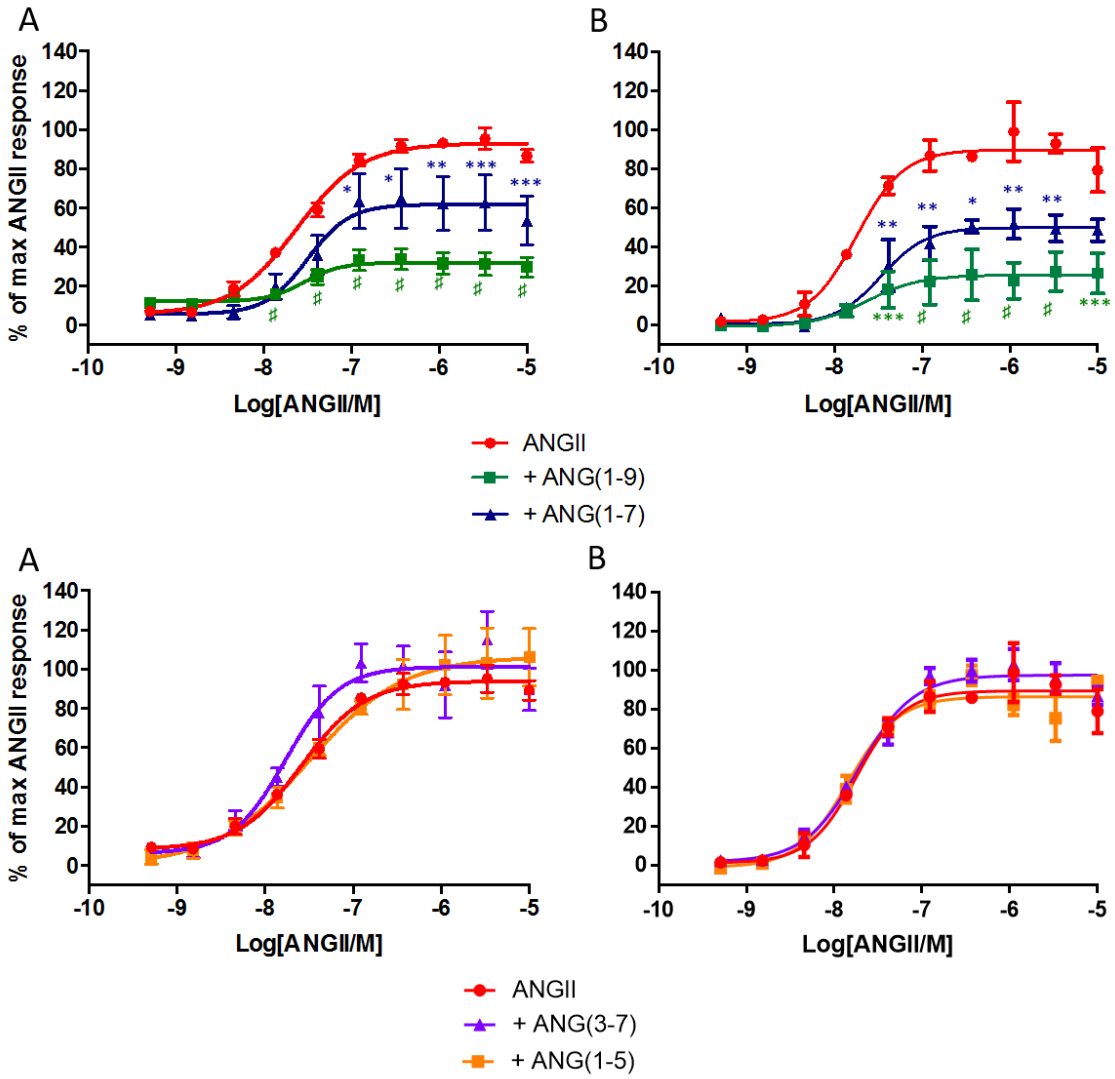

Figure 3-5. The ability of angiotensin peptides to inhibit ANGII. Pretreatment with ANG(1-7) or ANG(1-9) (10μM) for 15 minutes caused partial inhibition of ANGII induced Ca^{2+} responses in both healthy (A) (n=3 and n=5 respectively) and IPF fibroblasts (B) (n=5 and n=4 respectively). Pretreatment with ANG(1-5) or ANG(3-7) (10μM) had no significant effect on calcium mobilisation in healthy or IPF fibroblasts (C & D respectively). * indicates $p<0.05$, ** $p<0.01$, *** $p<0.001$ and # $p<0.0001$ when compared to the ANGII control (two way ANOVA). All data are expressed as percentage of the fitted maximum ANGII response and are the pooled mean ± SEM from all experiments.

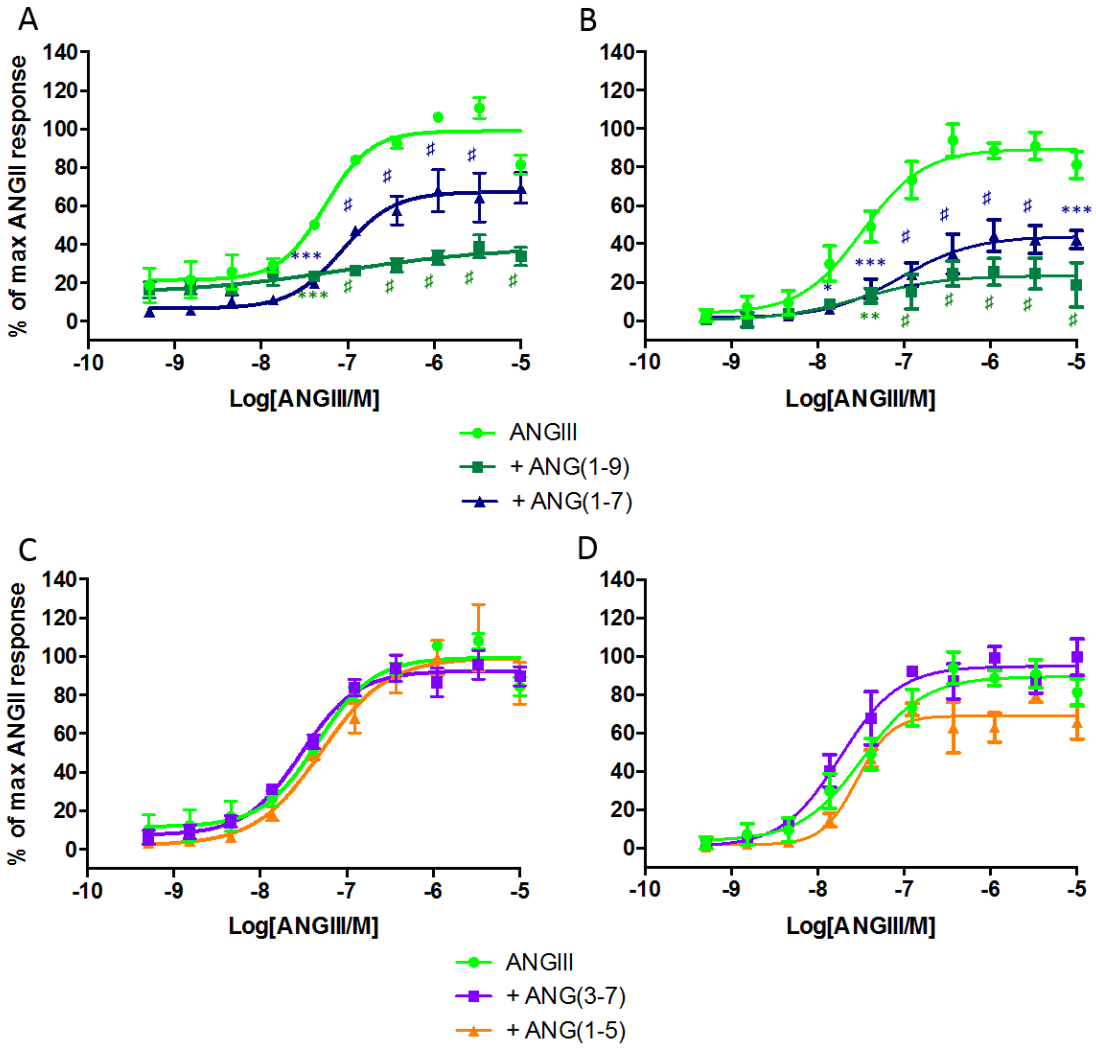

Figure 3-6. The ability of angiotensin peptides to inhibit ANGIII. Pretreatment with ANG(1-7) or ANG(1-9) (10μM) for 15 minutes caused partial inhibition of ANGIII induced Ca^{2+} responses in both healthy (A) (n=4 and n=3 respectively) and IPF fibroblasts (B) (n=3). Pretreatment with ANG(1-5) or ANG(3-7) (10μM) had no significant effect on Ca^{2+} mobilisation in healthy or IPF fibroblasts (C & D respectively). * indicates $p<0.05$, ** $p<0.01$, *** $p<0.001$ and # $p<0.0001$ when compared to ANGIII control (two way ANOVA). All data are expressed as percentage of the fitted maximum ANGII response and are the pooled mean ± SEM from all experiments.

The percentage of inhibition observed in the presence of ANG(1-7) or ANG(1-9) can be found in **Table 3-4** (healthy fibroblasts) and **Table 3-5** (IPF fibroblasts). ANG(1-5) and ANG(3-7) showed no ability to inhibit Ca^{2+} responses in this assay.

Agonist	Inhibitor	% inhibition
ANGII	ANG(1-9)	59.1 ± 5.5
ANGII	ANG(1-7)	40.5 ± 20.1
ANGIII	ANG(1-9)	55.6 ± 12.8
ANGIII	ANG(1-7)	29.0 ± 7.4

Table 3-4. The percentage of inhibition of ANGII and ANGIII in the presence of ANG(1-7) and ANG(1-9) in healthy fibroblasts. Percent inhibition of ANGII and ANGIII by ANG(1-7) (n=3 and n=4 respectively) and ANG(1-9) (n=5 and n=3 respectively). Data shown are mean ± SEM.

Agonist	Inhibitor	% inhibition
ANGII	ANG(1-9)	63.9 ± 10.9
ANGII	ANG(1-7)	46.1 ± 8.3
ANGIII	ANG(1-9)	77.0 ± 13.4
ANGIII	ANG(1-7)	63.8 ± 14.4

Table 3-5. The percentage of inhibition of ANGII and ANGIII in the presence of ANG(1-7) and ANG(1-9) in IPF fibroblasts. Percent inhibitions of ANGII and ANGIII in the presence of ANG(1-7) (n=5 and n=3 respectively) and ANG(1-9) (n=4 and n=3 respectively). Data shown are mean ± SEM.

Both ANG(1-7) and ANG(1-9) showed a trend towards a higher percentage inhibition of ANGIII than ANGII in IPF cells, although this did not reach statistical significance.

The potency of ANGII and ANGIII in the presence of inhibitors has been summarised for both healthy and IPF fibroblasts (**Table 3-6** and **Table 3-7** respectively). A significant decrease in the pEC_{50} for ANGII in IPF cells was observed in the presence of both ANG(1-7) (7.70 ± 0.04 versus 7.21 ± 0.07); $p<0.01$) and ANG(1-9) (7.67 ± 0.07 versus 7.56 ± 0.07; $p<0.05$). A trend towards lower ANGIII pEC_{50} values was also observed in the presence of both inhibitors but this failed to reach significance.

Agonist	**pEC_{50}**	**Inhibitor**	**pEC_{50}**	**Statistically significant?**
ANGII	7.51 ± 0.08	ANG(1-7)	7.41 ± 0.10	No
ANGII	7.48 ± 0.09	ANG(1-9)	7.61 ± 0.10	No
ANGIII	7.31 ± 0.11	ANG(1-7)	7.06 ± 0.07	No
ANGIII	7.39 ± 0.08	ANG(1-9)	7.08 ± 0.06	No

Table 3-6. Effects of ANG(1-7) and ANG(1-9) on ANGII and ANGIII pEC_{50} values in healthy fibroblasts. Paired pEC_{50} values for ANGII in the presence and absence of ANG(1-7) and ANG(1-9) (n=3 and n=5 respectively) and for ANGIII in the presence and absence of ANG(1-7) and ANG(1-9) (n=4 and n=3 respectively). All data expressed as mean ± SEM

Agonist	**pEC_{50}**	**Inhibitor**	**pEC_{50}**	**Statistically significant?**
ANGII	7.70 ± 0.04	ANG(1-7)	7.21 ± 0.07	$p<0.05$
ANGII	7.67 ± 0.07	ANG(1-9)	7.56 ± 0.07	$p<0.01$
ANGIII	7.51 ± 0.20	ANG(1-7)	7.09 ± 0.10	No
ANGIII	7.51 ± 0.20	ANG(1-9)	7.48 ± 0.10	No

Table 3-7. Effects of ANG(1-7) and ANG(1-9) on ANGII and ANGIII pEC_{50} values in IPF fibroblasts. Paired pEC_{50} values for ANGII in the presence and absence of ANG(1-7) and ANG(1-9) (n=4 and n=3 respectively) and for ANGIII in the presence and absence of ANG(1-7) and ANG(1-9) (n=3). All data expressed as mean ± SEM.

3.3.4 Further investigations into the activity of ANG(1-7) and ANG(1-9).

To attempt to determine the site of action of ANG(1-7) and ANG(1-9), dose-response curves to ANGII in the presence of 10μM of either peptide were constructed, this time in the presence of 1μM PD-123319, 10μM A-779 or 10μM D-Pro^7-ANG(1-7) (ANG(1-7) receptor antagonist) (**Figure 3-7** and **Figure 3-8**).

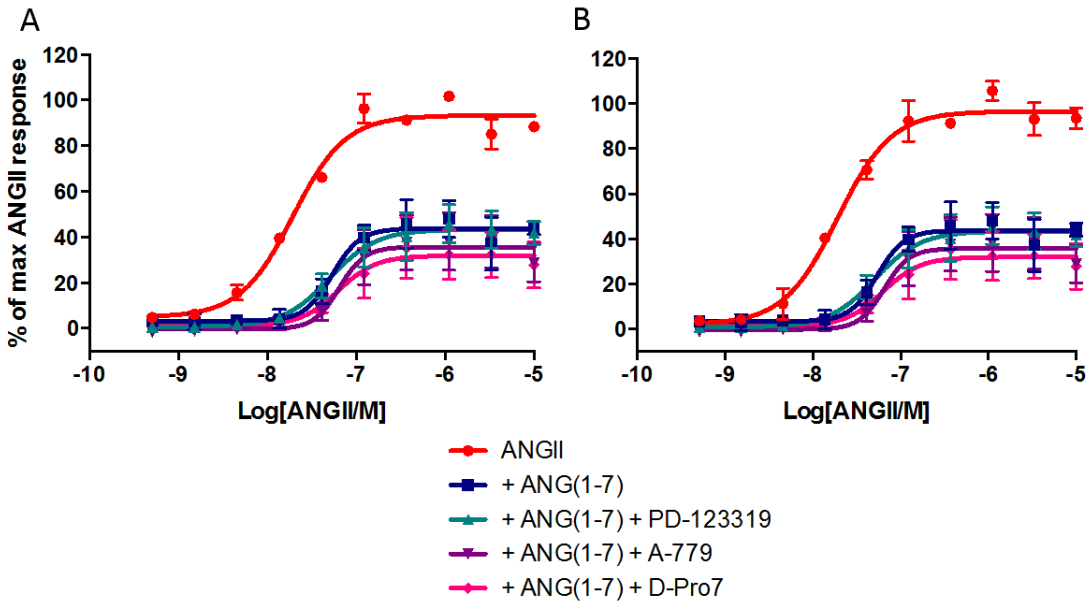

Figure 3-7. Effects of antagonists on ANG(1-7) induced inhibition. Dose response curves to ANGII were constructed in human lung fibroblasts following preincubation with PD-123319 (1μM), A-779 (10μM) or D-pro^7-ANG(1-7) (10μM) for 15 minutes, prior to subsequent pretreatment with ANG(1-7) (10μM) for a further 15 minutes. The inhibition of ANGII induced Ca^{2+} mobilisation observed in the presence of ANG(1-7) alone (dark blue) was not reversed in the presence of any of the three antagonists in either healthy (A) (n=1) or IPF fibroblasts (B) (n=3). ANGII control is shown in red. Data is expressed as percentage of the fitted maximum ANGII response, data in A is expressed as mean ± SEM for a single experiment run in duplicate, B is expressed as the pooled mean ± SEM from all experiments.

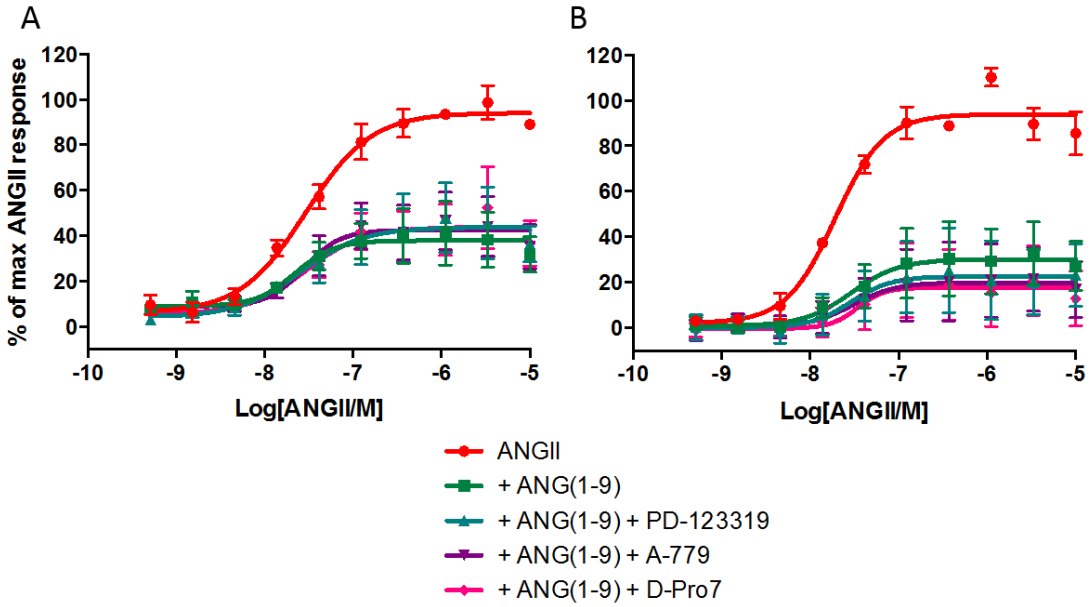

Figure 3-8. Effects of antagonists on ANG(1-9) induced inhibition. Dose response curves to ANGII were constructed in human lung fibroblasts following preincubation with PD-123319 (1μM), A-779 (10μM) or D-pro^7-ANG(1-7) (10μM) for 15 minutes, prior to subsequent pretreatment with ANG(1-9) (10μM) for a further 15 minutes. The inhibition of ANGII induced Ca^{2+} mobilisation observed in the presence of ANG(1-9) alone (dark green) was not reversed in the presence of any of the three antagonists in either healthy (A) (n=3) or IPF fibroblasts (B) (n=3). ANGII control is shown in red. Data is expressed as percentage of the fitted maximum ANGII response and are the pooled mean ± SEM from all experiments.

Of the three antagonists tested, none demonstrated the ability to reverse the inhibition caused by either ANG(1-7) or ANG(1-9), in either healthy or IPF fibroblasts.

To further characterise the activity of ANG(1-7) and ANG(1-9), inhibition curves to these peptides were constructed against three single concentrations of ANGII (0.1, 1 or 10μM). Inhibition curves were run in parallel to allow for potential shifts in the curve to be observed between different ANGII concentrations. ANG(1-9) inhibition curves in both healthy and IPF fibroblasts can be found in **Figure 3-9**, with pIC_{50} values of 5.54±0.09 and 5.49±0.3 (against 10μM ANGII) reported for healthy and IPF cells respectively. Similar pIC_{50} values were observed in the presence of 0.1 and 1μM ANGII (data not shown).

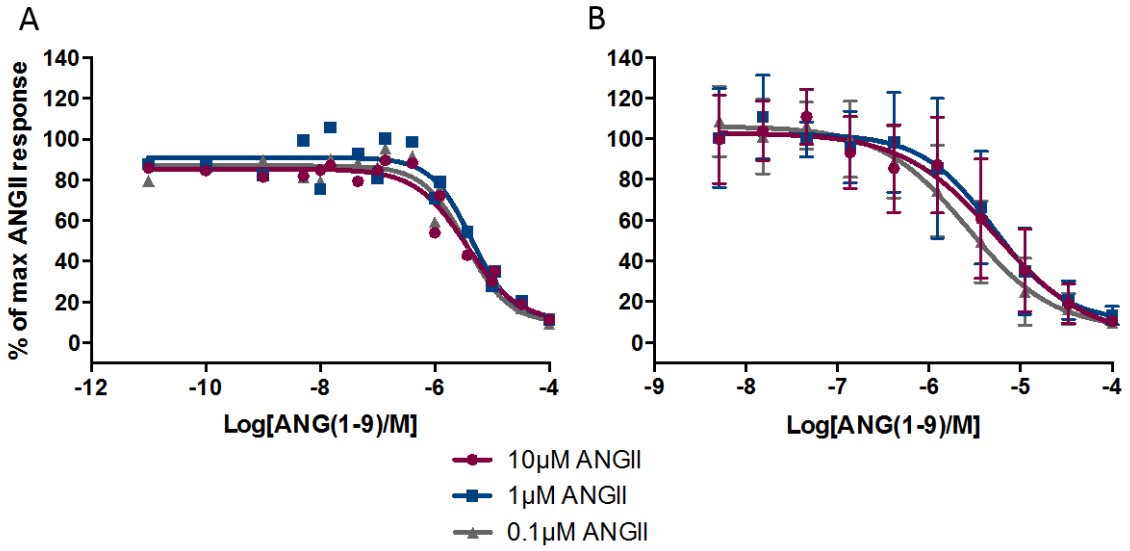

Figure 3-9. Inhibition curves to ANG(1-9). Human lung fibroblasts were pretreated with increasing concentrations of ANG(1-9) for 15 minutes before the addition of a single dose of ANGII at 0.1, 1 or 10μM. The response to the three ANGII concentrations was measured in both healthy (A) (n=3) and IPF fibroblasts (B) (n=3). All data are expressed as percentages of the fitted maximum ANGII response and are the pooled mean ± SEM from all experiments.

ANG(1-7) inhibition curves in IPF fibroblasts can be found in **Figure 3-10**, a pIC_{50} value of 5.71±0.25 for ANG(1-7) was reported in this cell type (against 10μM ANGII), with similar values again observed in the presence of 0.1 and 1μM ANGII (data not shown).

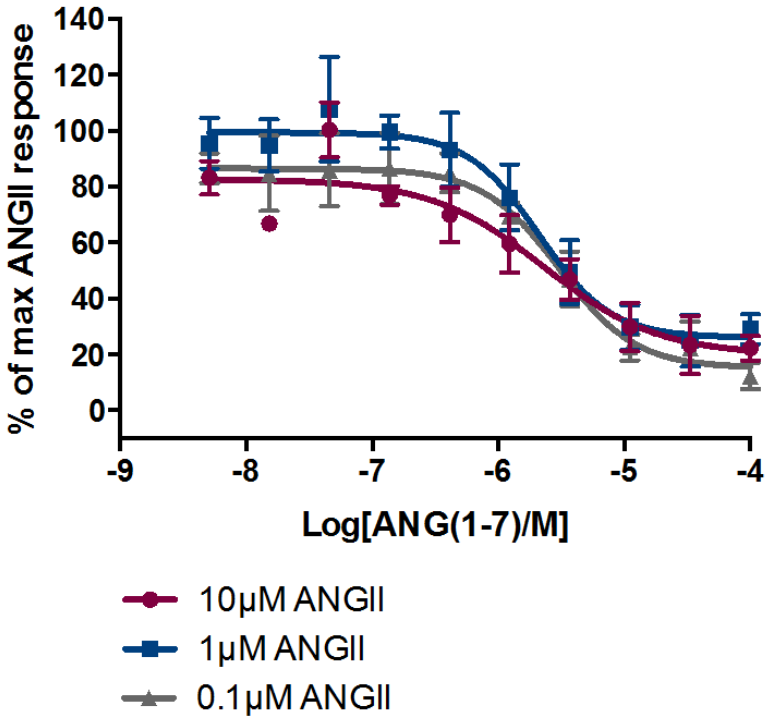

Figure 3-10. Inhibition curves to ANG(1-7). Human lung fibroblasts were pretreated with increasing concentrations of ANG(1-7) for 15 minutes before the addition of a single dose of ANGII at 0.1, 1 or 10µM. The response to the three ANGII concentrations was measured in IPF fibroblasts (n=3). All data are expressed as percentages of the fitted maximum ANGII response and are the pooled mean ± SEM from all experiments.

As ANG(1-9) is a known substrate for ACE (Schlüter and Wenzel, 2008), inhibition curves to ANG(1-9) against 10µM ANGII were constructed in the presence and absence of the ACE inhibitor captopril (100µM) (**Figure 3-11**). No change in the shape of the curve was observed in either healthy or IPF fibroblasts.

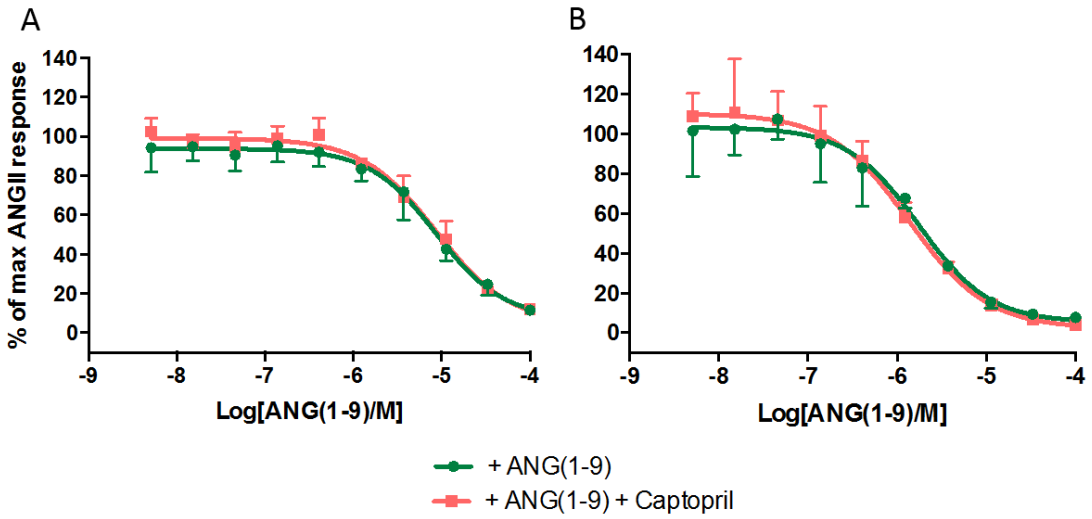

Figure 3-11. Inhibition curves to ANG(1-9) in the presence and absence of captopril. Human lung fibroblasts were pretreated with increasing concentrations of ANG(1-9) in the presence and absence of 100μM captopril before the subsequent addition of 10μM ANGII. Responses to ANGII were measured in healthy (A) (n=3) and IPF fibroblasts (B) (n=3). Data are expressed as percentages of the fitted maximum ANGII response and are the pooled mean ± SEM from all experiments.

3.3.5 Investigations into the activity of angiotensin I

As mentioned briefly in section 3.3.2, ANGI showed partial ability to mobilise calcium in both fibroblast cell types. Further investigations into the activity of this peptide were performed.

Pre-incubation of fibroblasts with ANGII for 15 minutes before the addition of a second dose of 10μM ANGII caused dose-dependent desensitisation of the Ca^{2+} response to the later dose of ANGII in both fibroblast types (**Figure 3-12**). ANGII desensitised the response by 91.25±0.65 and 94.76±5.07% in healthy and IPF cells respectively.

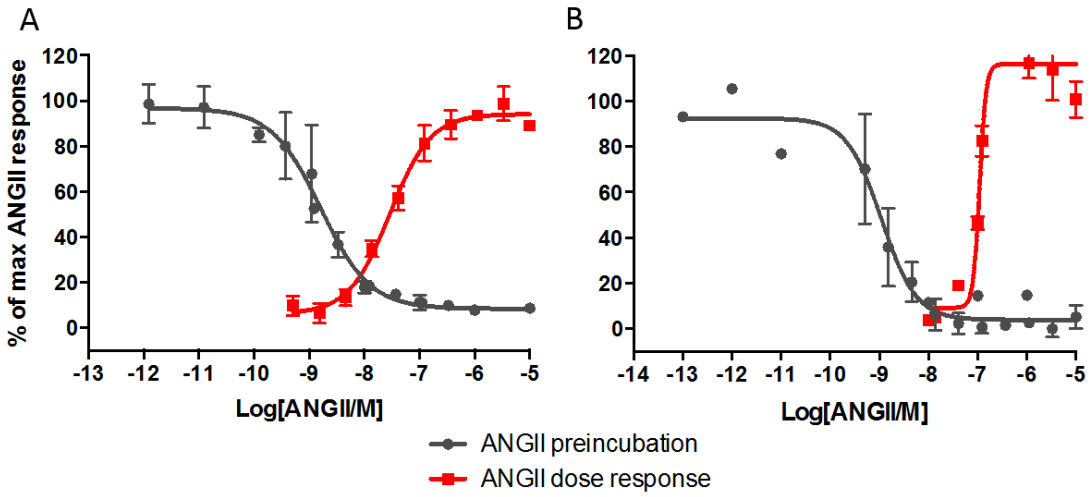

Figure 3-12. Desensitisation of the Ca^{2+} response to ANGII. Preincubation with increasing concentrations of ANGII caused desensitisation of the Ca^{2+} response to a subsequent dose of 10μM ANGII in both healthy (A) (n=3) and IPF fibroblasts (B) (n=3) (as indicated by grey line). Red line shows ANGII dose response control. Data are expressed as percentages of the fitted maximum ANGII response and are pooled mean ± SEM from all experiments.

Pre-incubation of fibroblasts with ANGI also showed a similar pattern of desensitisation of the response to 10μM ANGII in both healthy and IPF fibroblasts (91.8±1.11 and 96.6±1.46% respectively) as shown in **Figure 3-13**. No effect on the Ca^{2+} response was observed upon simultaneous addition of ANGI and ANGII.

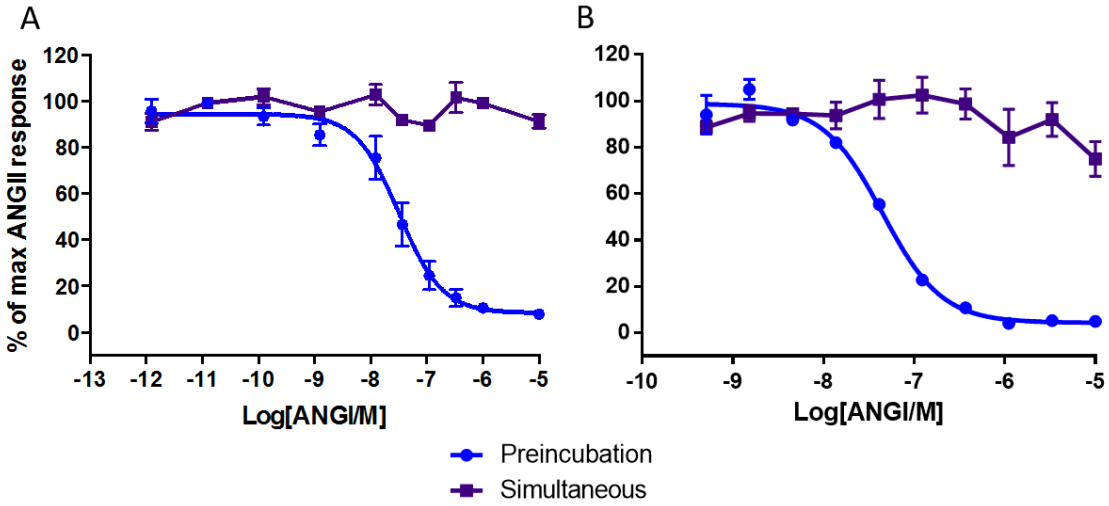

Figure 3-13. ANGI induced desensitisation of the Ca^{2+} response to ANGII. Preincubation with increasing concentrations of ANGI (light blue) caused desensitisation of the Ca^{2+} response to a subsequent dose of 10μM ANGII in both healthy (A) (n=3) and IPF fibroblasts (B) (n=3). ANGI had no effect on Ca^{2+} release in response to 10μM ANGII when added simultaneously (dark blue). Data are expressed as percentages of the fitted maximum ANGII response and are pooled mean ± SEM from all experiments.

To determine the role of ACE in the ability of ANGI to cause desensitisation, this experiment was repeated in the presence and absence of 100μM captopril (**Figure 3-14**).

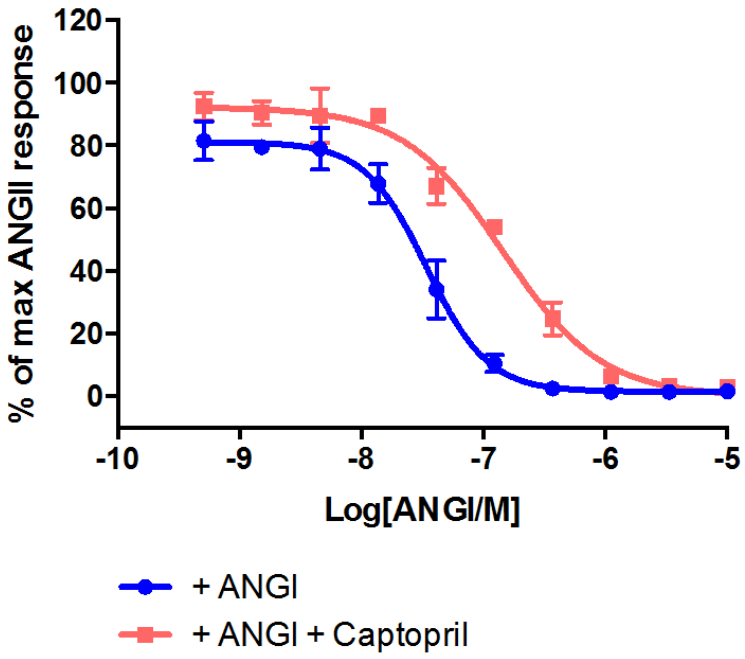

Figure 3-14. ANGI induced desensitisation of the Ca^{2+} response to ANGII in the presence and absence of captopril. Preincubation with increasing concentrations of ANGI followed by a single dose of 10μM ANGII was carried out in the presence and absence of 100μM captopril in IPF fibroblasts (n=2). Data are expressed as percentages of the fitted maximum ANGII response and are pooled mean ± SEM of all experiments.

The curve appeared to shift to the right in the presence of captopril, although these results are currently derived from two IPF fibroblast lines only so statistical comparison has not been performed.

Standard dose response curves to ANGI were also carried out in the presence and absence of 10μM captopril in both healthy and IPF fibroblasts (**Figure 3-15**).

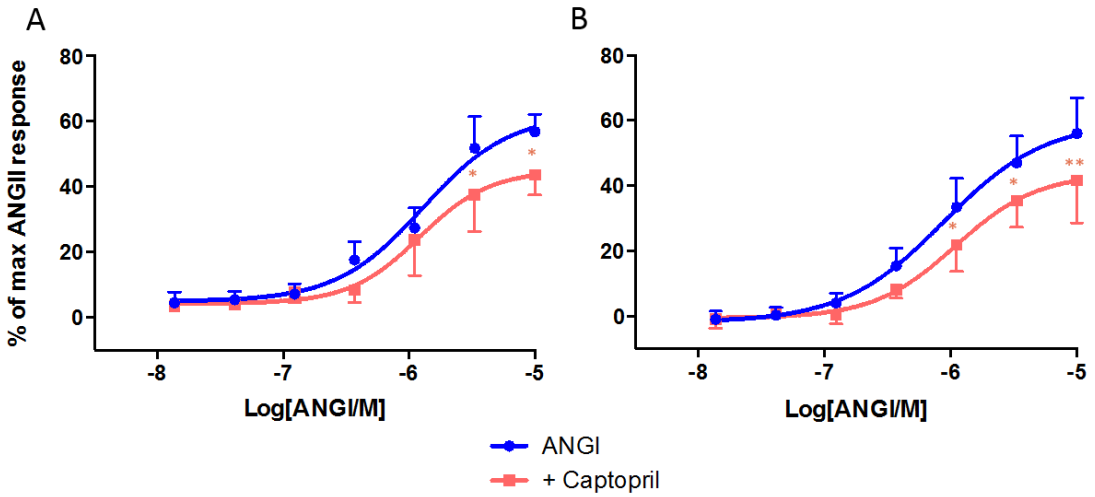

Figure 3-15. ANGI dose response curves in the presence and absence of captopril. Dose response curves to ANGI were carried out in the presence and absence of 100μM captopril in both healthy (n=3) (a) and IPF fibroblasts (n=4) (b) * indicates p<0.05, ** p<0.01 and ***p<0.001 when compared to ANGI alone (two way ANOVA). Data are expressed as percentages of the fitted maximum ANGII response and are mean ± SEM of all experiments.

The ANGI curve shifted to the right in the presence of captopril in both cell types. Also, lower responses to ANGI were observed in the presence of captopril in both healthy and IPF cells.

3.3.6 ERK Phosphorylation

As ANGII demonstrated consistent ability to induce intracellular Ca^{2+} release in HLFs, the ability of this peptide to induce ERK phosphorylation was investigated. This was to determine whether further downstream signalling pathways were activated following intracellular Ca^{2+} release.

Figure 3-16 shows a representative Western blot and **Figure 3-17** is the quantification of pooled data from three individual experiments.

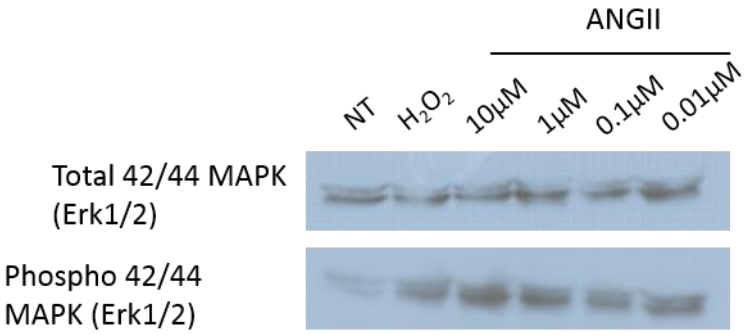

Figure 3-16. Western blot investigating ERK phosphorylation in response to ANGII. Representative Western blot showing the effects of ANGII on ERK phosphorylation. Human lung fibroblasts were incubated with 0.01 – 10μM ANGII or 8mM H_2O_2 (as a positive control) for 10 mins before cell lysate was analysed by Western blot.

ANGII demonstrated the ability to upregulate ERK phosphorylation at all concentrations tested, with both 1 and 10 μM phosphorylating ERK (4.19 ±1.95 and 3.79 ± 0.79 fold increase respectively) to a level similar to H_2O_2 (3.74 ± 0.94 fold increase from NT). ERK phosphorylation was still upregulated in the presence of 0.01 and 0.1μM ANGII but at a lower level than that observed with the higher ANGII concentrations.

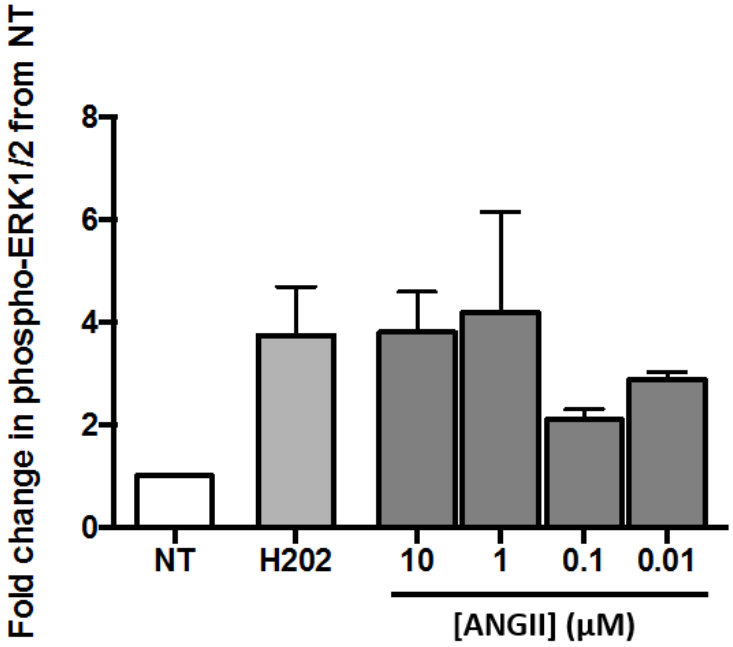

Figure 3-17. Western blot quantification. Quantification of Western blot shown in Figure 3-15. ANGII upregulated ERK phosphorylation at all concentrations tested, with the strongest upregulation observed in the presence of 1 and 10μM. H_2O_2 (8mM) was used as a positive control. Data shown are fold change from no treatment (NT) and mean ± SEM of three experiments.

3.4 Discussion

The main aim of this study was to determine the ability of eight ANG peptides to mobilise calcium in both healthy and IPF derived HLFs, and to determine the site of action of active peptides. The actions of these peptides have not been previously characterised in these cell types, and no difference in the effects of these peptides on healthy and IPF cells has been investigated.

Previous studies have shown that ANGII is able to mobilise calcium in human skin fibroblasts (Ceolotto *et al.*, 1998), this was also shown to be a purely AT_1R response, due to complete inhibition by losartan (AT_1R antagonist). The authors also reported no inhibition of the Ca^{2+} release in the presence of the AT_2R antagonist CGP42112A, indicating no AT_2R mediated response. These results were also confirmed in cardiac fibroblasts (Brilla *et al.*, 1998), where the AT_1R antagonist CV-11974 caused complete inhibition of ANGII induced Ca^{2+} mobilisation, with no effect observed in the presence of the AT_2R antagonist PD-123319. A pEC_{50} of 7.62 for ANGII was also reported in their investigation. These findings agree with the present study where a pEC_{50} of 7.67±0.01 was reported for ANGII in healthy lung fibroblasts and where the Ca^{2+} response to this peptide was completely inhibited by telmisartan (**Figure 3-4**), confirming that the response is mediated via AT_1R.

In another study (Ransom *et al.*, 1992), the ability of ANG peptides to mobilise calcium in neuroblastoma cells was tested. In this case, ANGI, ANGII and ANGIII were shown to mobilise calcium with pEC_{50} values of 6.36, 7.24 and 7.44 respectively. In the current study, pIC_{50} values of 5.87±0.17, 7.67±0.01 and 7.42±0.02 were reported for ANGI, ANGII and ANGIII respectively; these values are broadly similar to that from the on-going investigation, with ANGIII correlating particularly well. As ANGI acted as a fairly weak partial agonist in the present study, the top of the curve was not always well defined at the maximum concentration of 10μM. Ransom et al carried out ANGI dose response curves to a maximum concentration of 100μM, this could therefore provide better characterisation of the top of the dose response curve and hence provide a more accurate pEC_{50}. Ransom et al also demonstrated again, that ANGII and in this case ANGIII were mobilising Ca^{2+} via the AT_1 receptor (by the addition of AT_1R antagonist DUP-753). This again agrees with the findings from the current study, where telmisartan caused complete inhibition of the response to ANGIII (**Figure 3-4**). ANGIV showed no ability to mobilise calcium in the previous investigation (Ransom et al., 1992), whereas this peptide demonstrated weak ability to mobilise calcium in the existing study and also in a previous study (Chansel *et al.*, 2001), in rat mesangial cells. Chansel et al also demonstrated that ANGIV was inducing Ca^{2+} release via AT_1R and this was also confirmed in the present research. In the

current investigation, no inhibition of the calcium response to ANGI, ANGII, ANGIII and ANGIV was observed in the presence of either PD-123319 or A-779 (Mas receptor antagonist), demonstrating that no part of the Ca^{2+} response was due to either of these receptors. These results also indicate that neither AT_2R nor the Mas receptor negatively regulate Ca^{2+} signalling upon ANGII binding, as no increases in the response to ANGII were observed in the presence of the specific receptor antagonists.

ANG(1-5), ANG(1-7), ANG(1-9) and ANG(3-7) showed no ability to mobilise calcium in the present study. ANG(1-7) is the most studied of these peptides, and has been shown previously to have no effect on intracellular Ca^{2+} levels (Chansel *et al.*, 2001; Heitsch *et al.*, 2001); however the remaining three peptides and their effects on intracellular Ca^{2+} are relatively unexplored. To test whether any of these four peptides would act as antagonists in the existing study, fibroblasts were pre-incubated with 10μM of each peptide 15 minutes before the addition of either ANGII or ANGIII. In this assay, both ANG(1-7) and ANG(1-9) demonstrated the ability to partially inhibit the Ca^{2+} response to both ANGII and ANGIII (**Figure 3-5** and **Figure 3-6**). This finding correlates well with the previous research by Chansel et al, where ANG(1-7) was shown to inhibit the Ca^{2+} response to ANGII. Although as with the current research this was observed at high concentrations, with the authors only reporting significant inhibition ($p<0.05$) at 1μM ANG(1-7) and above, at 10μM ANG(1-7) the response to ANGII was still only partially inhibited. The mechanism of inhibition by ANG(1-7) was however, not investigated. The authors also demonstrated the ability of ANG(1-7) to completely inhibit the Ca^{2+} response to ANGIV, however this was not investigated in the current study. No comparable investigations into the activity of ANG(1-9) are currently available in the literature.

In a recent study on transfected HeLa cells (Flores-Muñoz *et al.*, 2011), radioligand binding studies showed that both ANG(1-7) and ANG(1-9) were capable of binding AT_2R, with pK_i values of 7.02 ± 0.14 and 6.28 ± 0.1 respectively. The authors also demonstrated that in rabbit cardiomyocytes, ANGII induced hypertrophy via AT_1R, whereas ANG(1-9) antagonised this hypertrophy via AT_2R. ANG(1-7) was also able to inhibit this ANGII induced hypertrophy but this was shown to be via the Mas receptor. ANG(1-7) has also been shown to bind AT_2R in competitive binding studies (Bosnyak *et al.*, 2011) with a pIC_{50} value of 6.61 reported for this peptide. To investigate whether in the present study ANG(1-7) or ANG(1-9) were causing inhibition of the Ca^{2+} response via AT_2R, Mas or the newly proposed ANG(1-7) receptor (discussed in section 1.5.2), ANGII dose response curves in the presence of either 10μM ANG(1-7) or ANG(1-9) were performed in the presence of PD-123319, A-779 or D-Pro^7-ANG(1-7) (**Figure 3-7** and **Figure 3-8**). No reversal of the inhibition caused by ANG(1-7) or ANG(1-9) was

observed in the presence of any of these inhibitors. From these results it was determined that neither ANG(1-7) nor ANG(1-9) were inducing inhibition via any of these three receptors.

To further characterise the inhibition observed and to attempt to determine whether ANG(1-7) or ANG(1-9) were competitively antagonising AT_1R, inhibition curves to these peptides were performed against 3 concentrations of ANGII (0.1, 1 and 10μM) (**Figure 3-9** and **Figure 3-10**). Competitive antagonism is characterised by a right shift in the inhibition curve at higher agonist concentrations (Cheng and Prusoff, 1973; Wyllie and Chen, 2007); however this shift was not observed for either ANG(1-7) or ANG(1-9), indicating that neither of these peptides were acting via simple competitive antagonism at AT_1R. For ANG(1-9), pIC_{50} values of 5.54±0.09 and 5.50±0.30 were recorded (against 10μM ANGII) in healthy and IPF cells respectively. A pIC_{50} value of 5.71±0.25 was recorded for ANG(1-7) (against 10μM ANGII) in IPF derived fibroblasts.

Also, competitive antagonists abide by the Cheng-Prusoff equation (Cheng and Prusoff, 1973; Lazareno and Birdsall, 1993) (**Equation 3-1**); when analysing the results obtained in these experiments, it becomes clear that this data does not fit this model well.

$$K_i = \frac{IC_{50}}{\frac{[A]}{EC_{50}} + 1}$$

Equation 3-1. Cheng-Prusoff equation. Cheng-Prusoff equation for competitive antagonism. K_i = Inhibition constant of antagonist (concentration of antagonist required to occupy half the receptors in the absence of agonist), *[A]* = Fixed agonist concentration, EC_{50} = Concentration of agonist causing 50% of maximal response. IC_{50} = Concentration of antagonist causing 50% of inhibitory effect.

No significant differences in the pIC_{50} values of either ANG(1-7) or ANG(1-9) were observed in the presence of varying concentrations of ANGII (0.1 and 1μM). As EC_{50} and K_i values remain constant, any change in the concentration of ANGII *[A]* should equate to a change in the IC_{50} of the antagonist. As this did not occur in the current experiments, it is very unlikely that either ANG(1-7) or ANG(1-9) are acting as competitive antagonists.

The potential non-competitive activity of ANG(1-7) observed is reinforced by previous investigations (Roks *et al.*, 1999), where 10μM ANG(1-7) was shown to inhibit ANGII induced arterial contractions by up to 60% in a non-competitive manner at AT_1R. This finding appears to correlate well with the results observed in the present study although the physiological relevance of these results may be questioned, as the effects of ANG(1-7) (and ANG(1-9)) occur at very high concentrations, not only in the present study but also in the studies by Roks et al and Chansel et al, when compared to the human plasma concentrations shown in **Table 3-8**

(Lawrence *et al.*, 1990; Matsui *et al.*, 1999). However, circulating plasma concentrations of these peptides are likely to be lower than that of pulmonary tissue, where the local RAS system comes into play, this local RAS system may also be up-regulated in lungs of patients with IPF (Li *et al.*, 2006).

Peptide	**Human plasma concentration (pM)**
ANGI	19.5±2.4 – 304±43
ANGII	13.9±2.0 - 32±6.0
ANGIII	2.9±1.0
ANGIV	>30
ANG(1-7)	1.0±0.2
ANG(1-9)	<2.1

Table 3-8. Human plasma concentrations of angiotensin peptides. Circulating human plasma concentrations from normotensive male subjects. (Lawrence *et al.*, 1990; Matsui *et al.*, 1999).

As ANG(1-9) does not appear to be acting via AT_1R, AT_2R, the Mas or ANG(1-7) receptor in either healthy or IPF cells, these results indicate that there is a further unknown site capable of binding ANG(1-9). From the results obtained in IPF fibroblasts, ANG(1-7) also appears to be acting via an uncharacterised novel binding site. Further investigation is required to determine the site of action of these peptides, and whether they are acting via the same binding site.

ANGI appeared to act as a partial agonist in this assay, with a maximum response of 54.9 ± 6.4% and 53.6 ± 10.9% of the ANGII response in healthy and IPF cells respectively. To determine whether ANGI was being broken down to ANGII over the course of the experiment, the ability of ANGI to cause desensitisation of the response to ANGII was investigated. This was tested as pre-incubation with ANGII was able to desensitise the response to a subsequent addition of ANGII (10μM) by 91.3 ± 0.65 and 94.8 ± 5.07% in healthy and IPF cells respectively (**Figure 3-12**). This mechanism of desensitisation could be due to internalisation of AT_1R, as this receptor is known to internalise when stimulated with ANGII (Hunyady *et al.*, 2000) or could be due to depletion of intracellular calcium stores. When added 15 minutes before the addition of ANGII, ANGI appeared to cause a similar, dose-dependent desensitisation to 10μM ANGII (91.8 ± 1.11 and 96.6 ± 1.46% in healthy and IPF cells respectively). When added simultaneously, ANGI appeared to have no effect on the response to 10μM ANGII at any of the

concentrations tested (**Figure 3-13**), indicating that this peptide was not competing for AT_1R in a simple manner. This was further confirmed, as a complete reduction in the ANGII response was observed in the presence of ANGI, whereas if competition were occurring, the ANGII response would only decrease to the point of the maximal ANGI response, due to the partial agonist characteristics of this peptide (Ariëns, 1983).

As these results suggest that ANGI was behaving in a similar manner to ANGII (indicating a breakdown of ANGI to ANGII), this desensitisation experiment was repeated in the presence of the ACE inhibitor captopril (**Figure 3-14**). The curve appears to shift to the right in the presence of captopril, indicating that the activity of ANGI is decreasing; although these results are currently derived from two IPF cell lines only, so further repeats are needed to confirm this result in both healthy and IPF cells. Simple dose response curves to ANGI in the presence and absence of 100μM captopril were also performed in both cell types (**Figure 3-15**), and as observed in **Figure 3-14** the curve shifted to the right in the presence of captopril, again demonstrating that the activity of ANGI is decreasing. ANGI dose response curves with captopril are statistically different from ANGI alone when compared with a two-way ANOVA in both healthy and IPF fibroblasts ($p<0.05$ in both cell types). These results indicate that both healthy and IPF fibroblasts may be locally producing ACE, which is, at least in part, responsible for the partial agonist characteristics of ANGI in this assay. If the Ca^{2+} mobilisation observed with this peptide is in fact due to cleavage to ANGII by ACE, then the factor limiting the production of ANGII is the amount of ACE present; in this system it is likely that ACE quickly becomes saturated by high concentrations of ANGI and therefore only a finite amount of ANGII is produced over the course of the experiment, giving rise to the partial Ca^{2+} response observed.

It has been demonstrated previously, that rat neonatal cardiac fibroblasts produce ACE in culture (van Kesteren *et al.*, 1999). In this study, ANGI was added to fibroblasts after 5 days of culture, with high levels of ANGII clearly detectable in the media within 10 minutes. The authors also reported a complete inhibition of this ANGII production in the presence of captopril, although in the present study captopril only partially inhibited the agonistic response to ANGI. In the previous study, captopril was used at a concentration of 500μM, which is higher than concentration of 100μM in the current study. Also in the present experiments, culture media is replaced with experimental buffer; this removes any ACE that may have been secreted into the media. Cell bound ACE has been demonstrated in human cardiac fibroblasts (Hafizi *et al.*, 1998), and this is likely to be the source of ACE in the current investigation.

When comparing the pEC_{50} values of ANGI, ANGII and ANGIII in the present study, no differences were observed between healthy and IPF fibroblasts. **Table 3-2** compiles pEC_{50} values

of the active peptides in this study. The maximal responses to ANGI, ANGII and ANGIII did however reach statistically significant difference between healthy and IPF cells, with responses in IPF cells consistently lower than those of healthy cells, details of which can be found in **Table 3-3**. No data for ANGIV is included in either **Table 3-2** or **Table 3-3**, as this peptide acted as an extremely weak agonist and therefore characterisation of dose-response curves to this peptide was not possible.

In the present study, no difference in the mechanism of action of any of the four active peptides was observed between healthy and IPF fibroblasts, with telmisartan causing complete inhibition of the Ca^{2+} response to all peptides in both cell types. This demonstrates that AT_1R is responsible for Ca^{2+} mobilisation in all cases. In a study investigating the differences in ANG receptor expression between healthy and IPF lungs (Königshoff *et al.*, 2007), an upregulation of both AT_1R and AT_2R was observed in IPF lungs, with staining for both receptor subtypes observed within fibroblastic foci. The same group also demonstrated that cell surface expression of AT_2R was upregulated in mouse fibrotic lung fibroblasts when compared to healthy lung fibroblasts, and also that AT_2R played a more important role in the signalling in this cell type. The authors also observed higher basal levels of proliferation and migration in fibrotic lung fibroblasts (regardless of ANGII addition) and saw that these were completely inhibited by PD-123319 but unaffected by losartan. These findings do not correlate well with the results from the current study, where no AT_2R mediated effects were observed in IPF fibroblasts. Although species variation needs to be considered, this may provide an explanation as to why Ca^{2+} responses in IPF fibroblasts are lower than that of healthy fibroblasts, as the results from Königshoff et al indicate that fibrotic fibroblasts could be locally producing ANGII and therefore this cell type could be partially desensitised to further stimulation with this peptide. This could be further investigated by Western blotting using antibodies for ANGII, or via PCR to look at ANGII mRNA levels. A previous investigation by Uhal et al (Uhal *et al.*, 2007) demonstrated that IPF derived fibroblasts express higher levels of angiotensinogen (AGT) mRNA and protein than HLFs. Renin mRNA levels have also been shown to be upregulated in IPF fibroblasts compared to HLFs (Montes *et al.*, 2012); these high levels of both AGT and renin could lead to a high breakdown of AGT in this cell type, leading to increased levels of ANGI, and eventually ANGII (due to ACE cleavage). This adds further weight to the hypothesis that IPF fibroblasts are partially desensitised to ANGII stimulation, due to a more active RAS in these cells.

In order to determine whether any processes known to be downstream of intracellular Ca^{2+} release were also activated. The ability of ANGII to induce ERK1/2 phosphorylation was explored (**Figure 3-16**). ANGII resulted in ERK1/2 phosphorylation, with a maximum effect

observed at 1μM (4.19 ±1.95 fold increase from NT). No further increase in ERK1/2 phosphorylation was observed in the presence of 10μM ANGII.

Many previous studies have demonstrated the ability of ANGII to cause ERK1/2 phosphorylation with maximum effects observed as quickly as 5 minutes in adult and neonatal rat cardiac fibroblasts (Sano *et al.*, 2001; Olson *et al.*, 2008). Lang et al (Lang *et al.*, 2010) showed an increase in ERK1/2 phosphorylation in response to 10μM ANGII, that was maintained until at least 1 hour after treatment in the MRC-5 human fibroblast cell line. The effects of ANGII on ERK1/2 phosphorylation in primary HLFs is extremely limited.

ERK1/2 phosphorylation has been shown to be downstream of intracellular Ca^{2+} signalling, increases in intracellular Ca^{2+} can be detected by the calcium binding protein calmodulin. Calmodulin is able to bind two molecules of Ca^{2+} and this calcium-calmodulin complex is then able to activate CaMKs (discussed in section 3.1). ANGII has been shown, at least in part, to induce ERK1/2 phosphorylation via CaMKII activation. Abraham et al (Abraham *et al.*, 1997) demonstrated a 60% inhibition of ANGII induced ERK1/2 phosphorylation in the presence of the CaMKII inhibitor KN-93 in rat VSMCs.

In studies involving fibroblasts, CaMKII inhibition has reduced cell proliferation (Martin *et al.*, 2014), ECM deposition and TGF-β1 secretion (Zhang *et al.*, 2010) in response to ANGII, further providing evidence for the importance of CaMKII in this signalling pathway. These two studies were, however, performed in mouse and rat cardiac fibroblasts respectively and differences may exist between rodent and human fibroblasts.

Another mechanism by which Ca^{2+} is able to induce ERK1/2 phosphorylation is via PKC. ANGII has been shown to induce phosphorylation in fibroblasts by two parallel mechanisms, a Ca^{2+} dependent, PKC independent pathway and a separate PKC dependent pathway (Booz *et al.*, 1994), ERK1/2 phosphorylation was only completely inhibited upon both buffering intracellular Ca^{2+} and inhibiting PKC simultaneously. Olson et al also confirmed ERK1/2 phosphorylation by ANGII was via these two parallel pathways, with inhibition of both required to completely knockdown the ANGII response. Booz et al also concluded that ERK1/2 phosphorylation alone was not sufficient to induce mitogenesis in the cell line under investigation (rat neonatal cardiac fibroblasts). This observation has also been backed up by a more recent study in adult human cardiac fibroblasts (Hou *et al.*, 2000), where ANGII induced protein synthesis and whilst being dependent a on PKC/Ca^{2+} signalling pathway, was not dependent on MAPKK, the kinase responsible for ERK1/2 activation. It is perfectly feasible, however, that ERK may be responsible for other cellular processes such as cell differentiation and collagen deposition in these circumstances.

Many previous studies into the profibrotic characteristics of the RAS have been focused on ANGII with little investigation into related ANG peptides. ANG(1-7) has however been shown recently in a number of studies to be antifibrotic (Uhal *et al.*, 2012). The results from the on-going investigation suggest that there are many other peptides in this system that may play a role locally in fibrosis, with ANGIII causing Ca^{2+} release in a manner similar to ANGII and two peptides (ANG(1-9) and ANG(1-7)) demonstrating the ability to partially inhibit Ca^{2+} release in this assay. This inhibition also appears to be occurring via a novel binding site that has not yet been characterised. It has also been indicated that both fibroblast types may be locally producing ACE and therefore may be capable of producing ANGII locally. This system may therefore play an important role in the pathogenesis of IPF and may provide beneficial therapeutic targets in the future.

Chapter 4. Effects of angiotensin peptides on human lung fibroblast function

4.1 Background

Many of the factors produced by fibroblasts play important roles in IPF disease progression. As discussed in section 1.2, dysregulated collagen production has been observed in the IPF lung (Fulmer *et al.*, 1980), which may be due to high enzymatic breakdown of already existing ECM. This subsequently produced, disorganised collagen structure becomes difficult to degrade, further driving lung fibrosis. One of the main enzymes responsible for the degradation of the structural type I and III collagens is MMP-1. Increases in MMP-1 have been reported in the IPF lung, with Selman et al (Selman *et al.*, 2000) hypothesising that this MMP plays an important role in the honeycombing features of IPF. Decreases in MMP-1 production by fibroblasts have been observed in the presence of TGF-β1 (section 1.3), lower levels of this enzyme would lead to less collagen degradation and also drive the fibrotic response. Increases in fibroblast number by proliferation or reduced apoptosis may also drive increased collagen deposition.

Increases in MMP-2 levels have also been observed in subepithelial myofibroblasts in IPF, close to areas of basement membrane degradation (Selman *et al.*, 2000). One substrate for MMP-2 is collagen type IV (Zeng *et al.*, 1999), which is an integral component of the basement membrane, disruption of which may lead to a dysregulated wound healing response. TGF-β1 has been shown in a number of studies to upregulate MMP-2 expression in human fibroblasts (Asano *et al.*, 2010; Lee *et al.*, 2010).

Elevated levels of IL-6 have also been observed in the lungs of patients with IPF, and activation of soluble IL-6Rα in mice induces increased fibroblast proliferation and collagen deposition (Le *et al.*, 2014). IL-6 has also been shown to differentially affect lung fibroblast proliferation, causing senescence of healthy HLFs and proliferation of fibroblasts derived from the IPF lung (Moodley *et al.*, 2003b).

ANGII is thought to modulate many of these factors, although literature is inconsistent on the effects of this peptide on fibroblast proliferation and collagen deposition. Little investigation into the effect of ANGII on HLFs has been performed, Marshall et al demonstrated an increase in HLF proliferation and collagen deposition (Marshall *et al.*, 2000; Marshall *et al.*, 2004), although most of this work was performed in a foetal lung fibroblast line and may not be representative of the adult primary lung fibroblast. Other studies in human cardiac fibroblasts have proved controversial and are discussed in detail in section 1.6.1.

ANGII has been shown to downregulate MMP-1 and MMP-2 but to upregulate MMP-9 in human cardiac fibroblasts (Pan *et al.*, 2008), however, most investigations into MMP production have been performed in murine fibroblasts. ANGII has been shown to reduce expression of the

gelatinases MMP-2 and MMP-9 in mouse cardiac fibroblasts (Stacy *et al.*, 2007) and also to reduce MMP-1 levels in rat cardiac fibroblasts (Chen *et al.*, 2004).

The effects of ANGII on IL-6 secretion is also limited and most of this work is performed in rodent fibroblasts, with ANGII inducing IL-6 expression in rat cardiac fibroblasts at both the mRNA and protein level (Sano *et al.*, 2000).

The AT_1 receptor is thought to be responsible for the profibrotic effects of ANGII, and many of the effects of this peptide (most noticeably collagen production) are widely accepted to be via induction of TGF-β1. A feedback loop between these two proteins has been hypothesised (Uhal *et al.*, 2007) and TGF-β1 has been shown to upregulate AT_1R mRNA and protein expression on primary HLFs (Renzoni *et al.*, 2004).

Studies into the effects of ANG(1-7) on the factors discussed above are extremely limited. ANG(1-7) has been shown to exert antifibrotic effects via the Mas receptor, however, most investigations into cell number and collagen production have been performed in rodent cardiac fibroblasts. Decreases in proliferation (McCollum *et al.*, 2012) and collagen deposition (Iwata *et al.*, 2005) have been observed in the presence of ANG(1-7) in rat cardiac fibroblasts, with these effects confirmed to be via the Mas receptor. ANG(1-7) has been shown to reduce MMP-9 levels in human cardiac fibroblasts (via the Mas receptor) and also to antagonise ANGII induced increases in MMP-9 (Pan *et al.*, 2008).

The ACE inhibitor captopril has also been shown to modulate fibroblast functions, Chen et al (Chen *et al.*, 2014) demonstrated a decrease in 10% FBS induced collagen deposition, TGF-β1 and PDGF secretion in primary human keloid fibroblasts. The ability of TGF-β1 to induce expression of ACE in rat cardiac fibroblasts has also been demonstrated (Petrov *et al.*, 2000), indicating that some of the effects of TGF-β1 may be via increased endogenous production of ANGII.

The effects of ANGII and ANG(1-7) on HLF function is relatively unexplored, therefore the functional response to both of these peptides in healthy HLFs will be explored in this chapter. The effects of captopril and telmisartan on fibroblast functions will also be examined to determine if there is any endogenous RAS activity in culture. The effect of PD-123319 on captopril modulated functions will also be investigated to determine any AT_2R mediated mechanisms.

4.2 Protocols

4.2.1 Patient characteristics

The fibroblasts that were used in this chapter were derived from patients undergoing surgery at Southampton General Hospital (as described in section 2.3.1). The below table summarises the patient characteristics of the donors from which these cells were isolated. Further details on the donors used for each experiment can be found in the Appendix.

Age	**63.4 ± 2.2 years**
Male / Female	**24 / 26**
Surgery - Bullectomy / Lobectomy	**5 / 55**
ACEi / AT_1R prescriptions	**10 / 4**
Smoking status - Current / Ex / Non / Cannabis	**12 / 31 / 6 / 1**
FEV_1/FVC	**>0.7**

Table 4-1. Summary of patient characteristics. Characteristics of the donors from which fibroblasts were isolated for functional studies.

4.2.2 Angiotensin II

To measure proliferation, cells were treated with 0.1, 1 or 10μM ANGII or 2ng/ml active TGF-β1 and cell number measured as described in section 2.6. The effects of serum starvation and the presence of different serum concentrations on ANGII and TGF-β1 effects were also investigated and are discussed in the results below.

To explore the interaction between ANGII and TGF-β1 in collagen experiments, HLFs were treated with 1nM - 10μM ANGII following a 16 hour pretreatment with either 2ng/ml active TGF-β1 or 0.5% NCS. Cells were also treated with 0.01 – 2ng/ml TGF-β1 in the presence and absence of 10μM ANGII. Cells were maintained as described in section 2.7 and collagen measured after 6 days.

To investigate MMP-2 and MMP-9, cells were treated with 0.1nM to 10μM ANGII or 2ng/ml TGF-β1 and supernatants were harvested at 48 hours before being run through gelatin zymography according to section 2.8.

For IL-6, MMP-1, latency associated peptide (LAP) and TGF-β1, cells were treated with 0.1 - 10μM ANGII or 2ng/ml TGF-β1. Supernatants were harvested at 24, 48 and 72 hours and run through sandwich ELISAs for the target protein (according to section 2.9).

4.2.3 Angiotensin(1-7)

In proliferation experiments, cells were incubated with 10% NCS in the presence and absence of 1 or 10μM ANG(1-7). To determine any Mas receptor effects, these experiments were also performed in the presence and absence of 10μM A-779 (added simultaneously with ANG(1-7)).

Collagen production in the presence of 0.5 – 10% NCS or 2ng/ml TGF-β1 was measured in the presence and absence of 0.1, 1 and 10μM ANG(1-7) (treatments added in unison). The effect of 10μM A-779 on the TGF-β1/ANG(1-7) collagen response was also explored. Collagen deposition in response to 2ng/ml TGF-β1 was also measured following a 16 hour preincubation with 1μM ANG(1-7), with ANG(1-7) also reintroduced upon TGF-β1 addition.

4.2.4 Angiotensin inhibitors

To investigate the potential presence of an endogenous angiotensin system in culture, the effects of angiotensin inhibitors on fibroblast functions were explored.

For collagen experiments HLFs were seeded in soton DMEM in the presence and absence of 100μM captopril (to prevent cleavage of any endogenous ANGI to ANGII) or 10nM or 1μM telmisartan (to block any endogenous ANGII from binding to AT_1R), before reintroducing the inhibitor in the presence of 0.5% NCS and cells were maintained for 6 days as described.

For IL-6, MMP-1 and TGF-β1 experiments, cells were treated with 0.5% NCS, 10% NCS or 2ng/ml TGF-β1 alone or in the presence of, 100μM captopril, 100μM captopril plus 1μM PD-123319 or 10nM telmisartan alone. Supernatants were harvested at 24 and 48 hours before being run through sandwich ELISAs.

The effects of inhibitors on 0.5% NCS were to investigate whether there were any endogenous RAS peptides present at basal conditions. The ability of inhibitors to modulate 10% NCS activity were explored to determine if any effects observed with 10% serum could be attributed to the presence of higher levels of ANG peptides. TGF-β1 functions were also investigated in the presence of RAS antagonists, to determine if any of the observed changes with this cytokine were via induced ANGII activity. TGF-β1 has been shown to upregulate both AT_1R on human lung fibroblasts (Renzoni *et al.*, 2004) and ACE expression in rat cardiac fibroblasts (Petrov *et al.*, 2000).

4.3 Results

Each individual replicate in this chapter represents one experiment performed with fibroblasts from one donor in duplicate.

For experiments that were run over multiple time points, i.e. 24, 48 and 72 hours, any donors that were used for the longer time points were also used at the lower time points. E.g. any fibroblasts that were tested at 72 hours were also tested at shorted time points. Not all donors that were used for 24 or 48 hours were continued to longer time points, usually due to low cell number when plating for experiments. Samples sizes are detailed in figure legends.

4.3.1 Angiotensin peptides and human lung fibroblast function

First the effects of the angiotensin peptides ANGII and ANG(1-7) on a wide variety of fibroblast functions were explored and results are presented below.

4.3.1.1 Proliferation

The effect of ANG peptides on fibroblast proliferation was the first factor to be explored. Increased cell number can lead to higher production of many of the profibrotic factors released by HLFs, such as MMPs and collagen.

A number of experimental parameters were altered to determine the most optimal conditions for this investigation. The first experiments were performed in HLFs that were serum starved for 24 hours prior to ANGII treatment in serum free media (**Figure 4-1**A), TGF-β1 (2ng/ml) was used as a positive control for all proliferation experiments.

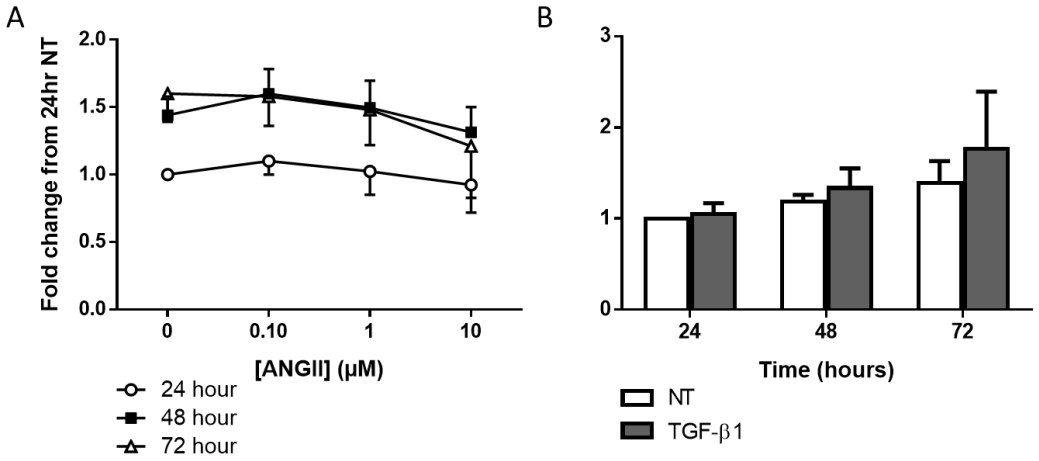

Figure 4-1. Initial proliferation experiments in serum free media. Human lung fibroblasts were serum starved overnight before treatment with either 0.1-10μM ANGII (**A**) or 2ng/ml TGF-β1 (**B**). Cells were then fixed at 24 (n=4), 48 (n=4) or 72 hours (n=3) and cell number measured with bromophenol blue. Data expressed are fold change from 24 hr no treatment (NT) and are pooled mean ± SEM of all experiments (Wilcoxon matched-pairs signed rank test).

Neither ANGII (at 0.1, 1 or 10μM) nor TGF-β1 induced proliferation of HLFs under these conditions. The lack of serum in these experiments also appeared to be detrimental to cell viability, HLFs were seeded at $1x10^4$ cells per well, however, the mean cell number recorded at 24 hours ranged from $5.61 \pm 1.38x10^3$ (no ANGII) to $6.36 \pm 1.83x10^3$ (0.1μM ANGII) indicating high levels of cell death in the initial steps of this experiment.

A number of other conditions, such as cell seeding density (0.5 - $1x10^4$ cells per well) and serum concentration present during the experiment (1 – 10%) were investigated (data not shown). The only experimental conditions that appeared to yield a positive effect of ANGII on HLF proliferation were, no serum starvation, followed by ANGII treatment in the presence of 10% NCS (**Figure 4-2**).

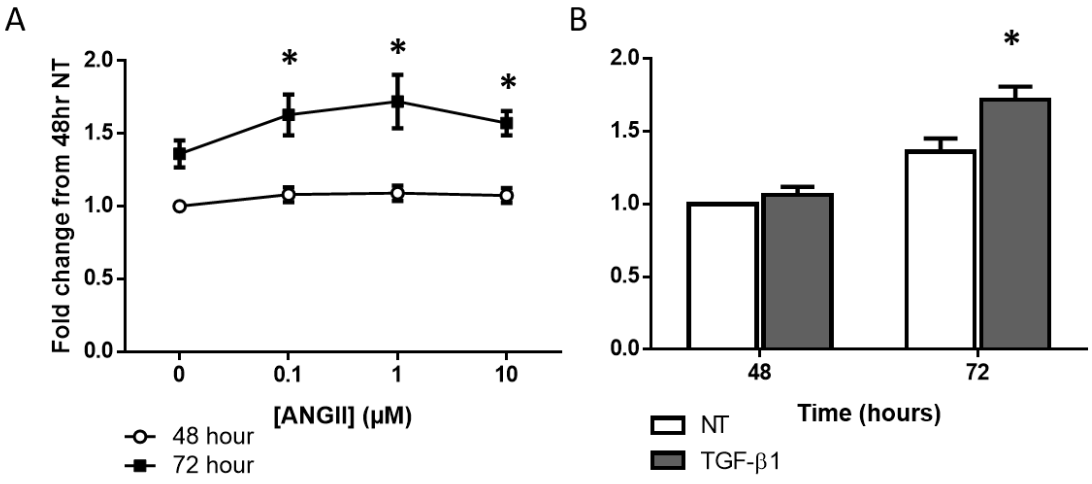

Figure 4-2. The effect of ANGII on human lung fibroblast proliferation in the presence of 10% newborn calf serum. Human lung fibroblasts were incubated overnight in 10% newborn calf serum (NCS) before treatment with either 0.1-10μM ANGII (**A**) or 2ng/ml TGF-β1 (**B**) in the presence of 10% NCS. Cells were fixed at 48 (n=6) and 72 hours (n=6) and cell count measured with bromophenol blue. Data expressed are fold change from 48hr no treatment (NT) and are pooled mean ± SEM of all experiments. *p<0.05 compared to 72 hr NT (Wilcoxon matched-pairs signed rank test).

These experimental conditions promoted baseline cell proliferation, with $15.5 \pm 3.0x10^4$ cells per well measured at 24 hour NT, an increase of 54.7 ± 30.2% from initial cell seeding density. Both ANGII and TGF-β1 appeared to upregulate proliferation at 72 hours under these conditions, with a maximum increase of 72.1 ± 6.80% (n=6) observed with 1μM ANGII (compared to 72 hour NT).

These experiments were the first with no serum starvation step, and were therefore repeated with the concentration of NCS reduced from 10 to 0.4% (**Figure 4-3**). This was to determine

whether it was the starvation step that reduced the ability of HLFs to proliferate in previous experiments rather than low serum conditions. Also as both ANGII and TGF-β1 only induced proliferation at 72 hours, a longer time point of 120 hours was included in this set of experiments.

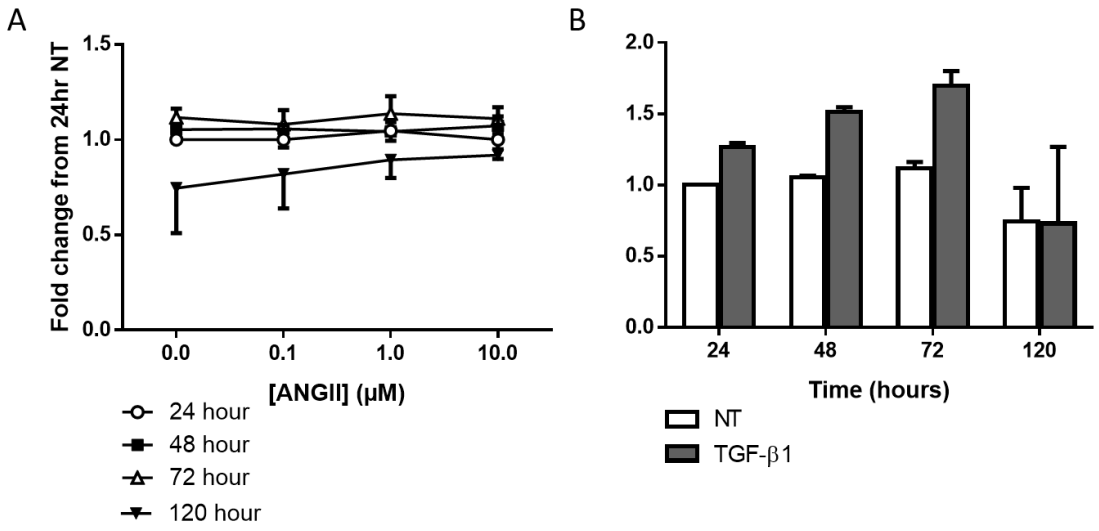

Figure 4-3. The effect of ANGII on human lung fibroblast proliferation in the presence of 0.4% newborn calf serum. Human lung fibroblasts were incubated overnight in 10% newborn calf serum (NCS) before treatment with either 0.1-10μM ANGII (**A**) or 2ng/ml TGF-β1 (**B**) in the presence of 0.4% NCS. Cells were fixed at 24, 48, 72 (n=3) and 120 hours (n=2) and cell count measured with bromophenol blue. Data expressed are fold change from 24 hour no treatment (NT) and are pooled mean ± SEM of all experiments (Wilcoxon matched-pairs signed rank test).

This set of conditions was optimal for maintaining cell viability, with 10.3 ± 1.04x10^4 cells per well measured at 24 hours NT. ANGII did not induce fibroblast proliferation at any of the time points investigated, however, the ability of TGF-β1 to induce proliferation was increased under these conditions. TGF-β1 increased cell number at 24, 48 and 72 hours and the largest increase was observed at 72 hours; TGF-β1 upregulated proliferation by 52.3 ± 8.91% compared to 72 hour NT. At 120 hours there was a decrease in cell number compared to 24 hour NT (as shown in **Figure 4-3** B), indicating a viability issue when maintaining cells in 0.4% serum conditions for this period of time.

The ability of the antifibrotic peptide ANG(1-7) to modulate HLF proliferation was also investigated. As 10% NCS induces HLF proliferation, the ability of ANG(1-7) and the Mas receptor antagonist A-779 to modulate 10% NCS induced effects were explored. Cells were seeded and maintained in 10% NCS, until treatment with 0.4% NCS, or 10% NCS in the presence and absence of 1μM (**Figure 4-4**) or 10μM ANG(1-7) (**Figure 4-5**) or A-779 (10μM). Cell

count was measured at both 48 and 72 hours. In these experiments NT refers to cells maintained in 0.4% NCS.

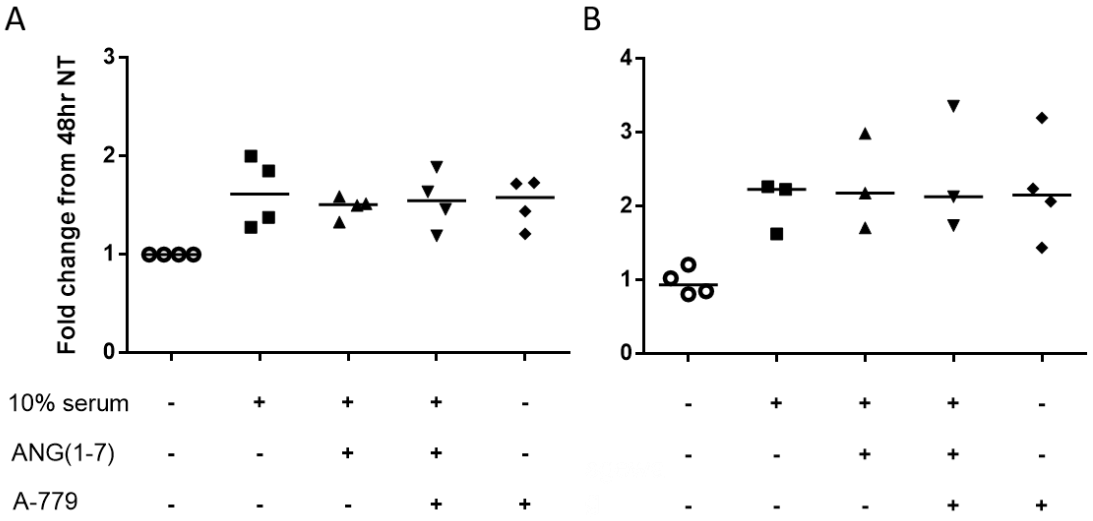

Figure 4-4. The effects of 1μM ANG(1-7) and 10μM A-779 on 10% newborn calf serum induced proliferation. Human lung fibroblasts were incubated overnight in 10% newborn calf serum (NCS) before treatment with 10% NCS alone or in the presence of 1μM ANG(1-7), 10μM A-779 or both. Cells were fixed at 48 (**A**, n=4) or 72 hours (**B**, n=3) and cell count measured with bromophenol blue. Data expressed are fold change from 48 hr 0.4% NCS, no treatment (NT) and plotted as individual data points plus median (Wilcoxon matched-pairs signed rank test).

At 48 hours, 10% NCS upregulated cell number by 62.7 ± 17.7% (**Figure 4-4**) when compared to 48 hour NT, this 10% NCS induced proliferation was reduced to 48.5 ± 17.7 % in the presence of 1μM ANG(1-7). Results were, however, variable between cell lines, with ANG(1-7) causing a median change of -7.0% (range of -20.5 – 8.7%) in 10% NCS induced proliferation. A-779 did not alter the effects of ANG(1-7) in this experiment.

At 72 hours, there was a small trend towards upregulation of 10% NCS effects observed in the presence of ANG(1-7). However, results in this instance were again variable with ANG(1-7) causing a median change of 4.9% (range of -2.2 – 31.7%) in 10% NCS induced cell number.

ANG(1-7) at a higher concentration of 10μM (**Figure 4-5**) did not affect 10% NCS induced proliferation at 48 hours, but upregulations in cell number were observed at 72 hours, with this consistent across the three cell lines that were tested. However, these increases were small, with 10% NCS induced proliferation increasing from 218.4 ± 30.6% to 247.3 ± 45.3% in the presence of ANG(1-7). A-779 did not affect the cell number observed in the presence of ANG(1-7).

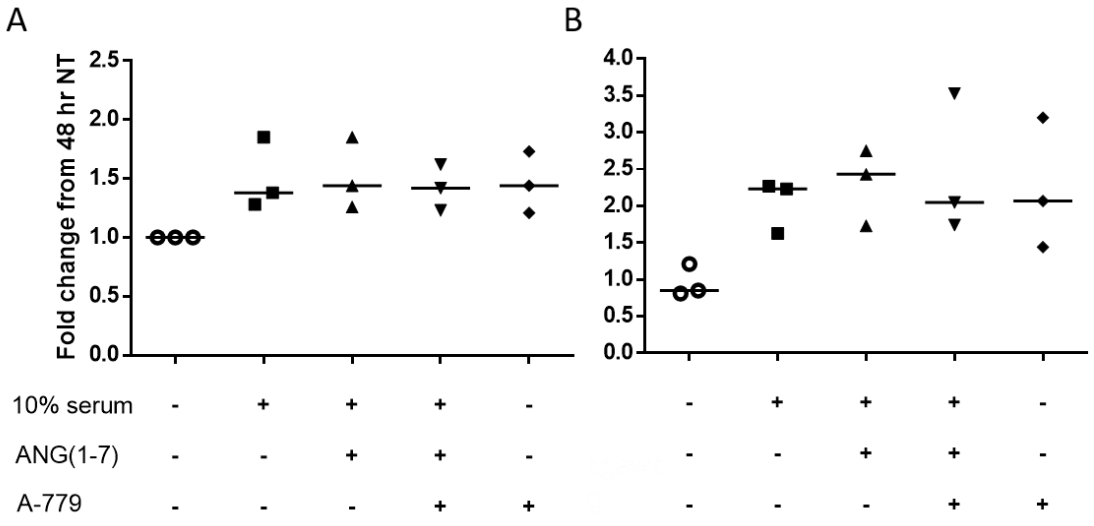

Figure 4-5. The effects of 10μM ANG(1-7) and 10μM A-779 on 10% newborn calf serum induced proliferation. Human lung fibroblasts were incubated overnight in 10% newborn calf serum (NCS) before treatment with 10% NCS alone or in the presence of 10μM ANG(1-7), 10μM A-779 or both. Cells were fixed at 48 (**A**, n=3) or 72 hour (**B**, n=3) and cell count measured with bromophenol blue. Data expressed are fold change from 48 hr no treatment (NT) and are plotted as individual data points plus median. (Wilcoxon matched-pairs signed rank test).

4.3.1.2 Collagen production

The next parameter to be explored was collagen production. Irreversible and increased ECM deposition is one of the hallmark features of IPF, collagen is the main component of ECM and fibroblasts are the key cell type involved its synthesis.

TGF-β1 is well known to induce collagen production in fibroblasts and was used as a positive control for these experiments. TGF-β1 consistently upregulated collagen production in HLFs (**Figure 4-6**), with an increase of 66.0 ± 7.97% observed (pooled data from 23 individual experiments).

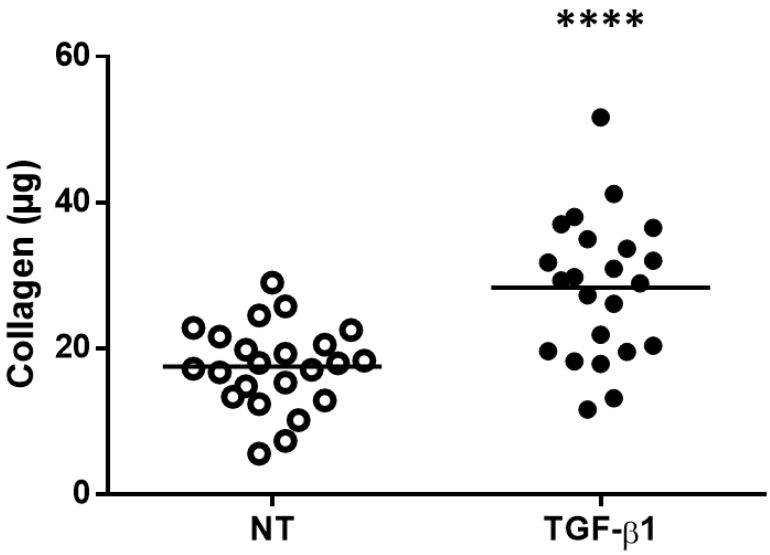

Figure 4-6. Effects of TGF-β1 on collagen production. Human lung fibroblasts were incubated overnight in soton DMEM before treatment with 2ng/ml TGF-β1 in the presence of 0.5% newborn calf serum and 100µM L-ascorbate. Cells were fixed after 6 days and collagen production measured with Sirius red dye. Data expressed are fold change from NT and plotted as individual experiments plus mean. ****p<0.0001 when compared to no treatment (NT) (Wilcoxon matched-pairs signed rank test).

The ability of ANGII to induce collagen production in HLFs was investigated. As TGF-β1 has been previously reported to upregulate AT_1R on fibroblasts, collagen production in response to ANGII was measured in cells that had a 16 hour pre-incubation with either 2ng/ml TGF-β1 or 0.5% NCS (**Figure 4-7**).

ANGII did not induce collagen synthesis in HLFs in either the presence or absence of TGF-β1 pre-treatment. There was, however, a consistently higher collagen production in the TGF-β1 treated group which was not unexpected.

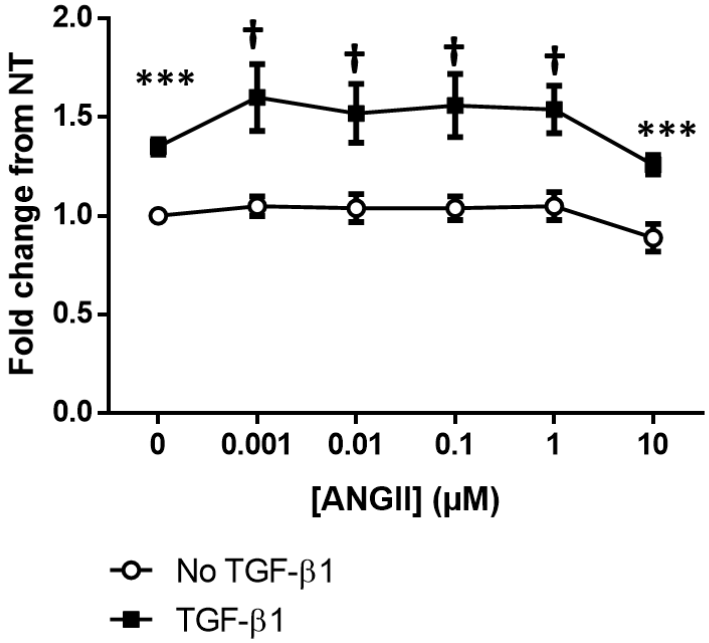

Figure 4-7. Effect of TGF-β1 on ANGII induced collagen production. Human lung fibroblasts were incubated overnight in soton DMEM, treated with either 2ng/ml TGF-β1 or 0.5% newborn calf serum (NCS) for 16 hours, before treatment with increasing concentrations of ANGII (0.001 - 10μM) (n=5). Cells were maintained in the presence of 0.5% newborn calf serum (NCS) and 100μM L-ascorbic acid. Cells were fixed after 6 days and collagen measured with Sirius red dye. Data expressed are fold change from 0.5% NCS maintained cells with no treatment (NT) and are pooled mean ± SEM of all experiments ***p<0.001 and †p<0.0001 when compared to the equal ANGII concentration on the no TGF-β1 control line (two-way ANOVA with multiple comparisons).

As 2ng/ml TGF-β1 is considered a maximal dose of this cytokine, fibroblasts under these conditions may be maximally stimulated to produce collagen. Therefore, no further increases in response to ANGII may be possible. To explore this, the effects of ANGII on TGF-β1 induced collagen production were also investigated (**Figure 4-8**). HLFs were treated with increasing concentrations of TGF-β1 (0.01-2ng/ml) in the presence and absence of 10μM ANGII. Lower concentrations of TGF-β1 may still lead to upregulated AT_1R without causing maximal collagen production.

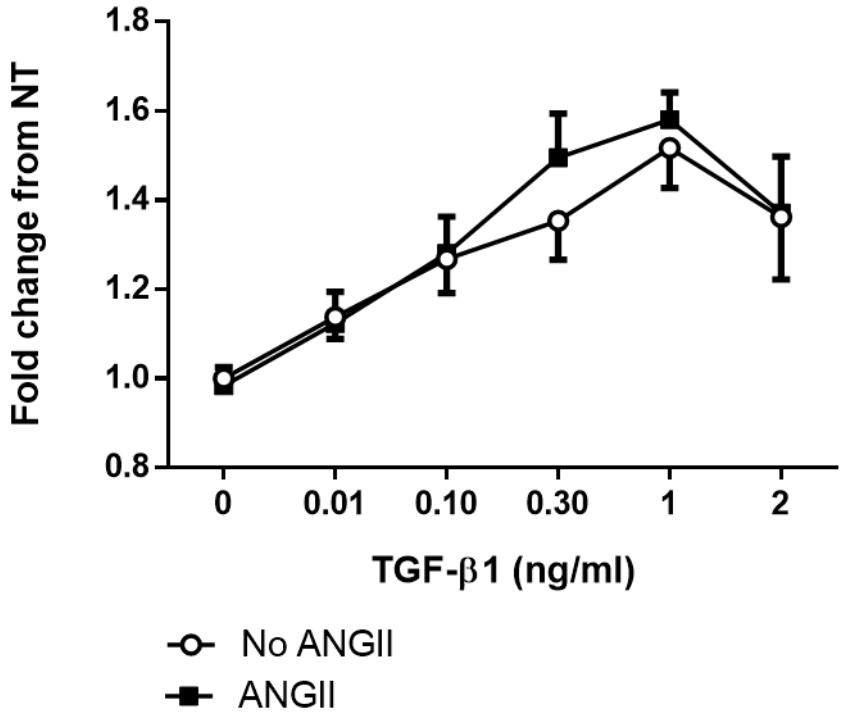

Figure 4-8. Effects of ANGII on TGF-β1 induced collagen production. Human lung fibroblasts were incubated overnight in soton DMEM before treatment with 0.01-2ng/ml of TGF-β1 in the presence or absence of ANGII (10μM). Experiment was maintained in 0.5% newborn calf serum (NCS) and 100μM L-ascorbic acid. Cells were fixed after 6 days and collagen measured with Sirius red dye. Data expressed are fold change from 0.5% NCS maintained cells with no treatment (NT) and are mean ± SEM (n=6). (Wilcoxon matched-pairs signed rank test performed at each TGF-β1 concentration).

As expected, TGF-β1 dose dependently increased collagen synthesis in HLFs. Although little difference was observed in the presence of ANGII, this peptide did cause a small increase in the response to 0.3ng/ml TGF-β1 of 10.6 ± 4.04%. Wilcoxon matched-pairs signed rank tests were performed on each TGF-β1 concentration to determine differences between individual points, this was used rather than a two-way ANOVA which looks for differences between the two lines as a whole. A Wilcoxon test provides a more accurate representation of the individual data points.

Next, the ability of ANG(1-7) to modulate collagen deposition by HLFs was explored. Cells were treated with increasing concentrations of NCS in the presence or absence of ANG(1-7) at 0.1, 1 and 10μM (**Figure 4-9** A,B and C respectively).

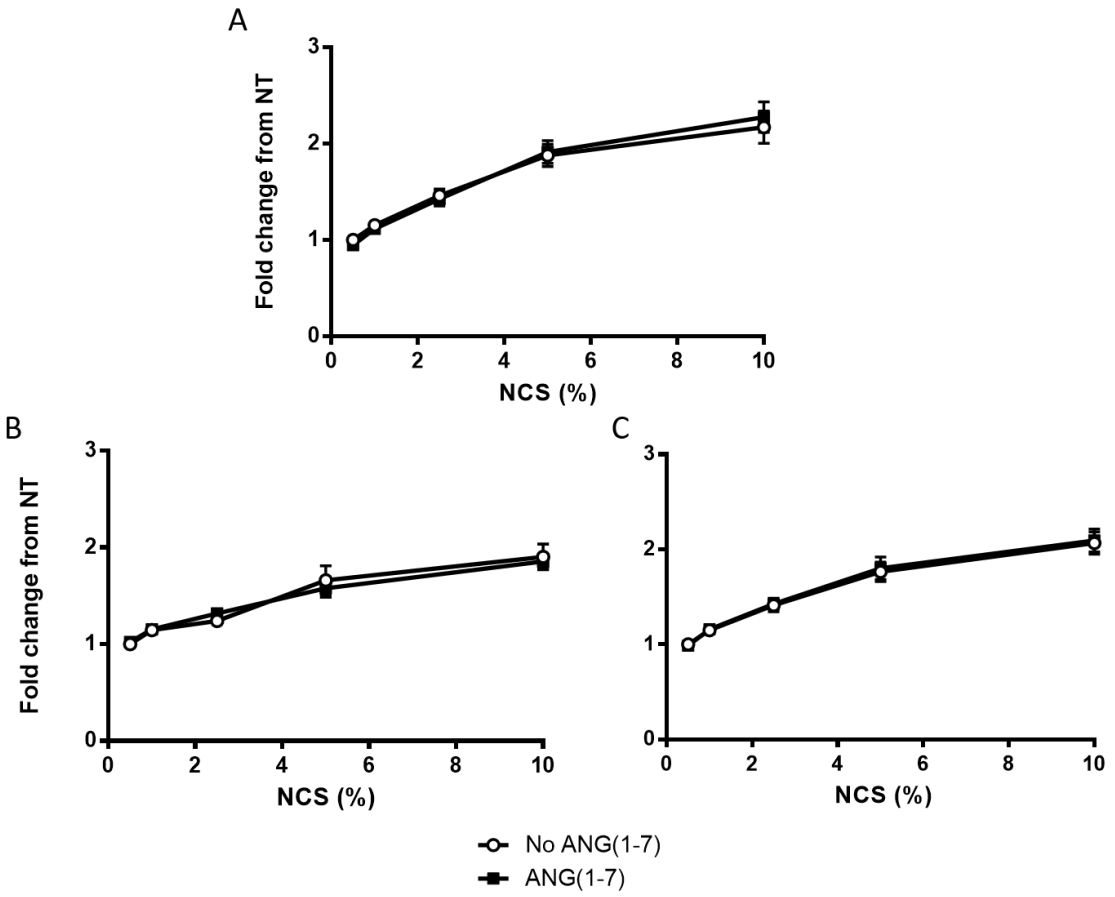

Figure 4-9. Effects of ANG(1-7) on serum induced collagen production. Human lung fibroblasts were incubated overnight in soton DMEM before treatment with 0.5-10% newborn calf serum (NCS) in the presence or absence of 0.1μM (**A**, n=7), 1μM (**B**, n=4) or 10μM ANG(1-7) (**C**, n=7). 100μM L-ascorbic acid was present for the duration of the experiment. Cells were fixed after 6 days and collagen measured with Sirius red dye. Data expressed are fold change from cells maintained in 0.5% NCS with no treatment (NT) and are mean ± SEM of all experiments (Two-way ANOVA with multiple comparisons).

ANG(1-7) did not affect NCS induced collagen production at any of the concentrations tested. The ability of this peptide to modulate TGF-β1 induced collagen production was also investigated. HLFs were treated with 2ng/ml TGF-β1 in the presence or absence of 0.1 or 10μM ANG(1-7) (**Figure 4-10** A and B respectively). Control cells (NT) were maintained in 0.5% NCS.

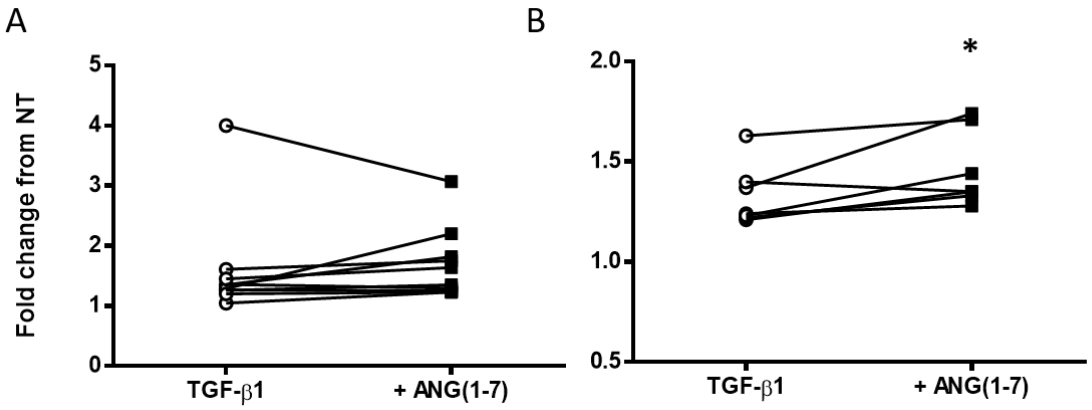

Figure 4-10. Effects of ANG(1-7) on TGF-B induced collagen production. Human lung fibroblasts were incubated overnight in soton DMEM before treatment with 2ng/ml TGF-β1 in the presence or absence of 0.1 (**A,** n=10) or 10μM ANG(1-7) (**B,** n=7). HLFs were maintained in 0.5% newborn calf serum (NCS) and 100μM L-ascorbic acid for the duration of the experiment. Cells were fixed after 6 days and collagen measured with Sirius red dye. Data expressed are fold change from cells maintained in 0.5% NCS with no treatment (NT). *p<0.05 when compared to 2ng/ml TGF-β1 alone (Wilcoxon matched-pairs signed rank test).

ANG(1-7) (0.1μM) did not affect TGF-β1 induced collagen production. However, the collagen response observed in the presence TGF-β1 was statistically upregulated in the presence of 10μM ANG(1-7) with an increase of 10.0 ± 3.88% reported. The biological significance of an increase of this size is, however, questionable.

In initial experiments performed in **Figure 4-10**, 0.1μM ANG(1-7) caused the greatest upregulation (19.7 ± 9.5%, n=7), therefore the ability of A-779 to modulate the effect of this concentration was tested (**Figure 4-11**). This was to determine any involvement of the Mas receptor in the observed result. Upon compiling the results from **Figure 4-11** with those initially performed in **Figure 4-10**, the upregulation in TGF-β1 induced collagen was reduced to 12.5 ± 8.0% (n=10).

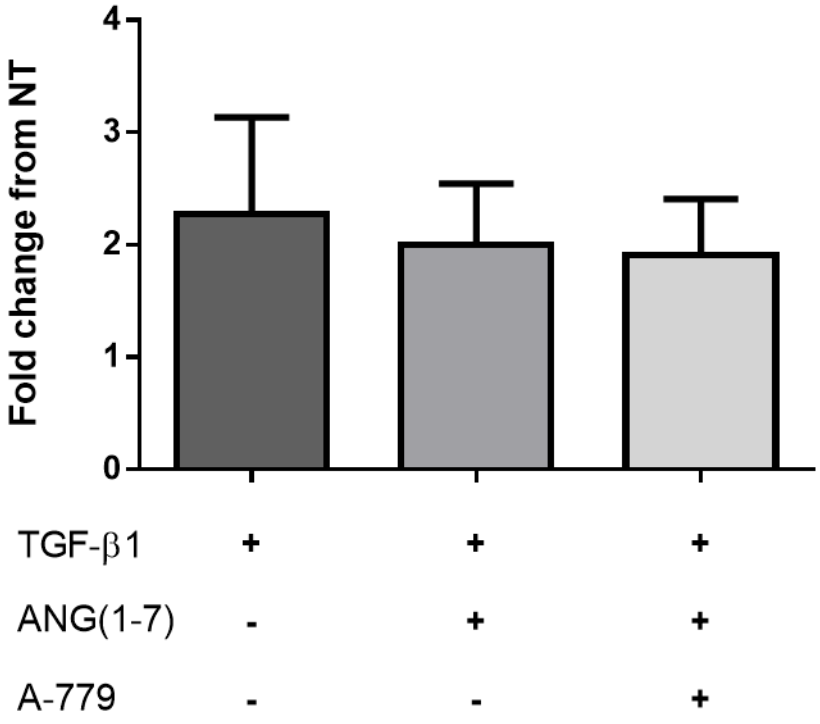

Figure 4-11. Effect of A-779 on ANG(1-7) modulated collagen production. Human lung fibroblasts were incubated overnight in soton DMEM before treatment with 2ng/ml TGF-β1 in the presence or absence of 0.1μM ANG(1-7) with or without 10μM A-779, n=3. Cells were maintained in 0.5% newborn calf serum (NCS) and 100μM L-ascorbic acid for the duration of the experiment. HLFs were fixed after 6 days and collagen measured with Sirius red dye. Data expressed are fold change from cells maintained in 0.5% NCS with no treatment (NT) and are mean ± SEM of all experiments. (Wilcoxon matched-pairs signed rank test)

In this set of experiments, 0.1μM ANG(1-7) did not cause an increase in TGF-β1 induced collagen production (-7.8 ± 12.2%) and again highlights the natural variability that exists between different fibroblast donors. Also, A-779 did not appear to affect the response to ANG(1-7), however, these experiments are currently n=3 so more repeats would be required to fully characterise the response to A-779.

The above experiments characterising the response to ANG(1-7) involved the addition of ANG(1-7) and positive stimulus (NCS or TGF-β1) simultaneously. Therefore, the effects of pretreating cells for 16 hours with 1μM ANG(1-7) before the addition of TGF-β1 were explored. The ability of ANG(1-7) to modulate baseline collagen levels in response to 0.5% NCS (NT) were also investigated in this set of experiments (**Figure 4-12**).

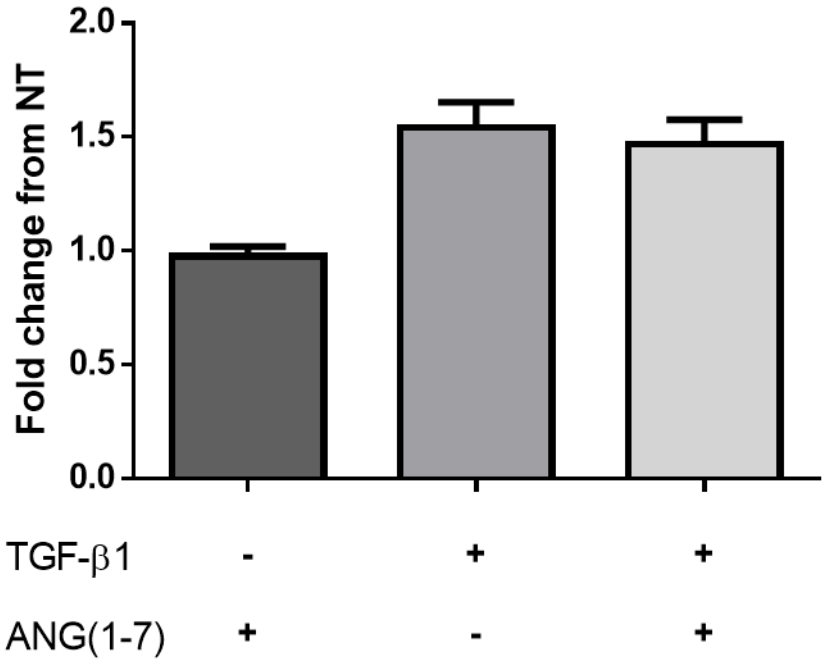

Figure 4-12. Effects of ANG(1-7) preincubation on TGF-β1 induced collagen production. Human lung fibroblasts were incubated overnight in soton DMEM with or without 1μM ANG(1-7). HLFs were then treated with either 0.5% newborn calf serum (NCS) or 2ng/ml TGF-β1, 1μM ANG(1-7) was then reintroduced to cells that had received ANG(1-7) pretreatment n=5. Cells were maintained in 0.5% NCS and 100μM L-ascorbic acid for the duration of the experiment. HLFs were fixed after 6 days and collagen measured with Sirius red dye. Data expressed are fold change from 0.5% NCS alone cells (no treatment – NT) and are mean ± SEM of all experiments (Wilcoxon matched-pairs signed rank test).

No effects of 1μM ANG(1-7) preincubation on either baseline or TGF-β1 induced collagen levels were observed in this set of experiments.

4.3.1.3 Matrix metalloproteinase-1

The ability of ANGII to modulate expression of MMP-1 in HLFs was investigated by sandwich ELISA. MMP-1 is one of the main MMPs involved in collagen degradation in the lung, any fluctuations in the levels of this enzyme could lead to either increased or dysregulated collagen deposition. Both of these instances could feasibly contribute to IPF disease progression.

Cells were treated with 0.1-10μM ANGII or 2ng/ml TGF-β1 and supernatants harvested at 24, 48 and 72 hours (**Figure 4-13**).

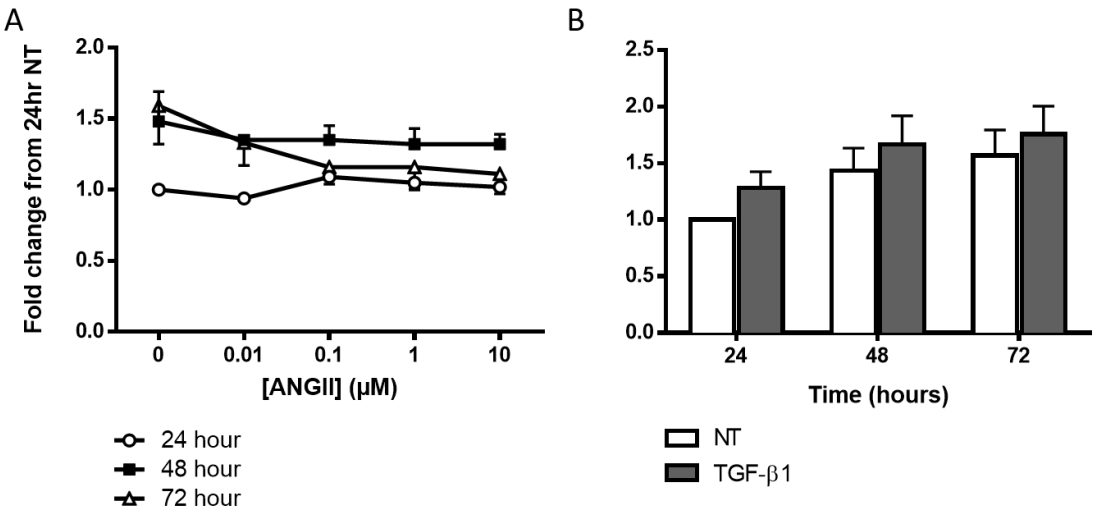

Figure 4-13. The effects of ANGII and TGF-β1 on matrix metalloproteinase-1 secretion. Human lung fibroblasts were incubated overnight in soton DMEM before treatment with either 0.1-10μM ANGII (**A**) or 2ng/ml TGF-β1 (**B**) in the presence of 0.5% newborn calf serum (NCS). Supernatants were harvested at 24, 48 or 72 hour (n=5) and run through a sandwich ELISA for MMP-1. Data shown are fold change from 24 hour no treatment (NT) are mean ± SEM of all experiments (Wilcoxon matched-pairs signed rank test).

ANGII did not appear to modulate the ability of HLFs to produce MMP-1, although a trend toward decreased production was observed at 72 hours (**Figure 4-13** A) (-24.4 ± 10.0% at 10μM ANGII) although this did not reach significance. There was no effect of TGF-β1 on MMP-1 production.

4.3.1.4 Matrix metalloproteinase-2 and 9

To investigate the effects of ANGII on the gelatinase subfamily of MMPs, gelatin zymography was performed to determine the secretion of MMP-2 and MMP-9 by HLFs. HLFs were treated with increasing concentrations of ANGII (0.1nM to 10μM) or TGF-β1 (2ng/ml). The levels of MMP-2 and MMP-9 in the supernatants were analysed 48 hours post dose by gelatin zymography (**Figure 4-14**).

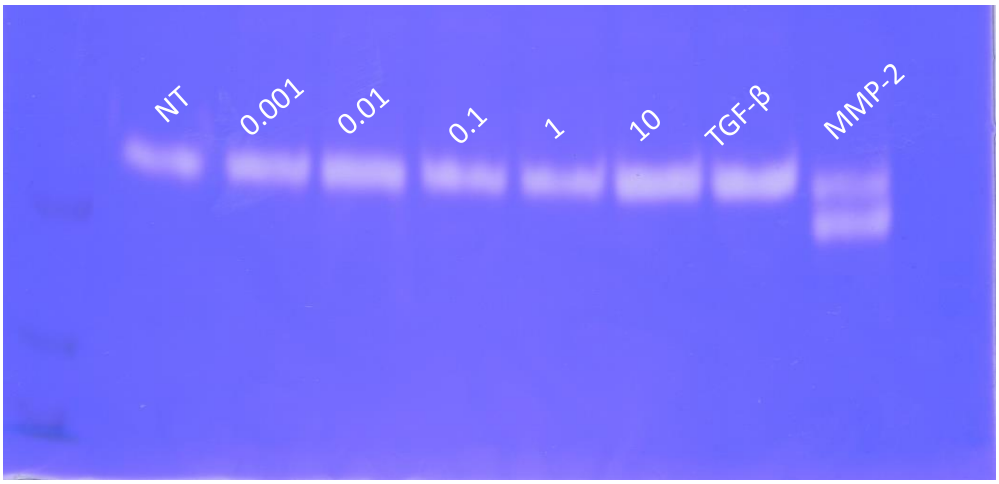

Figure 4-14. MMP-2 production in the presence of ANGII and TGF-β1. Human lung fibroblasts (n=3) were treated with increasing concentrations of ANGII (0.1nM to 10μM) or TGF-β1 (2ng/ml) for 48 hours. Cell supernatants were collected and analysed with gelatin zymography.

MMP-2 was detected in all cell supernatants regardless of treatment. MMP-9, however, was not detected in any supernatants from any cell line. Using densitometric analysis, changes in MMP-2 production relative to the NT sample were calculated (**Figure 4-15**). Upregulation in MMP-2 production was observed in the presence of both 10μM ANGII (35.7 ± 6.92%) and 2ng/ml TGF-β1 (47.8 ± 11.6%).

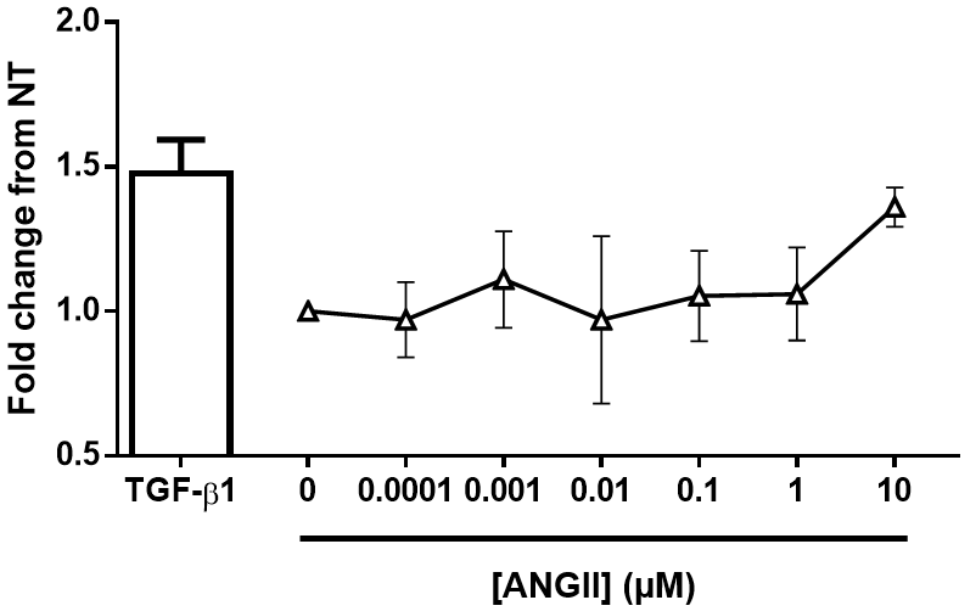

Figure 4-15. Relative changes in MMP-2 production in the presence of ANGII or TGF-β1. Human lung fibroblasts (n=3) were treated with increasing concentrations of ANGII (0.1nM to 10μM) or TGF-β1 (2ng/ml) for 48 hours and MMP-2 expression measured with gelatin zymography. Relative changes in MMP-2 expression (compared to no treatment) were analysed by densitometric analysis (Wilcoxon matched-pairs signed rank test).

4.3.1.5 Interleukin-6

The ability of ANGII to induce IL-6 secretion in HLFs was also explored. IL-6 signalling is known to play an important role in IPF, and this cytokine can differentially regulate HLF proliferation/apoptosis depending on the fibrotic phenotype of these cells (discussed in detail in section 1.4.2).

HLFs were treated with 0.1-10μM ANGII or 2ng/ml TGF-β1 in the presence of 0.5% NCS and supernatants harvested at 24, 48 and 72 hours (**Figure 4-16**).

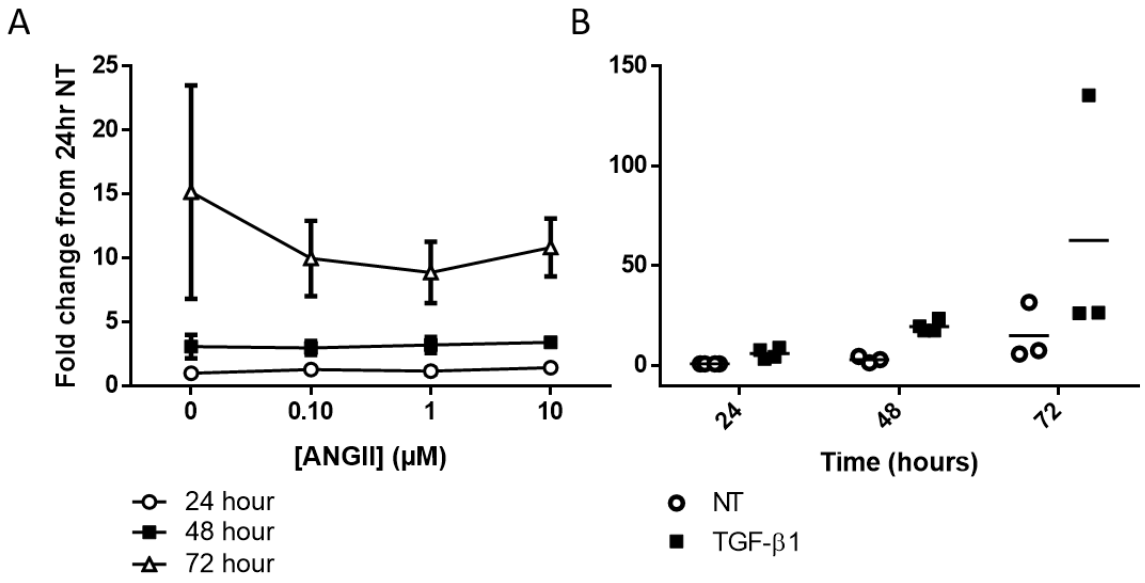

Figure 4-16. Effects of ANGII and TGF-β1 on interleukin-6 secretion. Human lung fibroblasts were incubated overnight in soton DMEM before treatment with either 0.1-10μM ANGII (**A**) or 2ng/ml TGF-β1 (**B**) in the presence of 0.5% newborn calf serum (NCS). Supernatants were harvested at 24, 48 and 72 hours (n=3) and run through sandwich ELISA for IL-6. Data shown are fold change from 24hr no treatment (NT) and are mean ± SEM of all experiments (Wilcoxon matched pairs-signed rank test).

ANGII did not induce IL-6 secretion in HLFs at 24, 48 or 72 hours. TGF-β1, however, strongly induced IL-6 release at all time points (**Figure 4-16** B). Large differences between NT and TGF-β1 were observed at 48 hours, with an increase of 757.9 ± 357.4% in the presence of TGF-β1. Similar increases were also observed at 72 hours (799.1 ± 689.4%), although results at this point were more variable due to high baseline secretion (NT) in one cell line at this time point. This is also the reason for the high variability observed at the 72 hour, no ANGII point in **Figure 4-16** A. The effects of TGF-β1 on IL-6 secretion did not reach statistical significance at any time point, likely due to the low sample size used for non-parametric testing.

4.3.1.6 Latency associated peptide

As many of the reported effects of ANGII on fibroblasts are widely accepted to be via TGF-β1 release, the secretion of TGF-β1 in response to ANGII was examined. TGF-β1 is secreted from cells in a complex with latency associated peptide (LAP) (discussed in more detail in section 1.3).

Measuring the levels of LAP secreted by HLFs, is a total measure of both inactive TGF-β1 (in complex with LAP) and active TGF-β1 (dissociated LAP) in the supernatant. As TGF-β1 is widely known to upregulate its own expression, this was again used as a positive control for these experiments.

HLFs were treated in the same manner as IL-6 experiments above, **Figure 4-17** shows the release of LAP to 0.1-10μM ANGII (A) and 2ng/ml TGF-β1 (B).

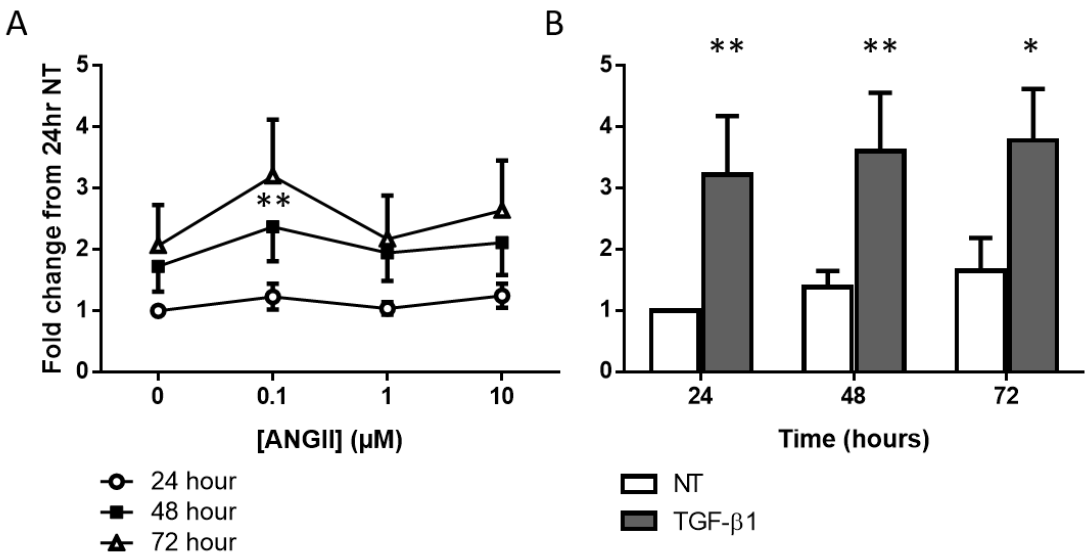

Figure 4-17. Effects of ANGII and TGF-β1 on latency associated peptide secretion. Human lung fibroblasts were incubated overnight in soton DMEM, before treatment with either 0.1-10μM ANGII (**A**) or 2ng/ml TGF-β1 (**B**) in the presence of 0.5% NCS. Supernatants were harvested at 24 (n=10), 48 (n=9) and 72 hours (n=7) and run through a sandwich ELISA for latency associated peptide (LAP). Data shown are fold change from 24hr no treatment (NT) and are mean ± SEM of all experiments. **A**: **p<0.01 when compared to 48hr no ANGII; **B**: *p<0.05, **p<0.01 when compared to NT from same day (Wilcoxon matched-pairs signed rank test).

ANGII (0.1μM) statistically upregulated LAP secretion in HLFs at both 48 hours, with an increase of 38.7 ± 19.3%. A trend towards increased LAP production was also observed with this concentration at 72 hours with an increase of 60.6 ± 20.1%y. No effects of 1 or 10μM ANGII were observed at any time point. A strong upregulation in LAP production was also induced in response to TGF-β1 at all the time points investigated.

Active TGF-β1 release in response to 0.1-10μM ANGII was also explored with a TGF-β1 sandwich ELISA, however, there was no detectable level of active TGF-β1 at 24, 48 or 72 hours (data not shown).

4.3.2 Angiotensin inhibitor effects

Next the effects of the ACE inhibitor captopril and AT_1R antagonist telmisartan on HLF function were explored. The AT_2R antagonist PD-123319 and its effect on captopril modified fibroblast function was also explored. These antagonists were utilised to determine whether there was an endogenously expressed RAS in the cell culture system.

4.3.2.1 Collagen

The ability of captopril to modulate baseline collagen levels was tested. HLFs were seeded in soton DMEM in the presence of 100μM captopril and incubated overnight before re-treatment with captopril in the presence of 0.5% NCS (**Figure 4-18**).

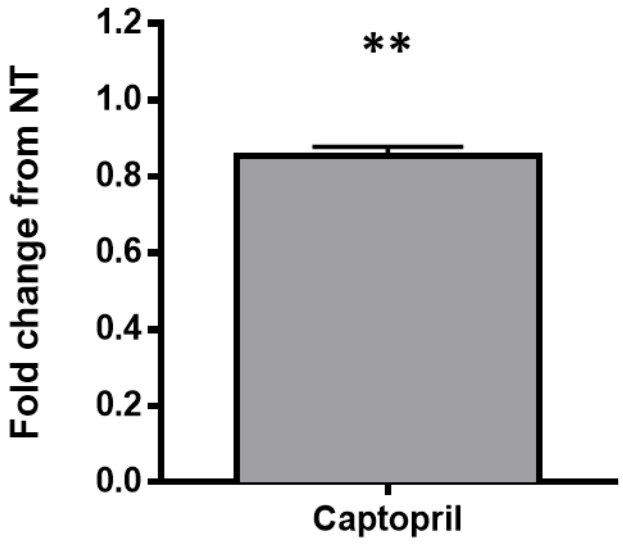

Figure 4-18. The effect of captopril on baseline collagen levels. Human lung fibroblasts (HLFs) were incubated overnight in soton DMEM with or without 100μM captopril, before treatment again with 100μM captopril in the presence of 0.5% newborn calf serum (NCS) and 100μM L-ascorbic acid, n=9. Cells were fixed after 6 days and collagen measured with Sirius red dye. Data shown are fold change from no treatment (NT) and are mean ± SEM of all experiments. **p<0.01 when compared with NT (Wilcoxon matched-pairs signed rank test).

Captopril significantly reduced baseline collagen levels by 14.6 ± 2.45%. To determine whether this was likely to be due to reduced production of endogenous ANGII, the ability of telmisartan

to induce a similar effect was explored, 10nM and 1μM telmisartan was used for these experiments (**Figure 4-19**).

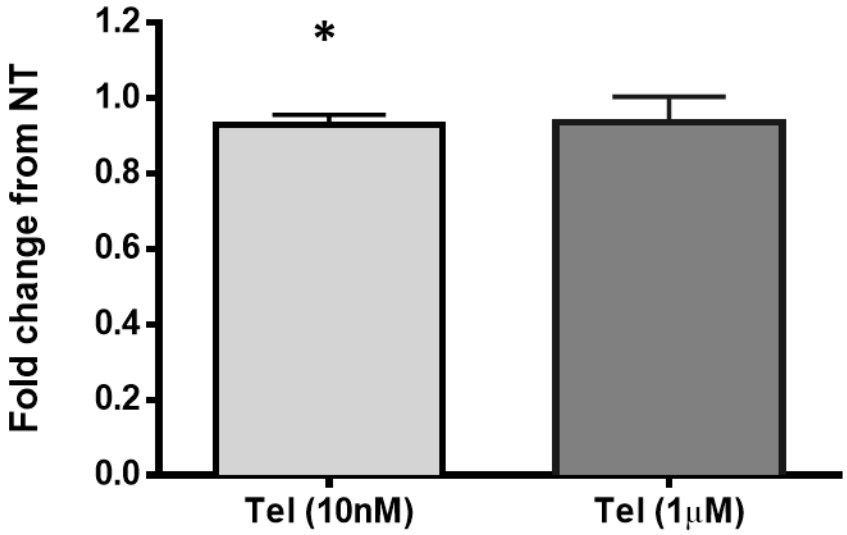

Figure 4-19. The effect of telmisartan on baseline collagen levels. Human lung fibroblasts (HLFs) were incubated overnight in soton DMEM alone or with 10nM (n=7) or 1μM telmisartan (n=3). HLFs were then treated with the same dose of telmisartan in the presence of 0.5% NCS and 100μM L-ascorbic acid, maintained for 6 days before fixing and staining with Sirius red dye. Data shown are fold change from no treatment (NT) and are mean ± SEM of all experiments. *p<0.01 when compared to NT (Wilcoxon matched-pairs signed rank test).

Telmisartan (10nM) significantly reduced baseline collagen levels by 7.0 ± 2.26%, although the biological significance of a decrease of this size is questionable. No further decrease in collagen was observed in the presence of 1μM telmisartan (5.04 ± 1.59%) indicating that the maximum effect was seen with 10nM.

4.3.2.2 Interleukin-6

Next, the ability of captopril to modulate IL-6 secretion in HLFs was investigated. In this instance the effects of 100μM captopril on 0.5% NCS, 10% NCS or 2ng/ml TGF-β1 treated fibroblasts were examined (**Figure 4-20** A, B and C respectively). Cells were seeded and incubated overnight before simultaneous addition of captopril plus 0.5 or 10% NCS or TGF-β1, IL-6 in the supernatants was measured at 24 and 48 hours.

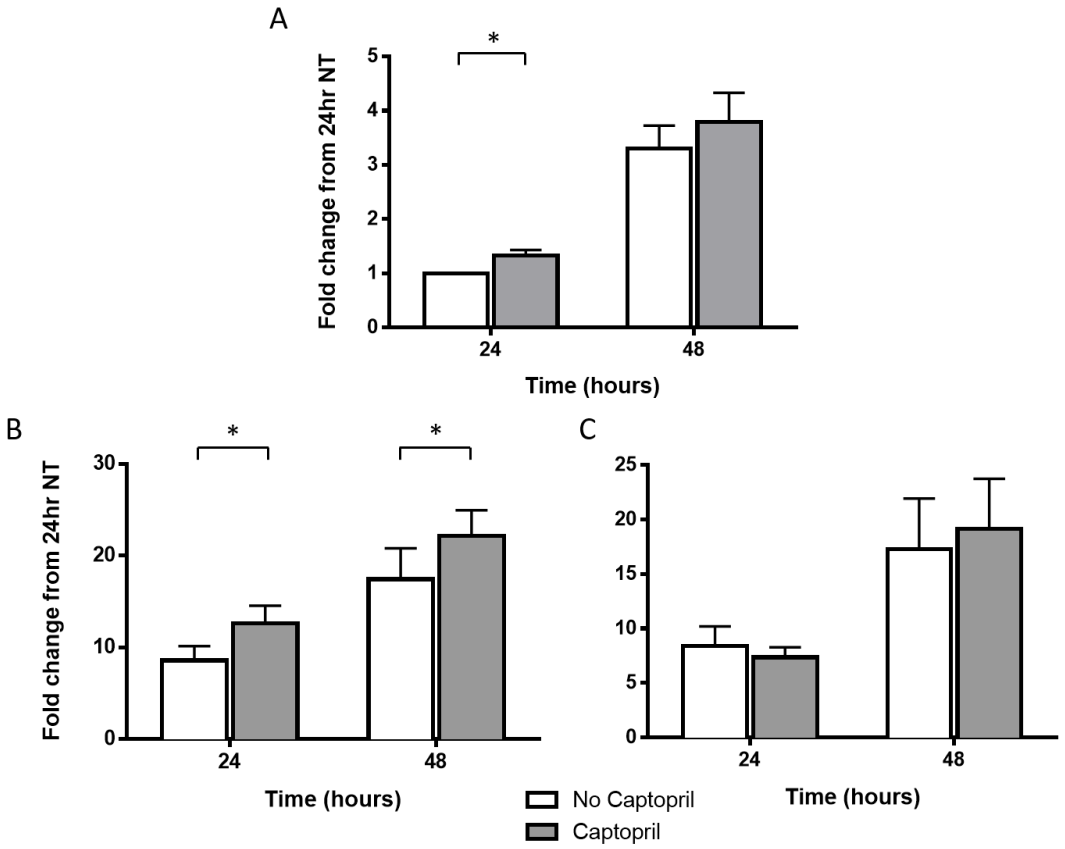

Figure 4-20. Effects of captopril on interleukin-6 secretion. Human lung fibroblasts were incubated overnight in soton DMEM before treatment with 0.5 (**A**) or 10% (**B**) newborn calf serum (NCS) or 2ng/ml TGF-β1 (**C**) in the presence or absence of 100μM captopril. Supernatants were harvested at 24 and 48 hours and run through a sandwich ELISA for IL-6, n=7 for all points. Data shown are fold change from 24 hour 0.5% alone (no treatment – NT) and are mean ± SEM of all experiments. *p<0.05 when compared to the paired no captopril group from the same time point (Wilcoxon matched-pairs signed rank test).

Captopril significantly upregulated 0.5% NCS induced IL-6 by 33.3 ± 10.7% at 24 hours, although this effect no longer reached significant at 48 hours. The IL-6 response to 10% NCS was also increased in the presence of captopril at both 24 (54.8 ± 16.7%) and 48 hours (34.2 ± 12.1%), although the effects were smaller at the later time point. There was no effect of captopril on TGF-β1 induced IL-6 secretion.

The effects of 1μM PD-123319 on captopril modulated IL-6 production were also explored, this was to determine whether any of the effects were due to increased levels of ANG(1-9) in the media. ANG(1-9) has been shown to have opposing effects to ANGII via AT_2R. The ability of 10nM telmisartan to modify IL-6 secretion in HLFs was also investigated in this set of experiments, **Figure 4-21** shows the effects of these inhibitors against 0.5% NCS treated cells.

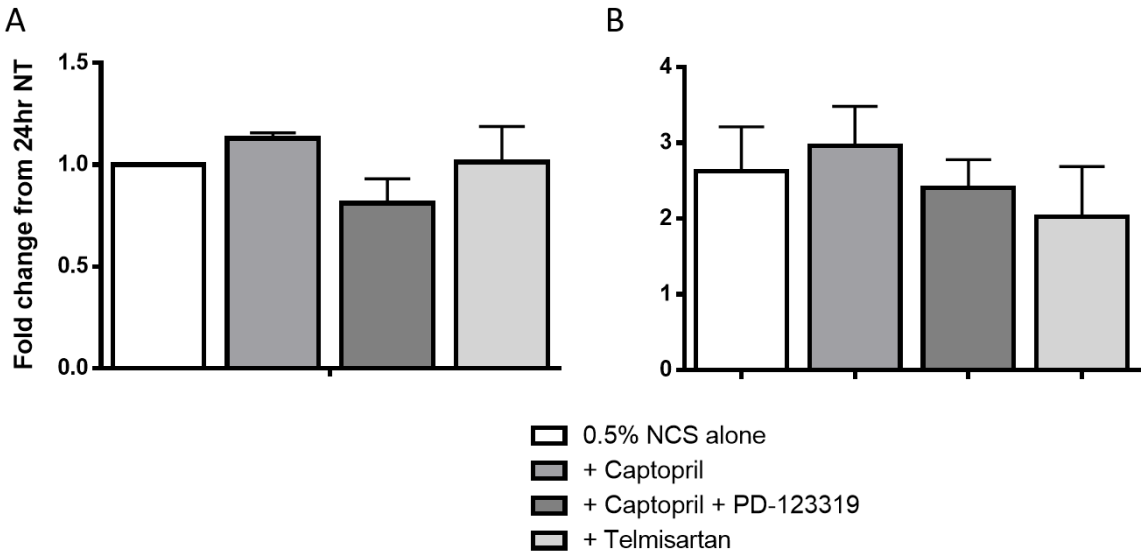

Figure 4-21. The effect of angiotensin inhibitors on baseline interleukin-6 secretion. Human lung fibroblasts were incubated overnight in soton DMEM before treatment with 0.5% newborn calf serum (NCS), 100μM captopril in the presence and absence of 1μM PD-123319 or 10nM telmisartan alone. Supernatants were harvested at 24 (**A**, n=3) and 48 hours (**B**, n=3), before being run through a sandwich ELISA for IL-6. Data shown are fold change from 24 hour no treatment (NT) and are mean ± SEM of all experiments (Wilcoxon matched-pairs signed rank test).

PD-123319 appears to reduce captopril induced IL-6 production at both 24 and 48 hours. Telmisartan does not appear to affect baseline IL-6 production at 24 hours, although a trend towards decreasing IL-6 in the presence of this antagonist was observed at 48 hours.

The effects of these angiotensin inhibitors on 10% NCS induced IL-6 were investigated in a similar manner and are shown below in **Figure 4-22**.

Captopril upregulated 10% NCS induced IL-6 as shown previously (**Figure 4-20**). PD-123319 inhibited this captopril induced IL-6 upregulation at both 24 and 48 hours, and is back to the level of 10% NCS treated cells by 48 hours. No effect of telmisartan on 10% NCS induced IL-6 was observed at either time point.

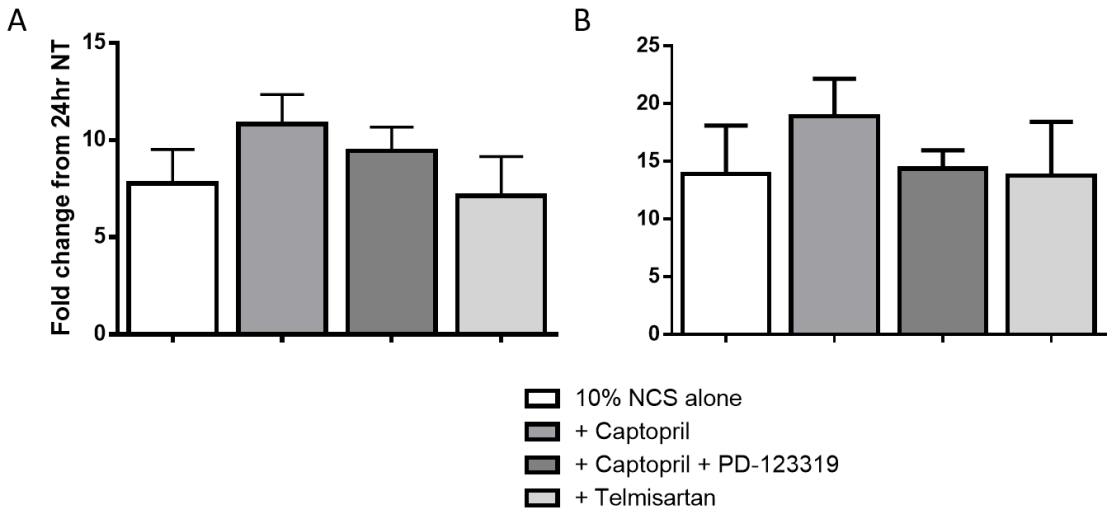

Figure 4-22. The effects of angiotensin inhibitors on 10% newborn calf serum induced interleukin-6. Human lung fibroblasts were incubated overnight in soton DMEM before treatment with 10% NCS, 100μM captopril in the presence and absence of 1μM PD-123319 or 10nM telmisartan alone. Supernatants were harvested at 24 (**A**, n=3) and 48 hours (**B**, n=3) before being run through a sandwich ELISA for IL-6. Data shown are fold change from 24 hour 0.5% NCS treated cells (no treatment – NT) and are mean ± SEM of all experiments (Wilcoxon matched-pairs signed rank test).

Although captopril did not affect TGF-β1 induced IL-6 in above experiments (**Figure 4-20**), the ability of the angiotensin inhibitors to modulate TGF-β1 induced IL-6 secretion were also tested (**Figure 4-23**).

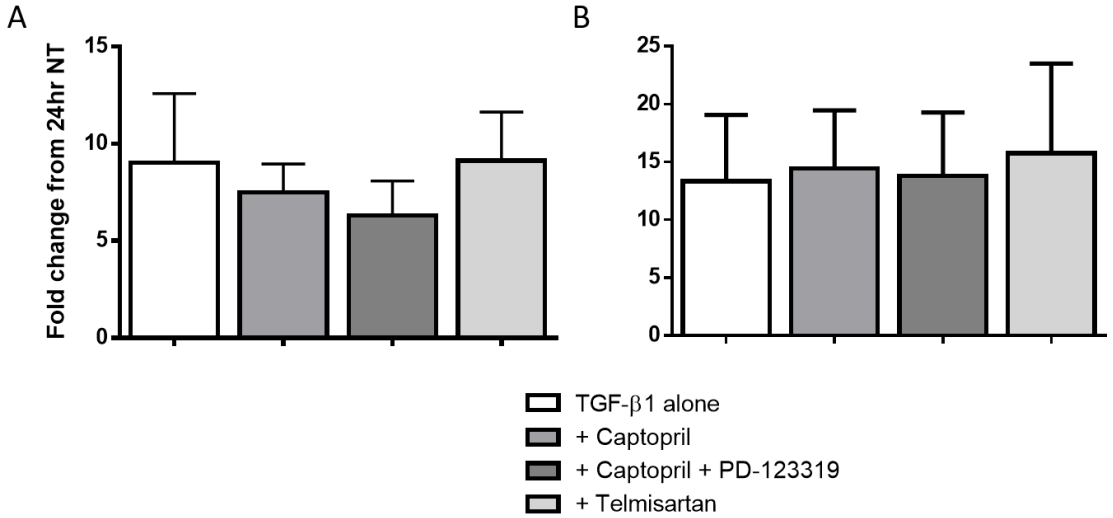

Figure 4-23. The effects of angiotensin inhibitors on TGF-β1 induced interleukin-6 secretion. Human lung fibroblasts were incubated overnight in soton DMEM before treatment with 2ng/ml TGF-β1 with or without 100μM captopril in the presence and absence of 1μM PD-123319, or 10nM telmisartan alone. Cells were maintained in 0.5% newborn calf serum (NCS) and supernatants harvested at 24 (**A**, n=3) and 48 hours (**B**, n=3). Data shown are fold change from 24 hour 0.5% NCS treated cells (no treatment – NT) and are mean ± SEM of all experiments. (Wilcoxon matched-pairs signed rank test).

Neither Captopril nor Telmisartan affected TGF-β1 induced IL-6 at either time point. However, Captopril in the presence of PD-123319 did appear to be lower than NT at 24 hours, with this effect lost by 48 hours.

4.3.2.3 Transforming growth factor-β1

The next soluble factor secreted by fibroblasts to be investigated was TGF-β1, the effects of 100μM captopril on 0.5% and 10% NCS induced TGF-β1 at 24 and 48 hours are shown below in **Figure 4-24.**

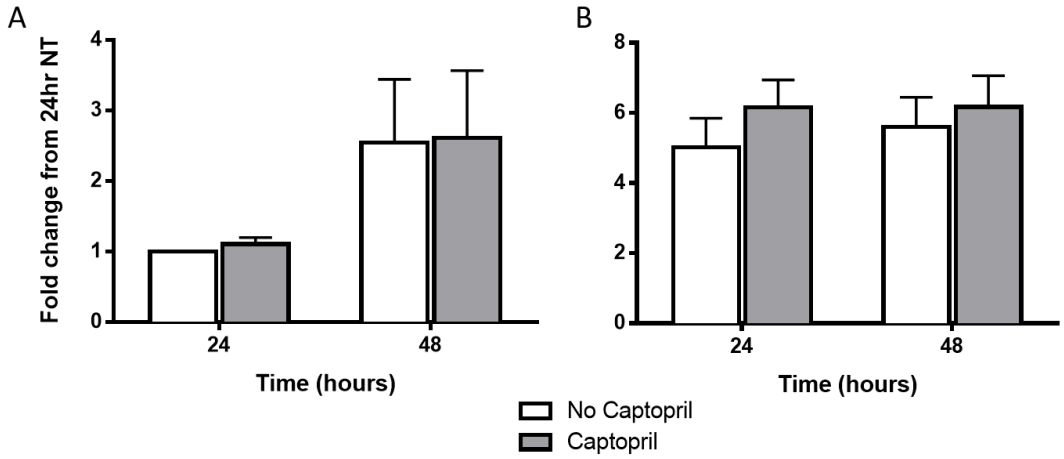

Figure 4-24. The effect of captopril on TGF-β1 secretion. Human lung fibroblasts were incubated overnight in soton DMEM before treatment with 0.5 (**A,** n=7) or 10% newborn calf serum (NCS) (**B,** n=7) in the presence and absence of 100μM captopril. Supernatants were harvested at 24 and 48 hours. Samples were acid treated and run through a sandwich ELISA to measure total TGF-β1. Data shown are fold change from 0.5% NCS treated cells (no treatment – NT) and are mean ± SEM of all experiments. (Wilcoxon matched-pairs signed rank test).

Captopril did not affect 0.5% NCS induced TGF-β1, however, a trend towards an increase in 10% NCS induced TGF-β1 was observed at 24 hours. The 24 hour 10% NCS group was 5.02 ± 0.82 fold higher than the NT group, in the presence of captopril, 10% NCS was 6.16 ± 0.78 fold higher than 24 hour NT. An average increase of 36.8 ± 27.4% was reported, although high variability between donor fibroblasts was observed.

The TGF-β1 levels seen in the presence of 0.5 and 10% NCS and captopril were measured in the presence of 1μM PD-123319. TGF-β1 levels in the presence of 10nM telmisartan were also explored. The effects of these antagonists against 0.5% NCS are shown in **Figure 4-25.**

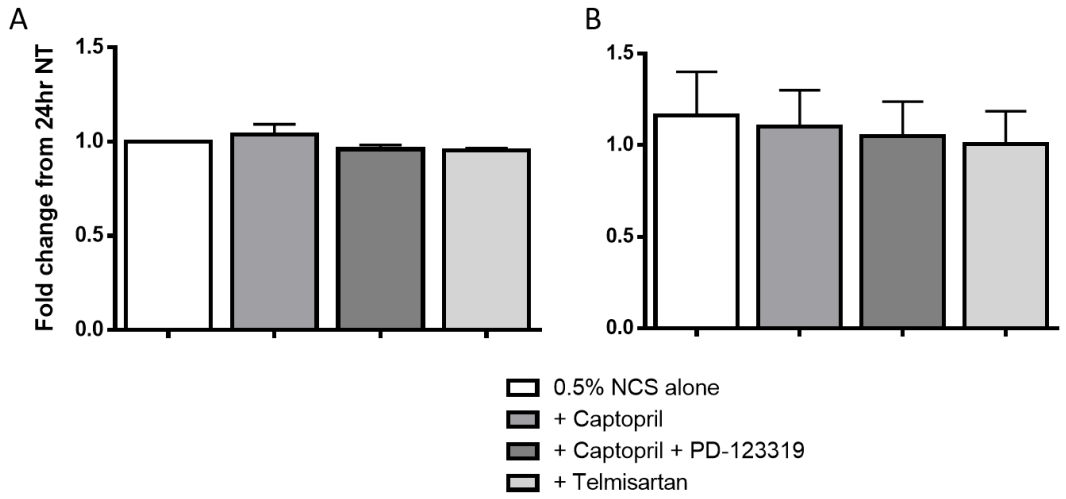

Figure 4-25. The effects of angiotensin inhibitors on baseline TGF-β1 secretion. Human lung fibroblasts were incubated overnight in soton DMEM before treatment with 0.5% newborn calf serum (NCS) with or without 100μM captopril in the presence and absence of 1μM PD-123319, or with 10nM telmisartan alone. Supernatants were harvested at 24 (**A**, n=3) and 48 hours (**B**, n=3), acid treated and run through a sandwich ELISA for total TGF-β1. Data shown are fold change from 24 hour no treatment (NT) and mean ± SEM of all experiments. (Wilcoxon matched-pairs signed rank test).

There does not appear to be any effects of captopril with or without PD-123319, or telmisartan on 0.5% NCS induced TGF-β1 at either time point.

The effects of angiotensin inhibitors on 10% NCS induced TGF-β1 were also explored (**Figure 4-26**) and there was no effect of captopril, PD-123319 or telmisartan observed at either time point.

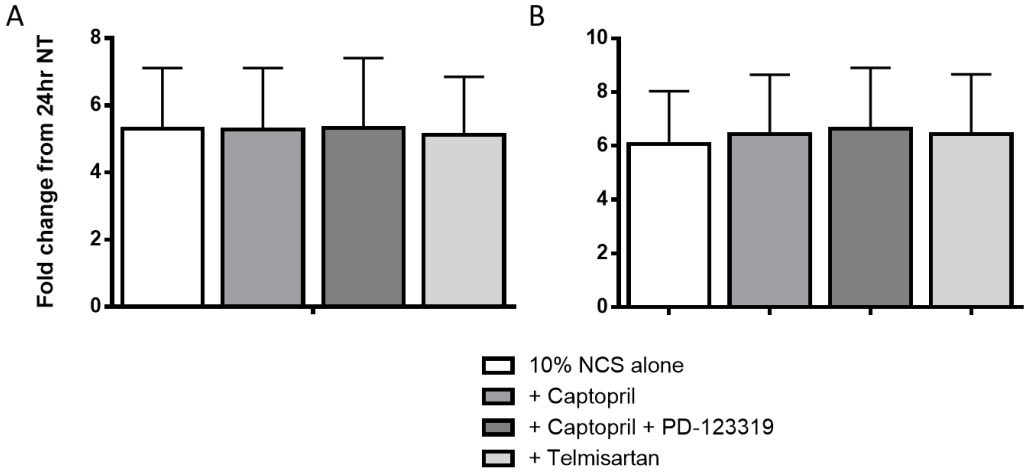

Figure 4-26. The effect of angiotensin inhibitors on 10% newborn calf serum induced TGF-β1. Human lung fibroblasts were incubated overnight in soton DMEM before treatment with 10% newborn calf serum (NCS) with or without 100μM captopril in the presence and absence of 1μM PD-123119, or with 10nM telmisartan alone. Supernatants were harvested at 24 (**A**, n=3) or 48 hours (**B**, n=3), acid treated and run through a sandwich ELISA for total TGF-β1. Data shown are fold change from 24 hour 0.5% NCS (no treatment – NT) and are mean ± SEM of all experiments. (Wilcoxon matched-pairs signed rank test).

4.3.2.4 Matrix metalloproteinase-1

The ability of HLFs to produce MMP-1 in response to 0.5% NCS, 10% NCS and TGF-β1 in the presence and absence of captopril was also investigated (**Figure 4-27**) in a similar manner to IL-6 and TGF-β1.

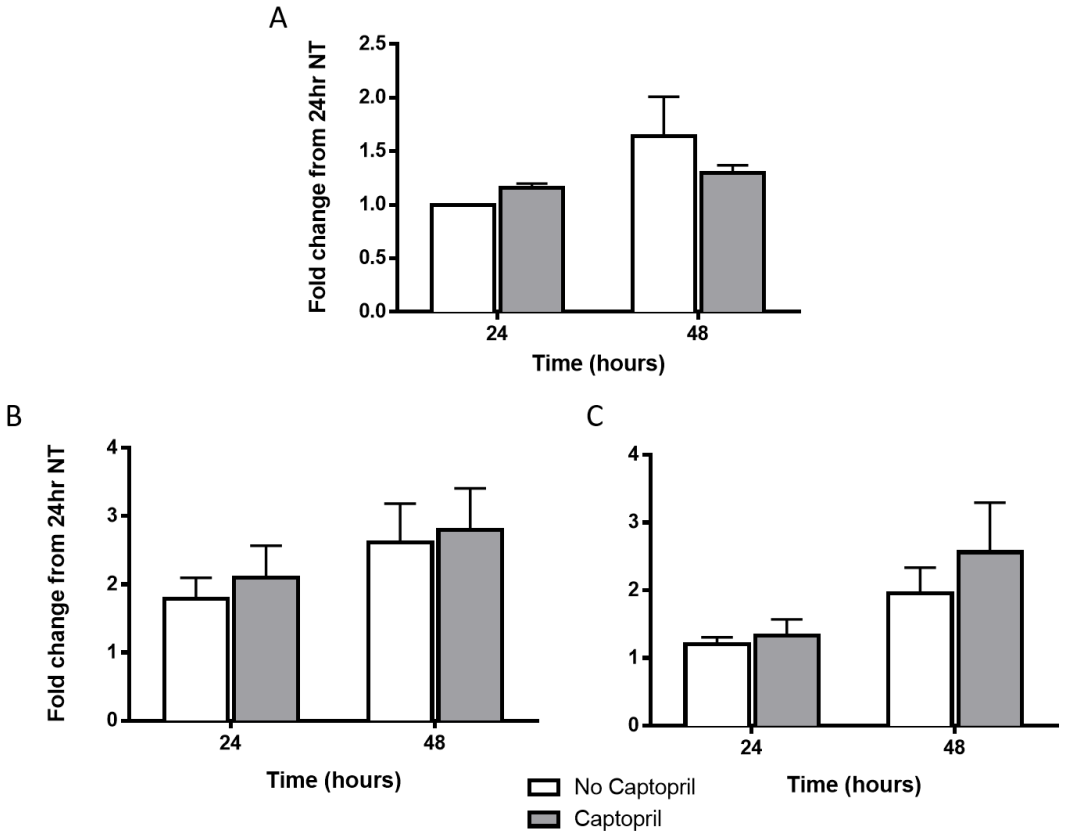

Figure 4-27. The effect of captopril on MMP-1 secretion. Human lung fibroblasts were incubated overnight in soton DMEM before treatment with 0.5% (**A**) or 10% newborn calf serum (NCS) (**B**) or 2ng/ml TGF-β1 (**C**) in the presence and absence of 100μM captopril. Supernatants were harvested at 24 and 48 hours, n=4, and run through a sandwich ELISA for MMP-1. Data shown are fold change from 24 hour 0.5% NCS treated cells (no treatment – NT) and are mean ± SEM of all experiments (Wilcoxon matched-pairs signed rank test).

The level of MMP-1 produced under the basal conditions of 0.5% NCS varied greatly between different fibroblast donors, with an MMP-1 level in a number of experiments that was too high to quantify. Therefore the sample size for these experiments was smaller (n=4) than the equivalent IL-6 and TGF-β1 captopril experiments (n=7), due to the need for further optimisation for this set of experiments.

Very little effect of captopril on MMP-1 was observed, although there did appear to be a trend towards reduced baseline MMP-1 secretion at 48 hours (**Figure 4-27** A). There also appeared to be a trend towards an upregulated response to TGF-β1 at 48 hours (**Figure 4-27** C) with an

increase of 25.5 ± 10.4% observed. However, due to the small sample size solid conclusions from this data are difficult.

The effect of PD-123319 on MMP-1 levels observed in the presence of captopril was also investigated. MMP-1 levels in the presence of telmisartan were also measured. **Figure 4-28** shows the effects of these antagonists on 0.5% NCS induced MMP-1 at 24 (A) and 48 hours (B).

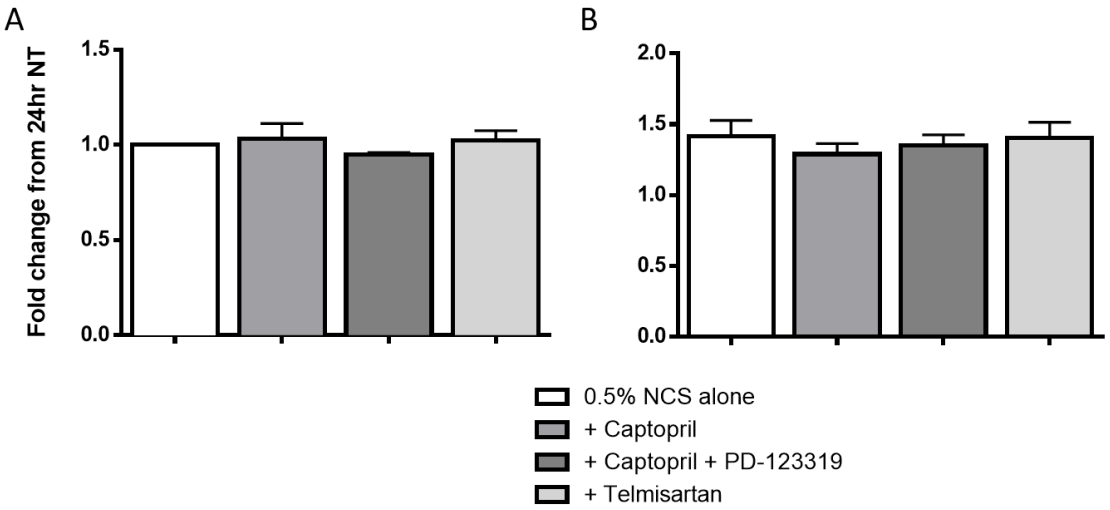

Figure 4-28. The effect of angiotensin inhibitors on baseline MMP-1 secretion. Human lung fibroblasts were incubated overnight in soton DMEM before treatment with 0.5% newborn calf serum (NCS) with or without 100μM captopril in the presence and absence of 1μM PD-123319, or with 10nM telmisartan alone. Supernatants were harvested at 24 (**A**, n=3) and 48 hours (**B**, n=3) and run through a sandwich ELISA for MMP-1. Data shown are fold change from 24 hour no treatment (NT) and are mean ± SEM of all experiments. (Wilcoxon matched-pairs signed rank test).

There was no effect of either captopril with or without PD-123319, or telmisartan on 0.5% NCS induced MMP-1 at either 24 or 48 hours. These inhibitors were retested against 10% NCS induced MMP-1 (**Figure 4-29**).

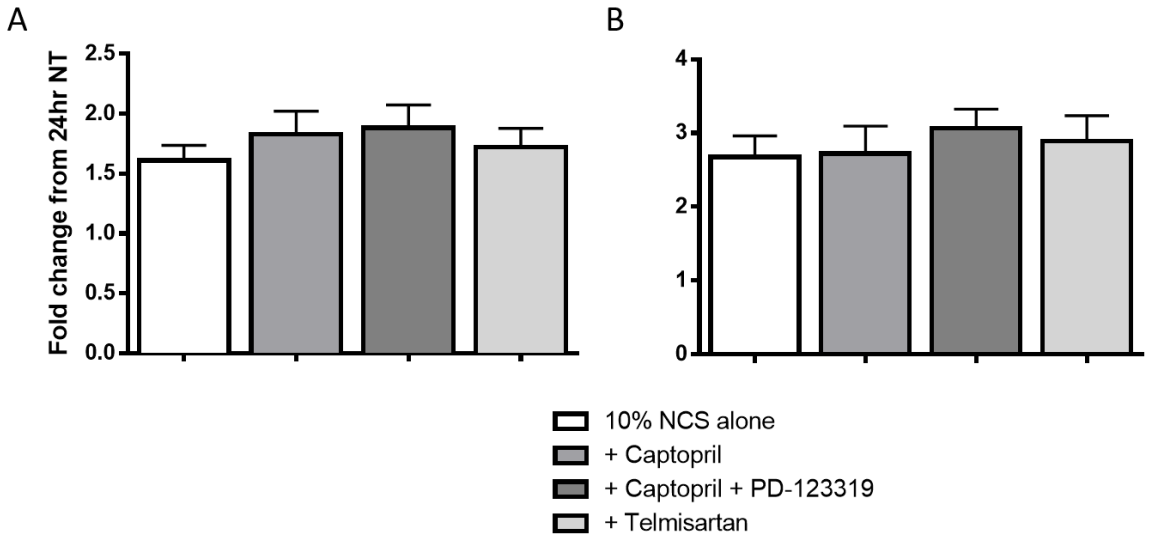

Figure 4-29. The effects of angiotensin inhibitors on 10% newborn calf serum induced MMP-1. Human lung fibroblasts were incubated overnight in soton DMEM before treatment with 10% newborn calf serum (NCS) with or without 100μM captopril in the presence and absence of 1μM PD-123319, or with 10nM telmisartan alone. Supernatants were harvested at 24 (**A**, n=3) and 48 hours (**B**, n=3) and run through a sandwich ELISA for MMP-1. Data shown are fold change from 24 hour 0.5% NCS treated cells (no treatment – NT) and are mean ± SEM of all experiments. (Wilcoxon matched-pairs signed rank test).

There does not appear to be any effects of captopril in the presence or absence of PD-123319, or telmisartan alone on 10% NCS induced MMP-1. The effects of these inhibitors on TGF-β1 induced MMP-1 are shown in **Figure 4-30** below.

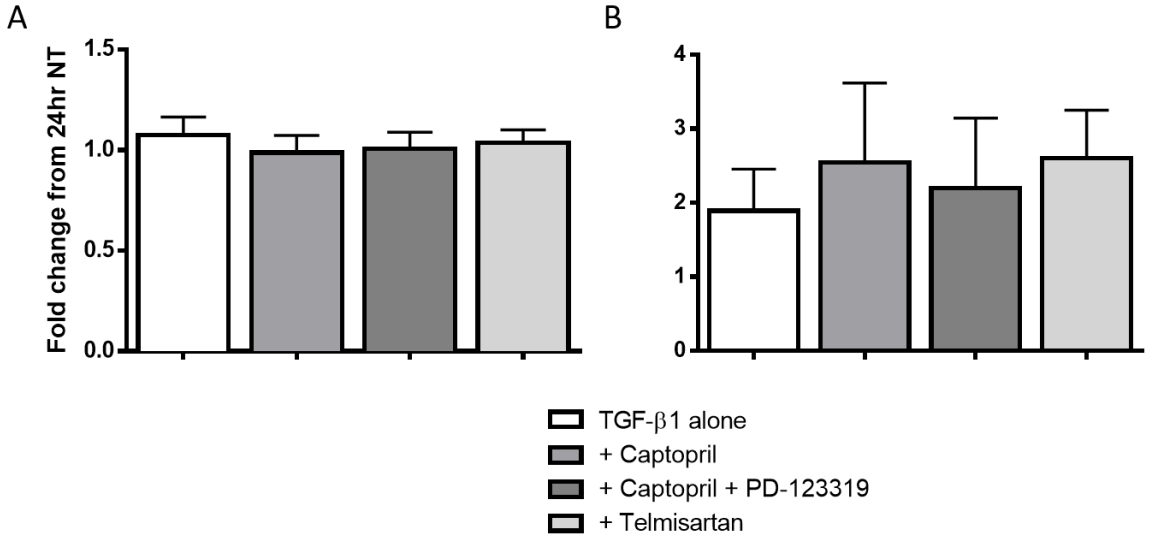

Figure 4-30. The effects of angiotensin inhibitors on TGF-β1 induced MMP-1. Human lung fibroblasts were incubated overnight in soton DMEM before treatment with 2ng/ml TGF-β1 with or without 100μM captopril in the presence and absence of 1μM PD-123319, or with 10nM telmisartan alone. Cells were maintained in the presence of 0.5% newborn calf serum (NCS). Supernatants were harvested at 24 (**A**, n=3) and 48 hours (**B**, n=3) and run through a sandwich ELISA for MMP-1. Data shown are fold change from 24 hour 0.5% NCS treated cells (no treatment – NT) and are mean ± SEM of all experiments. (Wilcoxon matched-pairs signed rank test).

Very little effect of any of the inhibitors was observed. Captopril may have induced small upregulations at 48 hours (similar to that observed in **Figure 4-27**), although PD-123319 does not appear to have much effect on this result. Due to the small sample size (n=3) and variability between cell lines, further repeats of this experiment are required to confirm this result.

4.4 Discussion

Previous experiments (as reported in Chapter 3) have demonstrated the ability of ANGII to induce intracellular Ca^{2+} release in HLFs via AT_1R. Activation of signalling pathways downstream of Ca^{2+} mobilisation were also observed, with ANGII shown to induce ERK1/2 phosphorylation. As these results indicate that ANGII is able to activate HLFs, effects of this peptide on downstream fibroblast functions were investigated. Results from Chapter 3 also showed inhibitory actions of ANG(1-7) on Ca^{2+} mobilisation, therefore, how this translates to fibroblast function was also examined. In addition, as ANGII is thought to mediate its effects, at least in part, by TGF-β1 induction (Uhal *et al.*, 2007), the effects of this cytokine on fibroblast function were also explored.

The first functional parameter to be investigated was proliferation. Initial experiments were performed following serum starvation for 24 hours, prior to treatment with ANGII or TGF-β1 in serum free DMEM (**Figure 4-1**). Neither treatment induced HLF proliferation under these circumstances, with a loss in cell number observed at 24 hours with these treatment conditions. An average loss of approximately 45% of the cell seeding density was seen at this time point, indicating high levels of cell death when maintaining cells in serum free DMEM. Previous literature has also reported apoptosis in a subset of mouse derived fibroblasts following serum starvation (Kulkarni and McCulloch, 1994), indicating that this condition may not be optimal for investigating fibroblast activity.

The effects of ANGII and TGF-β1 were also explored in the presence of 10% NCS in HLFs that were not serum starved. Both 0.1 and 1μM ANGII and 2ng/ml TGF-β1 upregulated proliferation of fibroblasts under these conditions (**Figure 4-2**), although these effects were only observed at the longer time point of 72 hours. The high NCS concentration present in this study also may not be the best condition for investigating fibroblast proliferation, as large increases in cell number were already observed in the presence of 10% NCS. This high level of background proliferation may therefore mask any early mitogenic effects of the peptides that were tested.

The proliferative effects of ANGII and TGF-β1 were also investigated in the presence of 0.4% NCS in HLFs that were not serum starved prior to treatments (**Figure 4-3**). It was hoped that lowering the concentration of NCS would increase the level of proliferation that could be observed with peptide treatments, by reducing the background proliferation observed in the presence of 10% NCS. ANGII did not induce proliferation under these conditions at any of the time points investigated. The mitogenic ability of TGF-β1 was, however, vastly improved under these conditions, and induced cell proliferation at all time points. Also 0.4% NCS appeared to provide a stable non-apoptotic, non-proliferative environment, with no change from the cell

seeding density observed with 24 hour no treatment. These results indicate that these conditions were the most optimal for study of cell proliferation.

ANGII only appeared to upregulate 10% NCS induced proliferation in HLFs that were not serum starved prior to experiments. No other experimental conditions yielded positive effects of ANGII on HLF cell number. This result is interesting, although the effects of the inhibitors telmisartan and PD-123319 on this ANGII activity need to be explored, to determine whether this was indeed a RAS induced effect.

There are a large number of previous studies investigating the effects of ANGII on human cardiac fibroblast (HCF) proliferation. The reported effects of both ANGII and TGF-β1 on fibroblast proliferation in the literature are extremely inconsistent. Agocha et al (Agocha *et al.*, 1997) reported an inhibitory effect of TGF-β1 and a stimulatory effect of ANGII on HCFs. These experiments were, however, performed on fibroblasts from one single donor (aged 25). The results from the current investigation highlight the natural variability that exists between different fibroblast donors, therefore the results obtained from just one donor derived cell line need to be interpreted with caution. Also, the younger age of the donor in the study by Agocha et al may also affect the proliferative ability of the fibroblasts, compared to the older ages of the HLF donors in the current study (57.3 ± 5.2 years). A number of previous investigations have shown that human dermal fibroblasts lose their proliferative capacity with age (Phillips *et al.*, 1994; Fedarko *et al.*, 1995), although comparable studies in HLFs are limited. Also Agocha et al used 10ng/ml TGF-β1 which is an extremely high concentration of this cytokine that is known to induce a shift to the less proliferative myofibroblastic phenotype (Midgley *et al.*, 2013). This may be a reason as to why no proliferation was observed with TGF-β1 in the published study.

The mitogenic effects of TGF-β1 have been explored in more detail in an older investigation in a human embryonic fibroblast cell line (Fine and Goldstein, 1987). Although there were small differences in the cell synchronisation (quiescing) step in the published study, results obtained by Fine and Goldstein fit well with results obtained from initial experiments in the current investigation. The authors quiesced cells in the presence of 0.4% bovine foetal serum (BFS) for either 24 or 48 hours, and experiments were performed in both serum free and 0.4% BFS environments. No effect of 0.1, 1 or 10ng/ml TGF-β1 on fibroblast nuclear number was reported. These results fit with the experiments conducted in serum free media in the current study, where no proliferation was observed in the presence of 2ng/ml TGF-β1 following cell synchronisation. TGF-β1 did, however, induce cell proliferation in the presence of 0.4% NCS, although these cells were not quiesced prior to experiments and therefore are not comparable

to those from Fine and Goldstein. Another study by Strutz et al (Strutz *et al.*, 2001) demonstrated a positive effect of TGF-β1 at 0.1, 1 and 10ng/ml in human kidney fibroblasts, with a peak maximal response observed at 1ng/ml. These fibroblasts were also serum starved for 24 hours prior to experimental treatments, but this was by replacing DMEM with Iscoves modified eagles media, which is a media tailored to highly proliferative cell phenotypes. This may have been less detrimental to fibroblast viability than the standard serum free DMEM used in most experiments.

Other investigations alongside the Agocha et al study discussed above have also demonstrated increased proliferation of HCFs in the presence of ANGII (Kawano *et al.*, 2000). Both of these investigations were performed in cells that had been quiesced in serum free media for either 24 (Agocha *et al.*, 1997) or 48 hours (Kawano *et al.*, 2000) before treatment with ANGII in serum free media. These results do not fit with those from the current study, as no proliferation with ANGII was observed in serum starved cells.

In contradiction, other studies have demonstrated no effect of ANGII on HCF proliferation, Hafizi et al saw no effect of ANGII, at concentrations ranging from 0.01- 10μM, again in cells that were quiesced in serum free media. Another study investigating the effects of ANGII on human lung, synovial and dermal fibroblasts also showed no effect of ANGII on cell proliferation (Galindo *et al.*, 2005). These authors quiesced fibroblasts with 0.1% serum for 24 hours and investigated the effects of 0.1 and 10μM ANGII in the presence of different serum concentrations (0.1, 5 and 10%), with no effect documented under any conditions. This fits well with preliminary data that was performed in the current study, with no effect of 0.01 - 10μM ANGII observed in the presence of 0, 1, 5 or 10% NCS following serum starvation (data not shown). The published study reported coexpression of AT_1R and AT_2R on all human fibroblast types and suggested the opposing roles of both receptors as a reason for the lack of overall ANGII effect. This was, however, contradicted by the fact that addition of the AT_2R antagonist PD-123319 prior to ANGII treatment, did not improve the proliferative ability of ANGII (via binding to AT_1R).

The ability of ANG(1-7) to modulate HLF proliferation was also explored in the current investigation. As previous literature has suggested an antifibrotic role for ANG(1-7), the ability of this peptide to inhibit 10% NCS induced proliferation was explored (**Figure 4-4** and **Figure 4-5**). The effects of the Mas antagonist A-779 on any ANG(1-7) results were also investigated, as well as the effects of A-779 alone.

As shown in experiments with ANGII, 10% NCS caused large increases in HLF proliferation. ANG(1-7) appeared to have little effect on this 10% NCS induced cell number at 48 hours, with

variable results between different donor fibroblast lines. Interestingly, small but consistent upregulations in cell number were observed in the presence of ANG(1-7) at 72 hours. One possible explanation for this is the high concentrations of ANG(1-7) used in this study. As mentioned earlier, there is likely to be a presence of ANG peptides in 10% NCS media. Therefore, there may be a basal level of ANG(1-7) present, which is causing a small suppression in HLF proliferation. By adding in high concentrations of exogenous ANG(1-7), this may cause Mas receptor desensitisation/internalisation (Gironacci *et al.*, 2011), leading to less activity of the endogenously present ANG(1-7) and hence may cause a small upregulation in proliferation. However, if this were the case, then these effects would have been expected at a shorter time point, as the Mas receptor has been shown to internalise within 10 minutes of ANG(1-7) treatment (Gironacci *et al.*, 2011).

The likelihood of this scenario is also questionable due to the lack of real effect observed with A-779. The addition of this antagonist alone had no real effect on 10% NCS induced proliferation. If the explanation above was indeed correct, increases in proliferation would be expected in the presence of A-779 alone (again due to inhibition of endogenous ANG(1-7) activity).

The lack of effect of A-779 on the upregulations observed in the presence of ANG(1-7) also suggests that this response is not simply mitogenic activity of ANG(1-7) via binding to the Mas receptor. However, due to the small sample size (n=3-4) used in these experiments and the variable nature between HLF donors, increasing the sample size of this investigation is required to allow for definitive conclusions to be made.

There is very little investigation into the effects of ANG(1-7) on fibroblast proliferation, with most published studies performed in rat cardiac fibroblasts. One study demonstrated the ability of ANG(1-7) to reduce FBS induced fibroblast proliferation. This inhibition was reversed in the presence of A-779, indicating that ANG(1-7) was causing inhibition via the Mas receptor (McCollum *et al.*, 2012). The ability of ANG(1-7) to dose dependently inhibit vasopressin induced rat cardiac fibroblast proliferation has also been shown to be via the Mas receptor (Niu *et al.*, 2014). These results do not fit well with those from the current investigation.

Increases in cell proliferation have been observed with ANG(1-7) in one study in human skin fibroblasts, in serum free conditions (Nickenig *et al.*, 1997). Dose dependent increases were observed with this peptide that were not blocked by the addition of either EXP-3174 (AT_1R antagonist) or PD-123319 (AT_2R antagonist), demonstrating that these responses were not via the classical ANGII receptors pathways. The same study also demonstrated the presence of a specific ANG(1-7) receptor on the cell surface, which was likely to be the Mas receptor.

Although this was not confirmed, as the Mas receptor was shown to be a receptor for ANG(1-7) in 2003 (Santos *et al.*, 2003b), which is after the described study was published.

The investigation by Nickenig et al is one of the few studies into ANG(1-7) functional responses performed in human derived fibroblasts, and this publication reported opposite effects to those observed in rat fibroblasts (discussed above). The results from the current investigation are also derived from human fibroblasts and fit better with the results observed by Nickenig et al, with potential proliferative activity of ANG(1-7). Although there are differences in the methodology between the current and published study (serum free vs 10% serum), these reported observations may suggest high species variability in the effects of ANG(1-7) on fibroblasts, and ANG(1-7) may in fact be mitogenic for fibroblasts derived from human organ systems.

However, care should be taken not to over compare the results from the current study with the study by Nickenig et al, as the published study utilised just one skin biopsy derived cell line for all experiments. The results from the current investigation demonstrate differences between fibroblasts from individual donors, therefore, had Nickenig et all used multiple cell lines, different results may have been observed.

The next fibroblast function investigated that is known to be extremely important in IPF disease progression was collagen deposition. There are multiple enzymes important in collagen synthesis, most notably lysyl hydroxylase, lysyl oxidase and prolyl hydroxylase. Lysyl hydroxylase is important in the hydroxylation of lysine to form hydroxylysine, which is then further glycosolated by the addition of galactose (Yamauchi and Sricholpech, 2012). These glycosylated hydroxylysine residues, as well as a small proportion of lysine residues, are then oxidised by lysyl oxidase (Feres-Filho *et al.*, 1995), causing the formation of reactive aldehydes. These reactive aldehydes can then undergo spontaneous reactions with other aldehyde containing residues in collagen, resulting in cross linking between collagen helices, helping to stabilise the collagen molecule (Csiszar, 2001). Prolyl hydroxylase is important in the formation of hydroxyproline, which is essential for the formation and stability of the collagen triple helix (Myllyharju, 2003).

Ascorbic acid is an important cofactor for both hydroxylases. In the absence of L-ascorbate, lysyl hydroxylase activity in human dermal fibroblasts was reduced to 8% of the maximum activity observed in the presence of this cofactor (Miller *et al.*, 1979). Prolyl hydroxylase activity has also been shown to be reduced by at least 90% in the absence of ascorbate (de Jong *et al.*, 1982). These observations demonstrate the need for the addition of ascorbate to the

culture media in order to observe any collagen production in response to stimuli, therefore 100μM L-ascorbate was added to the media for all collagen experiments.

Initial experiments saw no increase in collagen production in response to ANGII. Therefore the relationship between ANGII and TGF-β1 was explored. TGF-β1 is known to induce the expression of AT_1R on adult lung fibroblasts (Renzoni *et al.*, 2004), therefore HLFs in the current study were pretreated with 0.5% NCS with or without 2ng/ml TGF-β1 for 16 hours, before treatment with increasing concentrations of ANGII (**Figure 4-7**). The idea was that TGF-β1 may induce upregulation of AT_1R on HLFs, and therefore may 'boost' the response to a subsequent dose of ANGII. There was no ANGII dependent increase in collagen production in either 0.5% NCS or TGF-β1 treated cells. There was, however, an increase in collagen deposition in HLFs that received TGF-β1 pretreatment, highlighting the known profibrotic nature of this cytokine.

The 2ng/ml dose of TGF-β1 is considered to be a maximal dose. This may mean that HLFs are maximally stimulated to produce collagen at this concentration, therefore no additional effects of ANGII would be possible under these circumstances. This lead to investigating the effects of ANGII in the presence of lower TGF-β1 concentrations. HLFs were treated with increasing concentrations of TGF-β1 in the presence and absence of 10μM ANGII (**Figure 4-8**). TGF-β1 dose dependently increased collagen production, and a maximal response was observed at 2ng/ml in 3 cell lines and at 1ng/ml in the remaining 3 cell lines. No effect of ANGII on TGF-β1 induced collagen production was observed at any concentration. These results contradict the existence of the feedback loop that exists between these two peptides (Lee *et al.*, 1995; Renzoni *et al.*, 2004; Uhal *et al.*, 2007). TGF-β1 does not appear to upregulate the response to ANGII, nor does ANGII further enhance the response to TGF-β1 in these experiments.

The ability of ANG(1-7) to modulate collagen production in HLFs was also investigated. This peptide (0.1, 1 or 10μM) did not affect collagen deposition in response to increasing concentrations of NCS (**Figure 4-9**). This does not fit with previous literature investigating the effects of ANG(1-7) on collagen deposition in rat cardiac fibroblasts, with this peptide shown to reduce FBS induced collagen production in this cell type (McCollum *et al.*, 2012). Also the ability of ANG(1-7) to reduce the baseline collagen production observed in serum free media has been demonstrated (Iwata *et al.*, 2005), with the same study also demonstrating inhibitory effects of ANG(1-7) against ANGII induced collagen deposition, again in rat cardiac fibroblasts.

In the current investigation, 0.1μM ANG(1-7) had no effect on TGF-β1 induced collagen production (**Figure 4-10**). Also, upon closer evaluation the variable nature of fibroblasts becomes apparent, with a -30.3 – 70.5% change in TGF-β1 induced collagen production

observed between fibroblast lines. This, as well as the variation observed in the proliferation studies discussed above, suggests the potential existence of many different fibroblast phenotypes. Small but significant upregulations in TGF-β1 collagen production of 10% were observed in the presence of 10μM ANG(1-7), although these results again demonstrated high variation between individual experiments (-3.6 – 27.0%). Upon closer evaluation of the patient characteristics, there does not appear to be any discernible differences between donors that can account for the differences in the responses observed in any of the described experiments.

Also, no effect of A-779 on ANG(1-7) collagen production was observed (**Figure 4-11**), indicating that any differences in collagen that were observed with ANG(1-7) were not via the Mas receptor in this assay, although more experimental repeats are required to confirm this observation.

As the effects of ANG(1-7) on TGF-β1 collagen production discussed above were investigated by the simultaneous addition of ANG(1-7) and TGF-β1, the effect of ANG(1-7) pretreatment on TGF-β1 induced collagen was explored (**Figure 4-12**). Unlike previous experiments demonstrating increased collagen deposition, there was no effect of ANG(1-7) on TGF-β1 induced collagen production under these conditions. The expected effects of ANG(1-7) on TGF-β1 induced collagen production are unknown as there are no comparative studies into these effects of ANG(1-7) in the literature.

Collagen production was measured according to the methods used by Chen et al, where cells were treated and incubated for 6 days before staining with Sirius red dye. No media change was performed on the fibroblasts during this time which may not have been the most optimal culture conditions for maintaining these cells. During the course of the investigation, it was determined that shorter time points of 24 – 48 hours could have been used (due to the increases in collagen observed with just an overnight incubation with TGF-β1 in **Figure 4-7**), however this was not adopted to maintain continuity between all collagen experiments. This would be an important point to consider for further investigations into collagen deposition.

The next parameter to be investigated was MMP-1 secretion. There is limited data on the effects of ANGII on MMP production in fibroblasts although reported data is fairly consistent. ANGII has been shown to downregulate MMP-1 in HCFs (Pan *et al.*, 2008), and also in murine cardiac fibroblasts (Chen *et al.*, 2004; Stacy *et al.*, 2007).

MMP-1 was investigated by ELISA (**Figure 4-13**), and no difference in MMP-1 production was observed in the presence of ANGII at 24 or 48 hours. However, a trend towards decreasing MMP-1 in the presence of ANGII was observed at 72 hours, with an approximate decrease of

25% seen in response to 10μM ANGII (compared to no treatment). This was fairly consistent across all cell lines tested, with a decrease observed in 4 out of the 5 lines used for this experiment, although this did not reach significance. Decreases in MMP-1 would lead to less collagen degradation in the lung and therefore lead to increased collagen deposition and hence fibrosis, suggesting a potential profibrotic role for ANGII in these circumstances. To further characterise this potential response to ANGII an increased sample size is required, and these experiments need to be repeated in the presence of telmisartan and PD-123319 to determine receptor involvement.

This potential downregulation of MMP-1 by ANGII fits with that from Pan et al (2008) in HCFs, although the published study did not look at the expression of the MMP-1 protein, but rather the mRNA levels. The current work also fits loosely with the studies in murine cardiac fibroblasts (Chen *et al.*, 2004), although in the published study, differences in the protein level were seen as early as 6 hours post treatment with 0.1μM ANGII. Also, this reported downregulation was almost completely reversed by 24 hours. These results, coupled with those from the current work may in fact suggest a biphasic MMP-1 response to the addition of ANGII, and may also provide a reason as to why no inhibition was observed at 24 hours in the current study. Investigations into MMP-1 production at shorter time points would be required to confirm this hypothesis.

TGF-β1 caused small upregulations in MMP-1 production at all time points, however, this did not reach statistical significance. This trend is interesting, as this is different to that observed with ANGII, and is actually opposite to that seen in response to ANGII at 72 hours. ANGII is thought to mediate its effects via induction of TGF-β1 and has been shown to induce TGF-β1 secretion in fibroblasts (Lee *et al.*, 1995). If ANGII was indeed mediating its effects on MMP-1 production via induction of TGF-β1 then an increase in response to ANGII would be expected. This suggests that ANGII may be affecting MMP-1 secretion via a TGF-β1 independent mechanism.

The effects of ANGII and TGF-β1 on MMP production were also investigated by gelatin zymography. This method allows for the detection of the two gelatinases, MMP-2 and MMP-9, although no active MMP-9 was detected in the conditioned media from HLFs after 48 hours. This was not unexpected as Ramos et al (Ramos *et al.*, 2001) only detected low levels of MMP-9 in one out of three healthy fibroblast lines. In the currently study there was, however, an upregulation in MMP-2 production by HLFs in response to both 2ng/ml TGF-β1 and 10μM ANGII (**Figure 4-15**). These effects of TGF-β have been documented previously, with this cytokine shown to increase MMP-2 production in human gingival fibroblasts at both the

protein (Overall *et al.*, 1989) and RNA level (Overall *et al.*, 1991). MMP-2 has been shown not only to degrade gelatin, but also collagen type IV (Zeng *et al.*, 1999). As this collagen is responsible for the structural integrity of the basement membrane, upregulation of this MMP could lead to high degradation of the pulmonary epithelium, and hence initiate the dysregulated wound healing response and fibrosis that is typical of IPF. Selman et al (Selman *et al.*, 2000) observed MMP-2 expression in some subepithelial myofibroblasts in IPF lung samples, close to areas of basement membrane disruption. No MMP-2 staining was observed in healthy lung samples, further highlighting a potential role for this MMP in IPF.

ANGII has been shown to downregulate MMP-2 in both human (Pan *et al.*, 2008) and murine cardiac fibroblasts (Stacy *et al.*, 2007). The results from the current study do not fit well with these previous investigations. Although Pan et al only looked at mRNA levels 24 hours post treatment with 1μM ANGII. The study by Stacy et al, however, is easier to compare, with MMP activity measured after a 48 hour treatment with 1μM ANGII. MMP-2 activity was downregulated by 43% in this investigation. In the current study, 1μM ANGII had no effect on MMP-2 activity.

As the effects of ANGII on MMP-2 production in HLFs in the current study are only apparent at high concentrations (10μM), the physiological relevance of this observation is questionable. The circulating plasma concentration of ANGII is reported to range between 13.9 ± 2.0 – 32 ± 6.0pM (Lawrence *et al.*, 1990; Matsui *et al.*, 1999). Although the concentrations of ANGII in the pulmonary environment are likely to be higher, due to locally expressed ACE, they are unlikely to be at the concentrations required to upregulate MMP-2 production in this assay. Also as mentioned in section 1.6, ACE2 levels have been shown to be extremely downregulated in the lungs of IPF patients (Li *et al.*, 2008), which in turn is likely to lead to elevated ANGII levels in these patients, which could therefore be driving increased MMP-2 levels.

Very little effect of ANGII on HLF function has been reported in this study, therefore investigations into potential reasons for this were explored. The effects of ANGII on IL-6 secretion were examined, this parameter was chosen for investigation due to the effects of this cytokine on HLF proliferation. IL-6 has been reported previously to differentially affect HLF proliferation, depending on whether the fibroblasts were derived from healthy or IPF lung tissue (Moodley *et al.*, 2003b). A decreased proliferation of healthy derived HLFs was reported in the presence of IL-6, but increased proliferation was observed in IPF fibroblasts in response to this cytokine. The ability of ANGII to induce IL-6 secretion in HLFs was explored, as this peptide has been previously reported to induce expression of this cytokine in murine cardiac

fibroblasts (Sano *et al.*, 2000). If ANGII induces expression of IL-6 in HLFs then this may be a reason for the lack of proliferation observed in the presence of this peptide.

Preliminary experiments investigating the effects of ANGII and TGF-β1 on IL-6 looked at IL-6 in the supernatant 2, 4, 8 and 24 hours after treatment with 0.1 – 10μM ANGII or 2ng/ml TGF-β1. No IL-6 was detected in the supernatants at these time points (apart from 8 and 24 hour TGF-β1 treated cells), therefore longer time points were investigated. ANGII did not induce IL-6 expression at 24, 48 or 72 hours, but large increases in IL-6 were observed in response to TGF-β1 at all time points (**Figure 4-16**). These results do not support the suppressive effects of IL-6 on healthy HLF proliferation that have been previously reported. TGF-β1 demonstrated clear proliferative effects on HLFs in the presence of 0.4% NCS (**Figure 4-3**) and also induced large increases in IL-6 secretion under similar conditions, which according to Moodley et al, should be inducing senescence of this cell type. ANGII caused no proliferation of HLFs in the presence of 0.4% NCS and also did not induce IL-6 secretion.

Next, the ability of ANGII to induce TGF-β1 was investigated. It is widely accepted in the literature that many of the profibrotic actions of ANGII are mediated via the induction of TGF-β1 (Uhal *et al.*, 2007). The ability of TGF-β1 to positively upregulate secretion of itself in an autocrine feedback loop has also been documented (Van Obberghen-Schilling *et al.*, 1988). TGF-β1 *in vivo* exists in two forms, one form is in a complex bound to latency associated peptide (LAP), and the other is free TGF-β1 that has dissociated from LAP (**Figure 1-3** and **Figure 1-4**). Using an ELISA for the detection of LAP, allows for the measure of both of these TGF-β1 forms and so measures both free LAP (as a measure of free TGF-β1) and TGF-β1 bound LAP.

ANGII (at 0.1μM) caused significant upregulation in LAP secretion at both 48 and 72 hours (increases of approximately 40% and 60% respectively, **Figure 4-17**). However, no effect at either 1 or 10μM ANGII was observed, this may again be due to receptor internalisation at high concentrations of ANGII (mentioned previously). As expected (due to the autocrine feedback loop mentioned above), large increases in LAP production were observed at all time points following treatment with TGF-β1.

The effects of ANGII on active TGF-β1 were also examined with TGF-β1 ELISA, this only allows for detection of TGF-β1 that has dissociated from LAP and is in its free and active form. The effects of TGF-β1 in this assay could not be explored, as treatment with TGF-β1 would be detected in the supernatant giving a false positive. No detectable level of active TGF-β1 was seen in the presence or absence of ANGII.

Together, these results indicate that ANGII may indeed be inducing secretion of TGF-β1, although the secreted cytokine is in complex with LAP and is therefore rendered inactive. This may be a reason as to why very little effect of ANGII has been observed on HLF function. The ability of TGF-β1 to induce the active form of itself has not been investigated in this study.

Next, the ability of the ACE inhibitor captopril and AT_1R antagonist telmisartan to modulate baseline levels of HLF function were explored. This was to determine whether there may be a basally active RAS present in the cell culture system that is desensitising the response to exogenous additions of ANG peptides.

First the effects of these compounds on collagen production were explored. The inhibitors were added to the media at the cell seeding stage of the experiment, and left to incubate overnight before retreatment with these inhibitors in the presence of 0.5% NCS. Captopril did indeed cause a reduction in baseline collagen levels (**Figure 4-18**) of approximately 15%. As captopril was added at the cell seeding stage of the experiment, it is likely that this inhibitor was reducing the response to any peptides in the 10% NCS that would have occurred in the overnight incubation. Captopril has previously been shown to reduce 10% NCS induced collagen and TGF-β1 in keloid fibroblasts (Chen *et al.*, 2014). The ANG peptides are blood circulating peptides, therefore NCS is a likely source of ANGI. By adding in Captopril, inhibition of ACE could prevent the conversion of endogenous ANGI to ANGII, and hence could provide an explanation as to why decreases are observed. Also fibroblasts have been shown to express ACE (van Kesteren *et al.*, 1999; Hafizi *et al.*, 2004), so cleavage of ANGI to ANGII in the normal untreated culture system is a feasible scenario.

Confounding results were observed with telmisartan. This compound only caused an extremely small decrease in baseline collagen (**Figure 4-19**) of 7%. Although statistically significant, the physiological relevance of a reduction of this size is questionable. Maximum effects were also observed at 10nM, with no further effect observed in the presence of 1μM telmisartan. Although this decrease is small, this could suggest an AT_1R mediated mechanism, telmisartan will only prevent the binding of endogenous ANGII from binding to this receptor, whereas captopril (by blocking production of ANGII) will prevent binding of ANGII to both AT_1R and AT_2R. This could be a reason for the larger effect observed in the presence of this ACE inhibitor, to determine any AT_2R mediated mechanism these experiments could be repeated in the presence of the AT_2R antagonist PD-123319. Also, captopril will also stabilise any ANG(1-7) that is present in the cell culture media, as ACE degrades this peptide to ANG(1-5) under normal conditions (as shown in **Figure 1-8**). Therefore there could be some Mas receptor mediated effect following the addition of captopril, to confirm this, these experiments could be

repeated in the presence of the Mas antagonist A-779. The differences observed in the effects of captopril and telmisartan suggests that the results observed with captopril are not purely via an AT_1R mediated mechanism.

Captopril has been shown to inhibit human prolidase (Ganapathy *et al.*, 1985). Prolidase is an enzyme important in cleaving dipeptides and tripeptides containing C-terminal proline, as well as in the recycling of proline for the synthesis of new collagen (Jackson *et al.*, 1975). Proline is extremely important in stabilising the structure of collagen and human skin fibroblasts deficient in prolidase have been shown to have impaired collagen production (Dolenga and Hechtman, 1992). Cell culture media containing 10% FBS is known to contain many amino acids, therefore the 0.5% NCS present in the cell culture media in the current study is likely to be a small source of proline. However, at least part of this proline will exist in a dipeptide form, with proline in this form unavailable for incorporation into newly synthesised collagen, this is likely to be a limiting step in collagen production and therefore prolidase is required for cleavage of this dipeptide bound proline. In the current investigation, the culture media is also supplemented with MEM non-essential amino acids, which according to manufacturer's specification includes 0.1mM L-proline (when diluted 1 in 100 to a working concentration). Therefore whether inhibition of prolidase is a feasible action of captopril in this culture system in questionable. The concentration at which captopril causes inhibition of prolidases also varies greatly between species as well as different organs (Ganapathy *et al.*, 1985), with a K_i of 5 mM reported for captopril against human kidney prolidases, which is much higher than the 0.1mM used in the current investigation. Karna et al (Karna *et al.*, 2010) demonstrated a decrease in collagen synthesis in the presence of captopril, in human dermal fibroblasts that were cultured in media contained 10% FBS. Captopril (0.2 – 1mM) caused a dose dependent decrease in collagen, with a reduction of about 20% observed in the presence of 0.3mM captopril. This reduction in collagen synthesis was also shown to correlate with a decrease in prolidase activity. To determine if the effect of captopril in the current study was a collagen specific inhibition, the ability of captopril to modulate other fibroblast functions was explored.

Baseline IL-6 in response to 0.5% NCS was explored as well in as HLFs stimulated with 10% NCS or TGF-β1 (**Figure 4-20**). The effects of captopril on IL-6 levels under all conditions were examined. TGF-β1 induced IL-6 production was unaffected by the addition of captopril, indicating that this cytokine is inducing IL-6 via an ACE independent mechanism. Small but significant upregulations in 0.5% NCS treated cells were observed in the presence of captopril at 24 hours, however, this significance was lost by 48 hours. Most notable were the increases in 10% NCS induced IL-6 in the presence of captopril. These results first off do not suggest a RAS dependent mechanism, as ANGII has been reported to upregulate IL-6 in fibroblasts (Sano

et al., 2000). Blocking endogenous production of this peptide in 10% NCS should result in a decreased IL-6 response, but this was not observed in these experiments. However, the documented effects of ANGII on IL-6 production in fibroblasts is limited, with no previous studies performed in HLFs, therefore the exact effect expected in the presence of this peptide is relatively unknown.

The ANG peptides ANGI and ANG(1-7) are not the only substrates for ACE. Bradykinin is another known substrate for this enzyme (Hornig *et al.*, 1997), therefore by blocking ACE, higher levels of bradykinin result. Bradykinin has been shown to upregulate IL-6 production in primary HLFs (Hayashi *et al.*, 2000), and as this peptide (like ANG peptides) is an important vascular mediator, the presence of bradykinin in NCS is extremely likely. This could be the mechanism via which captopril is upregulating IL-6 in this assay, inhibition of ACE would lead to increased levels of bradykinin and hence increased IL-6 production.

Another RAS related hypothesis for the actions of captopril on the observed IL-6 response is the generation of ANG(1-9). By blocking the classical ANGI to ANGII pathway, the alternative degradation pathway for ANGI, the ACE2 pathway, is upregulated. The main peptide formed by cleavage of ANGI by ACE2 is ANG(1-9). Under normal circumstances, this ANG(1-9) is then further cleaved to ANG(1-7) by ACE or neprilysin (NEP) (**Figure 1-8**). HLFs have been shown to express cell bound NEP (Kondepudi and Johnson, 1993), which will cleave some of the ANG(1-9) present, but this degradation would still be reduced in the presence of captopril due to removal of ACE activity, causing higher levels of ANG(1-9) to remain in the media.

ANG(1-9) has been shown to have opposing actions to those generated by the ANGII/AT_1R pathway, via binding to AT_2R (Flores-Munoz *et al.*, 2012). Therefore the ability of the AT_2R antagonist PD-123319 to reverse the increased IL-6 production in response to captopril was investigated.

PD-123319 reduced captopril induced upregulation of both 0.5% (**Figure 4-21**) and 10% NCS IL-6 (**Figure 4-22**) at 24 and 48 hours. PD-123319 completely reversed the effects of captopril on 10% NCS by 48 hours. These results indicate that cells cultured in the presence of captopril have indeed shifted to the ACE2 pathway and have increased the production of ANG(1-9). ANG(1-9) has previously been reported to have antifibrotic actions via AT_2R, which have been inhibited in this system by the addition of PD-123319. However, care does need to be taken not to over interpret these results due to the small sample size for this set of experiments (n=3).

The effects of telmisartan on IL-6 production were also investigated, this was to determine whether any of the effects observed with captopril were an ANGII/AT_1R blockade response.

Telmisartan did not appear to have the same effect as captopril on 0.5 and 10% NCS induced IL-6, indicating that captopril is not acting via reduced production of ANGII.

The effects of captopril on total TGF-β1 secretion were also examined (**Figure 4-24**), there was no significant effect of captopril on 0.5% or 10% NCS induced TGF-β1. There did appear to be a trend towards higher 10% NCS induced TGF-β1 in the presence of captopril at 24 hours (an increase of 37% in the presence of captopril). The effect of captopril on 10% FBS induced TGF-β1 has been previously investigated (Chen *et al.*, 2014), however, a decrease in the presence of captopril was observed and is opposite to the results from the current study. The trend towards increased TGF-β1 in the presence of captopril is confounding to published evidence suggesting increased TGF-β1 in response to ANGII (Lee *et al.*, 1995). Indicating that the results from the current investigation are not ANGII dependent.

The effects of PD-123319 and telmisartan on TGF-β1 were also investigated (**Figure 4-25** and **Figure 4-26**). No effect of PD-123319 on TGF-β1 levels in the presence of captopril was observed in 0.5 or 10% NCS media. Telmisartan also did not affect 0.5 or 10% NCS induced TGF-β1. This suggests that any of the documented effects of captopril on TGF-β1 are not via a RAS dependent mechanism.

Effects of captopril on MMP-1 production were also examined (**Figure 4-27**). No clear effects of captopril on MMP-1 secretion were observed under any conditions. Small downregulations in 0.5% NCS induced MMP-1 were observed at 48 hours. This does not fit with previous results from the current investigation (and previous literature) suggesting downregulated MMP-1 in response to ANGII. If captopril blocked the endogenous production of ANGII, then an increase in MMP-1 would be expected. This again indicates that captopril is not working via an ANGII dependent mechanism.

Small upregulations in TGF-β1 induced MMP-1 were seen in the presence of both Captopril and Telmisartan. These results suggest that the observed trend could be ANGII and AT_1R dependent due to the similar actions of these two inhibitors. This effect of captopril on TGF-β1 does not appear to be reversed in the presence of PD-123319. However, due to the small sample size for these experiments, further repeats are required to allow for definitive conclusions to be made.

The results from this chapter suggest minimal effects of RAS peptides on HLF function. ANGII only appeared to upregulate proliferation in the presence of 10% NCS, however, upon assay optimisation this proliferative effect was lost in the presence of 0.4% NCS. ANGII did not significantly affect any other HLF function, which may be due to the lack of induction of active

TGF-β1. Treatment with TGF-β1 induced fibroblast proliferation, collagen deposition, IL-6 and MMP-2 production as well as small increases in MMP-1. These results suggest that this set of experiments were correctly optimised and provide confidence that the lack of effect seen with ANGII was indeed a real observation.

Captopril significantly upregulated 0.5 and 10% NCS induced IL-6 although this does not appear to be via inhibition of ANGII, due to the lack of effect of telmisartan in this assay. Interestingly, ANG(1-9) may play a role in this captopril induced effect as these responses were reversed in the presence of the AT_2R antagonist PD-123319. The only captopril induced effect that may have involvement of an ANGII dependent mechanism is TGF-β1 induced MMP-1, which may be upregulated due to inhibition of endogenously produced ANGII.

ANG(1-7) also does not appear to inhibit either cell proliferation or collagen production in response to 10% NCS, nor inhibit TGF-β1 stimulated collagen production. Any results in the presence of ANG(1-7) were also variable, with no effect of A-779 observed. This demonstrates no role for the Mas receptor in this investigation.

Together these results suggest limited involvement of the RAS in modulating HLF function, and suggest that this system may not play an important role in IPF pathogenesis. Although the effects of ANG peptides on IPF fibroblasts also need to be investigated to further confirm this observation.

Chapter 5. Angiotensin receptor expression in human lung fibroblasts

5.1 Background

Peptides of the renin-angiotensin system have been implicated in the pathogenesis of IPF (as discussed in section 1.6). ANGII, the most studied peptide of this system has been shown to exert profibrotic effects on fibroblasts, with many of these actions attributed to binding to AT_1R. Many studies investigating these effects have been performed in human cardiac fibroblasts (HCFs) (Hafizi *et al.*, 1998). Investigations into the role of AT_2R in fibrosis (if any) are extremely limited. In addition, ANG(1-7) has been shown to exert antifibrotic effects on fibroblasts via the Mas receptor (McCollum *et al.*, 2012). Most of this work has been carried out in rat cardiac fibroblasts, with extremely limited literature on the effects of this peptide in human fibroblasts.

As expected, due to the high number of investigations into the actions of ANGII, the expression of AT_1R and AT_2R on fibroblasts from a number of human organ systems has been explored. AT_1R was found to be expressed by both human skin (Nickenig *et al.*, 1997) and cardiac fibroblasts (Hafizi *et al.*, 1998), with neither study documenting the presence of AT_2R. One publication (Galindo *et al.*, 2005) did however, report co-expression of AT_1R and AT_2R in a number of different organ derived human fibroblasts, including pulmonary, cardiac and dermal. It was hypothesised that this co-expression of receptors leads to resistance against the profibrotic effects of ANGII.

Mas receptor expression on human fibroblasts is less widely explored, binding studies by Nickenig et al (Nickenig *et al.*, 1997) detected the presence of an ANG(1-7) binding site on human skin fibroblasts. This binding site was likely to be the Mas receptor although this was not investigated in detail, as this work preceded the hallmark publication that characterised the Mas receptor as a binding site for ANG(1-7) (Santos *et al.*, 2003b). Work by Iwata et al (Iwata *et al.*, 2005) also demonstrated an ANG(1-7) binding site on rat cardiac fibroblasts, that was inhibited by the Mas antagonist A-779.

The Mas receptor has been shown to internalise upon binding of 1μM ANG(1-7) in transfected HEK293T cells (Gironacci *et al.*, 2011), indicating a receptor desensitisation mechanism that is induced by high agonist concentrations. The authors also demonstrated that preincubation with A-779 was able to partially inhibit this agonist induced internalisation. The presence of a nuclear localisation sequence on the Mas protein has also been established (Lee *et al.*, 2004), indicating a preference for this receptor to locate to the cell nucleus.

Very little investigation into the expression of the Mas receptor on HLFs has been performed, therefore the main aim of this chapter was to determine whether HLFs express the Mas receptor. The expression of the ANGII receptors AT_1R and AT_2R on HLFs was also explored.

5.2 Protocols

5.2.1 Immunocytochemistry

Immunocytochemistry was performed according to Section 2.10. To determine Mas receptor expression on HLFs, two Anti-Mas rabbit IgG antibodies were used, one that binds a cytoplasmic domain of the Mas receptor and one that binds an extracellular domain. The effects of A-779 preincubation and a low serum environment (0.5% NCS) on Mas receptor expression were also investigated.

5.2.2 Radioligand binding

Radioligand binding studies were performed as described in Section 2.12. To allow characterisation of ANG(1-7) binding sites on fibroblast membrane samples, optimisation studies were performed on Mas transfected HEK293 cell membranes. Two radioligands were utilised for these experiments, [^{125}I]-(A-779) and [^{125}I]-ANG(1-7). ANG(1-7) (10μM) was used as the cold ligand to determine the NSB of both radioligands, however, the effectiveness of other cold ligands such as A-779 (Mas antagonist), AVE0991(non-peptidic analogue of ANG(1-7)) and ANGII were also explored.

To characterise ANGII binding sites on HLF membranes, [^{125}I]-[Sar^{1}Ile^8]-ANGII (Sarile) was used, with NSB defined by the addition of 10μM ANGII.

For homologous competition assays, 0.1 and 0.3nM [^{125}I]-Sarile was incubated with increasing concentrations of unlabelled [I]-Sarile. Heterologous competition assays were performed using increasing concentrations of telmisartan (AT_1R antagonist), PD-123319 (AT_2R antagonist), A-779 and ANGII to determine specific receptors present on HLF membrane samples.

5.3 Results

5.3.1 Mas receptor immunocytochemistry

Initial experiments investigated the effects of cell permeabilisation on the staining observed with cytoplasmic anti-Mas. Following permeabilisation with Triton-X, staining for the Mas receptor was clearly visible in the cell nuclei of HLFs (**Figure 5-1**), and this was confirmed by co-localisation of Hoechst stain and anti-Mas in **Figure 5-1** C.

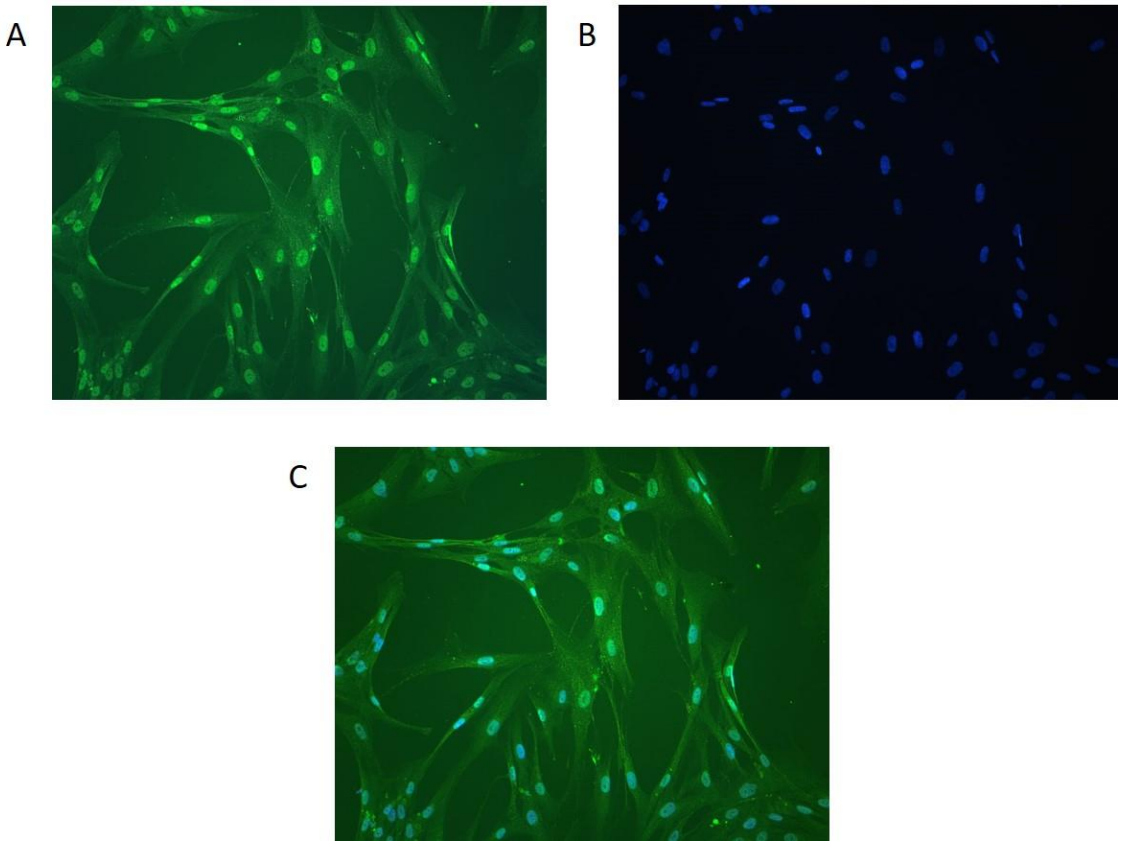

Figure 5-1. Cytoplasmic anti-Mas staining in permeabilised human lung fibroblasts. Human lung fibroblasts were permeabilised before staining with cytoplasmic anti-Mas, staining was then visualised with Alexo fluor 488™ conjugated secondary antibody. **A:** Staining for cytoplasmic anti-Mas was localised to the cell nucleus, **B:** Hoechst counter stain for cell nuclei, **C:** Combined cytoplasmic anti-Mas and Hoechst stain. Images shown are representative of 5 individual experiments.

These experiments were also performed in cells that had not been permeabilised with Triton-X. In non-permeabilised cells no nuclear staining was observed (**Figure 5-2**). These results provide weight that cells that were not treated with Triton-X were in fact 'non-permeabilsed', as cytoplasmic anti-Mas was unable to access the nucleus in this treatment group.

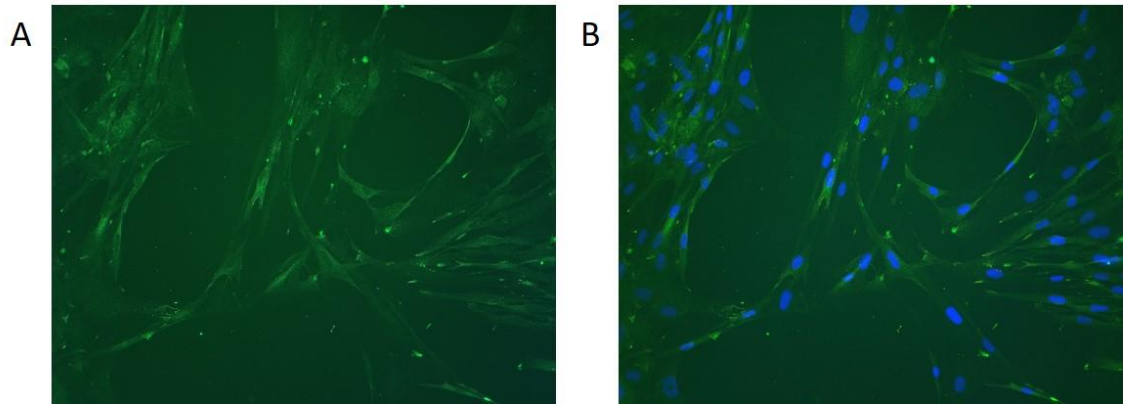

Figure 5-2. Cytoplasmic anti-Mas in non-permeabilised human lung fibroblasts. Human lung fibroblasts were stained with cytoplasmic anti-Mas, staining was then visualised with Alexo fluor 488™ conjugated secondary antibody. **A:** No nuclear staining was observed with cytoplasmic anti-Mas, **B:** Combined cytoplasmic anti-Mas and Hoechst nuclear stain.

Low levels of staining were still observed with this antibody in non-permeabilised cells, although these levels were similar to those observed with secondary antibody staining alone (shown in **Figure 5-3** below), indicating no permeabilisation of cells under these experimental conditions.

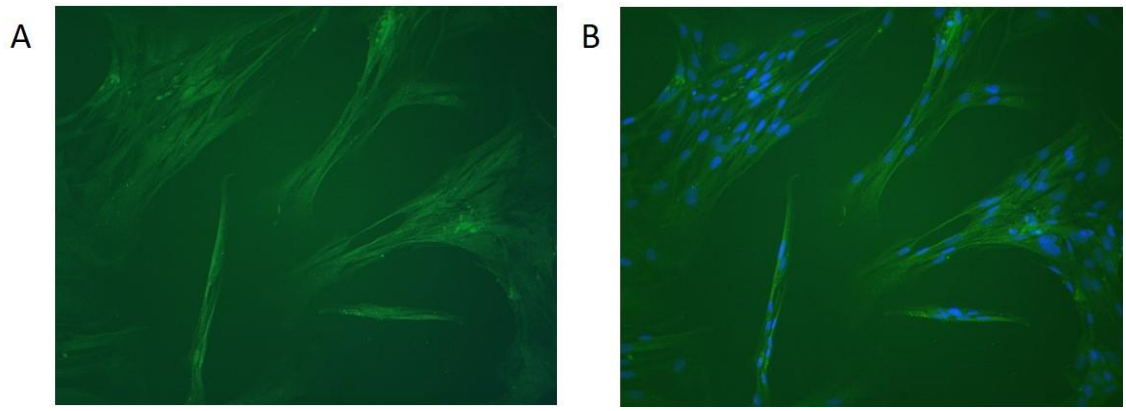

Figure 5-3. Secondary antibody staining alone. Human lung fibroblasts were stained with Alexo fluor 488™ conjugated goat anti-rabbit IgG antibody alone (**A**). Hoechst stain and secondary antibody combined is shown in (**B**). Low levels of background staining was observed with this antibody.

Following justification of the differences between permeabilised and non-permeabilised HLFs, detection of the Mas receptor by extracellular binding anti-Mas was investigated in non-permeabilised cells (**Figure 5-4**), minimal staining was observed with this antibody in initial experiments, at similar levels to secondary antibody alone (**Figure 5-3**).

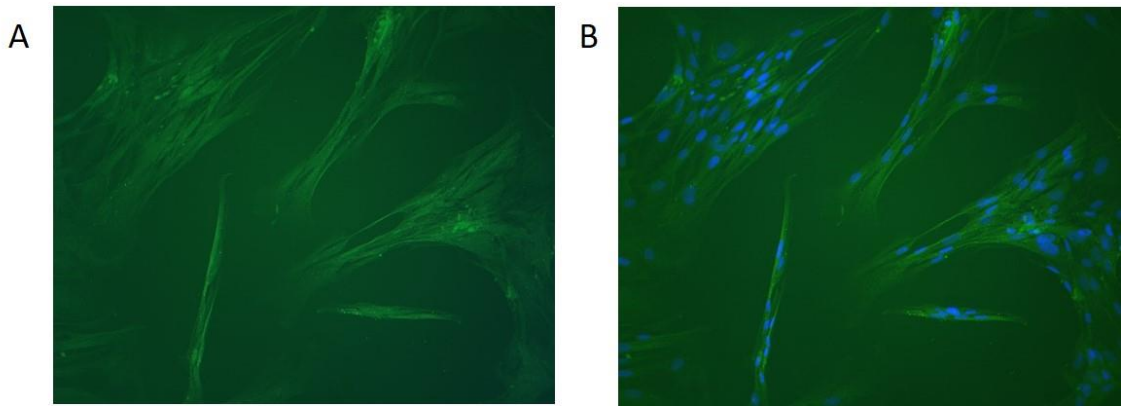

Figure 5-4. Staining with extracellular anti-Mas in non-permeabilised human lung fibroblasts. Human lung fibroblasts were stained with extracellular anti-Mas, staining was then visualised with Alexo fluor 488™ conjugated secondary antibody. **A:** Extracellular staining for the Mas receptor. **B:** Combined extracellular anti-Mas and Hoechst nuclear stain. Low levels of staining were observed in this cell line (TL0153).

Following staining with cytoplasmic anti-Mas, nuclear expression of the Mas receptor was observed in 6 out of the 7 cell lines used in this these experiments. However, this expression was not evident in one cell line, and this absent nuclear staining was coupled with higher levels of localised surface receptor expression when stained with extracellular anti-Mas (as indicated by the white arrows in **Figure 5-5**).

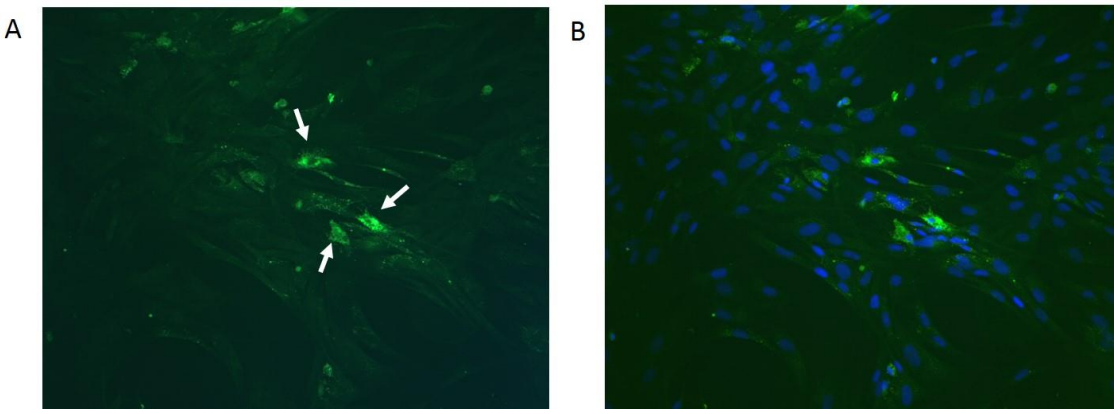

Figure 5-5. Staining with extracellular anti-Mas in non-permeabilised human lung fibroblasts. Human lung fibroblasts were stained with extracellular anti-Mas, staining was then visualised with Alexo fluor 488™ conjugated secondary antibody. **A:** Extracellular staining for the Mas receptor. **B:** Combined extracellular anti-Mas and Hoechst nuclear stain. Higher levels of staining were observed in this cell line (TL0163) compared to that observed in **Figure 5-4**.

As the Mas receptor clearly appears to be predominantly localised to the cell nucleus in HLFs, this could be due to receptor internalisation (due to the presence of ANG(1-7) in the cell media). Therefore the effects of 24 hour treatment with 10μM A-779 was investigated with extracellular anti-Mas (**Figure 5-6**).

Regardless of the level of Mas receptor staining observed with extracellular anti-Mas, no change in the surface expression was observed in cells pretreated with A-779.

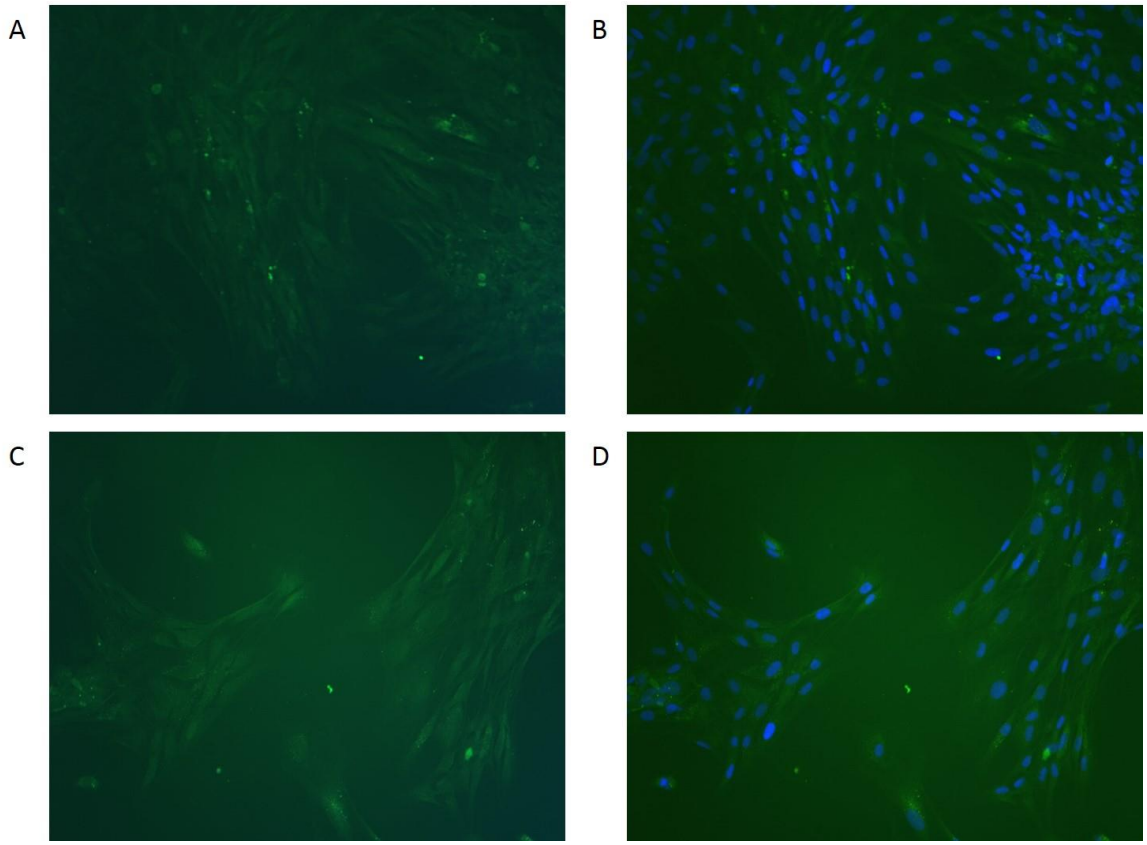

Figure 5-6. Effects of A-779 on extracellular anti-Mas staining. Human lung fibroblasts (HLFs) were stained with extracellular anti-Mas and staining visualised with Alexa fluor 488™ conjugated secondary antibody. Representative Mas receptor staining in **A:** HLFs maintained in 10% NCS and **C:** HLFs pretreated with 10μM A-779 for 24 hours. Figures **B** and **D** show combined anti-Mas and Hoechst stain for **A** and **C** respectively.

Due to the minimal staining observed with extracellular anti-Mas under most conditions, experiments with this antibody were not continued.

As higher levels of staining were observed with cytoplasmic anti-Mas, this antibody was chosen to further investigate the effects of 1 and 24 hour incubation with A-779. The effects of a 1 hr incubation in 0.5% NCS on nuclear staining were also explored (**Figure 5-7**).

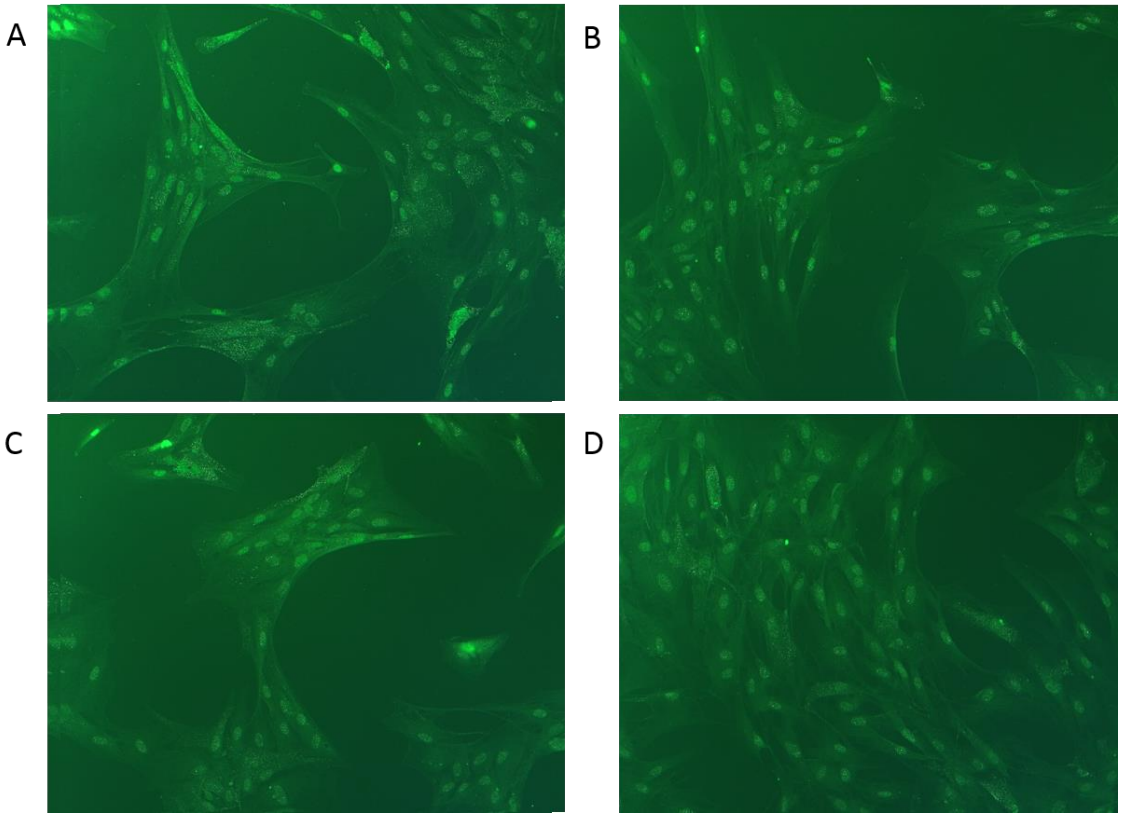

Figure 5-7. Effects of A-779 and 0.5% newborn calf serum on cytoplasmic anti-Mas staining. Human lung fibroblasts (HLFs) were stained with cytoplasmic anti-Mas and staining visualised with Alexo fluor 488™ conjugated secondary antibody. Representative Mas receptor staining in **A:** HLFs maintained in 10% newborn calf serum (NCS) (n=5). **B:** in HLFs pretreated with A-779 for 1 hour (n=2), **C:** in HLFs pretreated with A-779 for 24 hours (n=5). **D:** in HLFs incubated in 0.5% NCS (n=2).

Neither A-779 nor 0.5% NCS altered the staining observed in the presence of cytoplasmic anti-Mas, with the Mas receptor still localised to the nucleus under all treatment conditions. However, the sample size for cells treated for 1hr with A-779 and 0.5% serum needs to be increased as these experiments are currently n=2.

5.3.2 Radioligand binding

To allow for quantification of the Mas receptor staining observed in section 5.3.1, radioligand binding studies were performed with [^{125}I]-A-779 and [^{125}I]-ANG(1-7).

5.3.2.1 Mas receptor

Initial radioligand binding studies were performed with the radiolabelled Mas antagonist [^{125}I]-A-779 in both HLFs (**Figure 5-8 A** and **B**) and in Mas transfected HEK293 cell membrane preparations (**Figure 5-8 C** and **D**).

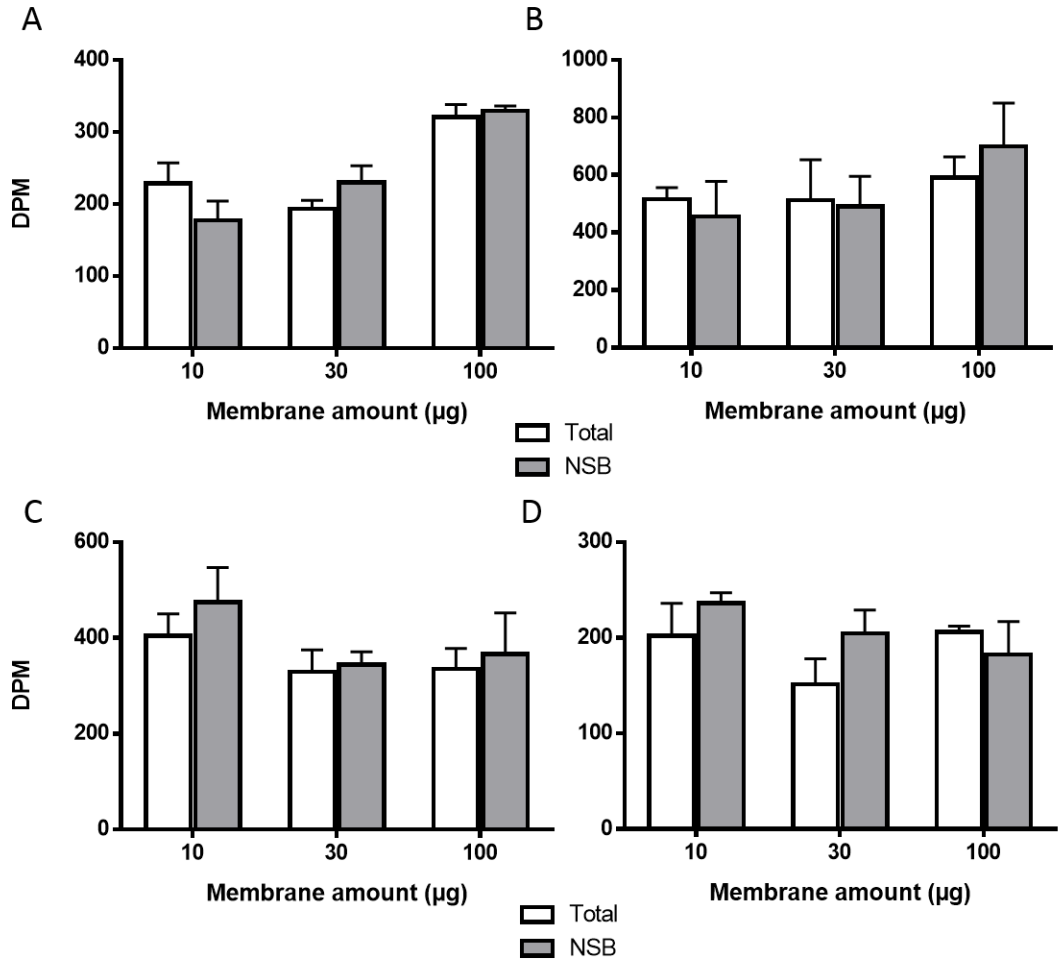

Figure 5-8. Total and non-specific binding of [^{125}I]-A-779. Total and non-specific binding (NSB) in the presence of varying concentrations of healthy lung fibroblast membrane (**A** & **B,** n=2) and HEK293 Mas transfected membrane protein (**C** & **D,** n=1), in the presence of 0.084nM (**A** & **C**) and 0.15nM radioligand (**B** & **D**). Data shown are mean ± SEM (from one experiment run in duplicate). NSB was determined with 10µM ANG(1-7)

As no specific binding was observed with this radioligand, and due to the lack of previous literature regarding the effectiveness of this radioligand in Mas receptor binding studies, experiments with this radioligand were not continued. All further experiments were performed with the better characterised radiolabelled Mas agonist [^{125}I]-ANG(1-7). Experiments with this radioligand were performed in Mas transfected HEK293 cells (**Figure 5-9**).

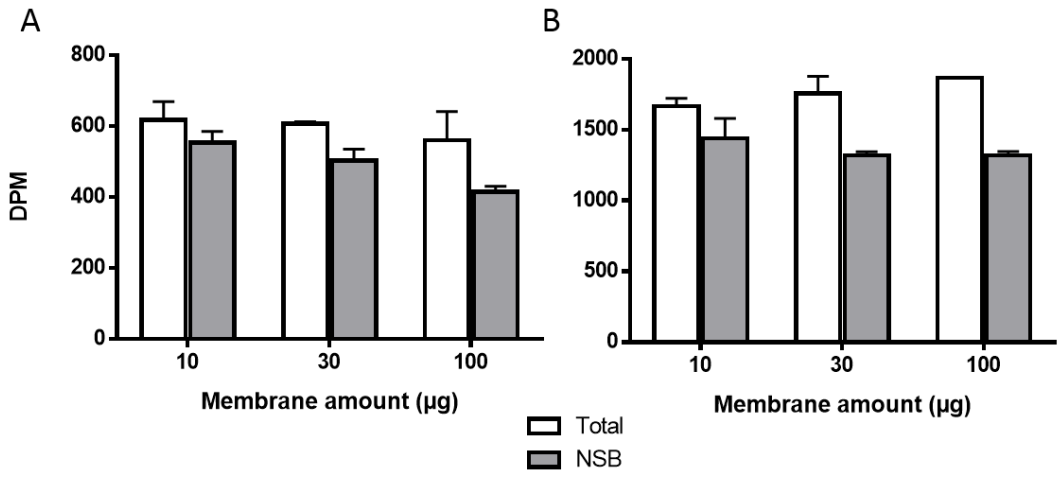

Figure 5-9. Total and non-specific binding of [^{125}I]-ANG(1-7). Total and non-specific binding (NSB) in the presence of varying amounts of Mas transfected HEK293 membrane protein (n=1) with 0.05nM (**A)** and 0.15nM [^{125}I]-ANG(1-7) (**B**). Data shown are mean ± SEM (from one experiment run in duplicate). NSB was determined with 10µM ANG(1-7)

The specific binding window improved with this radioligand but was still relatively small, with high NSB observed (≥70%). From these initial experiments, 30µg of membrane protein and the higher [^{125}I]-ANG(1-7) concentration (≈0.3nM) were chosen for further studies with this radioligand.

A number of experimental conditions were altered to try to decrease the NSB and optimise the binding window of [^{125}I]-ANG(1-7). Such conditions included, different cold ligands (ANG(1-7), A-779 and ANGII), the addition of protease inhibitors to the incubation step, increasing the number of washes during filtration and changing the filter buffer. No increase in the specific binding window was observed with any of these experimental conditions (data not shown).

One step that appeared to have a positive effect on the specific binding window was the addition of saponin, as shown in **Figure 5-10**, although the concentration at which saponin was effective fluctuated between experiments. Saponin is a detergent and was used to permeate any membrane vesicles that may have formed in the membrane suspension.

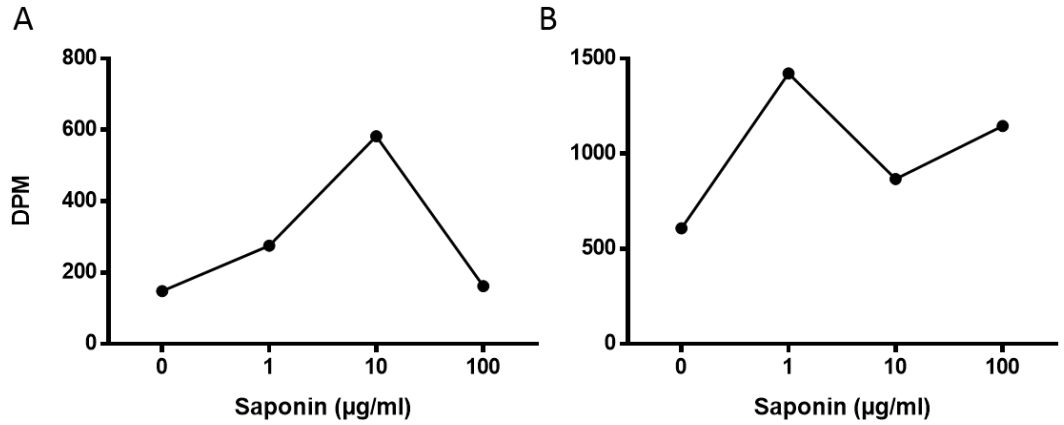

Figure 5-10. Specific binding in the presence of saponin. Specific binding of [^{125}I]-ANG(1-7) in Mas transfected HEK293 cells (n=4), in the presence of varying concentrations of saponin. Data shown from two individual experiments run in triplicate. NSB was defined with 10µM ANG(1-7).

From these results it was decided that saponin (10µg/ml) would be added to the incubation step in all future Mas receptor binding experiments.

Due to the variability in the specific binding observed between experiments, the addition of 100µg membrane protein was retested to see if an increase in the binding window could be observed, and hence reduce the variability between experiments.

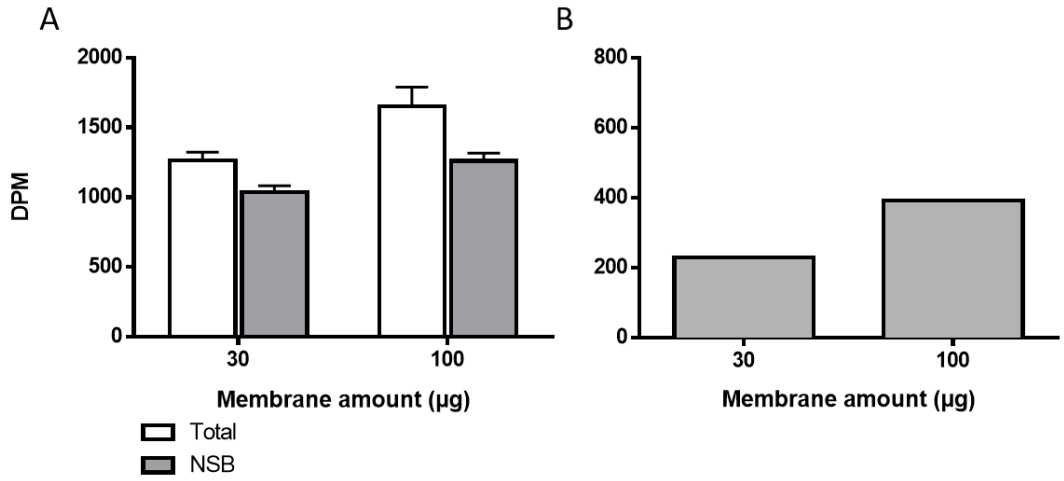

Figure 5-11. Binding of [^{125}I]-ANG(1-7) in the presence of increasing membrane protein. Total and non-specific binding (NSB) (**A**) and specific binding (**B**) in the presence of 30 and 100µg Mas transfected HEK293 membrane protein in the presence of 10µg/ml saponin. Data shown are mean ± SEM from one individual experiment with six replicates. NSB was defined with 10µM ANG(1-7).

The specific binding appeared to double in the presence of 100µg of membrane protein, therefore this amount was used for further binding experiments.

As the specific binding window observed with [^{125}I]-ANG(1-7) appeared to be at its optimum, a number of different ANG receptor ligands and antagonists (**Table 5-1**) were tested as the cold ligand. This was to ensure that [^{125}I]-ANG(1-7) was indeed binding to the Mas receptor and not another angiotensin related binding site. These experiments were performed in patient derived HLF membrane preparations.

Peptide/Antagonist	**Site of Action**
AVE0991	Mas receptor
D-ala^{7}-ANG(1-7) (A-779)	Mas receptor
ANG(1-7)	Mas receptor
ANGII	AT_1R, AT_2R
Saralasin	AT_1R, AT_2R
Telmisartan	AT_1R
PD-123319	AT_2R

Table 5-1. Different angiotensin receptor agonists/antagonists and their binding sites.

As the radioligand concentration for these two experiments was the same, at 0.2nM [^{125}I]-ANG(1-7), the results from these experiments were combined and are shown below in **Figure 5-12.**

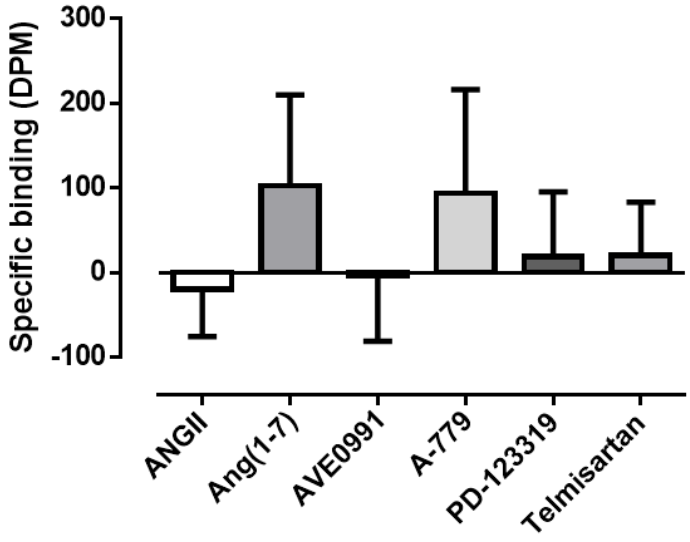

Figure 5-12. Binding of 0.2nM [^{125}I]-ANG(1-7) in presence of different cold ligands. Mean specific binding observed with 0.2nM [^{125}I]-ANG(1-7) in healthy lung fibroblast membranes (n=2), in presence of different angiotensin peptides and antagonists (10μM). Data shown are mean ± SEM of two pooled experiments

No clear specific binding was observed in the presence of any of the cold ligands tested. Specific binding of [^{125}I]-ANG(1-7) in the presence of ANG(1-7) also ranged from -5 to 210 DPM over two experiments. The specific binding in the presence of A-779 was similar and ranged from -28 to 216 DPM. These experiments were repeated in the presence of a 3-fold higher radioligand concentration (**Figure 5-13**).

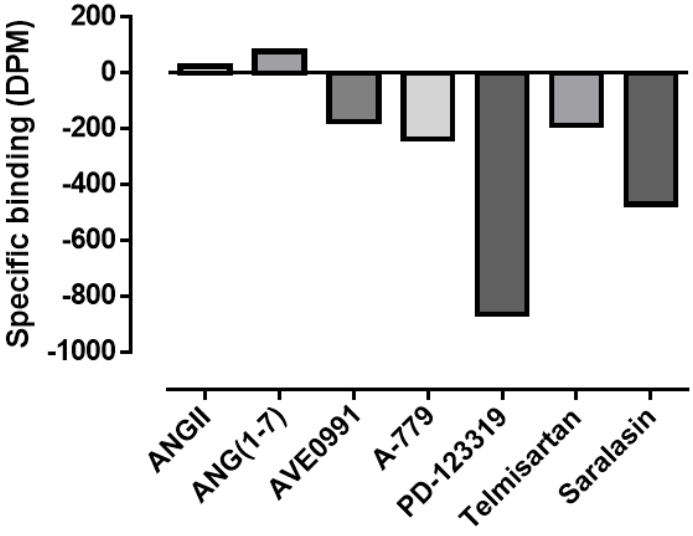

Figure 5-13. Binding of 0.52nM [^{125}I]-ANG(1-7) in the presence of different cold ligands. Binding of 0.52nM [^{125}I]-ANG(1-7) in healthy lung fibroblast membrane, in the presence of different angiotensin peptides and antagonists (10μM). Radioligand concentration ranged from 0.52-0.74nM for these experiments (n=3). Data shown are mean ± SEM from one representative experiment run in duplicate.

Results from these experiments were similar to those above and specific binding in the presence of ANG(1-7) ranged from 78 – 712.7 DPM over 3 experiments. Binding in the presence of A-779 ranged from -814.5 – 719.4 DPM.

Due to the variable nature of the results obtained with [^{125}I]-ANG(1-7), quantification of the Mas receptor on HLFs could not be performed with this radioligand.

5.3.2.2 Angiotensin receptors 1 and 2

The presence of ANGII binding sites on HLFs were also investigated using the radioligand [^{125}I]-Sarile.

Optimal experimental conditions for the binding of [^{125}I]-Sarile were quickly established, with an easily detectable specific binding window for this radioligand observed in the presence of 10, 30 and 100µg of fibroblast membrane protein (**Figure 5-14**). This window was observed with a low [^{125}I]-Sarile concentration of 0.07nM (**Figure 5-14 A**).

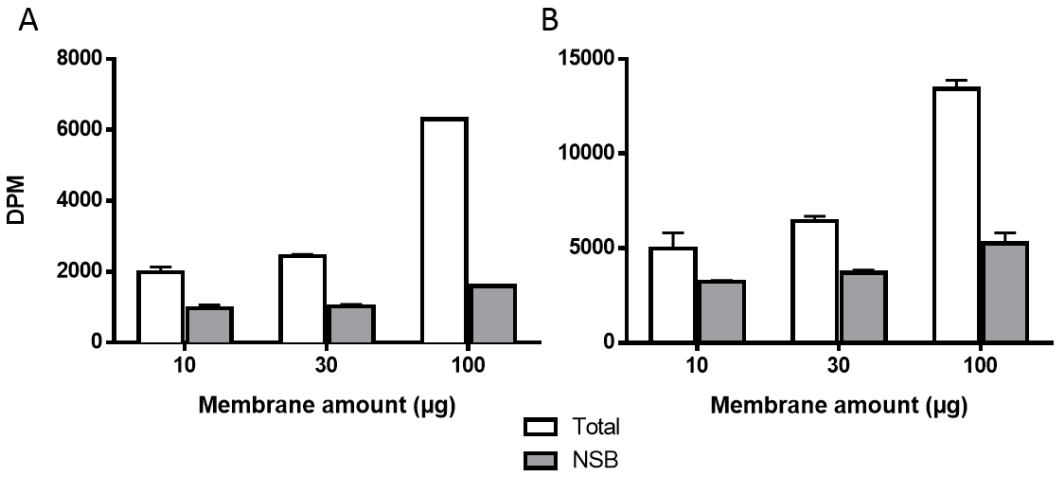

Figure 5-14. Total and NSB observed with [^{125}]I-Sarile. Total and non-specific binding (NSB) of 0.07 (**A**) and 0.24nM [^{125}I]-Sarile (**B**) in the presence of varying amounts of healthy lung fibroblast membrane (n=4). Data shown are mean ± SEM from one representative experiment run in duplicate. NSB was defined with 10µM ANGII.

The experimental parameters selected from these experiments were 0.1nM radioligand with 30µg of membrane protein. In the experiment above, [^{125}I]-Sarile was incubated with membrane protein for 4 hours to ensure that maximal binding was observed. The next step in

optimisation was to determine the length of incubation required to reach maximal specific binding (**Figure 5-15**).

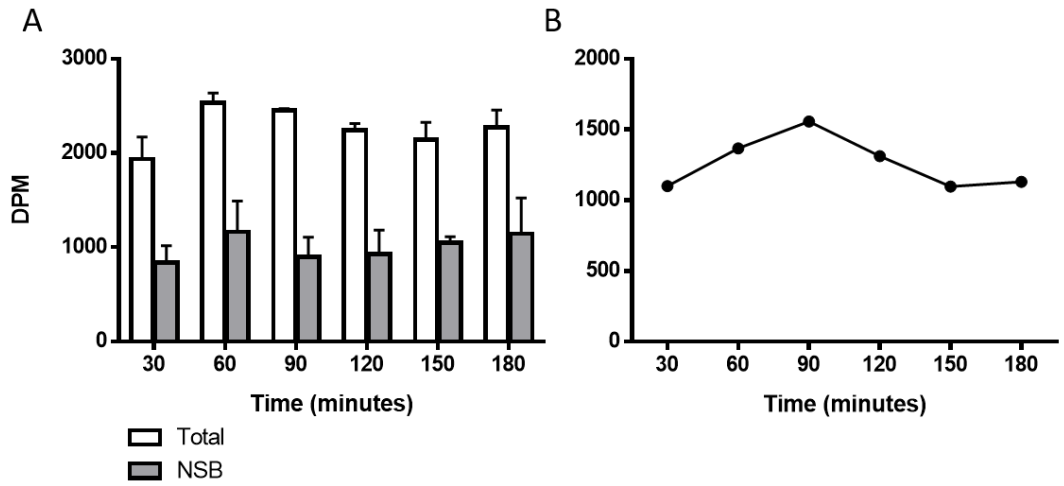

Figure 5-15. Specific binding of [^{125}I]-Sarile over time. Total and non-specific binding (NSB) (**A**) and specific binding (**B**) of 0.09nM [^{125}I]-Sarile over time with 30µg healthy lung fibroblast membrane (n=3). Data shown are mean ± SEM from one representative experiment run in duplicate. NSB was defined with 10µM ANGII.

Although high specific binding was observed after a 30 minute incubation, maximal specific binding was observed after 90 minutes in these experiments. However, to account for potential variability between cell lines, 120 minutes was chosen as the membrane and radioligand incubation time for [^{125}I]-Sarile experiments.

To characterise the binding of [^{125}I]-Sarile to fibroblast membranes and to identify the receptors present, homologous competition assays were performed with the 'cold' ligand I-sarile (as shown in **Figure 5-16** and **Figure 5-17**)

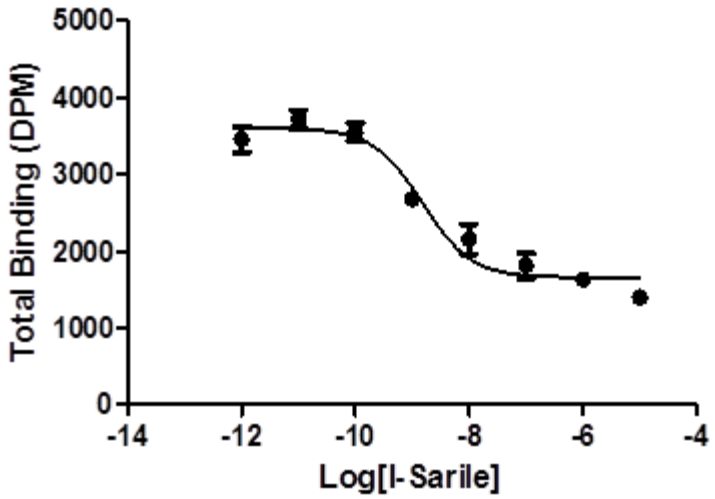

Figure 5-16. Homologous competition assays with [^{125}I]-Sarile. Concentrations of cold I-sarile were increased in the presence of 0.1nM [^{125}I]-Sarile with 30µg of healthy lung membrane (n=1). Data shown are mean ± SEM (experiment run in duplicate).

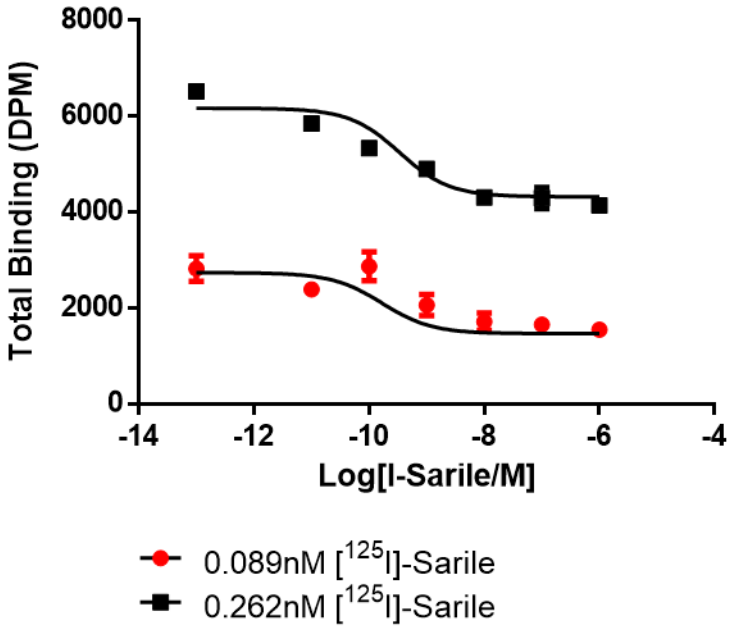

Figure 5-17. Homologous competition assays with [^{125}I]-Sarile. Concentrations of cold I-Sarile were increased in the presence of 0.09 and 0.26nM [^{125}I]-Sarile with 30µg healthy lung fibroblast membrane (n=2). Data shown are mean ± SEM for one experiment run in duplicate.

K_d values for [^{125}I]-Sarile in these experiments were calculated and **Figure 5-16** yielded a value of -8.85. The two experiments that were performed in the presence of two radioligand concentrations in parallel estimated K_d values of -10.10 (graph shown in **Figure 5-17**) and -8.28.

The number of binding sites (B_{max}) were also calculated and ranged from 16.42 – 248.9 fmol/mg of membrane protein between all three experiments.

To determine the receptors that [^{125}I]-Sarile was binding to in this assay, preliminary heterologous competition assays were performed in the presence of increasing concentrations of ANGII, telmisartan, PD-123319 or the non-peptidic ANG(1-7) analogue AVE0991, as shown in **Figure 5-18**. NSB was determined by the addition of 10µM ANGII.

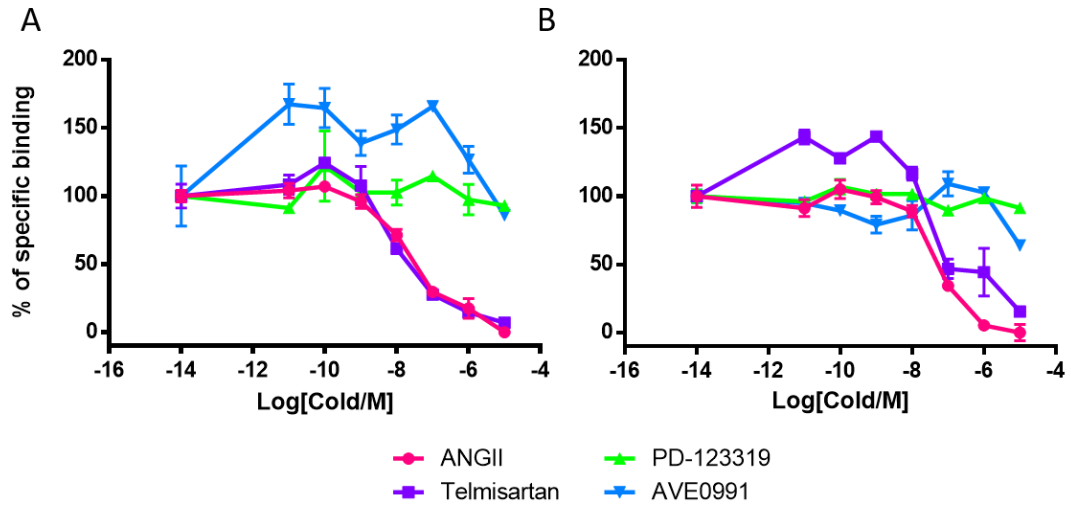

Figure 5-18. Heterologous competition of [^{125}I]-Sarile. Inhibition of the mean maximal specific binding of **A:** 0.05 - 0.09nM [^{125}I]-Sarile and **B:** 0.21 - 0.27nM [^{125}I]-Sarile, in IPF derived lung fibroblast membrane (n=1), (ANGII inhibition curves were run against 0.05 and 0.21nM radioligand, the remaining antagonists were run against 0.09 and 0.27nM radioligand). Data shown as percentage of specific binding (non-specific binding was defined with 10µM ANGII). Data shown are mean ± SEM (experiment run in duplicate).

As both ANGII and telmisartan caused dose-dependent decreases in the specific binding of [^{125}I]-Sarile, inhibition curves were fit to these data and are shown in **Figure 5-19**.

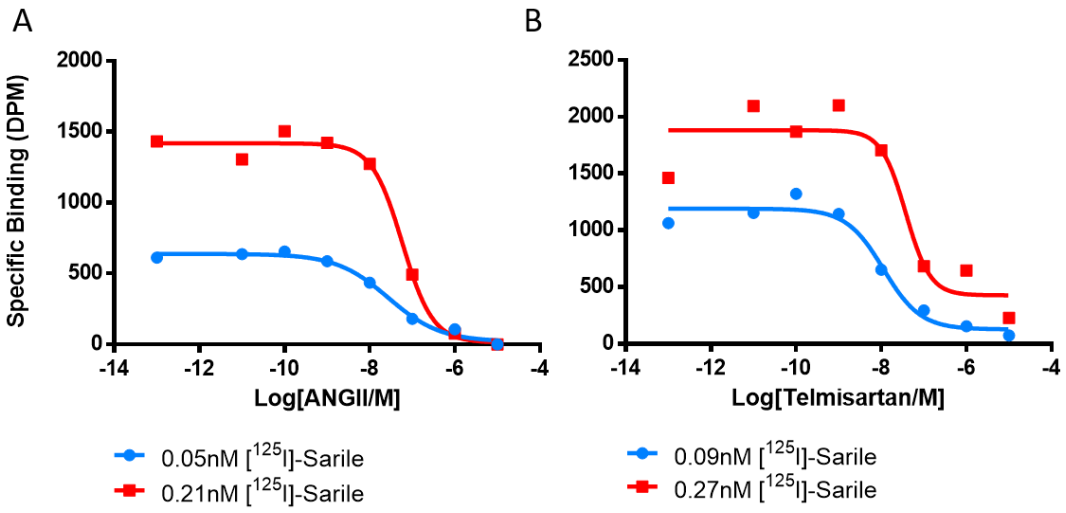

Figure 5-19. Inhibition of [^{125}I]-Sarile with ANGII and telmisartan. Inhibition curves with **A**: ANGII against 0.05 and 0.21nM [^{125}I]-Sarile and **B**: Telmisartan against 0.09 and 0.27nM [^{125}I]-Sarile, in IPF derived lung fibroblast membrane (n=1). Non-specific binding was defined with 10μM ANGII. Data shown are mean ± SEM (experiment run in duplicate).

ANGII and telmisartan had similar pIC_{50} values of 7.85 and 8.0 respectively against lower radioligand concentrations. Against higher radioligand concentrations, pIC_{50} values of 7.23 and 7.52 were observed for ANGII and telmisartan respectively. PD-123319 had no effect on the specific binding of [^{125}I]-Sarile, but small decreases in specific binding were observed at high concentrations (10μM) of AVE0991.

5.4 Discussion

Very little is known about Mas receptor expression in HLFs, initial experiments to investigate this expression were performed with immunocytochemistry. Two anti-Mas antibodies were utilised for this research, one targeted to a cytoplasmic domain of the receptor, and one targeted to an extracellular domain.

Initial experiments were performed with cytoplasmic anti-Mas and demonstrated highly localised nuclear expression of the Mas receptor in cells permeabilised with Triton-X (**Figure 5-1**). No nuclear staining was observed in cells that had not been permeabilised prior to investigation (**Figure 5-2**). These results were compared to confirm that the protocol for experiments in non-permeabilised cells, were in fact not causing permeabilisation of HLFs.

Experiments performed with extracellular anti-Mas were performed in non-permeabilised cells, to ensure that this antibody only had access to the external cell surface. Little to no staining was observed with this antibody (**Figure 5-4**), with levels similar to those of cells treated with secondary fluorescent antibody alone (**Figure 5-3**).

One cell line did not express nuclear expression of the Mas receptor, with higher levels of extracellular staining observed in this fibroblast line (**Figure 5-5**). Upon closer examination of the patient characteristics, no discernible difference can be observed between this donor and others used in the same study. This patient had been prescribed the ACE inhibitor ramipril, but another fibroblast line from the same experimental set was also derived from a patient prescribed this drug and still demonstrated nuclear Mas receptor expression. ACE inhibition could limit downstream production of ANG(1-7) from ANGI in the media and hence decrease receptor desensitisation. However, culturing cells in the absence of ramipril for approximately four weeks prior to experiments, means any residual effects are unlikely.

Nuclear expression of the Mas receptor is not completely unexpected. Lee et al (Lee *et al.*, 2004) identified a nuclear localisation sequence on the Mas protein, indicating a preference for this receptor to locate to the cell nucleus. The Mas receptor has also been shown to internalise upon binding by ANG(1-7) (Gironacci *et al.*, 2011), however, in this publication no intranuclear staining was observed. The authors also reported accumulation of the Mas receptor in the cell cytoplasm, close to the nucleus, in areas likely to be the endoplasmic reticulum.

Nuclear staining of Mas in sheep kidney sections was also observed in a study by Gwathmey et al (Gwathmey *et al.*, 2010), although complete localisation of ANG(1-7) to the nucleus was not observed in this investigation. However, as these experiments were performed in kidney tissue sections and not in cell populations, care needs to be taken not to over-compare these results.

Binding studies from the same publication also demonstrated the existence of a receptor binding site in isolated renal nuclei that was substantially blocked by the addition of A-779. This was therefore likely to be Mas receptor expression, the authors also demonstrated functional capabilities of the nuclear Mas expression observed, as A-779 significantly blocked ANG(1-7) induced nitric oxide (NO) in these isolated nuclear preparations.

To investigate the possibility of endogenous ANG(1-7) in the culture system causing Mas receptor internalisation, immunocytochemistry with extracellular anti-Mas was again performed, this time in cells pretreated with 10μM A-779 for 24 hours (**Figure 5-6**). The idea behind this was that blocking any low level Mas receptor expression on the cell surface would cause return of the receptor to the cell membrane, as it is no longer stimulated by any existing ANG(1-7) in the media. However, no upregulated Mas surface expression was observed in the presence of A-779 in these experiments. Also, experiments with cytoplasmic anti-Mas showed no decrease in nuclear Mas expression following a 1 or 24 hour treatment with A-779 (**Figure 5-7**). The expression of cytoplasmic Mas receptor was also examined in cells treated with 0.5% NCS. By reducing the amount of NCS in the media, the level of endogenous ANG(1-7) would likely decrease and hence upregulation in surface levels of the Mas receptor (and downregulation of nuclear expression) would be expected. This was, however, not observed in these experiments.

These results indicate that the Mas receptor expression in the nucleus is not induced by endogenously expressed ANG(1-7). One theory is that upon leaving the Golgi apparatus after packaging into vesicles, the Mas receptor is immediately trafficked to the nucleus due to the localisation sequence present, with this receptor never reaching the cell surface in HLFs under these experimental conditions.

Radioligand binding work with [^{125}I]-ANG(1-7) did not give a clear binding signal to indicate the presence of the Mas receptor, in either Mas transfected HEK293 or HLF membrane preparations (**Figure 5-9**). Initial experiments in both cell types demonstrated high NSB, which may be a characteristic of [^{125}I]-ANG(1-7), as high NSB with this radioligand has been reported previously (Iwata *et al.*, 2005).

As mentioned previously, a number of parameters were altered to try to improve the specific binding signal observed with this radioligand in Mas transfected HEK293 cells. A number of these conditions were changed to investigate whether binding of unbound [^{125}I]-ANG(1-7) to the filter mat was occurring and whether this could be reduced, in turn increasing the specific binding. The filter mats were soaked in a number of different buffers with increasing concentrations of polyethylenimine (PEI) with and without BSA. PEI is a cationic polymer than

attracts negatively charged cell membrane and therefore aids anchoring of the membrane-[^{125}I]-ANG(1-7) complex to the filter mat. However, altering these conditions did not reduce the NSB of [^{125}I]-ANG(1-7) in this assay. The number of washes during the filtration step was also increased from three washes up to five to help reduce potential filter mat binding. Increasing washes completely abolished both the total and NSB signal (data not shown) indicating that binding of free [^{125}I]-ANG(1-7) to the filter mat was not the cause of high NSB. Extra washing steps are likely to have removed even membrane bound [^{125}I]-ANG(1-7).

Another factor to be altered during these experiments was the addition of saponin to the membrane-radioligand incubation step. Saponin is a detergent and may permeate any membrane vesicles that may have formed upon membrane preparation. This would allow the radioligand to bind to any Mas receptor present on the internal surface of these vesicles. This appeared to have a positive effect of the binding window (**Figure 5-10**) of [^{125}I]-ANG(1-7), therefore 10μg/ml saponin was added to the incubation step for remaining experiments.

The binding observed with [^{125}I]-ANG(1-7) was still variable and at low levels, even in the presence of different cold ligands (**Figure 5-12** and **Figure 5-13**), with high amounts of NSB still occurring. These results indicate that [^{125}I]-ANG(1-7) was unlikely to be binding to either AT_1R or AT_2R. High NSB was also still observed in the presence of the three cold ligands targeted to the Mas receptor (ANG(1-7), A-779 and AVE0991). From these results it was concluded that radioligand binding with [^{125}I]-ANG(1-7) was not an optimal technique to quantify Mas receptor expression in the current investigation.

One previous publication has successfully demonstrated a binding signal with [^{125}I]-ANG(1-7) in bovine aortic endothelial cell membranes (Tallant *et al.*, 1997). Many of the experimental procedures used in this study were repeated in the current investigation, such as the addition of protease inhibitors and the presence of BSA during the filtration step, although little change in the specific binding of [^{125}I]-ANG(1-7) was observed. Tallant et al also observed low levels of NSB in the presence of unlabelled ANG(1-7), which does not compare to the ≥70% observed in the current study. One reason for this could be differences in the NSB sites between the two cells types investigated.

Other studies that have explored Mas receptor expression in adult rat cardiac fibroblasts have been performed on whole cell preparations (Iwata *et al.*, 2005). This group demonstrated high levels of NSB (approximately 50%) in the presence of unlabelled ANG(1-7), and also observed radioligand solution interference at high concentrations of [^{125}I]-ANG(1-7). These observations provide weight to the difficult nature of using [^{125}I]-ANG(1-7) for Mas receptor

characterisation. The published study also indicates that a high number of NSB sites for this radioligand are present on fibroblasts.

Radioligand binding with [^{125}I]-ANG(1-7) was not able to detect a specific binding window for the Mas receptor, even in HEK293 cells with known cell surface Mas expression. These results therefore do not allow for definitive proof of the absence of Mas receptor expression on the surface of HLFs. Although experiments with Mas fluorescent antibodies suggest that there is no cell surface expression of Mas, these antibodies have not been widely used in the literature. Therefore, further characterisation of these would be advantageous to confirm their specificity for the Mas receptor. Checking the binding of these antibodies in Mas transfected HEK293 cells would be one method that could be utilized for this purpose. Also radioligand binding studies in whole cell preparations could be performed to further investigate HLF surface expression, this may provide a larger specific binding window due to the lack of intracellular NSB sites.

Binding experiments with the non-selective AT_1R/AT_2R antagonist [^{125}I]-Sarile, indicated that an ANGII receptor population was present on HLF membrane preparations (**Figure 5-14**). The number of binding sites (B_{max}) for this cell population was estimated to range between 16.42 and 248.9 fmol/mg. As there is little published work characterising the receptor populations on HLFs, direct comparisons to these data are difficult. Nickenig et al (Nickenig *et al.*, 1997), however, did characterise the ANG receptors present on human skin fibroblasts and determined that AT_1R was present with a B_{max} of 17.9 fmol/mg. This is comparable to the data derived from **Figure 5-17** in the current study which estimated the B_{max} of this cell type to be 16.42 fmol/mg. Radioligand binding work with [^{125}I]-Sarile in HLFs is also limited, however, previous binding experiments estimate the K_d of [^{125}I]-Sarile to be -9.42 in murine neuroblastoma cells (Fluharty and Reagan, 1989) and -9.12 in hamster heart membranes (Lambert *et al.*, 1995). These values are broadly similar to those obtained in this study, with a mean K_d of -9.08 ± 0.54.

Data achieved by running two concentrations of radioligand in parallel are likely to be more reliable than the data achieved from a single radioligand concentration (as shown in **Figure 5-16**). Although the value obtained from **Figure 5-16** fits extremely well with one of the experiments run in duplicate (K_d of -8.28 to -8.85 and B_{max} of 171.9 – 248.9 fmol/mg). This suggests that the values obtained from **Figure 5-17** appear to be the outlying results. As the experiments running two concentrations of radioligand in parallel have only been conducted twice, further repeats of this may reduce the variability and confirm any outlying data points, providing more accurate estimations of the K_d and B_{max}.

Upon preliminary investigation in IPF derived fibroblasts, it was determined that AT_1R was responsible for the binding signal observed with [^{125}I]-Sarile, with telmisartan causing complete inhibition of the binding signal recorded with this radioligand (**Figure 5-18**). This was also comparable to the inhibition observed with ANGII. PD-123319 had no effect on the binding observed with [^{125}I]-Sarile, indicating no presence of AT_2R on this cell type. This result is comparable to that of previous research in HCFs (Hafizi *et al.*, 1998), where losartan caused complete dose dependent decreases in the specific binding of [^{125}I]-Sarile, with no reduction in the binding seen with PD-123319. In the current research, small decreases in total binding were also observed in the presence of high concentrations of AVE0991 (10μM), however this is unlikely to be due to binding of [^{125}I]-Sarile to the Mas receptor, and is more likely low affinity binding of AVE0991 to AT_1R.

Telmisartan had pIC_{50} values of 8.0 and 7.52 against two concentrations of [^{125}I]-Sarile (0.09 and 0.27nM respectively), with a half log shift to the right observed in the presence of the higher radioligand concentration (**Figure 5-19 B**). This is characteristic of competitive binding (Wyllie and Chen, 2007), and demonstrates the competitive nature of telmisartan when added in unison with a competing ligand (Maillard *et al.*, 2002), in this case [^{125}I]-Sarile. Also the specific binding observed with 0.09 and 0.27nM [^{125}I]-Sarile in the presence of 10μM telmisartan increased from 74.3 to 227.1 DPM, this was a threefold increase in specific binding, correlating with a threefold increase in radioligand concentration. This indicates surmountable inhibition by telmisartan and again this is only typical of telmisartan when adding simultaneously with competing ligands. A similar competitive profile was observed with ANGII, with pIC_{50} values of 7.85 and 7.23 recorded against 0.05 and 0.21nM [^{125}I]-Sarile respectively, again representing a half log shift to the right in the presence of the higher radioligand concentration. As this experiment has only been performed once, care needs to be taken not to over interpret these results. Further work is required to confirm this result in both IPF and HLF membranes.

The results from the current investigation demonstrate clear nuclear expression of the Mas receptor in HLFs, with little to no cytoplasmic or extracellular expression observed. This nuclear expression could not be quantified with radioligand binding, with low and variable specific binding observed between experiments performed in HLF membrane preparations. Carrying out binding studies on membrane preparations would have allowed access to the nuclear Mas receptor observed in HLFs, although this did not appear to be detected. Also, little to no specific binding was observed with [^{125}I]-ANG(1-7) even in Mas transfected cells with known Mas receptor expression. These results suggest that [^{125}I]-ANG(1-7) may not be a suitable tool for the quantification of the Mas receptor in either cell type. This may be due to

high numbers of NSB binding sites, with low specificity of the radioligand, or this may be due to the fact that this radioligand is not actually a ligand for the Mas receptor.

Chapter 6. Final discussion

6.1 Discussion

IPF is a progressive, irreversible disease of the lung involving ECM deposition and loss of pulmonary function, eventually leading to death of these patients within a few years of diagnosis. Fibroblasts are thought to be a key effector cell in this disease, being the precursor to the more active myofibroblast phenotype, which is in turn responsible for deposition of ECM components (discussed in more detail in sections 1.1 and 1.4).

The renin-angiotensin system (RAS) is an important system involved in blood pressure regulation, with the main peptide of this system, ANGII, known to induce vasoconstriction and increase blood pressure. Prolonged hypertension can lead to remodelling of the vascular system leading to increased risk of cardiac hypertrophy and fibrosis (Díez, 2007). Peptides of the RAS have also been implicated in the pathogenesis of IPF. ANGII has been shown to exert many profibrotic effects on a number of different organ derived fibroblasts, such an increased collagen deposition and proliferation (as discussed in section 1.6.1). These profibrotic effects are thought to be via induction of TGF-β1, with increased production of this cytokine observed in fibroblasts in response to ANGII (Lee *et al.*, 1995). ANGII is known to act via two main receptors, AT_1R and AT_2R, with many of the fibrotic effects of this peptide known to be via AT_1R. The presence of this receptor has been widely characterised on human skin and cardiac derived fibroblasts (Nickenig *et al.*, 1997; Hafizi *et al.*, 1998), however, the effects of ANGII and the receptors present on primary HLFs remain relatively unexplored.

Although early studies focused on the roles of ANGII in fibrosis, there are many other RAS peptides that may play a role in IPF, the most notable of which is ANG(1-7). A number of antifibrotic effects of ANG(1-7) have been demonstrated (section 1.6.2), including inhibition of both fibroblast proliferation and collagen deposition induced by FBS, as well as inhibiting those effects induced by ANGII (Iwata *et al.*, 2005; McCollum *et al.*, 2012). These observed actions of ANG(1-7) are attributed to the Mas receptor, with the presence of this receptor reported on rat cardiac fibroblasts (Iwata *et al.*, 2005). An ANG(1-7) binding site has also been detected on human skin fibroblasts (Nickenig *et al.*, 1997), although this was not confirmed as the Mas receptor. Again, studies investigating the effects of this peptide and Mas receptor expression on HLFs are lacking.

Although there is a large body of *in vivo* evidence implicating peptides of the RAS in lung fibrosis, the *in vitro* evidence for not only these two peptides, but also related peptides, is very limited and variable; therefore the main aims of this study were:

1. To determine the effects of ANGII, ANG(1-7) and related peptides on fibroblast activity, such as intracellular calcium release, collagen and MMP production.

2. To determine any differences in the effects of ANG peptides on fibroblast activity between healthy and IPF derived HLFs.

3. To investigate the ANG receptors present on HLFs, with the main focus on the Mas receptor.

The first investigations performed in this study were to determine the ability of eight angiotensin peptides (as shown in colour in **Figure 1-8**) to regulate intracellular Ca^{2+} release in HLFs. The differences in the Ca^{2+} responses between healthy and IPF derived fibroblasts were also investigated in this set of experiments.

The two peptides that acted as full agonists in these experiments were ANGII and ANGIII. These results were not unexpected, as intracellular Ca^{2+} release in response to both of these peptides has been documented previously in neuroblastoma cells (Ransom *et al.*, 1992). ANGIII has also been shown to bind to AT_1R with similar potencies to ANGII (Bosnyak *et al.*, 2011). ANGI was also shown to be acting as a partial agonist in these experiments. All peptides were shown to be inducing intracellular Ca^{2+} release via AT_1R, with complete inhibition reported in the presence of the AT_1R antagonist telmisartan. No AT_2R or Mas receptor mediated response was observed with any of these active peptides (determined by the addition of the AT_2R antagonist PD-123319 and the Mas antagonist A-779).

Fibroblasts derived from the IPF lung demonstrated smaller maximal Ca^{2+} responses to all peptides when compared with HLFs, although no difference in peptide potency was observed between the two cell phenotypes. ANGI, ANGII and ANGIII were again all shown to be causing intracellular Ca^{2+} release purely via AT_1R. One hypothesis for the difference in maximal responses between the two cell types, is that IPF cells are more basally active than healthy HLFs. Königshoff et al (Königshoff *et al.*, 2007) demonstrated that mouse fibrotic lung fibroblasts had higher basal levels of proliferation and migration compared to controls and that these effects were completely inhibited by PD-123319, indicating an ANGII mediated mechanism in culture. Although there are limited investigations into the differences in RAS receptors and activity between healthy HLFs and IPF derived fibroblasts, many basal activities have been shown to differ between the two cell phenotypes. IPF cells in culture have higher levels of collagen production, TGF-β1 secretion and decreased cell proliferation compared to non-fibrotic fibroblasts (Ramos *et al.*, 2001), although the role of the RAS in these activities was not explored. IPF fibroblasts have been shown in other studies to express higher levels of AGT

(Uhal *et al.*, 2007) and renin (Montes *et al.*, 2012), providing further evidence to suggest that this cell phenotype has a more basally active RAS in culture.

To determine if signalling events downstream of intracellular Ca^{2+} release were also being activated by ANGII, the ability of this peptide to induce ERK phosphorylation was examined. Increases in intracellular Ca^{2+} can act on plasma membrane Ca^{2+} channels, causing them to open, resulting in an influx of Ca^{2+} from the extracellular environment. This can then cause downstream ERK phosphorylation (potential mechanisms discussed in section 3.1). ANGII induced large increases in ERK phosphorylation, to levels comparable to the H_2O_2 positive control, with maximal ERK phosphorylation seen in response to 1μM ANGII. These observations provide weight that signalling pathways downstream of intracellular Ca^{2+} were indeed activated by ANGII.

The ability of ANGII to activate intracellular signalling pathways did not appear to translate to fibroblast function. Intracellular Ca^{2+} release was observed in response to ANGII in HLFs that were serum starved for 16 hours prior to experiments. However, ANGII did not induce proliferation in HLFs in similar serum free conditions. This may be due to the time frame of the experiment in question, HLFs used in Ca^{2+} assays were serum starved for a maximum of 24 hours, whereas proliferation experiments were performed in serum free conditions for 96 hours (including the serum starvation step prior to treatments). It was determined that serum free conditions may not provide the most optimal environment to investigate fibroblast functions, therefore all further experiments were performed in 0.5% NCS.

ANGII caused significant upregulation of latency associated peptide (LAP) at concentrations of 0.1μM. *In vivo,* TGF-β1 exists in two forms, one in complex with LAP (therefore in its inactive state) and one in its dissociated, active state. Measurement of LAP allows for the measure of both of these forms of TGF-β1. Upon further investigation with an ELISA for dissociated (active) TGF-β1, it appeared that no active TGF-β1 was induced by ANGII. Therefore any LAP measured in the initial experiments was likely to be in complex with TGF-β1. As ANGII is thought to exert many of its profibrotic effects via active TGF-β1 release (Lee *et al.*, 1995; Uhal *et al.*, 2007), this may be the reason as to why ANGII does not significantly affect proliferation, collagen deposition, MMP-1, MMP-2 or IL-6 secretion in this study. Due to the lack of availability of IPF derived fibroblasts at the University of Southampton, the effects of ANG peptides on functions in this cell type were not investigated.

ANG(1-7) and ANG(1-9) demonstrated inhibitory properties in the Ca^{2+} mobilisation assay, with both peptides causing partial reduction of the responses to both ANGII and ANGIII. These antagonistic effects of ANG(1-7) on ANGII mediated calcium release have been observed

previously in mesangial cells (Chansel *et al.*, 2001), with ANG(1-7) causing partial inhibition at 10μM. Upon further investigation, there did not appear to be a role of the Mas receptor or AT_2R in the inhibitory effects of either ANG(1-7) or ANG(1-9) in the current study (no reversal of the inhibition was observed in the presence of PD-123319 or A-779). These peptides also did not appear to be competing for AT_1R, with no change in the IC_{50} of ANG(1-7) or ANG(1-9) observed in the presence of increasing ANGII concentrations (0.1 – 10μM). These results indicate a novel binding site for these two peptides, with preliminary work suggesting that this could be via activation of a Ca^{2+}-independent PKC (see further work below for more information).

As with ANGII, the effects of ANG(1-7) did not appear to translate to fibroblast function. Although, due to the lack of positive effect observed with ANGII, the inhibitory effects of ANG(1-7) on ANGII actions could not be investigated. ANG(1-7), however, did not inhibit NCS induced fibroblast proliferation or NCS or TGF-β1 induced collagen production. Small upregulations in cell number were observed in the presence of ANG(1-7), although there was no effect of the Mas antagonist A-779 on this response. Proliferative effects of ANG(1-7) have been shown previously in human skin fibroblasts (Nickenig *et al.*, 1997). Any antifibrotic effects of ANG(1-7) on fibroblast proliferation and collagen deposition have only been reported in rat cardiac fibroblasts (Iwata *et al.*, 2005; McCollum *et al.*, 2012). This may suggest high species variability and ANG(1-7) may actually be mitogenic for human derived fibroblasts, with results from the current study suggesting that this may be a Mas independent mechanism.

Investigations into Mas receptor expression on HLFs by immunocytochemistry indicated that the Mas receptor was localised to the nuclei under normal 10% NCS culture conditions, and also in cells treated with 0.5% NCS. The lack of surface expressed Mas receptor on HLFs may be the reason for the lack of antifibrotic effects observed with ANG(1-7) in this study.

To further characterise Mas receptor expression on HLFs, [^{125}I]-ANG(1-7) was used. This radioligand did not give a clear specific binding window for the Mas receptor, either in HLF membrane preparations that have been shown to express nuclear Mas receptor or in Mas transfected HEK293 cells. High non-specific binding (NSB) was observed with this radioligand in all experiments (≈ 70%). Fairly high NSB (40 – 60%) has also been reported previously with this radioligand in both Mas transfected CHO cells and rat cardiac fibroblasts (Santos *et al.*, 2003b; Iwata *et al.*, 2005). The higher levels of NSB in the current investigation made quantification of the Mas receptor difficult and also suggests that this radioligand may not be binding to the Mas receptor, suggesting that [^{125}I]-ANG(1-7) is not a good tool for Mas receptor characterisation and quantification.

As mentioned previously, ANGI acted as a partial agonist in the Ca^{2+} signalling assay. This peptide also demonstrated the ability to desensitise the response to a subsequent dose of ANGII. To further characterise these responses to ANGI, the effects of the ACE inhibitor captopril on the actions of this peptide were explored. Captopril reduced the maximum Ca^{2+} response to ANGI in both healthy and IPF derived lung fibroblasts, and preliminary experiments in IPF cells showed that captopril reduced the ability of ANGI to desensitise the response to ANGII. These results indicate that fibroblasts may express ACE. Functional ACE expression by both human and rat cardiac fibroblasts has been demonstrated previously (Hafizi *et al.*, 1998; van Kesteren *et al.*, 1999). The study by Hafizi et al also demonstrated that the ACE expression observed was bound to the surface of human cardiac fibroblasts. In the current investigation, DMEM was removed from fibroblasts and the cells were washed and incubated in loading buffer for 1 hour prior to Ca^{2+} experiments, this step was likely to remove most soluble ACE. It is therefore possible that HLFs also express cell bound ACE, although this was not investigated further. This could be measured, however, by using a radiolabelled ACE inhibitor on whole cell fibroblast preparations. The presence of ACE in these experiments would mean that exogenously added ANGI could be converted to ANGII, and this production of ANGII could be responsible for the activity observed. The limiting factor would be the amount of ACE present, and is likely to be the cause of the partial agonist properties observed with ANGI.

Due to the demonstrated ability of AT_1R to desensitise upon agonist binding in the current investigation, and the evidence to suggest fibroblast expression of ACE, the effects of captopril on HLF function were explored. This was to investigate the hypothesis of a basally active RAS existing in the cell culture system. Endogenous conversion of any ANGI in the media to ANGII could lead to AT_1R desensitisation and hence prevent any further effects of exogenous ANGII from being observed.

Captopril significantly reduced baseline collagen production in HLFs and there are multiple RAS related hypotheses that could explain these effects. Reducing the production of ANGII would prevent binding of this peptide to both AT_1R and AT_2R. As telmisartan induced much smaller responses than captopril, this suggests that the results observed with this ACE inhibitor are not purely via AT_1R. Part of this effect could also be via ANG(1-7), due to stabilisation of this peptide in the media by captopril (preventing breakdown to ANG(1-5) by ACE), although further work would be required to confirm this hypothesis (e.g. via the addition of the Mas antagonist A-779).

Captopril is also known to inhibit prolidase, which is an important enzyme involved in recycling proline for incorporation into newly synthesised collagen. Although the levels of captopril required to inhibit human prolidase have been reported to be much higher than the 100μM used in the current study (Ganapathy *et al.*, 1985). Also as the cell culture media in the current investigation is supplemented with MEM non-essential amino acids (containing a final concentration of 0.1mM L-proline), the likelihood of prolidase inhibition being responsible for the decrease in collagen production in questionable. To determine whether the effect observed in this study could be due to an RAS independent mechanism such as the inhibition of prolidase, or whether this was indeed likely to be an ACE dependent effect, the ability of captopril to modulate other activities such as MMP-1, IL-6 and TGF-β1 secretion was also explored. Captopril has been shown previously to reduce proliferation, collagen production and TGF-β1 secretion in human keloid fibroblasts (Chen *et al.*, 2014), indicating that captopril's effects on collagen are not just due to prolidase inhibition.

The main effect seen with Captopril was the upregulation of both 0.5 and 10% NCS induced IL-6 production. There are many possible explanations for the observed effects of captopril, one is the reduced production of ANGII in the media, although this was unlikely to be the case as no comparable effects were seen in the presence of telmisartan. Another explanation is through a bradykinin dependent mechanism as this peptide is also a substrate for ACE. Bradykinin has been shown to induce IL-6 secretion in HLFs (Hayashi *et al.*, 2000), therefore blocking the degradation of bradykinin may cause upregulated IL-6 production. Another scenario is the upregulation of the ACE2 pathway and hence increased production of ANG(1-9), which has been reported to bind to AT_2R and oppose the effects of ANGII (Flores-Munoz *et al.*, 2012). The addition of the AT_2R antagonist PD-123319, appeared to reduce captopril induced IL-6 in response to both 0.5 and 10% NCS, which provides evidence to support the production of ANG(1-9); although further repeats of this experiment would be required to confirm this result.

This observation of a potential AT_2R mediated mechanism is contradictory to preliminary [^{125}I]-Sarile binding studies (shown in chapter 5), where PD-123319 caused no inhibition of binding of the radioligand, indicating no presence of AT_2R. However, these binding results were obtaining from an IPF derived fibroblast line, whereas the captopril and PD-123319 effects discussed above were observed in non-fibrotic, healthy, HLFs. There may be differences in AT_1R and AT_2R expression levels between the two cell phenotypes, which needs to be explored further (see further work below), Galindo et al detected the presence of both AT_1R and AT_2R on HLFs and suggested that this co-expression of receptors leads to resistance to ANGII effects (Galindo *et al.*, 2005). This could be a reason for the lack of effect of ANGII on HLF activity in the current study. There is limited literature on the differences in ANG receptor expression

between healthy and IPF lung fibroblasts, although Königshoff et al did investigate the differences in AT_1R and AT_2R mRNA expression levels between the two lung types. Both AT_1R and AT_2R mRNA expression was shown to be upregulated in IPF lung and this was associated with increased expression of both receptor types in interstitial fibroblasts (staining in fibroblasts was absent in control lungs). This does not fit well with the preliminary work performed with IPF lung fibroblasts in the current study, although more repeats would be required to confirm this. There are currently no comparable investigations into Mas receptor mRNA expression between healthy and IPF lung available in the literature.

Together these results indicate that many peptides of the RAS are capable of manipulating intracellular signalling pathways in both healthy HLFs and IPF derived fibroblasts. ANGII caused large increases in intracellular Ca^{2+} release and also induced ERK phosphorylation. However, the effects of this peptide did not appear to translate to HLF function, and this may be due to the lack of induction of active TGF-β1.

ANG(1-7) and ANG(1-9) were able to partially inhibit the Ca^{2+} response to ANGII and this appeared to be via a novel binding site. Upon further investigation into the effects of ANG(1-7), it was shown that this peptide did not inhibit serum or TGF-β1 induced fibroblast function, in fact, small upregulations in NCS induced cell number and TGF-β1 induced collagen deposition were observed. Also, the Mas antagonist A-779 did not affect these ANG(1-7) actions, indicating no role for the Mas receptor in this set of experiments.

Captopril also modulated some fibroblast functions, most notably collagen deposition and IL-6 secretion. Although the lack of effect of telmisartan in these experiments suggests that these results are not purely ANGII/AT_1R mediated effects and may be via different mechanisms (such as AT_2R or ANG(1-7) and bradykinin or ANG(1-9) respectively).

One point to consider regarding the results obtained in this thesis is the relatively high concentrations of ANG peptides required to induce the observed effects. The IC_{50} values for ANG(1-9) were reported to be 2.88×10^{-5} M and 3.16×10^{-5}M against ANGII in healthy and IPF cell respectively. A similar value of 1.95×10^{-5}M was reported for ANG(1-7) in IPF cells. Any limited effects of ANGII reported in this study (MMP-2 production, LAP production etc) also all occurred at concentrations of 0.1μM or greater. These values are much higher than the circulating concentrations of peptides that are documented in **Table 3-8**, for example, 13.9 – 32pM ANGII.

It is feasible however, that lung tissue concentrations of these ANG peptides would be higher than circulating concentrations, due to locally expressed ACE and ACE2 (see section 1.6). The

tissue concentrations of these peptides have been explored in other organ systems; human heart homogenate for example, has been shown to contain as much as 170nM ANGI, with up to 85% of this rapidly converted to ANGII and ANG(1-9) (Kokkonen *et al.*, 1997). Production rates of these two peptides were also shown to be 1.37±0.23 and 1.60±0.40 $nmol \cdot min^{-1} \cdot mg^{-1}$ respectively, although these values were from patients with end stage congestive heart failure and may not be representative of the healthy cardiac environment. No comparable studies into the peptide levels present in the human lung are currently available. Investigations into these would be extremely valuable in allowing the concentrations of the peptides required in the current study, to be compared to lung tissue levels. This would allow for the question of physiological relevance to be addressed.

Very limited effects of ANG peptides on HLF function have been observed in the current investigation. ANGII did not induce proliferation, collagen deposition, active TGF-β1 secretion or MMP production. ANG(1-7) also did not exert antifibrotic effects on fibroblasts, with no reduction in NCS induced proliferation or collagen deposition. Upon further investigation there does not appear to be any Mas receptor expressed on the surface of this cell type, which is likely to be the reason for the lack of effect observed with this peptide.

These results, together with the high concentrations of peptides required in the signalling experiments, suggest limited involvement of the RAS in the modified fibroblast behaviours observed in the IPF lung. This suggests that this system may not be a suitable therapeutic target for treatment of this disease.

6.2 Further work

A number of future experiments could be performed to further investigate the actions of ANG peptides and receptor expression on fibroblasts. Many ideas for further work are discussed in the sections below.

6.2.1 Calcium mobilisation in human lung fibroblasts

- Investigations in the mechanism of inhibition by ANG(1-7) and ANG(1-9)

Preliminary studies using Gö6976 (an selective Ca^{2+}-dependent PKC inhibitor) and GF109203 (a non-selective PKC inhibitor) indicate that ANG(1-7) may be acting via activation of a Ca^{2+}-independent PKC in these experiments. This potential mechanism of ANG(1-7) needs to be confirmed. Also, the ability of PKC inhibitors to modulate the inhibitory activity of ANG(1-9)

needs to be explored, to determine whether this peptide is acting in a similar manner to ANG(1-7).

6.2.2 ERK phosphorylation

- Inhibition of the ANGII response.

The effects of the angiotensin antagonists telmisartan and PD-123319 on ANGII induced ERK phosphorylation needs to be investigated to determine receptor involvement. Also the ability of ANG(1-7) and ANG(1-9) to inhibit this phosphorylation also needs to be investigated to further explore the ability of these peptides to inhibit signalling mechanisms.

6.2.3 Receptor Expression

- Whole cell radioligand binding with [^{125}I]-ANG(1-7)

High levels of NSB observed with [^{125}I]-ANG(1-7) could be due to a high number of intracellular NSB binding sites available in membrane suspensions. A number of successful radioligand binding studies characterising Mas receptor expression with [^{125}I]-ANG(1-7) have been performed in whole cell preparations (Santos *et al.*, 2003b; Iwata *et al.*, 2005), therefore this could be a more optimal method for radioligand binding studies.

- Effects of ANG(1-7) on Mas receptor expression with immunocytochemistry.

The effects of ANG(1-7) treatment on Mas receptor expression in HLFs needs to be investigated. If no modification of expression is observed following preincubation with this peptide, then this may provide evidence to suggest that the Mas receptor is not an ANG(1-7) binding site.

- Further investigations with [^{125}I]-Sarile binding studies.

Preliminary experiments indicate that only AT_1R is present on IPF derived fibroblasts, with no AT_2R detected. The sample size for experiments performed with [^{125}I]-Sarile needs to be increased in both healthy and IPF derived fibroblasts, to allow for more accurate characterisation of both the radioligand and its receptor sites. This would also allow for differences between healthy and IPF fibroblasts to be investigated. Galindo et al (Galindo *et al.*, 2005) detected both AT_1R and AT_2R on HLFs, and suggested that co-expression of these receptors leads to resistance to ANGII. The receptor population on healthy HLFs in this study needs to be investigated to determine if AT_1R and AT_2R co-expression exists in this cell type.

6.2.4 Fibroblast functions

- Investigation into the effects of ANG peptides on IPF derived lung fibroblast functions

The effects of ANGII and ANG(1-7) on proliferation, collagen deposition, MMP, TGF-β1 and IL-6 secretion need to be explored to determine if any differences in the action of these peptides exist between the two cell phenotypes.

- Effects of ANGII receptor inhibitors on fibroblast function

ANGII significantly upregulated HLF proliferation in the presence of 10% NCS and also significantly upregulated LAP secretion. Also other trends such as a decrease in MMP-1 were observed. The effect of telmisartan and PD-123319 on these functional changes needs to be investigated to determine whether these are AT_1R or AT_2R mediated effects.

Although the current work suggests that RAS peptides do not modulate healthy HLF function, this research would benefit from the further work mentioned above; especially the investigations into the actions of ANG peptides in IPF derived fibroblasts, to fully characterise their potential roles in IPF.

List of References

Abraham, S.T., Benscoter, H.A., Schworer, C.M. and Singer, H.A. (1997) A role for Ca2+/calmodulin-dependent protein kinase II in the mitogen-activated protein kinase signaling cascade of cultured rat aortic vascular smooth muscle cells. *Circ Res,* 81 (4), 575-584.

Agocha, A., Lee, H.W. and Eghbali-Webb, M. (1997) Hypoxia regulates basal and induced DNA synthesis and collagen type I production in human cardiac fibroblasts: effects of transforming growth factor-beta1, thyroid hormone, angiotensin II and basic fibroblast growth factor. *J Mol Cell Cardiol,* 29 (8), 2233-2244.

Antoniades, H.N., Bravo, M.A., Avila, R.E., Galanopoulos, T., Neville-Golden, J., Maxwell, M. and Selman, M. (1990) Platelet-derived growth factor in idiopathic pulmonary fibrosis. *J Clin Invest,* 86 (4), 1055-1064.

Ariëns, E.J. (1983) Intrinsic activity: partial agonists and partial antagonists. *J Cardiovasc Pharmacol,* 5 Suppl 1, S8-15.

Asano, K., Shikama, Y., Shoji, N., Hirano, K., Suzaki, H. and Nakajima, H. (2010) Tiotropium bromide inhibits TGF-β-induced MMP production from lung fibroblasts by interfering with Smad and MAPK pathways in vitro. *Int J Chron Obstruct Pulmon Dis,* 5, 277-286.

Ats/Ers (2000) American Thoracic Society. Idiopathic pulmonary fibrosis: diagnosis and treatment. International consensus statement. American Thoracic Society (ATS), and the European Respiratory Society (ERS). *Am J Respir Crit Care Med,* 161 (2 Pt 1), 646-664.

Ben Henda, Y., Labidi, A., Arnaudin, I., Bridiau, N., Delatouche, R., Maugard, T., Piot, J.M., Sannier, F., Thiéry, V. and Bordenave-Juchereau, S. (2013) Measuring angiotensin-I converting enzyme inhibitory activity by micro plate assays: comparison using marine cryptides and tentative threshold determinations with captopril and losartan. *J Agric Food Chem,* 61 (45), 10685-10690.

Benter, I.F., Diz, D.I. and Ferrario, C.M. (1993) Cardiovascular actions of angiotensin(1-7). *Peptides,* 14 (4), 679-684.

Berg, J.T., Breen, E.C., Fu, Z., Mathieu-Costello, O. and West, J.B. (1998) Alveolar hypoxia increases gene expression of extracellular matrix proteins and platelet-derived growth factor-B in lung parenchyma. *Am J Respir Crit Care Med,* 158 (6), 1920-1928.

Bergeron, A., Soler, P., Kambouchner, M., Loiseau, P., Milleron, B., Valeyre, D., Hance, A.J. and Tazi, A. (2003) Cytokine profiles in idiopathic pulmonary

fibrosis suggest an important role for TGF-beta and IL-10. *Eur Respir J,* 22 (1), 69-76.

Birkedal-Hansen, H., Moore, W.G., Bodden, M.K., Windsor, L.J., Birkedal-Hansen, B., Decarlo, A. and Engler, J.A. (1993) Matrix metalloproteinases: a review. *Crit Rev Oral Biol Med,* 4 (2), 197-250.

Blankley, C.J., Hodges, J.C., Klutchko, S.R., Himmelsbach, R.J., Chucholowski, A., Connolly, C.J., Neergaard, S.J., Van Nieuwenhze, M.S., Sebastian, A. and Quin, J. (1991) Synthesis and structure-activity relationships of a novel series of non-peptide angiotensin II receptor binding inhibitors specific for the AT2 subtype. *J Med Chem,* 34 (11), 3248-3260.

Bocchino, M., Agnese, S., Fagone, E., Svegliati, S., Grieco, D., Vancheri, C., Gabrielli, A., Sanduzzi, A. and Avvedimento, E.V. (2010) Reactive oxygen species are required for maintenance and differentiation of primary lung fibroblasts in idiopathic pulmonary fibrosis. *PLoS One,* 5 (11), e14003.

Booz, G.W., Dostal, D.E., Singer, H.A. and Baker, K.M. (1994) Involvement of protein kianse C and Ca2+ in angiotensin II-induced mitogenesis of cardiac fibroblasts. *Am J Physiol,* 267 (5 Pt 1), C1308-1318.

Borzone, G., Moreno, R., Urrea, R., Meneses, M., Oyarzún, M. and Lisboa, C. (2001) Bleomycin-induced chronic lung damage does not resemble human idiopathic pulmonary fibrosis. *Am J Respir Crit Care Med,* 163 (7), 1648-1653.

Bosnyak, S., Jones, E.S., Christopoulos, A., Aguilar, M.I., Thomas, W.G. and Widdop, R.E. (2011) Relative affinity of angiotensin peptides and novel ligands at AT1 and AT2 receptors. *Clin Sci (Lond),* 121 (7), 297-303.

Boucard, A.A., Wilkes, B.C., Laporte, S.A., Escher, E., Guillemette, G. and Leduc, R. (2000) Photolabeling identifies position 172 of the human AT(1) receptor as a ligand contact point: receptor-bound angiotensin II adopts an extended structure. *Biochemistry,* 39 (32), 9662-9670.

Brilla, C.G., Scheer, C. and Rupp, H. (1998) Angiotensin II and intracellular calcium of adult cardiac fibroblasts. *J Mol Cell Cardiol,* 30 (6), 1237-1246.

Brodsky, B. and Ramshaw, J.A. (1997) The collagen triple-helix structure. *Matrix Biol,* 15 (8-9), 545-554.

Capponi, A.M. and Catt, K.J. (1979) Angiotensin II receptors in adrenal cortex and uterus. Binding and activation properties of angiotensin analogues. *J Biol Chem,* 254 (12), 5120-5127.

Ceolotto, G., Pessina, A.C., Iori, E., Monari, A., Trevisan, R., Winkleswski, P. and Semplicini, A. (1998) Modulatory effect of insulin on release of calcium from human fibroblasts by angiotensin II. *J Hypertens,* 16 (4), 487-493.

Cha, S.A., Park, B.M., Gao, S. and Kim, S.H. (2013) Stimulation of ANP by angiotensin-(1-9) via the angiotensin type 2 receptor. *Life Sci,* 93 (24), 934-940.

Chansel, D., Vandermeersch, S., Oko, A., Curat, C. and Ardaillou, R. (2001) Effects of angiotensin IV and angiotensin-(1-7) on basal and angiotensin II-stimulated cytosolic Ca2+ in mesangial cells. *Eur J Pharmacol,* 414 (2-3), 165-175.

Chen, C.Z., Peng, Y.X., Wang, Z.B., Fish, P.V., Kaar, J.L., Koepsel, R.R., Russell, A.J., Lareu, R.R. and Raghunath, M. (2009) The Scar-in-a-Jar: studying potential antifibrotic compounds from the epigenetic to extracellular level in a single well. *Br J Pharmacol,* 158 (5), 1196-1209.

Chen, J., Zhao, S., Liu, Y., Cen, Y. and Nicolas, C. (2014) Effect of captopril on collagen metabolisms in keloid fibroblast cells. *ANZ J Surg*.

Chen, K., Chen, J., Li, D., Zhang, X. and Mehta, J.L. (2004) Angiotensin II regulation of collagen type I expression in cardiac fibroblasts: modulation by PPAR-gamma ligand pioglitazone. *Hypertension,* 44 (5), 655-661.

Chen, Q., Yang, Y., Huang, Y., Pan, C., Liu, L. and Qiu, H. (2013) Angiotensin-(1-7) attenuates lung fibrosis by way of Mas receptor in acute lung injury. *J Surg Res,* 185 (2), 740-747.

Cheng, Y. and Prusoff, W.H. (1973) Relationship between the inhibition constant (K1) and the concentration of inhibitor which causes 50 per cent inhibition (I50) of an enzymatic reaction. *Biochem Pharmacol,* 22 (23), 3099-3108.

Chiu, A.T., Herblin, W.F., Mccall, D.E., Ardecky, R.J., Carini, D.J., Duncia, J.V., Pease, L.J., Wong, P.C., Wexler, R.R. and Johnson, A.L. (1989) Identification of angiotensin II receptor subtypes. *Biochem Biophys Res Commun,* 165 (1), 196-203.

Chou, C.H., Chuang, L.Y., Lu, C.Y. and Guh, J.Y. (2013) Interaction between TGF-β and ACE2-Ang-(1-7)-Mas pathway in high glucose-cultured NRK-52E cells. *Mol Cell Endocrinol,* 366 (1), 21-30.

Clapham, D.E. (2007) Calcium signaling. *Cell,* 131 (6), 1047-1058.

Couluris, M., Kinder, B.W., Xu, P., Gross-King, M., Krischer, J. and Panos, R.J. (2012) Treatment of idiopathic pulmonary fibrosis with losartan: a pilot project. *Lung,* 190 (5), 523-527.

Coutinho, D.C., Foureaux, G., Rodrigues, K.D., Salles, R.L., Moraes, P.L., Murça, T.M., De Maria, M.L., Gomes, E.R., Santos, R.A., Guatimosim, S. and Ferreira, A.J. (2014) Cardiovascular effects of angiotensin A: a novel peptide of the renin-angiotensin system. *J Renin Angiotensin Aldosterone Syst,* 15 (4), 480-486.

Crosby, L.M. and Waters, C.M. (2010) Epithelial repair mechanisms in the lung. *Am J Physiol Lung Cell Mol Physiol,* 298 (6), L715-731.

Csiszar, K. (2001) Lysyl oxidases: a novel multifunctional amine oxidase family. *Prog Nucleic Acid Res Mol Biol,* 70, 1-32.

De Gasparo, M., Catt, K.J., Inagami, T., Wright, J.W. and Unger, T. (2000) International union of pharmacology. XXIII. The angiotensin II receptors. *Pharmacol Rev,* 52 (3), 415-472.

De Jong, L., Albracht, S.P. and Kemp, A. (1982) Prolyl 4-hydroxylase activity in relation to the oxidation state of enzyme-bound iron. The role of ascorbate in peptidyl proline hydroxylation. *Biochim Biophys Acta,* 704 (2), 326-332.

Di Sario, A., Bendia, E., Svegliati Baroni, G., Ridolfi, F., Casini, A., Ceni, E., Saccomanno, S., Marzioni, M., Trozzi, L., Sterpetti, P., Taffetani, S. and Benedetti, A. (2002) Effect of pirfenidone on rat hepatic stellate cell proliferation and collagen production. *J Hepatol,* 37 (5), 584-591.

Dolenga, M. and Hechtman, P. (1992) Prolidase deficiency in cultured human fibroblasts: biochemical pathology and iminodipeptide-enhanced growth. *Pediatr Res,* 32 (4), 479-482.

Donoghue, M., Hsieh, F., Baronas, E., Godbout, K., Gosselin, M., Stagliano, N., Donovan, M., Woolf, B., Robison, K., Jeyaseelan, R., Breitbart, R.E. and Acton, S. (2000) A novel angiotensin-converting enzyme-related carboxypeptidase (ACE2) converts angiotensin I to angiotensin 1-9. *Circ Res,* 87 (5), E1-9.

Díez, J. (2007) Mechanisms of cardiac fibrosis in hypertension. *J Clin Hypertens (Greenwich),* 9 (7), 546-550.

Eggena, P., Chu, C.L., Barrett, J.D. and Sambhi, M.P. (1976) Purification and partial characterization of human angiotensinogen. *Biochim Biophys Acta,* 427 (1), 208-217.

Eickelberg, O., Köhler, E., Reichenberger, F., Bertschin, S., Woodtli, T., Erne, P., Perruchoud, A.P. and Roth, M. (1999) Extracellular matrix deposition by primary human lung fibroblasts in response to TGF-beta1 and TGF-beta3. *Am J Physiol,* 276 (5 Pt 1), L814-824.

Fareh, J., Touyz, R.M., Thibault, G. and Schiffrin, E.L. (1995) Basal and angiotensin II-induced cytosolic free calcium in adult rat cardiomyocytes and fibroblasts after volume overload. *Hypertension,* 26 (6 Pt 2), 1149-1153.

Fedarko, N.S., D'avis, P., Frazier, C.R., Burrill, M.J., Fergusson, V., Tayback, M., Sponseller, P.D. and Shapiro, J.R. (1995) Cell proliferation of human fibroblasts and osteoblasts in osteogenesis imperfecta: influence of age. *J Bone Miner Res,* 10 (11), 1705-1712.

Feres-Filho, E.J., Choi, Y.J., Han, X., Takala, T.E. and Trackman, P.C. (1995) Pre- and post-translational regulation of lysyl oxidase by transforming growth factor-beta 1 in osteoblastic MC3T3-E1 cells. *J Biol Chem,* 270 (51), 30797-30803.

Fillion, D., Cabana, J., Guillemette, G., Leduc, R., Lavigne, P. and Escher, E. (2013) Structure of the human angiotensin II type 1 (AT1) receptor bound to angiotensin II from multiple chemoselective photoprobe contacts reveals a unique peptide binding mode. *J Biol Chem,* 288 (12), 8187-8197.

Fine, A. and Goldstein, R.H. (1987) The effect of transforming growth factor-beta on cell proliferation and collagen formation by lung fibroblasts. *J Biol Chem,* 262 (8), 3897-3902.

Fjellbirkeland, L., Cambier, S., Broaddus, V.C., Hill, A., Brunetta, P., Dolganov, G., Jablons, D. and Nishimura, S.L. (2003) Integrin alphavbeta8-mediated activation of transforming growth factor-beta inhibits human airway epithelial proliferation in intact bronchial tissue. *Am J Pathol,* 163 (2), 533-542.

Flores-Munoz, M., Work, L.M., Douglas, K., Denby, L., Dominiczak, A.F., Graham, D. and Nicklin, S.A. (2012) Angiotensin-(1-9) attenuates cardiac fibrosis in the stroke-prone spontaneously hypertensive rat via the angiotensin type 2 receptor. *Hypertension,* 59 (2), 300-307.

Flores-Muñoz, M., Smith, N.J., Haggerty, C., Milligan, G. and Nicklin, S.A. (2011) Angiotensin1-9 antagonises pro-hypertrophic signalling in cardiomyocytes via the angiotensin type 2 receptor. *J Physiol,* 589 (Pt 4), 939-951.

Fluharty, S.J. and Reagan, L.P. (1989) Characterization of binding sites for the angiotensin II antagonist 125I-[Sarc1,Ile8]-angiotensin II on murine neuroblastoma N1E-115 cells. *J Neurochem,* 52 (5), 1393-1400.

Fukuda, Y., Ishizaki, M., Kudoh, S., Kitaichi, M. and Yamanaka, N. (1998) Localization of matrix metalloproteinases-1, -2, and -9 and tissue inhibitor of metalloproteinase-2 in interstitial lung diseases. *Lab Invest,* 78 (6), 687-698.

Fulmer, J.D., Bienkowski, R.S., Cowan, M.J., Breul, S.D., Bradley, K.M., Ferrans, V.J., Roberts, W.C. and Crystal, R.G. (1980) Collagen concentration and rates of synthesis in idiopathic pulmonary fibrosis. *Am Rev Respir Dis,* 122 (2), 289-301.

Gadek, J.E., Kelman, J.A., Fells, G., Weinberger, S.E., Horwitz, A.L., Reynolds, H.Y., Fulmer, J.D. and Crystal, R.G. (1979) Collagenase in the lower respiratory tract of patients with idiopathic pulmonary fibrosis. *N Engl J Med,* 301 (14), 737-742.

Galindo, M., Santiago, B., Palao, G., Gutierrez-Cañas, I., Ramirez, J.C. and Pablos, J.L. (2005) Coexpression of AT1 and AT2 receptors by human fibroblasts is associated with resistance to angiotensin II. *Peptides,* 26 (9), 1647-1653.

Ganapathy, V., Pashley, S.J., Roesel, R.A., Pashley, D.H. and Leibach, F.H. (1985) Inhibition of rat and human prolidases by captopril. *Biochem Pharmacol,* 34 (8), 1287-1291.

Gauldie, J. and Kolb, M. (2008) Animal models of pulmonary fibrosis: how far from effective reality? *Am J Physiol Lung Cell Mol Physiol,* 294 (2), L151.

Gembardt, F., Grajewski, S., Vahl, M., Schultheiss, H.P. and Walther, T. (2008) Angiotensin metabolites can stimulate receptors of the Mas-related genes family. *Mol Cell Biochem,* 319 (1-2), 115-123.

Gironacci, M.M., Adamo, H.P., Corradi, G., Santos, R.A., Ortiz, P. and Carretero, O.A. (2011) Angiotensin (1-7) induces MAS receptor internalization. *Hypertension,* 58 (2), 176-181.

Grima, M., Welsch, C., Michel, B., Barthelmebs, M. and Imbs, J.L. (1991) In vitro tissue potencies of converting enzyme inhibitors. Prodrug activation by kidney esterase. *Hypertension,* 17 (4), 492-496.

Gross, T.J. and Hunninghake, G.W. (2001) Idiopathic pulmonary fibrosis. *N Engl J Med,* 345 (7), 517-525.

Grynkiewicz, G., Poenie, M. and Tsien, R.Y. (1985) A new generation of Ca2+ indicators with greatly improved fluorescence properties. *J Biol Chem,* 260 (6), 3440-3450.

Guinee, D., Brambilla, E., Fleming, M., Hayashi, T., Rahn, M., Koss, M., Ferrans, V. and Travis, W. (1997) The potential role of BAX and BCL-2 expression in diffuse alveolar damage. *Am J Pathol,* 151 (4), 999-1007.

Gwathmey, T.M., Westwood, B.M., Pirro, N.T., Tang, L., Rose, J.C., Diz, D.I. and Chappell, M.C. (2010) Nuclear angiotensin-(1-7) receptor is functionally coupled to the formation of nitric oxide. *Am J Physiol Renal Physiol,* 299 (5), F983-990.

Hafizi, S., Chester, A.H. and Yacoub, M.H. (2004) Differential response of human cardiac fibroblasts to angiotensin I and angiotensin II. *Peptides,* 25 (6), 1031-1033.

Hafizi, S., Wharton, J., Morgan, K., Allen, S.P., Chester, A.H., Catravas, J.D., Polak, J.M. and Yacoub, M.H. (1998) Expression of functional angiotensin-converting enzyme and AT1 receptors in cultured human cardiac fibroblasts. *Circulation,* 98 (23), 2553-2559.

Handa, R.K. (2000) Metabolism alters the selectivity of angiotensin-(1-7) receptor ligands for angiotensin receptors. *J Am Soc Nephrol,* 11 (8), 1377-1386.

Hayashi, R., Yamashita, N., Matsui, S., Fujita, T., Araya, J., Sassa, K., Arai, N., Yoshida, Y., Kashii, T., Maruyama, M., Sugiyama, E. and Kobayashi, M. (2000)

Bradykinin stimulates IL-6 and IL-8 production by human lung fibroblasts through ERK- and p38 MAPK-dependent mechanisms. *Eur Respir J,* 16 (3), 452-458.

Heitsch, H., Brovkovych, S., Malinski, T. and Wiemer, G. (2001) Angiotensin-(1-7)-Stimulated Nitric Oxide and Superoxide Release From Endothelial Cells. *Hypertension,* 37 (1), 72-76.

Herath, C.B., Mak, K., Burrell, L.M. and Angus, P.W. (2013) Angiotensin-(1-7) reduces the perfusion pressure response to angiotensin II and methoxamine via an endothelial nitric oxide-mediated pathway in cirrhotic rat liver. *Am J Physiol Gastrointest Liver Physiol,* 304 (1), G99-108.

Hornig, B., Kohler, C. and Drexler, H. (1997) Role of bradykinin in mediating vascular effects of angiotensin-converting enzyme inhibitors in humans. *Circulation,* 95 (5), 1115-1118.

Horowitz, J.C. and Thannickal, V.J. (2006) Epithelial-mesenchymal interactions in pulmonary fibrosis. *Semin Respir Crit Care Med,* 27 (6), 600-612.

Hou, M., Pantev, E., Möller, S., Erlinge, D. and Edvinsson, L. (2000) Angiotensin II type 1 receptors stimulate protein synthesis in human cardiac fibroblasts via a Ca2+-sensitive PKC-dependent tyrosine kinase pathway. *Acta Physiol Scand,* 168 (2), 301-309.

Hunyady, L., Catt, K.J., Clark, A.J. and Gáborik, Z. (2000) Mechanisms and functions of AT(1) angiotensin receptor internalization. *Regul Pept,* 91 (1-3), 29-44.

Iwata, M., Cowling, R.T., Gurantz, D., Moore, C., Zhang, S., Yuan, J.X. and Greenberg, B.H. (2005) Angiotensin-(1-7) binds to specific receptors on cardiac fibroblasts to initiate antifibrotic and antitrophic effects. *Am J Physiol Heart Circ Physiol,* 289 (6), H2356-2363.

Jackson, S.H., Dennis, A.W. and Greenberg, M. (1975) Iminodipeptiduria: a genetic defect in recycling collagen; a method for determining prolidase in erythrocytes. *Can Med Assoc J,* 113 (8), 759, 762-753.

Jankowski, V., Vanholder, R., Van Der Giet, M., Tölle, M., Karadogan, S., Gobom, J., Furkert, J., Oksche, A., Krause, E., Tran, T.N., Tepel, M., Schuchardt, M., Schlüter, H., Wiedon, A., Beyermann, M., Bader, M., Todiras, M., Zidek, W. and Jankowski, J. (2007) Mass-spectrometric identification of a novel angiotensin peptide in human plasma. *Arterioscler Thromb Vasc Biol,* 27 (2), 297-302.

Jia, H.P., Look, D.C., Shi, L., Hickey, M., Pewe, L., Netland, J., Farzan, M., Wohlford-Lenane, C., Perlman, S. and Mccray, P.B. (2005) ACE2 receptor expression and severe acute respiratory syndrome coronavirus infection depend on differentiation of human airway epithelia. *J Virol,* 79 (23), 14614-14621.

Jordana, M., Schulman, J., Mcsharry, C., Irving, L.B., Newhouse, M.T., Jordana, G. and Gauldie, J. (1988) Heterogeneous proliferative characteristics of human adult lung fibroblast lines and clonally derived fibroblasts from control and fibrotic tissue. *Am Rev Respir Dis,* 137 (3), 579-584.

Kambayashi, Y., Bardhan, S., Takahashi, K., Tsuzuki, S., Inui, H., Hamakubo, T. and Inagami, T. (1993) Molecular cloning of a novel angiotensin II receptor isoform involved in phosphotyrosine phosphatase inhibition. *J Biol Chem,* 268 (33), 24543-24546.

Karna, E., Szoka, L. and Palka, J.A. (2010) Captopril-dependent inhibition of collagen biosynthesis in cultured fibroblasts. *Pharmazie,* 65 (8), 614-617.

Kasai, H., Allen, J.T., Mason, R.M., Kamimura, T. and Zhang, Z. (2005) TGF-beta1 induces human alveolar epithelial to mesenchymal cell transition (EMT). *Respir Res,* 6, 56.

Katzenstein, A.L., Mukhopadhyay, S. and Myers, J.L. (2008) Diagnosis of usual interstitial pneumonia and distinction from other fibrosing interstitial lung diseases. *Hum Pathol,* 39 (9), 1275-1294.

Kawano, H., Do, Y.S., Kawano, Y., Starnes, V., Barr, M., Law, R.E. and Hsueh, W.A. (2000) Angiotensin II has multiple profibrotic effects in human cardiac fibroblasts. *Circulation,* 101 (10), 1130-1137.

Kay, E.P., Lee, H.K., Park, K.S. and Lee, S.C. (1998) Indirect mitogenic effect of transforming growth factor-beta on cell proliferation of subconjunctival fibroblasts. *Invest Ophthalmol Vis Sci,* 39 (3), 481-486.

Khalil, N., O'connor, R.N., Flanders, K.C. and Unruh, H. (1996) TGF-beta 1, but not TGF-beta 2 or TGF-beta 3, is differentially present in epithelial cells of advanced pulmonary fibrosis: an immunohistochemical study. *Am J Respir Cell Mol Biol,* 14 (2), 131-138.

Khalil, N., Parekh, T.V., O'connor, R., Antman, N., Kepron, W., Yehaulaeshet, T., Xu, Y.D. and Gold, L.I. (2001) Regulation of the effects of TGF-beta 1 by activation of latent TGF-beta 1 and differential expression of TGF-beta receptors (T beta R-I and T beta R-II) in idiopathic pulmonary fibrosis. *Thorax,* 56 (12), 907-915.

King, T.E., Pardo, A. and Selman, M. (2011) Idiopathic pulmonary fibrosis. *Lancet,* 378 (9807), 1949-1961.

Kingsley, D.M. (1994) The TGF-beta superfamily: new members, new receptors, and new genetic tests of function in different organisms. *Genes Dev,* 8 (2), 133-146.

Kokkonen, J.O., Saarinen, J. and Kovanen, P.T. (1997) Regulation of local angiotensin II formation in the human heart in the presence of interstitial

fluid. Inhibition of chymase by protease inhibitors of interstitial fluid and of angiotensin-converting enzyme by Ang-(1-9) formed by heart carboxypeptidase A-like activity. *Circulation,* 95 (6), 1455-1463.

Kondepudi, A. and Johnson, A. (1993) Cytokines increase neutral endopeptidase activity in lung fibroblasts. *Am J Respir Cell Mol Biol,* 8 (1), 43-49.

Kulkarni, G.V. and Mcculloch, C.A. (1994) Serum deprivation induces apoptotic cell death in a subset of Balb/c 3T3 fibroblasts. *J Cell Sci,* 107 (Pt 5), 1169-1179.

Königshoff, M., Wilhelm, A., Jahn, A., Sedding, D., Amarie, O.V., Eul, B., Seeger, W., Fink, L., Günther, A., Eickelberg, O. and Rose, F. (2007) The angiotensin II receptor 2 is expressed and mediates angiotensin II signaling in lung fibrosis. *Am J Respir Cell Mol Biol,* 37 (6), 640-650.

Lambert, C., Massillon, Y. and Meloche, S. (1995) Upregulation of cardiac angiotensin II AT1 receptors in congenital cardiomyopathic hamsters. *Circ Res,* 77 (5), 1001-1007.

Lang, Y.D., Hung, C.L., Wu, T.Y., Wang, L.F. and Chen, C.M. (2010) The renin-angiotensin system mediates hyperoxia-induced collagen production in human lung fibroblasts. *Free Radic Biol Med,* 49 (1), 88-95.

Lautner, R.Q., Villela, D.C., Fraga-Silva, R.A., Silva, N., Verano-Braga, T., Costa-Fraga, F., Jankowski, J., Jankowski, V., Sousa, F., Alzamora, A., Soares, E., Barbosa, C., Kjeldsen, F., Oliveira, A., Braga, J., Savergnini, S., Maia, G., Peluso, A.B., Passos-Silva, D., Ferreira, A., Alves, F., Martins, A., Raizada, M., Paula, R., Motta-Santos, D., Klempin, F., Kemplin, F., Pimenta, A., Alenina, N., Sinisterra, R., Bader, M., Campagnole-Santos, M.J. and Santos, R.A. (2013) Discovery and characterization of alamandine: a novel component of the renin-angiotensin system. *Circ Res,* 112 (8), 1104-1111.

Lawrence, A.C., Evin, G., Kladis, A. and Campbell, D.J. (1990) An alternative strategy for the radioimmunoassay of angiotensin peptides using amino-terminal-directed antisera: measurement of eight angiotensin peptides in human plasma. *J Hypertens,* 8 (8), 715-724.

Lazareno, S. and Birdsall, N.J. (1993) Estimation of competitive antagonist affinity from functional inhibition curves using the Gaddum, Schild and Cheng-Prusoff equations. *Br J Pharmacol,* 109 (4), 1110-1119.

Le, T.T., Karmouty-Quintana, H., Melicoff, E., Weng, T., Chen, N.Y., Pedroza, M., Zhou, Y., Davies, J., Philip, K., Molina, J., Luo, F., George, A.T., Garcia-Morales, L.J., Bunge, R.R., Bruckner, B.A., Loebe, M., Seethamraju, H., Agarwal, S.K. and Blackburn, M.R. (2014) Blockade of IL-6 Trans signaling attenuates pulmonary fibrosis. *J Immunol,* 193 (7), 3755-3768.

Lee, A.A., Dillmann, W.H., Mcculloch, A.D. and Villarreal, F.J. (1995) Angiotensin II stimulates the autocrine production of transforming growth factor-beta 1 in adult rat cardiac fibroblasts. *J Mol Cell Cardiol,* 27 (10), 2347-2357.

Lee, C.H., Hong, C.H., Yu, H.S., Chen, G.S. and Yang, K.C. (2010) Transforming growth factor-β enhances matrix metalloproteinase-2 expression and activity through AKT in fibroblasts derived from angiofibromas in patients with tuberous sclerosis complex. *Br J Dermatol,* 163 (6), 1238-1244.

Lee, D.K., Lança, A.J., Cheng, R., Nguyen, T., Ji, X.D., Gobeil, F., Chemtob, S., George, S.R. and O'dowd, B.F. (2004) Agonist-independent nuclear localization of the Apelin, angiotensin AT1, and bradykinin B2 receptors. *J Biol Chem,* 279 (9), 7901-7908.

Leeming, D.J., Sand, J.M., Nielsen, M.J., Genovese, F., Martinez, F.J., Hogaboam, C.M., Han, M.K., Klickstein, L.B. and Karsdal, M.A. (2012) Serological investigation of the collagen degradation profile of patients with chronic obstructive pulmonary disease or idiopathic pulmonary fibrosis. *Biomark Insights,* 7, 119-126.

Lemjabbar, H., Gosset, P., Lechapt-Zalcman, E., Franco-Montoya, M.L., Wallaert, B., Harf, A. and Lafuma, C. (1999) Overexpression of alveolar macrophage gelatinase B (MMP-9) in patients with idiopathic pulmonary fibrosis: effects of steroid and immunosuppressive treatment. *Am J Respir Cell Mol Biol,* 20 (5), 903-913.

Li, X., Molina-Molina, M., Abdul-Hafez, A., Ramirez, J., Serrano-Mollar, A., Xaubet, A. and Uhal, B.D. (2006) Extravascular sources of lung angiotensin peptide synthesis in idiopathic pulmonary fibrosis. *Am J Physiol Lung Cell Mol Physiol,* 291 (5), L887-895.

Li, X., Molina-Molina, M., Abdul-Hafez, A., Uhal, V., Xaubet, A. and Uhal, B.D. (2008) Angiotensin converting enzyme-2 is protective but downregulated in human and experimental lung fibrosis. *Am J Physiol Lung Cell Mol Physiol,* 295 (1), L178-185.

Lin, X., Yu, M., Wu, K., Yuan, H. and Zhong, H. (2009) Effects of pirfenidone on proliferation, migration, and collagen contraction of human Tenon's fibroblasts in vitro. *Invest Ophthalmol Vis Sci,* 50 (8), 3763-3770.

Lyons, R.M., Keski-Oja, J. and Moses, H.L. (1988) Proteolytic activation of latent transforming growth factor-beta from fibroblast-conditioned medium. *J Cell Biol,* 106 (5), 1659-1665.

Maher, T.M. (2010) Pirfenidone in idiopathic pulmonary fibrosis. *Drugs Today (Barc),* 46 (7), 473-482.

Maillard, M.P., Perregaux, C., Centeno, C., Stangier, J., Wienen, W., Brunner, H.R. and Burnier, M. (2002) In vitro and in vivo characterization of the activity of telmisartan: an insurmountable angiotensin II receptor antagonist. *J Pharmacol Exp Ther,* 302 (3), 1089-1095.

Marinković, A., Liu, F. and Tschumperlin, D.J. (2013) Matrices of physiologic stiffness potently inactivate idiopathic pulmonary fibrosis fibroblasts. *Am J Respir Cell Mol Biol,* 48 (4), 422-430.

Marshall, R.P., Gohlke, P., Chambers, R.C., Howell, D.C., Bottoms, S.E., Unger, T., Mcanulty, R.J. and Laurent, G.J. (2004) Angiotensin II and the fibroproliferative response to acute lung injury. *Am J Physiol Lung Cell Mol Physiol,* 286 (1), L156-164.

Marshall, R.P., Mcanulty, R.J. and Laurent, G.J. (2000) Angiotensin II is mitogenic for human lung fibroblasts via activation of the type 1 receptor. *Am J Respir Crit Care Med,* 161 (6), 1999-2004.

Martin, T.P., Lawan, A., Robinson, E., Grieve, D.J., Plevin, R., Paul, A. and Currie, S. (2014) Adult cardiac fibroblast proliferation is modulated by calcium/calmodulin-dependent protein kinase II in normal and hypertrophied hearts. *Pflugers Arch,* 466 (2), 319-330.

Matsui, T., Tamaya, K., Matsumoto, K., Osajima, Y., Uezono, K. and Kawasaki, T. (1999) Plasma concentrations of angiotensin metabolites in young male normotensive and mild hypertensive subjects. *Hypertens Res,* 22 (4), 273-277.

May, V., Clason, T.A., Buttolph, T.R., Girard, B.M. and Parsons, R.L. (2014) Calcium influx, but not intracellular calcium release, supports PACAP-mediated ERK activation in HEK PAC1 receptor cells. *J Mol Neurosci,* 54 (3), 342-350.

Mccartney-Francis, N., Mizel, D., Wong, H., Wahl, L. and Wahl, S. (1990) TGF-beta regulates production of growth factors and TGF-beta by human peripheral blood monocytes. *Growth Factors,* 4 (1), 27-35.

Mccollum, L.T., Gallagher, P.E. and Tallant, E.A. (2012) Angiotensin-(1-7) abrogates mitogen-stimulated proliferation of cardiac fibroblasts. *Peptides,* 34 (2), 380-388.

Metukuri, M.R., Namas, R., Gladstone, C., Clermont, T., Jefferson, B., Barclay, D., Hermus, L., Billiar, T.R., Zamora, R. and Vodovotz, Y. (2009) Activation of latent transforming growth factor-beta1 by nitric oxide in macrophages: role of soluble guanylate cyclase and MAP kinases. *Wound Repair Regen,* 17 (4), 578-588.

Midgley, A.C., Rogers, M., Hallett, M.B., Clayton, A., Bowen, T., Phillips, A.O. and Steadman, R. (2013) Transforming growth factor-β1 (TGF-β1)-stimulated fibroblast to myofibroblast differentiation is mediated by hyaluronan (HA)-facilitated epidermal growth factor receptor (EGFR) and CD44 co-localization in lipid rafts. *J Biol Chem,* 288 (21), 14824-14838.

Milasta, S., Pediani, J., Appelbe, S., Trim, S., Wyatt, M., Cox, P., Fidock, M. and Milligan, G. (2006) Interactions between the Mas-related receptors MrgD and

MrgE alter signalling and trafficking of MrgD. *Mol Pharmacol,* 69 (2), 479-491.

Miller, R.L., Elsas, L.J. and Priest, R.E. (1979) Ascorbate action on normal and mutant human lysyl hydroxylases from cultured dermal fibroblasts. *J Invest Dermatol,* 72 (5), 241-247.

Miura, S., Feng, Y.H., Husain, A. and Karnik, S.S. (1999) Role of aromaticity of agonist switches of angiotensin II in the activation of the AT1 receptor. *J Biol Chem,* 274 (11), 7103-7110.

Miyazono, K. (2000) Positive and negative regulation of TGF-beta signaling. *J Cell Sci,* 113 (Pt 7), 1101-1109.

Moeller, A., Gilpin, S.E., Ask, K., Cox, G., Cook, D., Gauldie, J., Margetts, P.J., Farkas, L., Dobranowski, J., Boylan, C., O'byrne, P.M., Strieter, R.M. and Kolb, M. (2009) Circulating fibrocytes are an indicator of poor prognosis in idiopathic pulmonary fibrosis. *Am J Respir Crit Care Med,* 179 (7), 588-594.

Moeller, A., Rodriguez-Lecompte, J.C., Wang, L., Gauldie, J. and Kolb, M. (2006) Models of pulmonary fibrosis. *Drug Discovery Today: Disease Models,* 3 (3), 243-249.

Molteni, A., Wolfe, L.F., Ward, W.F., Ts'ao, C.H., Molteni, L.B., Veno, P., Fish, B.L., Taylor, J.M., Quintanilla, N., Herndon, B. and Moulder, J.E. (2007) Effect of an angiotensin II receptor blocker and two angiotensin converting enzyme inhibitors on transforming growth factor-beta (TGF-beta) and alpha-actomyosin (alpha SMA), important mediators of radiation-induced pneumopathy and lung fibrosis. *Curr Pharm Des,* 13 (13), 1307-1316.

Montes, E., Ruiz, V., Checa, M., Maldonado, V., Melendez-Zajgla, J., Montaño, M., Ordoñez-Razo, R., Cisneros, J., García-De-Alba, C., Pardo, A. and Selman, M. (2012) Renin is an angiotensin-independent profibrotic mediator: role in pulmonary fibrosis. *Eur Respir J,* 39 (1), 141-148.

Moodley, Y.P., Caterina, P., Scaffidi, A.K., Misso, N.L., Papadimitriou, J.M., Mcanulty, R.J., Laurent, G.J., Thompson, P.J. and Knight, D.A. (2004) Comparison of the morphological and biochemical changes in normal human lung fibroblasts and fibroblasts derived from lungs of patients with idiopathic pulmonary fibrosis during FasL-induced apoptosis. *J Pathol,* 202 (4), 486-495.

Moodley, Y.P., Misso, N.L., Scaffidi, A.K., Fogel-Petrovic, M., Mcanulty, R.J., Laurent, G.J., Thompson, P.J. and Knight, D.A. (2003a) Inverse effects of interleukin-6 on apoptosis of fibroblasts from pulmonary fibrosis and normal lungs. *Am J Respir Cell Mol Biol,* 29 (4), 490-498.

Moodley, Y.P., Scaffidi, A.K., Misso, N.L., Keerthisingam, C., Mcanulty, R.J., Laurent, G.J., Mutsaers, S.E., Thompson, P.J. and Knight, D.A. (2003b) Fibroblasts isolated from normal lungs and those with idiopathic pulmonary fibrosis

differ in interleukin-6/gp130-mediated cell signaling and proliferation. *Am J Pathol,* 163 (1), 345-354.

Moore, B.B. and Hogaboam, C.M. (2008) Murine models of pulmonary fibrosis. *Am J Physiol Lung Cell Mol Physiol,* 294 (2), L152-160.

Morales, M.G., Abrigo, J., Meneses, C., Simon, F., Cisternas, F., Rivera, J.C., Vazquez, Y. and Cabello-Verrugio, C. (2014) The Ang-(1-7)/Mas-1 axis attenuates the expression and signalling of TGF-β1 induced by AngII in mouse skeletal muscle. *Clin Sci (Lond),* 127 (4), 251-264.

Mulsow, J.J., Watson, R.W., Fitzpatrick, J.M. and O'connell, P.R. (2005) Transforming growth factor-beta promotes pro-fibrotic behavior by serosal fibroblasts via PKC and ERK1/2 mitogen activated protein kinase cell signaling. *Ann Surg,* 242 (6), 880-887, discussion 887-889.

Munger, J.S., Huang, X., Kawakatsu, H., Griffiths, M.J., Dalton, S.L., Wu, J., Pittet, J.F., Kaminski, N., Garat, C., Matthay, M.A., Rifkin, D.B. and Sheppard, D. (1999) The integrin alpha v beta 6 binds and activates latent TGF beta 1: a mechanism for regulating pulmonary inflammation and fibrosis. *Cell,* 96 (3), 319-328.

Myllyharju, J. (2003) Prolyl 4-hydroxylases, the key enzymes of collagen biosynthesis. *Matrix Biol,* 22 (1), 15-24.

Nadrous, H.F., Ryu, J.H., Douglas, W.W., Decker, P.A. and Olson, E.J. (2004) Impact of angiotensin-converting enzyme inhibitors and statins on survival in idiopathic pulmonary fibrosis. *Chest,* 126 (2), 438-446.

Nho, R.S., Hergert, P., Kahm, J., Jessurun, J. and Henke, C. (2011) Pathological alteration of FoxO3a activity promotes idiopathic pulmonary fibrosis fibroblast proliferation on type i collagen matrix. *Am J Pathol,* 179 (5), 2420-2430.

Nho, R.S., Peterson, M., Hergert, P. and Henke, C.A. (2013) FoxO3a (Forkhead Box O3a) deficiency protects Idiopathic Pulmonary Fibrosis (IPF) fibroblasts from type I polymerized collagen matrix-induced apoptosis via caveolin-1 (cav-1) and Fas. *PLoS One,* 8 (4), e61017.

Nho, R.S., Xia, H., Kahm, J., Kleidon, J., Diebold, D. and Henke, C.A. (2005) Role of integrin-linked kinase in regulating phosphorylation of Akt and fibroblast survival in type I collagen matrices through a beta1 integrin viability signaling pathway. *J Biol Chem,* 280 (28), 26630-26639.

Nickenig, G., Geisen, G., Vetter, H. and Sachinidis, A. (1997) Characterization of angiotensin receptors on human skin fibroblasts. *J Mol Med (Berl),* 75 (3), 217-222.

Niu, X., Xue, Y., Li, X., He, Y., Zhao, X., Xu, M. and Zhao, L. (2014) Effects of angiotensin-(1-7) on the proliferation and collagen synthesis of arginine vasopressin-stimulated rat cardiac fibroblasts: role of mas receptor-calcineurin-NF-κB signaling pathway. *J Cardiovasc Pharmacol,* 64 (6), 536-542.

Oliveira, L., Costa-Neto, C.M., Nakaie, C.R., Schreier, S., Shimuta, S.I. and Paiva, A.C. (2007) The angiotensin II AT1 receptor structure-activity correlations in the light of rhodopsin structure. *Physiol Rev,* 87 (2), 565-592.

Olson, E.R., Shamhart, P.E., Naugle, J.E. and Meszaros, J.G. (2008) Angiotensin II-induced extracellular signal-regulated kinase 1/2 activation is mediated by protein kinase Cdelta and intracellular calcium in adult rat cardiac fibroblasts. *Hypertension,* 51 (3), 704-711.

Orte, C., Polak, J.M., Haworth, S.G., Yacoub, M.H. and Morrell, N.W. (2000) Expression of pulmonary vascular angiotensin-converting enzyme in primary and secondary plexiform pulmonary hypertension. *J Pathol,* 192 (3), 379-384.

Otsuka, M., Takahashi, H., Shiratori, M., Chiba, H. and Abe, S. (2004) Reduction of bleomycin induced lung fibrosis by candesartan cilexetil, an angiotensin II type 1 receptor antagonist. *Thorax,* 59 (1), 31-38.

Overall, C.M., Wrana, J.L. and Sodek, J. (1989) Independent regulation of collagenase, 72-kDa progelatinase, and metalloendoproteinase inhibitor expression in human fibroblasts by transforming growth factor-beta. *J Biol Chem,* 264 (3), 1860-1869.

Overall, C.M., Wrana, J.L. and Sodek, J. (1991) Transcriptional and post-transcriptional regulation of 72-kDa gelatinase/type IV collagenase by transforming growth factor-beta 1 in human fibroblasts. Comparisons with collagenase and tissue inhibitor of matrix metalloproteinase gene expression. *J Biol Chem,* 266 (21), 14064-14071.

Pan, C.H., Wen, C.H. and Lin, C.S. (2008) Interplay of angiotensin II and angiotensin(1-7) in the regulation of matrix metalloproteinases of human cardiocytes. *Exp Physiol,* 93 (5), 599-612.

Papp, M., Li, X., Zhuang, J., Wang, R. and Uhal, B.D. (2002) Angiotensin receptor subtype AT(1) mediates alveolar epithelial cell apoptosis in response to ANG II. *Am J Physiol Lung Cell Mol Physiol,* 282 (4), L713-718.

Pardo, A., Selman, M. and Kaminski, N. (2008) Approaching the degradome in idiopathic pulmonary fibrosis. *Int J Biochem Cell Biol,* 40 (6-7), 1141-1155.

Patel, J.M., Martens, J.R., Li, Y.D., Gelband, C.H., Raizada, M.K. and Block, E.R. (1998) Angiotensin IV receptor-mediated activation of lung endothelial NOS is associated with vasorelaxation. *Am J Physiol,* 275 (6 Pt 1), L1061-1068.

Paul, M., Poyan Mehr, A. and Kreutz, R. (2006) Physiology of local renin-angiotensin systems. *Physiol Rev,* 86 (3), 747-803.

Petrov, V.V., Fagard, R.H. and Lijnen, P.J. (2000) Transforming growth factor-beta(1) induces angiotensin-converting enzyme synthesis in rat cardiac fibroblasts during their differentiation to myofibroblasts. *J Renin Angiotensin Aldosterone Syst,* 1 (4), 342-352.

Phillips, C.L., Combs, S.B. and Pinnell, S.R. (1994) Effects of ascorbic acid on proliferation and collagen synthesis in relation to the donor age of human dermal fibroblasts. *J Invest Dermatol,* 103 (2), 228-232.

Raghu, G., Chen, Y.Y., Rusch, V. and Rabinovitch, P.S. (1988) Differential proliferation of fibroblasts cultured from normal and fibrotic human lungs. *Am Rev Respir Dis,* 138 (3), 703-708.

Raghu, G. and Thickett, D.R. (2013) Pirfenidone for IPF: pro/con debate; the 'con' viewpoint. *Thorax,* 68 (7), 605-608.

Raghu, G., Weycker, D., Edelsberg, J., Bradford, W.Z. and Oster, G. (2006) Incidence and prevalence of idiopathic pulmonary fibrosis. *Am J Respir Crit Care Med,* 174 (7), 810-816.

Ramos, C., Montaño, M., García-Alvarez, J., Ruiz, V., Uhal, B.D., Selman, M. and Pardo, A. (2001) Fibroblasts from idiopathic pulmonary fibrosis and normal lungs differ in growth rate, apoptosis, and tissue inhibitor of metalloproteinases expression. *Am J Respir Cell Mol Biol,* 24 (5), 591-598.

Ransom, J.T., Sharif, N.A., Dunne, J.F., Momiyama, M. and Melching, G. (1992) AT1 angiotensin receptors mobilize intracellular calcium in a subclone of NG108-15 neuroblastoma cells. *J Neurochem,* 58 (5), 1883-1888.

Renzoni, E.A., Abraham, D.J., Howat, S., Shi-Wen, X., Sestini, P., Bou-Gharios, G., Wells, A.U., Veeraraghavan, S., Nicholson, A.G., Denton, C.P., Leask, A., Pearson, J.D., Black, C.M., Welsh, K.I. and Du Bois, R.M. (2004) Gene expression profiling reveals novel TGFbeta targets in adult lung fibroblasts. *Respir Res,* 5, 24.

Richeldi, L., Du Bois, R.M., Raghu, G., Azuma, A., Brown, K.K., Costabel, U., Cottin, V., Flaherty, K.R., Hansell, D.M., Inoue, Y., Kim, D.S., Kolb, M., Nicholson, A.G., Noble, P.W., Selman, M., Taniguchi, H., Brun, M., Le Maulf, F., Girard, M., Stowasser, S., Schlenker-Herceg, R., Disse, B., Collard, H.R. and Investigators, I.T. (2014) Efficacy and safety of nintedanib in idiopathic pulmonary fibrosis. *N Engl J Med,* 370 (22), 2071-2082.

Roks, A.J., Van Geel, P.P., Pinto, Y.M., Buikema, H., Henning, R.H., De Zeeuw, D. and Van Gilst, W.H. (1999) Angiotensin-(1-7) is a modulator of the human renin-angiotensin system. *Hypertension,* 34 (2), 296-301.

Ruiz-Ortega, M., Lorenzo, O. and Egido, J. (1998) Angiotensin III up-regulates genes involved in kidney damage in mesangial cells and renal interstitial fibroblasts. *Kidney Int Suppl,* 68, S41-45.

Sacco, O., Silvestri, M., Sabatini, F., Sale, R., Defilippi, A.C. and Rossi, G.A. (2004) Epithelial cells and fibroblasts: structural repair and remodelling in the airways. *Paediatr Respir Rev,* 5 Suppl A, S35-40.

Saharinen, J., Hyytiäinen, M., Taipale, J. and Keski-Oja, J. (1999) Latent transforming growth factor-beta binding proteins (LTBPs)--structural extracellular matrix proteins for targeting TGF-beta action. *Cytokine Growth Factor Rev,* 10 (2), 99-117.

Sano, M., Fukuda, K., Kodama, H., Pan, J., Saito, M., Matsuzaki, J., Takahashi, T., Makino, S., Kato, T. and Ogawa, S. (2000) Interleukin-6 family of cytokines mediate angiotensin II-induced cardiac hypertrophy in rodent cardiomyocytes. *J Biol Chem,* 275 (38), 29717-29723.

Sano, M., Fukuda, K., Sato, T., Kawaguchi, H., Suematsu, M., Matsuda, S., Koyasu, S., Matsui, H., Yamauchi-Takihara, K., Harada, M., Saito, Y. and Ogawa, S. (2001) ERK and p38 MAPK, but not NF-kappaB, are critically involved in reactive oxygen species-mediated induction of IL-6 by angiotensin II in cardiac fibroblasts. *Circ Res,* 89 (8), 661-669.

Santos, R.A., Campagnole-Santos, M.J., Baracho, N.C., Fontes, M.A., Silva, L.C., Neves, L.A., Oliveira, D.R., Caligiorne, S.M., Rodrigues, A.R. and Gropen Júnior, C. (1994) Characterization of a new angiotensin antagonist selective for angiotensin-(1-7): evidence that the actions of angiotensin-(1-7) are mediated by specific angiotensin receptors. *Brain Res Bull,* 35 (4), 293-298.

Santos, R.A., Haibara, A.S., Campagnole-Santos, M.J., Simões E Silva, A.C., Paula, R.D., Pinheiro, S.V., Leite, M.F., Lemos, V.S., Silva, D.M., Guerra, M.T. and Khosla, M.C. (2003a) Characterization of a new selective antagonist for angiotensin-(1-7), D-pro7-angiotensin-(1-7). *Hypertension,* 41 (3 Pt 2), 737-743.

Santos, R.A., Simoes E Silva, A.C., Maric, C., Silva, D.M., Machado, R.P., De Buhr, I., Heringer-Walther, S., Pinheiro, S.V., Lopes, M.T., Bader, M., Mendes, E.P., Lemos, V.S., Campagnole-Santos, M.J., Schultheiss, H.P., Speth, R. and Walther, T. (2003b) Angiotensin-(1-7) is an endogenous ligand for the G protein-coupled receptor Mas. *Proc Natl Acad Sci U S A,* 100 (14), 8258-8263.

Schlüter, K.D. and Wenzel, S. (2008) Angiotensin II: a hormone involved in and contributing to pro-hypertrophic cardiac networks and target of anti-hypertrophic cross-talks. *Pharmacol Ther,* 119 (3), 311-325.

Schwacke, J.H., Spainhour, J.C., Ierardi, J.L., Chaves, J.M., Arthur, J.M., Janech, M.G. and Velez, J.C. (2013) Network modeling reveals steps in angiotensin peptide processing. *Hypertension,* 61 (3), 690-700.

Selman, M., King, T.E., Pardo, A., Society, A.T., Society, E.R. and Physicians, A.C.O.C. (2001) Idiopathic pulmonary fibrosis: prevailing and evolving hypotheses about its pathogenesis and implications for therapy. *Ann Intern Med,* 134 (2), 136-151.

Selman, M., Montaño, M., Ramos, C. and Chapela, R. (1986) Concentration, biosynthesis and degradation of collagen in idiopathic pulmonary fibrosis. *Thorax,* 41 (5), 355-359.

Selman, M. and Pardo, A. (2006) Role of epithelial cells in idiopathic pulmonary fibrosis: from innocent targets to serial killers. *Proc Am Thorac Soc,* 3 (4), 364-372.

Selman, M., Ruiz, V., Cabrera, S., Segura, L., Ramírez, R., Barrios, R. and Pardo, A. (2000) TIMP-1, -2, -3, and -4 in idiopathic pulmonary fibrosis. A prevailing nondegradative lung microenvironment? *Am J Physiol Lung Cell Mol Physiol,* 279 (3), L562-574.

Seyer, J.M., Hutcheson, E.T. and Kang, A.H. (1976) Collagen polymorphism in idiopathic chronic pulmonary fibrosis. *J Clin Invest,* 57 (6), 1498-1507.

Shenoy, V., Ferreira, A.J., Qi, Y., Fraga-Silva, R.A., Díez-Freire, C., Dooies, A., Jun, J.Y., Sriramula, S., Mariappan, N., Pourang, D., Venugopal, C.S., Francis, J., Reudelhuber, T., Santos, R.A., Patel, J.M., Raizada, M.K. and Katovich, M.J. (2010) The angiotensin-converting enzyme 2/angiogenesis-(1-7)/Mas axis confers cardiopulmonary protection against lung fibrosis and pulmonary hypertension. *Am J Respir Crit Care Med,* 182 (8), 1065-1072.

Silva, D.M., Vianna, H.R., Cortes, S.F., Campagnole-Santos, M.J., Santos, R.A. and Lemos, V.S. (2007) Evidence for a new angiotensin-(1-7) receptor subtype in the aorta of Sprague-Dawley rats. *Peptides,* 28 (3), 702-707.

Specks, U., Martin, W.J. and Rohrbach, M.S. (1990) Bronchoalveolar lavage fluid angiotensin-converting enzyme in interstitial lung diseases. *Am Rev Respir Dis,* 141 (1), 117-123.

Stacy, L.B., Yu, Q., Horak, K. and Larson, D.F. (2007) Effect of angiotensin II on primary cardiac fibroblast matrix metalloproteinase activities. *Perfusion,* 22 (1), 51-55.

Strutz, F., Zeisberg, M., Renziehausen, A., Raschke, B., Becker, V., Van Kooten, C. and Müller, G. (2001) TGF-beta 1 induces proliferation in human renal fibroblasts via induction of basic fibroblast growth factor (FGF-2). *Kidney Int,* 59 (2), 579-592.

Suki, B., Ito, S., Stamenovic, D., Lutchen, K.R. and Ingenito, E.P. (2005) Biomechanics of the lung parenchyma: critical roles of collagen and mechanical forces. *J Appl Physiol (1985),* 98 (5), 1892-1899.

Suzuki, S., Doi, Y., Aoi, W., Kuramochi, M. and Hashiba, K. (1984) Effect of angiotensin III on blood pressure, renin-angiotensin-aldosterone system in normal and hypertensive subjects. *Jpn Heart J,* 25 (1), 75-85.

Tallant, E.A., Lu, X., Weiss, R.B., Chappell, M.C. and Ferrario, C.M. (1997) Bovine aortic endothelial cells contain an angiotensin-(1-7) receptor. *Hypertension,* 29 (1 Pt 2), 388-393.

Taniguchi, H., Ebina, M., Kondoh, Y., Ogura, T., Azuma, A., Suga, M., Taguchi, Y., Takahashi, H., Nakata, K., Sato, A., Takeuchi, M., Raghu, G., Kudoh, S., Nukiwa, T. and Japan, P.C.S.G.I. (2010) Pirfenidone in idiopathic pulmonary fibrosis. *Eur Respir J,* 35 (4), 821-829.

Thomas, W.G., Thekkumkara, T.J. and Baker, K.M. (1996) Molecular mechanisms of angiotensin II (AT1A) receptor endocytosis. *Clin Exp Pharmacol Physiol Suppl,* 3, S74-80.

Tipnis, S.R., Hooper, N.M., Hyde, R., Karran, E., Christie, G. and Turner, A.J. (2000) A human homolog of angiotensin-converting enzyme. Cloning and functional expression as a captopril-insensitive carboxypeptidase. *J Biol Chem,* 275 (43), 33238-33243.

Tom, B., De Vries, R., Saxena, P.R. and Danser, A.H. (2001) Bradykinin potentiation by angiotensin-(1-7) and ACE inhibitors correlates with ACE C- and N-domain blockade. *Hypertension,* 38 (1), 95-99.

Tullberg-Reinert, H. and Jundt, G. (1999) In situ measurement of collagen synthesis by human bone cells with a sirius red-based colorimetric microassay: effects of transforming growth factor beta2 and ascorbic acid 2-phosphate. *Histochem Cell Biol,* 112 (4), 271-276.

Uhal, B.D., Gidea, C., Bargout, R., Bifero, A., Ibarra-Sunga, O., Papp, M., Flynn, K. and Filippatos, G. (1998) Captopril inhibits apoptosis in human lung epithelial cells: a potential antifibrotic mechanism. *Am J Physiol,* 275 (5 Pt 1), L1013-1017.

Uhal, B.D., Kim, J.K., Li, X. and Molina-Molina, M. (2007) Angiotensin-TGF-beta 1 crosstalk in human idiopathic pulmonary fibrosis: autocrine mechanisms in myofibroblasts and macrophages. *Curr Pharm Des,* 13 (12), 1247-1256.

Uhal, B.D., Li, X., Piasecki, C.C. and Molina-Molina, M. (2012) Angiotensin signalling in pulmonary fibrosis. *Int J Biochem Cell Biol,* 44 (3), 465-468.

Unger, T., Paulis, L. and Sica, D.A. (2011) Therapeutic perspectives in hypertension: novel means for renin-angiotensin-aldosterone system modulation and emerging device-based approaches. *Eur Heart J,* 32 (22), 2739-2747.

Van Kesteren, C.A., Saris, J.J., Dekkers, D.H., Lamers, J.M., Saxena, P.R., Schalekamp, M.A. and Danser, A.H. (1999) Cultured neonatal rat cardiac

myocytes and fibroblasts do not synthesize renin or angiotensinogen: evidence for stretch-induced cardiomyocyte hypertrophy independent of angiotensin II. *Cardiovasc Res,* 43 (1), 148-156.

Van Kuppevelt, T.H., Veerkamp, J.H. and Timmermans, J.A. (1995) Immunoquantification of type I, III, IV and V collagen in small samples of human lung parenchyma. *Int J Biochem Cell Biol,* 27 (8), 775-782.

Van Obberghen-Schilling, E., Roche, N.S., Flanders, K.C., Sporn, M.B. and Roberts, A.B. (1988) Transforming growth factor beta 1 positively regulates its own expression in normal and transformed cells. *J Biol Chem,* 263 (16), 7741-7746.

Verma, R.P. and Hansch, C. (2007) Matrix metalloproteinases (MMPs): chemical-biological functions and (Q)SARs. *Bioorg Med Chem,* 15 (6), 2223-2268.

Wang, L., Eberhard, M. and Erne, P. (1995) Stimulation of DNA and RNA synthesis in cultured rabbit cardiac fibroblasts by angiotensin IV. *Clin Sci (Lond),* 88 (5), 557-562.

Wang, R., Ibarra-Sunga, O., Verlinski, L., Pick, R. and Uhal, B.D. (2000) Abrogation of bleomycin-induced epithelial apoptosis and lung fibrosis by captopril or by a caspase inhibitor. *Am J Physiol Lung Cell Mol Physiol,* 279 (1), L143-151.

Wang, R., Zagariya, A., Ibarra-Sunga, O., Gidea, C., Ang, E., Deshmukh, S., Chaudhary, G., Baraboutis, J., Filippatos, G. and Uhal, B.D. (1999) Angiotensin II induces apoptosis in human and rat alveolar epithelial cells. *Am J Physiol,* 276 (5 Pt 1), L885-889.

Waseda, Y., Yasui, M., Nishizawa, Y., Inuzuka, K., Takato, H., Ichikawa, Y., Tagami, A., Fujimura, M. and Nakao, S. (2008) Angiotensin II type 2 receptor antagonist reduces bleomycin-induced pulmonary fibrosis in mice. *Respir Res,* 9, 43.

Wienen, W., Hauel, N., Van Meel, J.C., Narr, B., Ries, U. and Entzeroth, M. (1993) Pharmacological characterization of the novel nonpeptide angiotensin II receptor antagonist, BIBR 277. *Br J Pharmacol,* 110 (1), 245-252.

Willems, S., Stijn, W., Verleden, S.E., Vanaudenaerde, B.M., Wynants, M., Marijke, W., Dooms, C., Christophe, D., Yserbyt, J., Jonas, Y., Somers, J., Jana, S., Verbeken, E.K., Verleden, G.M. and Wuyts, W.A. (2013) Multiplex protein profiling of bronchoalveolar lavage in idiopathic pulmonary fibrosis and hypersensitivity pneumonitis. *Ann Thorac Med,* 8 (1), 38-45.

Willis, B.C., Liebler, J.M., Luby-Phelps, K., Nicholson, A.G., Crandall, E.D., Du Bois, R.M. and Borok, Z. (2005) Induction of epithelial-mesenchymal transition in alveolar epithelial cells by transforming growth factor-beta1: potential role in idiopathic pulmonary fibrosis. *Am J Pathol,* 166 (5), 1321-1332.

Wollin, L., Wex, E., Pautsch, A., Schnapp, G., Hostettler, K.E., Stowasser, S. and Kolb, M. (2015) Mode of action of nintedanib in the treatment of idiopathic pulmonary fibrosis. *Eur Respir J,* 45 (5), 1434-1445.

Wyllie, D.J. and Chen, P.E. (2007) Taking the time to study competitive antagonism. *Br J Pharmacol,* 150 (5), 541-551.

Wynn, T.A. (2011) Integrating mechanisms of pulmonary fibrosis. *J Exp Med,* 208 (7), 1339-1350.

Xia, H., Nho, R.S., Kahm, J., Kleidon, J. and Henke, C.A. (2004) Focal adhesion kinase is upstream of phosphatidylinositol 3-kinase/Akt in regulating fibroblast survival in response to contraction of type I collagen matrices via a beta 1 integrin viability signaling pathway. *J Biol Chem,* 279 (31), 33024-33034.

Yamashita, C.M., Dolgonos, L., Zemans, R.L., Young, S.K., Robertson, J., Briones, N., Suzuki, T., Campbell, M.N., Gauldie, J., Radisky, D.C., Riches, D.W., Yu, G., Kaminski, N., Mcculloch, C.A. and Downey, G.P. (2011) Matrix metalloproteinase 3 is a mediator of pulmonary fibrosis. *Am J Pathol,* 179 (4), 1733-1745.

Yamashita, M., Yamauchi, K., Chiba, R., Iwama, N., Date, F., Shibata, N., Kumagai, H., Risteli, J., Sato, S., Takahashi, T. and Ono, M. (2009) The definition of fibrogenic processes in fibroblastic foci of idiopathic pulmonary fibrosis based on morphometric quantification of extracellular matrices. *Hum Pathol,* 40 (9), 1278-1287.

Yamauchi, M. and Sricholpech, M. (2012) Lysine post-translational modifications of collagen. *Essays Biochem,* 52, 113-133.

Yao, H.W., Zhu, J.P., Zhao, M.H. and Lu, Y. (2006) Losartan attenuates bleomycin-induced pulmonary fibrosis in rats. *Respiration,* 73 (2), 236-242.

Yu, Q. and Stamenkovic, I. (2000) Cell surface-localized matrix metalloproteinase-9 proteolytically activates TGF-beta and promotes tumor invasion and angiogenesis. *Genes Dev,* 14 (2), 163-176.

Yuan, W. and Varga, J. (2001) Transforming growth factor-beta repression of matrix metalloproteinase-1 in dermal fibroblasts involves Smad3. *J Biol Chem,* 276 (42), 38502-38510.

Zeng, Z.S., Cohen, A.M. and Guillem, J.G. (1999) Loss of basement membrane type IV collagen is associated with increased expression of metalloproteinases 2 and 9 (MMP-2 and MMP-9) during human colorectal tumorigenesis. *Carcinogenesis,* 20 (5), 749-755.

Zhang, H., Unal, H., Desnoyer, R., Han, G.W., Patel, N., Katritch, V., Karnik, S.S., Cherezov, V. and Stevens, R.C. (2015a) Structural Basis for Ligand

Recognition and Functional Selectivity at Angiotensin Receptor. *J Biol Chem,* 290 (49), 29127-29139.

Zhang, H., Unal, H., Gati, C., Han, G.W., Liu, W., Zatsepin, N.A., James, D., Wang, D., Nelson, G., Weierstall, U., Sawaya, M.R., Xu, Q., Messerschmidt, M., Williams, G.J., Boutet, S., Yefanov, O.M., White, T.A., Wang, C., Ishchenko, A., Tirupula, K.C., Desnoyer, R., Coe, J., Conrad, C.E., Fromme, P., Stevens, R.C., Katritch, V., Karnik, S.S. and Cherezov, V. (2015b) Structure of the Angiotensin receptor revealed by serial femtosecond crystallography. *Cell,* 161 (4), 833-844.

Zhang, W., Chen, D.Q., Qi, F., Wang, J., Xiao, W.Y. and Zhu, W.Z. (2010) Inhibition of calcium-calmodulin-dependent kinase II suppresses cardiac fibroblast proliferation and extracellular matrix secretion. *J Cardiovasc Pharmacol,* 55 (1), 96-105.

Zimpelmann, J. and Burns, K.D. (2009) Angiotensin-(1-7) activates growth-stimulatory pathways in human mesangial cells. *Am J Physiol Renal Physiol,* 296 (2), F337-346.

8. Appendix

The tables below show the patient characteristics of the fibroblast lines that were used for each individual figure in chapter 4.

N.B All donor fibroblasts chosen for investigation were from patients whose FEV_1/FVC ratio was >0.7, indicating no significant obstructive lung disease. This data is therefore not included in the tables below.

Sample	Age	Gender	Operation	Prescribed ACEi or AT_1R antags?	Smoking status
HL303	21	M	Bullectomy	No	Non
EV169	66	F	Wedge resection	No	Non
EV178	71	M	Lobectomy	No	Ex
HL312	32	M	Bullectomy	No	Cannabis

Appendix 1. Patient characteristic of the fibroblast lines that were used in Figure 4.1.

Sample	Age	Gender	Operation	Prescribed ACEi or AT_1R antags?	Smoking status
HL357	70	F	Lobectomy	Ramipril	Ex
HL361	78	F	Lobectomy	No	Ex
HL362	76	F	Lobectomy	No	Ex
HL373	50	F	Lobectomy	No	Ex
HL380	62	F	Lobectomy	No	Current
HL385	72	M	Lobectomy	No	Ex

Appendix 2. Patient characteristic of the fibroblast lines that were used in Figure 4.2.

Sample	Age	Gender	Operation	Prescribed ACEi or AT_1R antags?	Smoking status
HL303	21	M	Bullectomy	No	Non
EV178	71	M	Lobectomy	No	Ex
EV169	66	F	Wedge	No	Non
HL312	32	M	Bullectomy	No	Cannabis

Appendix 3. Patient characteristic of the fibroblast lines that were used in Figure 4.3.

Sample	Age	Gender	Operation	Prescribed ACEi or AT_1R antags?	Smoking status
HL409	61	F	Lobectomy	No	Current
HL386	21	M	Bullectomy	No	Non
HL385	72	M	Lobectomy	No	Ex
HL380	62	F	Lobectomy	No	Current

Appendix 4. Patient characteristic of the fibroblast lines that were used in Figure 4.4 and Figure 4.5.

Sample	Age	Gender	Operation	Prescribed ACEi or AT_1R antags?	Smoking status
HL442	73	F	Lobectomy	No	Ex
HL443	55	F	Lobectomy	No	Ex
HL452	62	F	Lobectomy	Candesartan	Ex
HL453	28	M	Bullectomy	No	Ex
HL454	65	F	Lobectomy	No	Current
HL456	80	M	Lobectomy	No	Ex
HL463	74	M	Lobectomy	No	Ex
TL0079	N/A	F	Lobectomy	No	Ex
TL0042	84	M	Lobectomy	Candesartan	Ex
TL0070	83	F	Lobectomy	No	Current
TL0076	68	M	Lobectomy	No	Ex

Appendix 5. Patient characteristic of the fibroblast lines that were used in Figure 4.6.

Sample	Age	Gender	Operation	Prescribed ACEi or AT_1R antags?	Smoking status
HL463	74	M	Lobectomy	No	Ex
TL0079	N/A	F	Lobectomy	Candesartan	Ex
TL0042	84	M	Lobectomy	Candesartan	Ex
TL0070	83	F	Lobectomy	No	Current
TL0076	68	M	Lobectomy	No	Ex

Appendix 6. Patient characteristic of the fibroblast lines that were used in Figure 4.7.

Sample	Age	Gender	Operation	Prescribed ACEi or AT_1R antags?	Smoking status
HL442	73	F	Lobectomy	No	Ex
HL443	55	F	Lobectomy	No	Ex
HL463	74	M	Lobectomy	No	Ex
TL0079	N/A	F	Lobectomy	Candesartan	Ex
TL0070	83	F	Lobectomy	No	Current
TL0076	68	M	Lobectomy	No	Ex

Appendix 7. Patient characteristic of the fibroblast lines that were used in Figure 4.8.

Sample	Age	Gender	Operation	Prescribed ACEi or AT_1R antags?	Smoking status
HL424	63	M	Wedge resection	No	Ex
HL429	51	M	Bullectomy	No	Current
HL442	73	F	Lobectomy	No	Ex
HL443	55	F	Lobectomy	No	Ex
HL452	62	F	Lobectomy	Candesartan	Ex
HL453	28	M	Bullectomy	No	Ex
HL454	65	F	Lobectomy	No	Current
HL456	80	M	Lobectomy	No	Ex

Appendix 8. Patient characteristic of the fibroblast lines that were used in Figure 4.9.

Sample	Age	Gender	Operation	Prescribed ACEi or AT_1R antags?	Smoking status
HL442	73	F	Lobectomy	No	Ex
HL443	55	F	Lobectomy	No	Ex
HL452	62	F	Lobectomy	Candesartan	Ex
HL453	28	M	Bullectomy	No	Ex
HL454	65	F	Lobectomy	No	Current
HL456	80	M	Lobectomy	No	Ex
HL466	55	F	Lobectomy	No	Ex
TL0208	59	M	Lobectomy	No	Ex
TL0398	70	F	Lobectomy	No	Ex

Appendix 9. Patient characteristic of the fibroblast lines that were used in Figure 4.10.

Sample	Age	Gender	Operation	Prescribed ACEi or AT_1R antags?	Smoking status
HL466	55	F	Lobectomy	No	Ex
TL0208	59	M	Lobectomy	No	Ex
TL0398	70	F	Lobectomy	No	Ex

Appendix 10. Patient characteristic of the fibroblast lines that were used in Figure 4.11.

Sample	Age	Gender	Operation	Prescribed ACEi or AT_1R antags?	Smoking status
HL456	80	M	Lobectomy	No	Ex
TL0156	50	F	Lobectomy	Losartan	Current
TL0167	76	M	Lobectomy	No	Ex
TL0261	50	M	Lobectomy	No	Non
TL0398	70	F	Lobectomy	No	Ex

Appendix 11. Patient characteristic of the fibroblast lines that were used in Figure 4.12.

Sample	Age	Gender	Operation	Prescribed ACEi or AT_1R antags?	Smoking status
TL0098	78	M	Lobectomy	Ramipril	Ex
HL324	50	M	Lobectomy	Lisinopril	Current
TL0153	76	F	Lobectomy	No	Ex
HL466	55	F	Lobectomy	No	Ex
TL0208	59	M	Lobectomy	No	Ex

Appendix 12. Patient characteristic of the fibroblast lines that were used in Figure 4.13.

Sample	Age	Gender	Operation	Prescribed ACEi or AT_1R antags?	Smoking status
HL312	32	M	Bullectomy	No	Cannabis
HL315	47	M	Wedge Resection	No	Current
HL319	68	F	Lobectomy	No	Ex

Appendix 13. Patient characteristic of the fibroblast lines that were used in Figure 4.14 and Figure 4.15.

Sample	Age	Gender	Operation	Prescribed ACEi or AT_1R antags?	Smoking status
TL0208	59	M	Lobectomy	No	Ex
HL324	50	M	Lobectomy	Lisinopril	Current
HL466	55	F	Lobectomy	No	Ex

Appendix 14. Patient characteristic of the fibroblast lines that were used in Figure 4.16.

Sample	Age	Gender	Operation	Prescribed ACEi or AT_1R antags?	Smoking status
HL452	62	F	Lobectomy	Candesartan	Ex
HL454	65	F	Lobectomy	No	Current
HL455	63	M	Lobectomy	Ramipril	Non
HL460	52	M	Lobectomy	Ramipril	Current
HL461	65	F	Lobectomy	No	Current
HL463	74	M	Lobectomy	No	Ex
TL0068	66	M	Lobectomy	Ramipril	Ex
TL0079	N/A	F	Lobectomy	No	Ex
TL0098	78	M	Lobectomy	Ramipril	Ex
TL0153	76	F	Lobectomy	No	Ex

Appendix 15. Patient characteristic of the fibroblast lines that were used in Figure 4.17.

Sample	Age	Gender	Operation	Prescribed ACEi or AT_1R antags?	Smoking status
TL0108	68	F	Lobectomy	Ramipril	Current
TL0156	50	F	Lobectomy	Candesartan	Current
TL0163	68	F	Lobectomy	Ramipril	Ex
TL0167	76	M	Lobectomy	No	Ex
TL0172	73	M	Lobectomy	No	Ex
TL0181	72	F	Lobetomy	No	Ex
TL0191	72	F	Lobetomy	No	Non
HL466	55	F	Lobectomy	No	Ex
TL0208	59	M	Lobectomy	No	Ex

Appendix 16. Patient characteristic of the fibroblast lines that were used in Figure 18 and Figure 4.19.

Sample	Age	Gender	Operation	Prescribed ACEi or AT_1R antags?	Smoking status
TL0208	59	M	Lobectomy	No	Ex
TL0261	56	M	Lobectomy	No	Non
HL324	50	M	Lobectomy	Lisinopril	Current
HL466	55	F	Lobectomy	No	Ex
TL0398	70	F	Lobectomy	No	Ex

Appendix 17. Patient characteristic of the fibroblast lines that were used in Figure 4.20.

Sample	Age	Gender	Operation	Prescribed ACEi or AT_1R antags?	Smoking status
TL0043	79	F	Lobectomy	Ramipril	Current
TL0208	59	M	Lobectomy	No	Ex
TL0261	56	M	Lobectomy	No	Non
HL324	50	M	Lobectomy	Lisinopril	Current
HL466	55	F	Lobectomy	No	Ex

Appendix 18. Patient characteristic of the fibroblast lines that were used in Figure 4.24.

Sample	Age	Gender	Operation	Prescribed ACEi or AT_1R antags?	Smoking status
HL324	50	M	Lobectomy	Lisinopril	Current
HL466	59	M	Lobectomy	No	Ex
TL0208	59	M	Lobectomy	No	Ex
TL0398	70	F	Lobectomy	No	Ex

Appendix 19. Patient characteristic of the fibroblast lines that were used in Figure 4.27.

Sample	Age	Gender	Operation	Prescribed ACEi or AT_1R antags?	Smoking status
TL0208	59	M	Lobectomy	No	Ex
HL466	55	F	Lobectomy	No	Ex
TL0398	70	F	Lobectomy	No	Ex

Appendix 20. Patient characteristic of the fibroblast lines that were used in Figure 4.21, Figure 4.22, Figure 4.23, Figure 4.25, Figure 4.26, Figure 4.28, Figure 4.29 and Figure 4.30